Final Report

STUDY THERMOGRAPHIC FLAW DETECTION

Contract Number: NAS8-38609
Delivery order: 148

Prepared by and Co-Principle Investigator

James L. Walker
Center for Automation and Robotics
University of Alabama in Huntsville
Huntsville, AL 35899
(205)-895-6578*207

Co-Principle Investigator

Gary L. Workman
Center for Automation and Robotics
University of Alabama in Huntsville
Huntsville, AL 35899
(205)-895-6578*240

Submitted to

Samuel Russell
EH13
National Aeronautics and Space Administration
Marshall Space Flight Center, AL 35812
(205)-544-4411

July, 1996

TABLE OF CONTENTS

ABSTRACT

The development of thermographic inspection methods for use on aerospace structures is under investigation. Several different material systems, structural geometries and defect types have been included in this study so as to establish a baseline from which future IRT testing can be made. This study examines various thermal loading techniques in an attempt to enhance the likelihood of capturing and identifying critically sized flaws under "non laboratory" actual working conditions. Qualification techniques and calibration standards are also being investigated to standardize the thermographic method.

In conjunction with the thermographic inspections, advanced image processing techniques including digital filtering and neural networks have been investigated to increase the ability of detecting and sizing flaws. Here, the digitized thermographic images are mathematically manipulated through various filtering techniques and/or artificial neural mapping schemes to enhance its overall quality, permitting accurate flaw identification even when the signal-to-noise ratio is low.

1.0 INTRODUCTION

Advances in materials and manufacturing processes have lead to vast improvements in today's aerospace structures. As a result, structural efficiencies have risen to a level where even slight material or process anomalies can detrimentally effect the performance of the vehicle or structure. To keep pace with these advances and to verify the quality of "advanced" structures, new and innovative nondestructive evaluation (NDE) techniques must be developed. In order to prevent costly downtime and disassembly of a structure and to provide adequate feedback to designers in a realistic amount of time the NDE approach must provide rapid assessment of a large portion of the structure in as near to the actual service environment as possible. No single NDE technique has the capability of providing 100% detectability for all service environments and conditions, so complementory techniques must be developed to fully monitor components. This particular research effort investigates the potential of infrared thermography (IRT) to assess the quality of composite, and other aerospace structures, as well as to create post analysis tools that will make data interpretation of the thermographic images more effective.

Thermographic NDE techniques allow subsurface defects to be visualized by means of variations in the structural surface temperature arising from distortion of an injected heat field, from an external source such as a heat lamp, or from within the structure as a result of rubbing, such as from a fatigue process. Thermograms are produced "at distance" requiring no direct contact with the structure and can be produced over relatively large surface areas. The temperature variations though are often very small, requiring specialized highly sensitive detection systems to locate small material abnormalities.

Up until recent times the results of a thermographic inspection were only qualitative in nature, providing no direct measure of material quality. Research at the NASA Langley Research Center has shown that to some degree a quantitative measure of flaw depth could be measured using thermography along with post test image processing. The purpose of this project is to mirror and then extend that work, developing new and innovative methods for acquiring and analyzing thermographic data, so that quantitative nondestructive measurements can be made of composite structures in near real time. Emphasis is to be placed upon assembling and qualifying a portable NDE thermographic flaw detection system capable of taking controlled measurements, performing data analysis, and generating documentable results in the field.

Recent advancements in digital thermal imagery along with the increase in personal computer computational power have brought thermography into the forefront of NDE as a viable approach for locating defects or other material abnormalities in aerospace structures. Thermography has been used to qualitatively detect subsurface corrosion in the wing skins of aircraft, locate delaminations and disbonds in honeycomb and foam core composite panels and find cracks in thin aluminum sheet. A major problem with thermography though, has been the lack of repeatability and quantitative results.

Several factors have a significant effect on the detectability of thermography including size and depth of the flaw, local emissivity, environmental stability, material thermal conductivity and diffusivity, heating cycle, detector resolution, etc. Each of these factors needs to be addressed in order to make thermographic measurements repeatable and transferable.

Advances in image processing through the use of neural networks, Laplacian operators and multivariate statistical methods should permit quantitative measures of the thermography data. Features within the thermal image obscured by background noise may be enhanced with these mathematical techniques providing valuable information on the integrity of the component under test.

This report outlines IRT inspections performed on various test panels, as well as actual aerospcae hardware. The design of support hardware and software for the enhancement of the thermographic technique. Also, post analysis image processing is studied as a means to improve the resolution of thermal images.

2.0 STANDARDIZED FLAW PANELS

2.1 MONOLITHIC PANELS (Disbonds)

Using the facilities at UAH, three 12 inch square, two @ 17 ply and one @ 16 ply, graphite/epoxy (IM6/3501-6) panels have been constructed with built in flaws. The purpose of this work was to generate disbond type defects of known size and orientation without resorting to insertion of foreign material into the laminate. The panels were inspected with infrared thermography, ultrasonics and shearography at MSFC before being sent to NASA Langley (LaRC) to be further inspected thermographically. Upon return of the panels from LaRC they will be dissected to determine the quality of the defects so that improvements can be made to the manufacturing process.

The three panels feature different manufacturing approaches, each with the goal of generating carefully sized "realistic looking" voids, delaminations and/or disbonds.

2.1.1 Fabrication (Panel 1M)

The first panel utilized 17 plies and measured approximately 0.10 inch thick. The defects in this panel were formed by cutting small sections of the midply away and then sandwiching it between two previously cured 8 ply cover panels. The general procedure for making panel 1 is as follows.

1. Position peel ply on tooling plate.
2. Lay-up two (0,45,-45,90,90,-45,45,0) Gr/Ep panels.
3. Cover laminate with peel ply, breather, bleeder and vacuum bag.
   Cure for 2 hrs at 350 °F/cool to 250 °F in oven with fan on/Cool to 150 °F in oven with fan on and top of door open/Cool to 100 °F out of oven then remove vacuum bag and peel ply.
4. Make pattern for middle layer cut-outs on scrap prepreg backing (Figure 1).
5. Using template, cut pattern from middle layer.
6. Sandwich middle layer between panels made in Step 1 though 3. Place peel ply on top of sandwich. Cover with vacuum bag and cure for 1.5 hrs at 300 °F. Raise temperature to 350 °F for 0.5 hrs. Cool as in Step 3.
7. Sand edges smooth.

The finished panel was inspected using thermography, shearography and ultrasonics. The shearographic inspection was not able to locate the defects. Using back side heating from a single 500 W quartz heat lamp the image shown in Figure 2 was generated thermographically. All of the scheduled flaws were found although the smallest (0.36 inch circle and 1/4 inch square) of the planned defects were very close to the threshold of detectability. The C-scan image indicated that the planned defects had remained open; i.e. looked like voids; during cure. Some resin could be seen to fill in around the edge of each cut-out region and the smallest planned defects were all but totally filled with resin and unrecognizable.

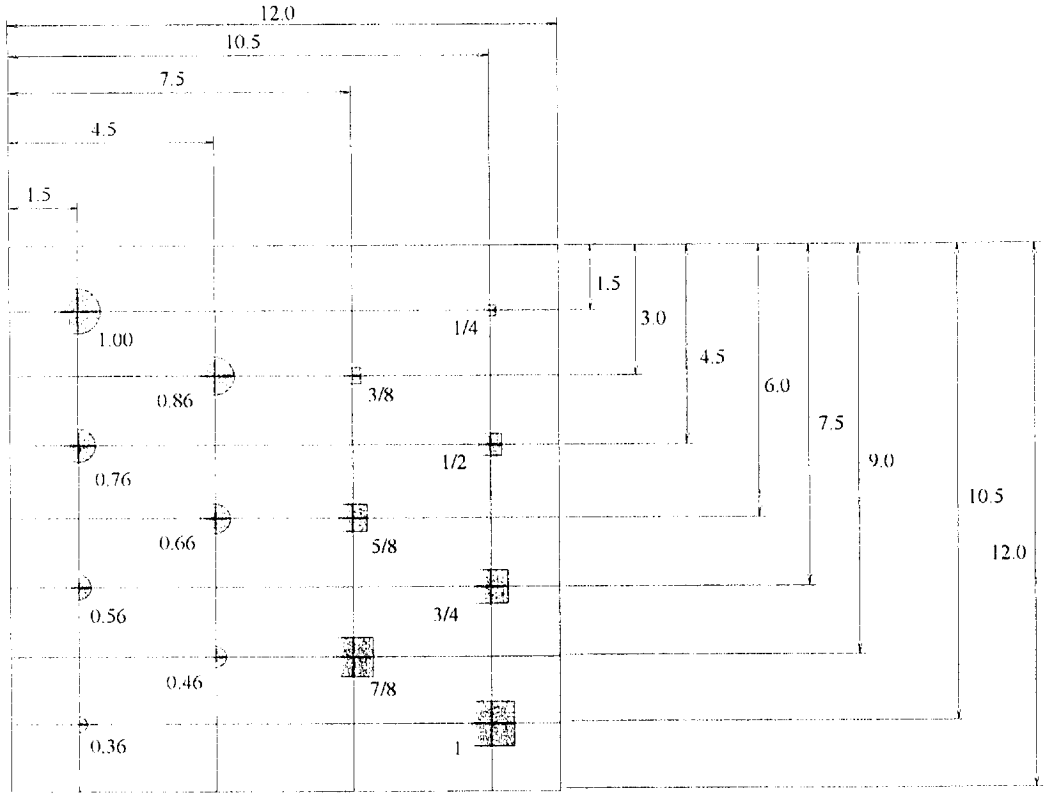

Figure 1. Monolithic panel 1M layout.

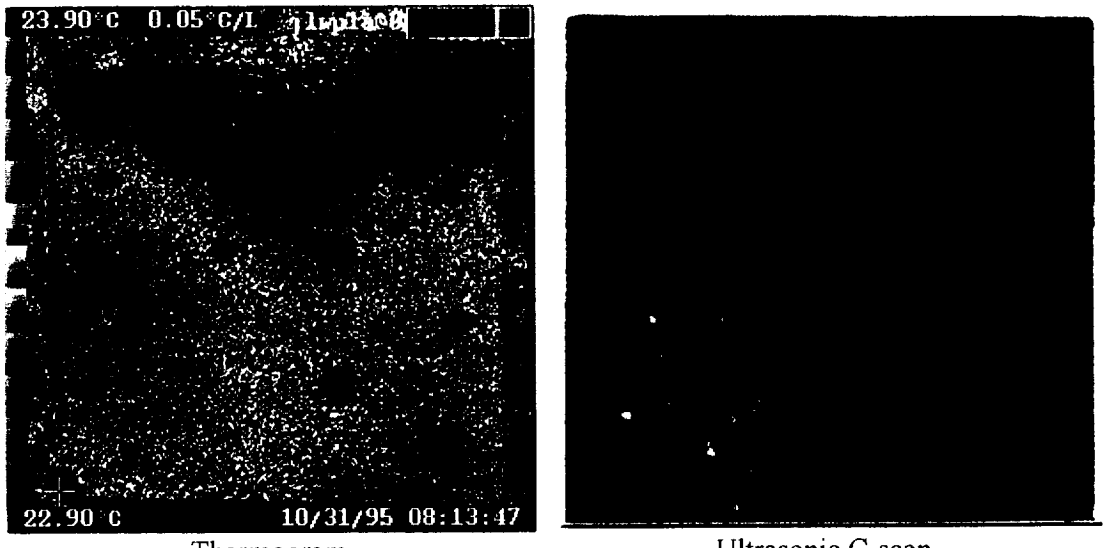

Thermogram

Ultrasonic C-scan

Figure 2. Monolithic panel 1M results.

2.1.2 Fabrication (Panel 2M)

The defects in the second panel were made by dimpling the midply surface of the laminate with brass shimstock (0.003, 0.004 and 0.006 inch thick). Again a 17 ply laminate is constructed with the defects residing between ply 9 and 10. The general procedure for constructing the panel is as follows.

1. Position peel ply on tooling plate.
2. Lay-up two (0,45,-45,90,90,-45,45,0) Gr/Ep panels
   One panel will have release coated brass shim-stock inserts positioned as shown in Figure 4 between the tooling plate and the first layer of material. (Note: no peel ply is placed below the panel with the shim stock.)
3. Cover laminate with peel ply, breather, bleeder and vacuum bag.
   Cure for 2 hrs at 350 °F/cool to 250 °F in oven with fan on/Cool to 150 °F in oven with fan on and top of door open/Cool to 100 °F out of oven then remove vacuum bag and peel ply.
4. Remove inserts from panel.
5. Sandwich a middle prepreg layer between panels made in Step 1 though 3. First position middle layer on top of faceplate without inserts. Preheat to 200 °F, remove from oven, cover with backing paper and press prepreg tightly against faceplate. Lay faceplate with prepreg middle layer on tooling plate and position insert panel on top. Place peel ply on top of sandwich. Cover with vacuum bag and cure for 1.5 hrs at 300 °F. Raise temperature to 350 °F for 0.5 hrs. Cool as in Step 3.
6. Sand edges smooth.

The finished panel was inspected with thermography and C-scan ultrasonics (Figure 3). The IRT scan utilized back side heating with a 500 W heat lamp and was able to detect all the defects. IRT was not able to distinguish the finer detail of the lower, V-shaped, flaws. When the panel was inspected ultrasonically resin flow could be seen along the edge of the dimpled regions. The C-scan confirmed that the V-shaped indentations had partially filled with resin, which was the reason that the thermographic scan could not resolve their planned shape.

Unavailable at time of print

Thermogram

Ultrasonic C-scan

Figure 3. Monolithic panel 2M results.

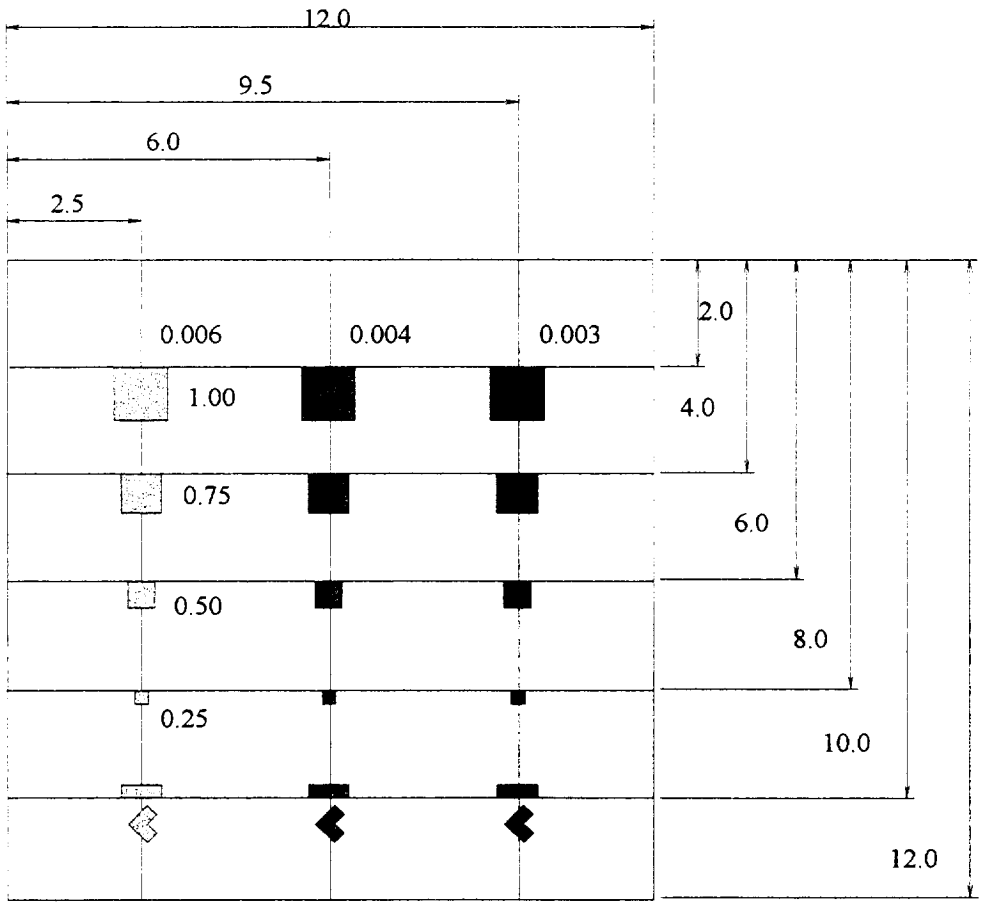

Figure 4. Monolithic panel 2M and 3M layout.

2.1.3 Fabrication (Panel 3M)

The third panel was constructed from two precured 8 ply faceplates bonded together with a layer of prepreg cobond adhesive. Patterns were cut in the cobond tape in an attempt to produce tight disbonds between the two faceplates. The construction procedure is s follows.

1. Position peel ply on tooling plate.
2. Lay-up two (0,45,-45,90,90,-45,45,0) Gr/Ep panels
3. Cover laminate with peel ply, breather, bleeder and vacuum bag.
   Cure for 2 hrs at 350 °F/cool to 250 °F in oven with fan on/Cool to 150 °F in oven with fan on and top of door open/Cool to 100 °F out of oven then remove vacuum bag and peel ply.
3. Make pattern for middle layer cut-outs on scrap prepreg backing (Figure 4) similar to panel 1.
4. Using template, cut pattern from middle layer of cobond tape.
5. Sandwich middle layer of cobond tape between panels made in Step 1. Place peel ply on top of sandwich. Cover with vacuum bag and cure for 2 hrs at 250 °F. Cool as in Step 1.
5. Sand edges smooth.

The thermographic results obtained using backside heating with a 500 W heat lamp was unable to recognize the planned defects (Figure 5). The C-scan results indicated that the cobond adhesive had flowed into the cutout regions, thus all but eliminating the disbond regions.

Unavailable at time of print

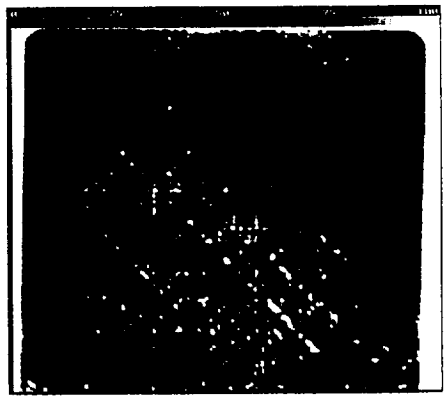

Thermogram

Ultrasonic C-scan

Figure 5. Monolithic panel 3M results.

Based upon the results of these tests it would appear that method two would be the most realistic way of generating controlled disbond regions inside a monolithic gr/ep panel. Additional work will be required though the gain control over the amount of resin that flows into the depressed region of the planned defect.

2.2 MONOLITHIC PANELS (Inclusions)

An 8 ply panel was constructed with backing paper, peal ply (Dacron fiber), bagging film and latex glove inclusions. The inclusions were cut into 1 inch squares and placed at mid-laminate as well as between the second and third ply. The tip off of a latex glove was also included at the center of the panel. The construction procedure is as follows.

1. Position peel ply on tooling plate.
2. Lay-up a single (0,90, 45,-45,-45,45,90,0) Gr/Ep panel with inclusions as specified in Table 1.
3. Cover laminate with peel ply, breather, bleeder and vacuum bag.
   Cure for 2 hrs at 350 °F/cool to 250 °F in oven with fan on/Cool to 150 °F in oven with fan on and top of door open/Cool to 100 °F out of oven then remove vacuum bag and peel ply.
4. Sand edges smooth.

Flaw I.D.	Materials	Depth (Ply)
A	Peal ply	4
B	Waxed backing paper	4
C	Backing paper	4
D	Bagging film	2
E	Latex glove	4
F	Bagging film	4
G	Backing paper	2
H	Waxed backing paper	2

Table 1. Inclusions.

The finished panel was inspected using front surface flash heating. The panel was placed 32 inches from the imager, under the spectral hood, and flashed with an equivalent energy level of 1400 V (power setting of the Bales Scientific flash unit). Figure 6 shown the thermal image 120 msec after the flash when all of the inclusions were visible. Inclusions "D, G and H" which were only two plies deep, were visible 20 msec after the flash. The remaining inclusions became apperant after 60 msec indicating the thermal lag through the panel.

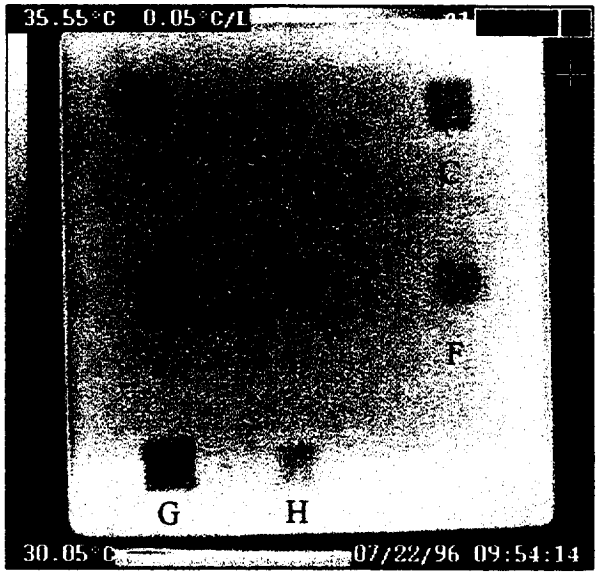

Figure 6. Thermographic results from inclusion panel.

2.3 HONEYCOMB PANELS

Three 15 inch square aluminum honeycomb graphite/epoxy composite panels were constructed with planned manufactured defects and tested thermographically. The defects were designed to simulate delaminations and disbonds between the faceplate and core. The defects were produced by altering the bondline between the faceplate and core material mechanically and as such did not utilize any foreign material such as Teflon tape.

As will be described in a latter section of this report, nine aluminum honeycomb graphite/epoxy panels that make up an inter tank structure were inspected at the MSFC NDE Lab using the Bales Thermographic Inspection System. An inter tank panel featuring Teflon inserts had been constructed to test the various NDE techniques that would ultimately be used to validate the integrity of each production panel. Thermography had little problems locating the built in Teflon inserts "flaws", see Section 4.0. The problem was though that most of the flaws could be seen visually and a question was posed as to the validity of using a foreign material as a means to simulate real core to face plate separations as well as delaminations between the various plies. Therefor a study intended to help answer those questions and to develop more realistic "standard" flaw panels was initiated to be used to certify the inspection process.

A scrap sheet of 1.0 inch aluminum honeycomb, similar to that used in the mid-region of the production unit inter tank panels, was acquired from Bill McMahon of MSFC to be used as the core for the test panels. Graphite/epoxy (IM6/3501-6) prepreg and cobond adhesive donated to UAH was used for the face plates. Each face plate was stacked using a (0, 90, 45, -45)s laminate and cured for 2 hours at 350 °F under a vacuum pressure. Several concepts for building in known defects were attempted and will be described in the following sub-sections.

2.3.1 Fabrication (Panel 1H)

Panel 1H was constructed in a manner similar to that of the monolithic panel 3M. That is cobond adhesive with planned holes cut in it was used to bond a faceplate to the core. The construction procedure is as follows.

1. Position a 15 inch square piece of peal ply on a large tooling plate.
2. Lay-up first 14.5 inch square Gr/Ep prepreg face plate (0,45,-45,90,90,-45,45,0)
3. Cover lay-up with a single ply of prepreg cobond adhesive tape.
4. Position honeycomb on cobond tape.
5. Center a small tooling plate on the top of the honeycomb panel.
6. Position a 15 inch square piece of peal ply on top of small tooling plate.
7. Lay-up second 14.5 inch square Gr/Ep prepreg face plate (0,45,-45,90,90,-45,45,0).
8. Cover top face plate with peal ply, breather and bleeder.
9. Vacuum bag the entire part. and ensure that there are no leaks.
   Cure for 2 hrs at 350 °F/cool to 250 °F in oven with fan on/Cool to 150 °F in oven with fan on and top of door open/Cool to 100 °F out of oven then remove vacuum bag and peel ply.
10. Using a template (Figure 7), cut defect pattern from cobond tape.
11. Apply defect cobond tape to inside surface of top face plate (the laminate cured on the small tooling plate.
12. Place top face plate, cobond tape side down, on exposed honey comb. Place a piece of peal ply on top of sandwich. Cover with vacuum bag and cure for 2 hrs at 250 °F. Cool as in Step 9.
13. Sand edges smooth.

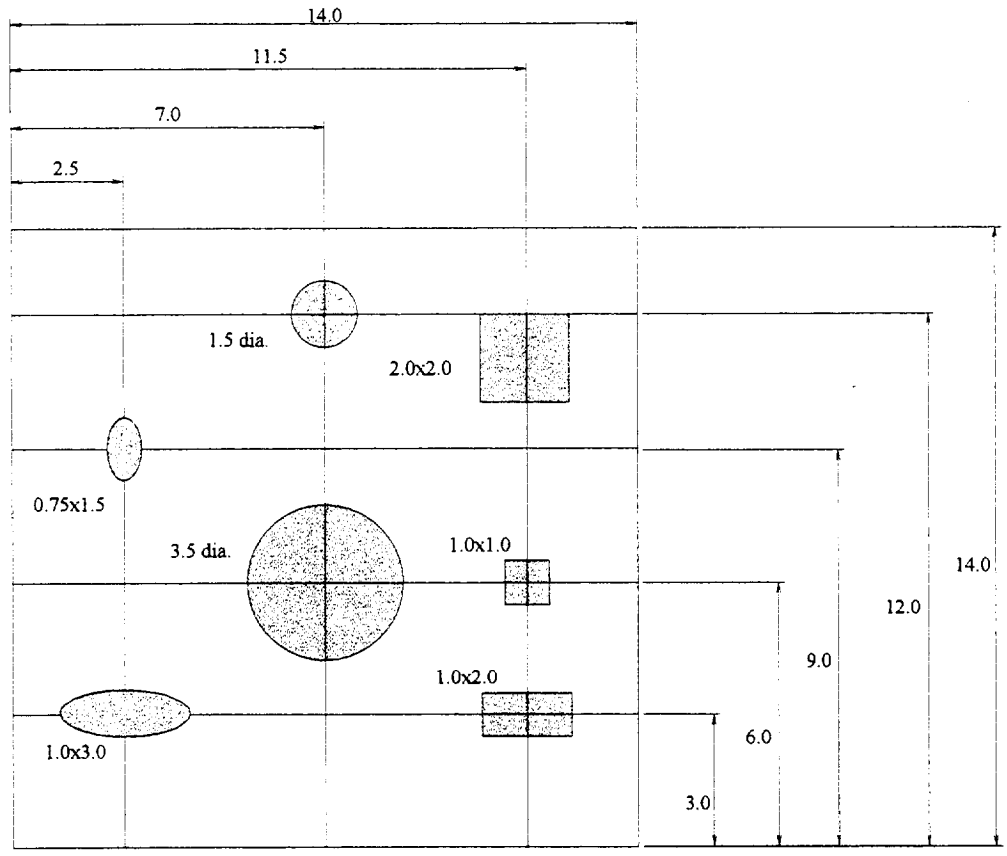

Figure 7. Honeycomb panel 1 layout.

Using a similar procedure as was performed on the production inter tank panels (Section 4.0) a thermographic inspection of the test panel was performed. The results are presented for panel 1H in Figure 8. The scheduled flaws showed up as cold spots in the thermograms during back surface heating by the two 500 Watt shop lamps. The flaws were barely detectable when they faced the heat source, i.e. face away from the camera. This result indicates the importance of having access to both sides of a honeycomb panel when performing thermographic inspections.

In addition to the backside heating, flash heating by means of the Bales Spectral Hood was conducted to the test panels. This technique was not used on the inter tank panels. The thermograms resulting from the flash heating though were much clearer than those from backside lamp heating.

Provided access is available to both sides of a honeycomb structural panel, it is therefor recommended that that flash heating be used to conduct the thermal scans. When access to only one side of the panel is available for viewing, and heat can be applied to the back face, then high intensity long duration heating should be used. If only one side of the panel is available for viewing and heating then there is little hope for inspecting the back faceplate and bondline with IRT.

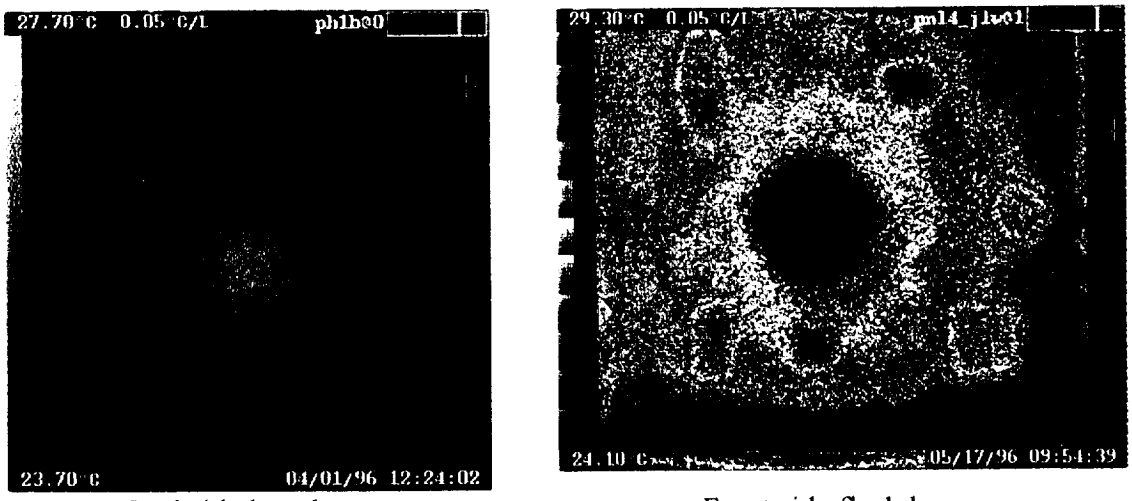

Backside heat lamp

Front side flash lamp

Figure 8. Honeycomb panel 1H.

Using digital filtering techniques an attempt to enhance the back surface heated image was made by applying the Winfree (Laplacian) filter and several self developed filters. The Laplacian filter was unable to resolve the thermal profile of the part. On the other hand a simple "edge enhancement" filter proved to be very useful by defining the shapes of each planned defect (Figure 9). The filter consisted of a 7 x 7 array in the form shown in Table 2.

0	0	0	0	0	0	0
0	2	2	2	2	2	0
0	2	0	0	0	2	0
0	2	0	10	0	2	0
0	2	0	0	0	2	0
0	2	2	2	2	2	0
0	0	0	0	0	0	0

Table 2. Digital filter.

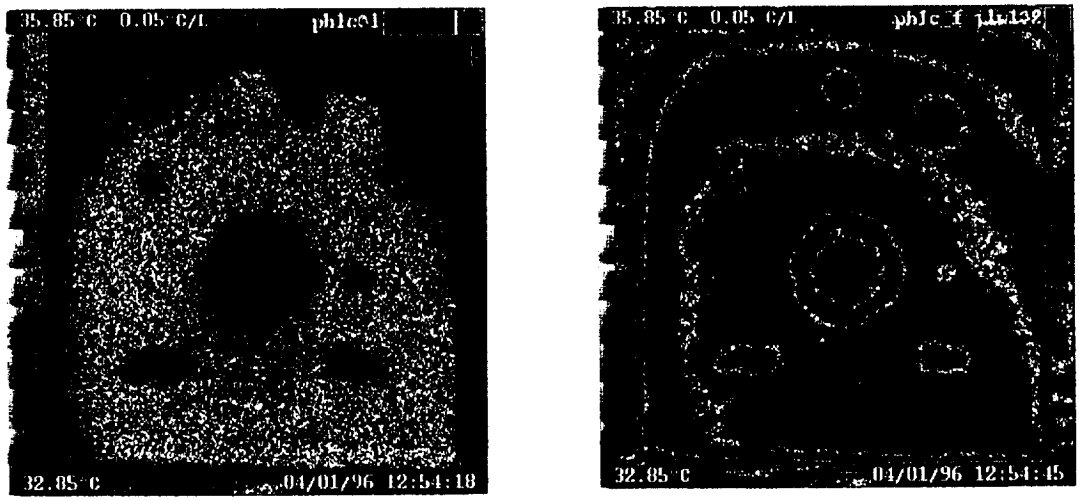

Figure 9. Image before and after digital filter.

Assuming that the thermal properties of the test panel and inter tank are similar, the thermographic procedures used for the inspection of the inter tank panels appears to be adequate for locating disbond over 1.0 inch square between the core and face plate based upon the results of this first test panel.

2.3.2 Fabrication (Panel 2H)

The second honeycomb panel built utilized a procedure similar to that of the second monolithic panel to generate disbonds between the core and faceplate by means of shim stock to depress a faceplate during a precure cycle. The procedures to construct such a panel are as follows.

1. Position a 15 inch square piece of peal ply on a large tooling plate.
2. Lay-up first 14.5 inch square Gr/Ep prepreg face plate (0,45,-45,90,90,-45,45,0)
3. Cover lay-up with a single ply of prepreg cobond adhesive tape.
4. Position honeycomb on cobond tape.
5. Center a small tooling plate on the top of the honeycomb panel.
6. Lay-up second 14.5 inch square Gr/Ep prepreg face plate (0,45,-45,90,90,-45,45,0).
7. Turn lay-up over and position inserts, then flip back over so that inserts face tooling plate.
8. Cover top face plate with peal ply, breather and bleeder.
9. Vacuum bag the entire part. and ensure that there are no leaks.
   Cure for 2 hrs at 350 °F/cool to 250 °F in oven with fan on/Cool to 150 °F in oven with fan on and top of door open/Cool to 100 °F out of oven then remove vacuum bag and peel ply.
10. Remove inserts from top face plate.
11. Apply cobond tape to honeycomb core.
12. Place top face plate, insert side down, on exposed honey comb. Place a piece of peal ply on top of sandwich. Cover with vacuum bag and cure for 2 hrs at 250 °F. Cool as in Step 9.
13. Sand edges smooth.

All the planned defect were found using both backside (500 W heat lamp) and flash heating as shown in Figures 10 and 11.

Figure 10. Backside heating of panel 2H.

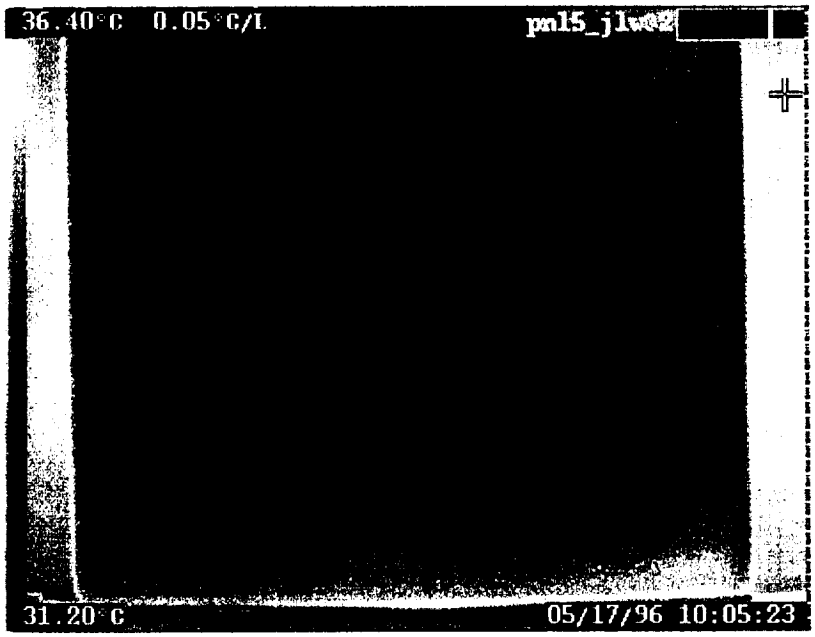

Figure 11. Front side flash heating of Panel 2H.

2.3.3 Fabrication (Panel 3H)

The third honeycomb core panel was constructed with embedded midfaceplate, type 2M, flaws and type 1H core to faceplate disbonds. The procedure for the construction of the panel are given below.

1. Position a 15 inch square piece of peal ply on a large tooling plate.
2. Lay-up first 14.5 inch square Gr/Ep prepreg face plate (0,90,45,-45,-45,45,90,0)
3. Cover lay-up with a single ply of prepreg cobond adhesive tape.
4. Position honeycomb on cobond tape.
5. Center a small tooling plate on the top of the honeycomb panel.
6. Lay-up half of second 14.5 inch square Gr/Ep prepreg face plate (0,90,45,-45).
7. Turn lay-up over and position inserts, then flip back over so that inserts face tooling plate.
8. Cover top face plate with peal ply, breather and bleeder.
9. Vacuum bag the entire part. and ensure that there are no leaks.
   Cure for 2 hrs at 350 °F/cool to 250 °F in oven with fan on/Cool to 150 °F in oven with fan on and top of door open/Cool to 100 °F out of oven then remove vacuum bag and peel ply.
10. Remove inserts from top face plate.
11. Lay-up second half of second 14.5 inch square Gr/Ep prepreg face plate (-45,45,90,0) on tooling plate. Place first half of faceplate "B" face down on uncured laminate.
12. Cover top face plate with peal ply, breather and bleeder.
13. Vacuum bag the entire part. and ensure that there are no leaks.
    Cure for 2 hrs at 350 °F/cool to 250 °F in oven with fan on/Cool to 150 °F in oven with fan on and top of door open/Cool to 100 °F out of oven then remove vacuum bag and peel ply.
14. Using template, cut defect pattern from cobond tape.
15. Apply defect cobond tape to inside surface of top face plate (the laminate cured on the small tooling plate.
16. Place top face plate, cobond tape side down, on exposed honey comb. Place a piece of peal ply on top of sandwich. Cover with vacuum bag and cure for 2 hrs at 250 °F. Cool as in Step 9.
17. Sand edges smooth.

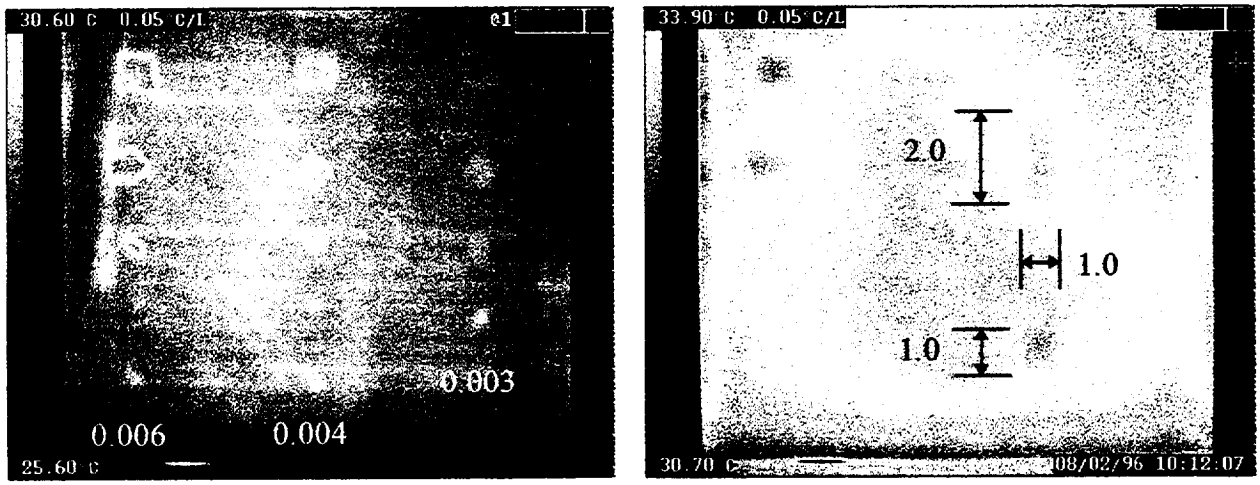

220 msec

780 msec

Figure 11. Flash heating of panel 3H.

3.0 IMPACT DAMAGED GRAPHITE/PHENOLIC SPECIMENS

During the thermographic inspection of the NPU-3 graphite/phenolic external tank nose cone, Section 5 of this report, a question was posed as to the validity of using Teflon inserts to simulate delamination type flaws. The main doubt was whether or not the thermographic inspection procedure used for identifying artificial defects would be representative of a similar inspection for locating "real" flaws. As a test to this dilemma, eleven, 3.0 inch square by 0.25 inch thick, specimens were cut from a section of external tank nose cone and impacted using a 5 pound impact hammer, with either a 0.0625, 0.25 or 0.5 inch tup, dropped from various heights to produce a wide range of damage states. A summary of the impact energies and tup sizes for the specimens are provided in Table 3.

Specimen I.D.	Impact Energy (Ft-lb)	Tup Size
GL2	4.39	0.25
GL4	12.58	0.25
GL5	17.53	0.0625
BL2	10.16	0.25
GR1	3.34	0.0625
GR2	8.76	0.0625
GR3	5.18	0.0625
GR4	6.54	0.25
GR5	18.76	0.5
GR6	9.22	0.5
GR7	18.78	0.25

Table 3. Impact samples.

Three thermal loading techniques were performed to assess the nature of the impact damage. First, the Bales Scientific TIP was used to scan the back of each specimen as heat was applied, with a hot air gun to their front face. The front face was not scanned due the presence of markings that had been used to identify the specimens and locate their impact point. These marking would have biased the interpretation of the impact location and size. The specimens were positioned 6 inches from the face of the camera and the same image size used for each scan so that a direct comparison of the thermographically measured flaw sizes could be made. A DOS *.TIF image of each thermally loaded specimen was saved in "repeat all" color format and then printed on an EPSON color printer (Figures 13a and 13b). The flaw size of each image was measured and normalized from the "TIF" images for the subsequent comparison with impact energy. Several of the specimens experienced large scale delaminations due to their small size, the brittle nature of the graphite/phenolic material and the large magnitude of some of the impact energies. Ply splitting could be seen on the edge of specimen GL4, GR5 and GR7 while specimen GL5 broke into two pieces as a result of the impact. The remaining specimens showed varying degrees of surface damage from the impact test but no evidence of edge splitting.

With exception to the specimens that showed gross interlaminar splitting, the delamination zones had fairly clear boundaries similar to those made by inserting Teflon patches. The impact point of specimens GR5 and GR7 were barely noticeable in the thermographic image, instead the color maps were somewhat uniform indicating that the most of the specimen had suffered some degree of delamination. Specimen GL4 was not as severe damaged, but the delamination zone still extended to the edge of the sample. The color map of the impact damage for the remaining specimens were generally circular in shape, varying in size depending upon the damage level. The results shown in Figure 12 indicate that flaw size increases linearly with impact damage. The samples will have to be cross sectioned and photomicrographed to determine how well the thermographic images actually mapped the damage regions.

The thermographic images of the flaws produced as a result of the impacts appears to behave similarly to those produced by using Teflon inserts. That is, the defect shows up as a cold spot on the temperature map as heat is initially applied to the back side of the sample. Without a direct comparison though, it is impossible to draw any valid conclusions as to the acceptability of Teflon inserts for simulating defects.

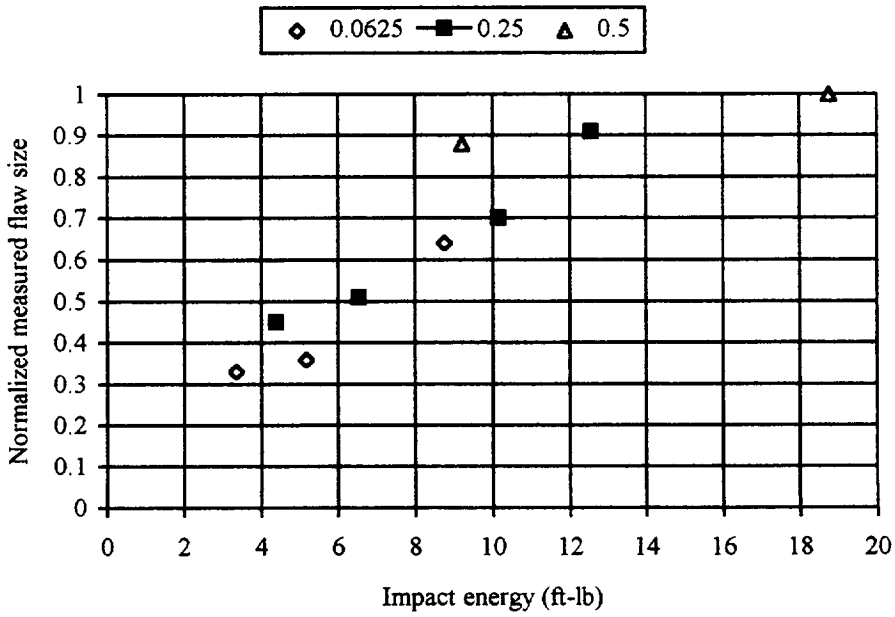

Figure 12. Flaw size versus impact energy.

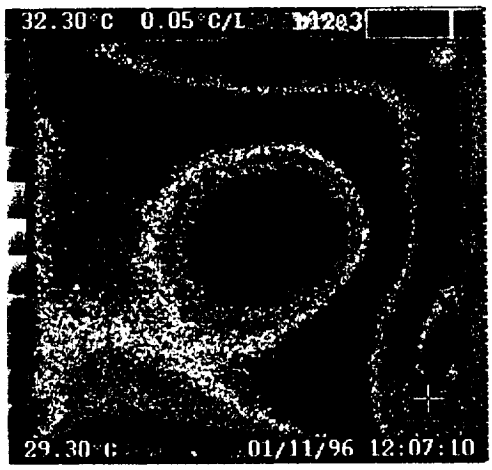

BL2 - 10.16 ft-lb

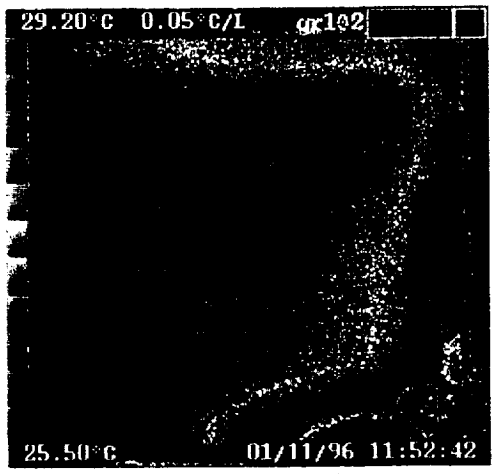

GR1 - 3.34 ft-lb

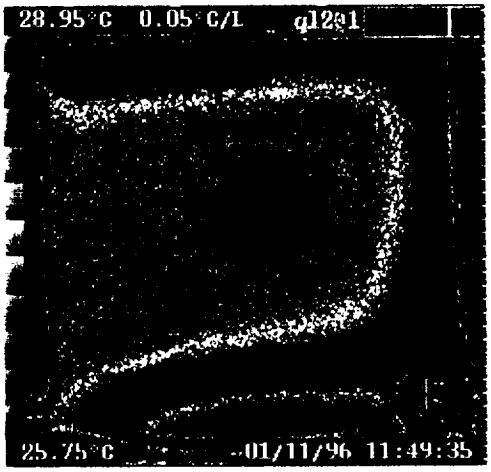

GL2 - 4.49 ft-lb

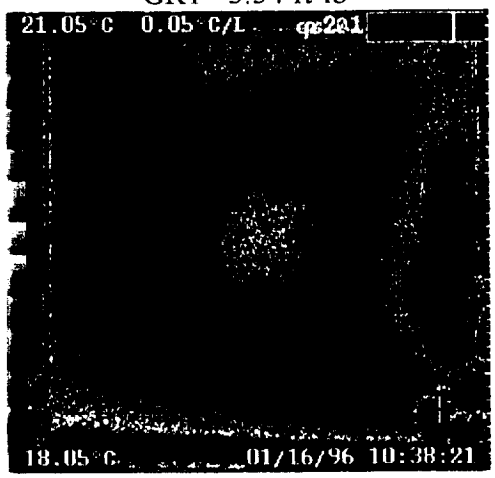

GR2 - 8.76 ft-lb

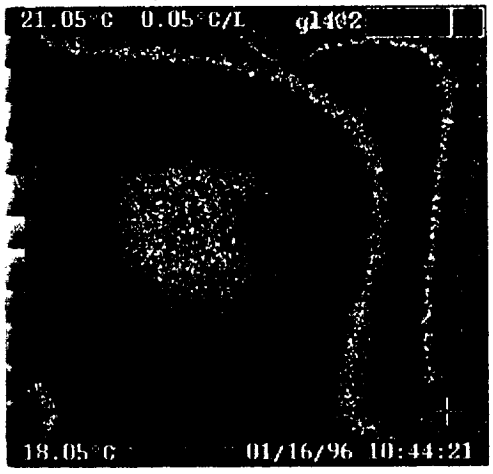

GL4 - 12.58 ft-lb

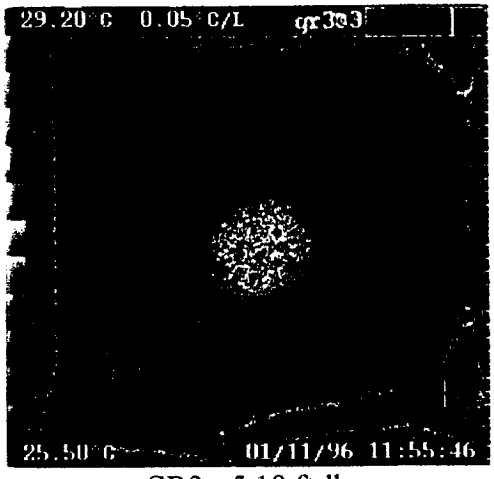

GR3 - 5.18 ft-lb

Figure 13a. Thermograms from impact specimens.

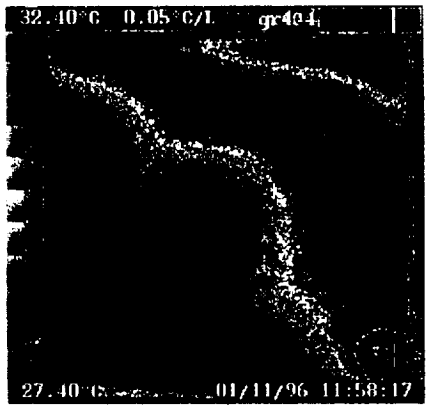

GR4 - 6.54 ft-lb

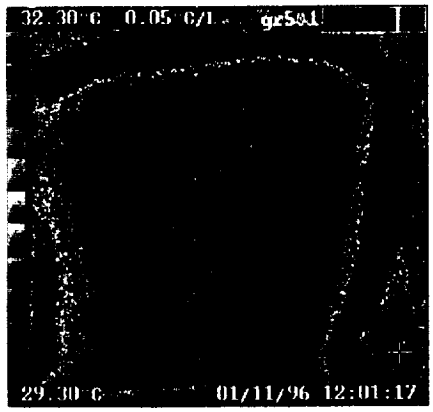

GR5 - 18.76 ft-lb

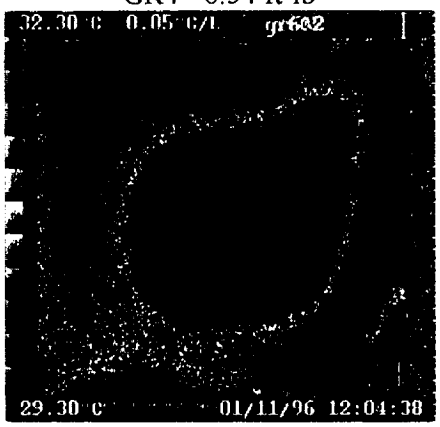

GR6 - 9.22 ft-lb

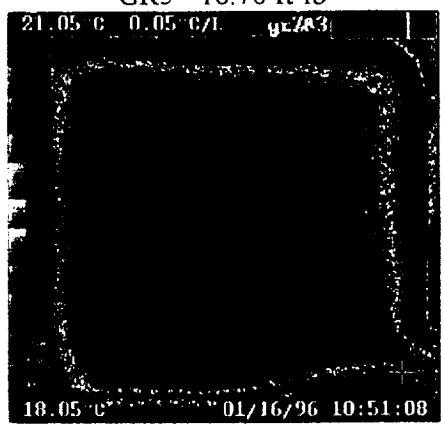

GR7 - 18.78 ft-lb

Figure 13b. Thermograms from imapct specimens (continued).

To better test how well the thermographic procedure used to inspect the nose cone would identify such an impact, two of the impact samples were clamped to the inside of a cut out region of the NPU-3 and inspected. Figure 14 shows the thermal image from that test. It is clearly evident that the inspection process is capable of identifying impact related damage and that the scheduled Teflon insert defects do to some degree behave thermographically as artificial impact damage.

Figure 14. Impact coupons in NPU-3.

Finally, front surface flash heating of the coupons was used to demonstrate it potential for future inspection of nose cone structures (Figure 15).

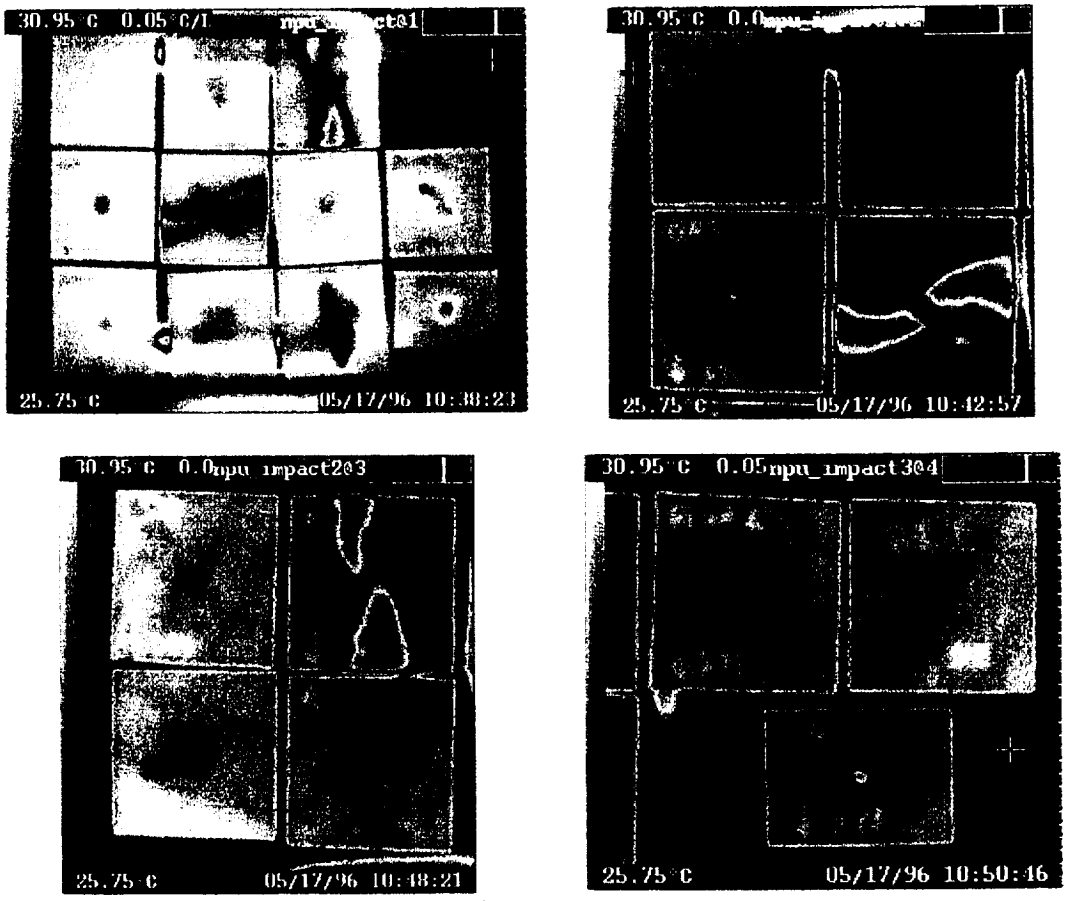

Figure 15. Flash heating of impact samples.

4.0 INTER TANK PANELS

The thermographic inspection of 10, eighty inch by forty inch, curved graphite/epoxy inter tank panels are now discussed. A Bales Scientific Thermal Image Processor positioned 64 inches from the panel was used to scan the panel in 10 passes (5 front and 5 back). The top and bottom of the panel, where the front and back faces merge, were scanned independent of the middle honeycomb section to avoid large variations in the thermal profile that would have made the images hard to interpret. Two 500 W heat lamps, mounted end to end, were held 1 to 2 inches from the back surface of the panel to provide the required thermal excitation. The panel was hand scanned from left to right facing rear surface with an overlapping semicircular motion covering the region of interest.

A test panel featuring many built in defects, 17 of which were visible as surface discontinuities and are labeled as A through Q, is shown in Figure 16 was inspected first to determine the proper settings for the thermal NDE of the 9 production panels..

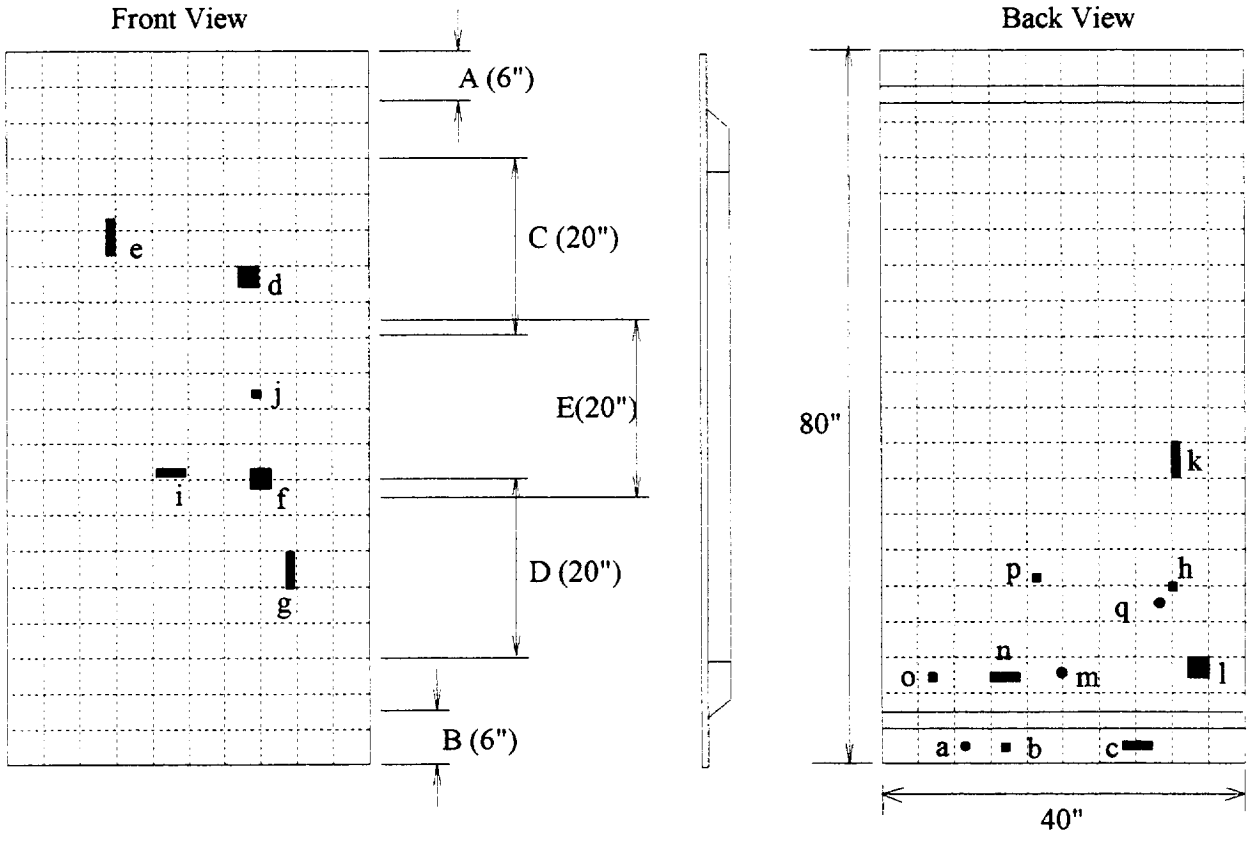

Figure 16. Panel configuration.

The color map was set to "repeat all" for each of the images to provide the best resolution for the entire image field. Since, the panel was scanned over a period of about 15 seconds, if the color map had not been set to "repeat all" the temperature range would have had to be set much larger to encompass the hot region directly behind the heat source and the cold region where heat had not been applied. Otherwise, only a small band of the image would have been legible on the color map.

The three flaws labeled A, B and C were viewed from both the front side scan, Figures 17 and 18, and the back side scan, Figure 28. Flaws A and B resembled their surface features, but flaw C showed up as a large circle, not the rectangular shape of the surface feature, indicating the possibility that other flaws were embedded deeper into the panel.

Flaws D and E showed up clearly on pass "C" as shown in Figures 19 and 20. When the flaws were positioned on the heat side of the panel for the back scan neither one was visible to the thermographic system.

Pass "D" yielded many flaws including F, G, H, I and Q shown in Figures 21 and 22. A better indication of the shapes of flaws F and I were found in pass "E" where Figure 24 clearly shows flaw F as a square and flaw I as a rectangle. It also appears that another vertical rectangular shape is present below flaw I. The back surface flaws, H and Q show up as a single indication in Figure 22 due to their heat signatures being smeared by the front surface of the panel.

Besides flaws F and I, pass "E" was able to locate flaw J in Figure 23.

The panel was reversed so that the back surface flaws could be more readily detected. When the center of the panel was scanned, pass "ER", flaws F, J and K were found, Figures 25 and 26. Note that flaws J and F were found as surface features on the front side of the panel.

During pass "BR" flaws A, B and C were again apparent, Figure 28, but this time flaws L, M, N and O were also visible (Figures 27 and 28). Figures 29 and 30 show that during pass "DR", flaws L, M and N were again visible.

Finally, during pass "DR" the two small flaws labeled H and Q were made identifiable as shown in Figure 29. Flaw P also showed up very lightly on Figure 30.

A long rectangular feature extending nearly half way across the panel was found during pass "AR" that was not apparent on the surface of the panel (Figure 31). Without any knowledge of the make-up of the panel in that region it is hard to tell if this is a defect or not. Since, a similar feature was not found on the other end of the panel during pass "B" or "BR" it is suspicious.

The 9 production unit inter tank panels were inspected in a similar fashion to the test panel. The thermograms for the production panels are give in Appendix 12.5. No major indications were found on the production panels.

Figure 17. Flaws A and B viewed from pass B.

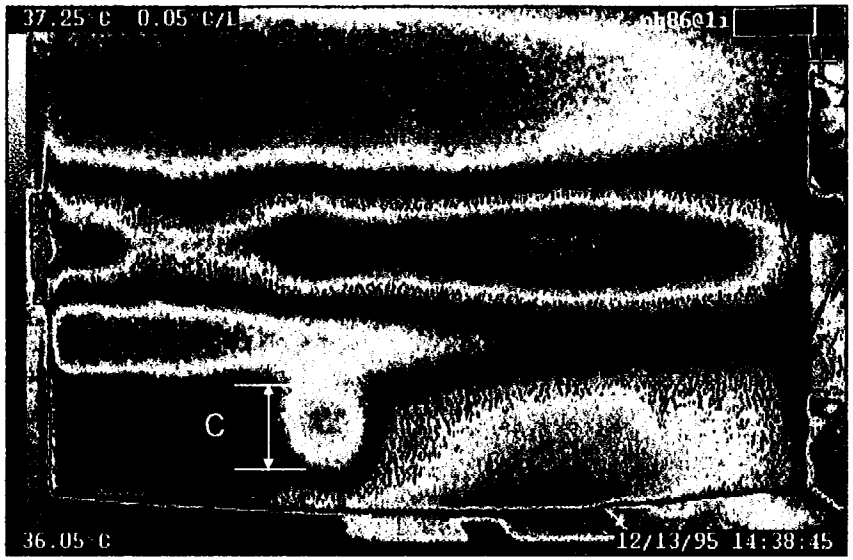

Figure 18. Flaw C viewed from pass B.

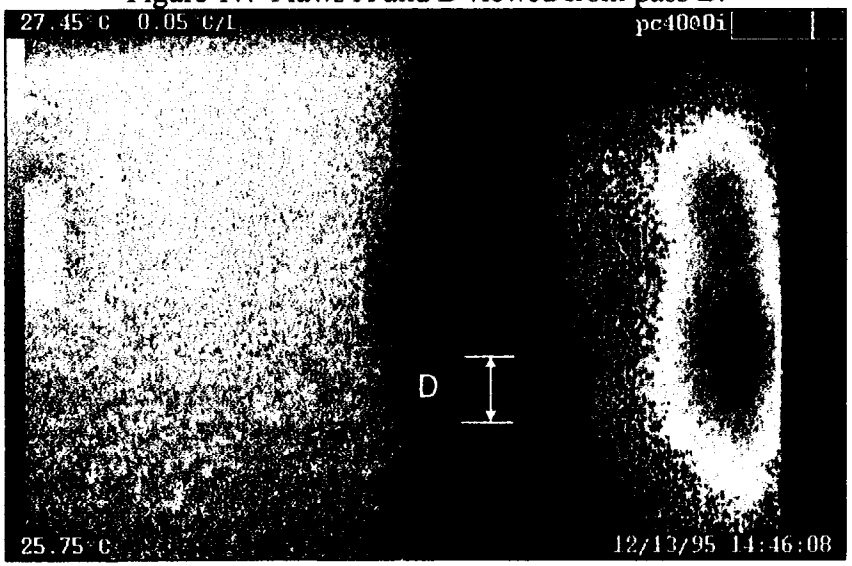

Figure 19. Flaw D viewed from pass C.

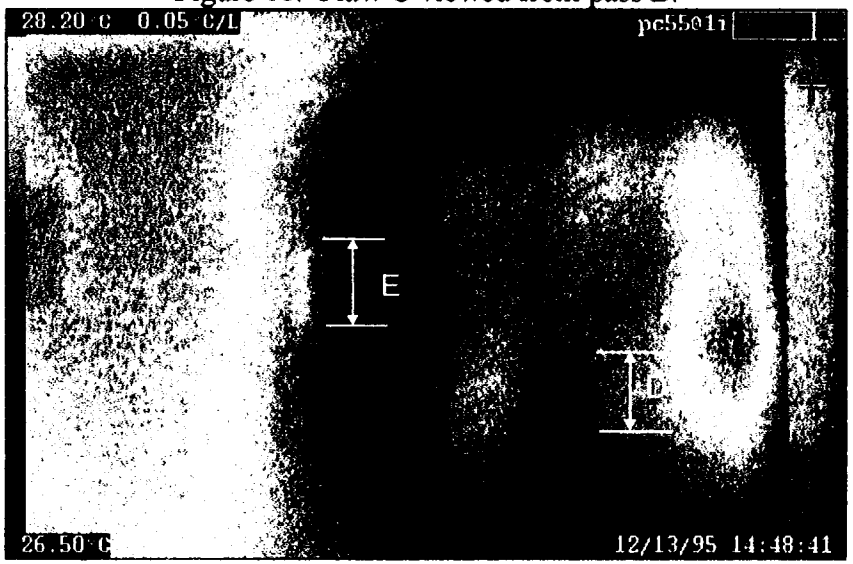

Figure 20. Flaws D and E viewed from pass C.

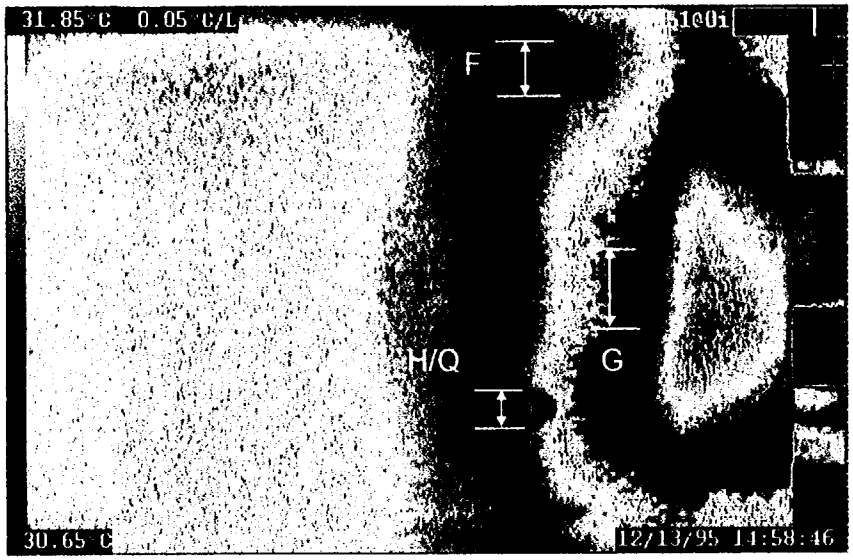

Figure 21. Flaws F, G, H and Q viewed from pass D.

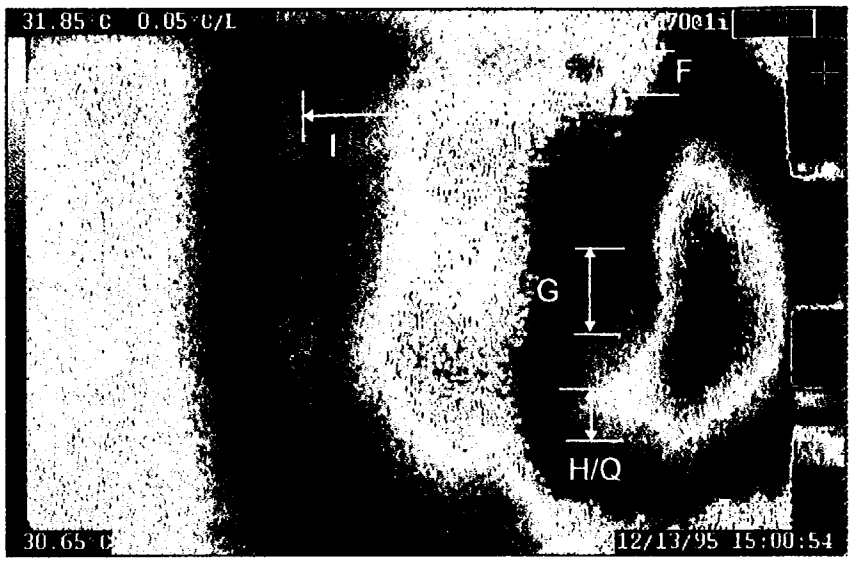

Figure 22. Flaws F, G, I, H and Q viewed from pass D.

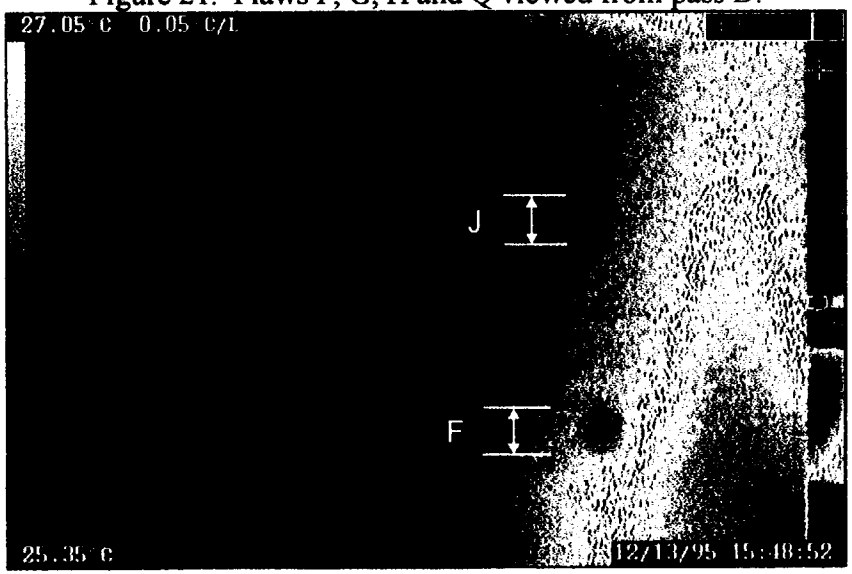

Figure 23. Flaws J and F viewed from pass E.

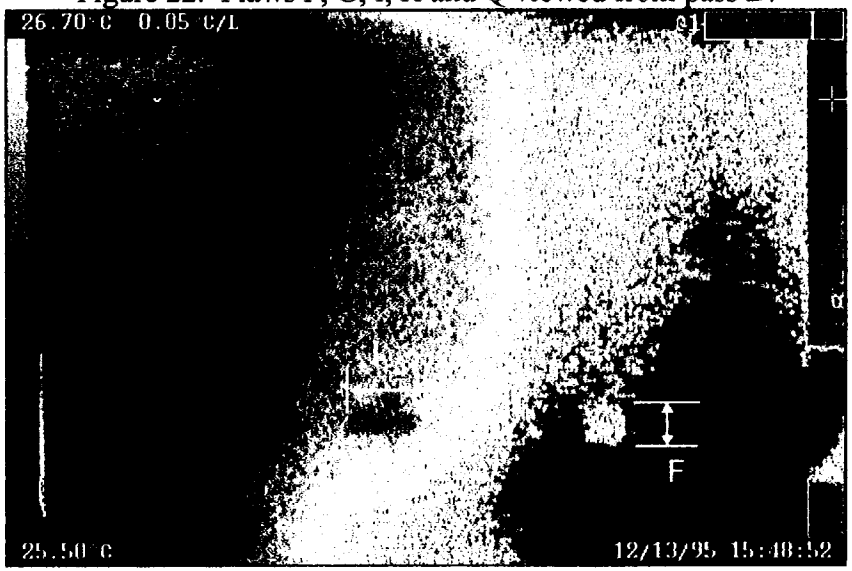

Figure 24. Flaws F and I viewed from pass E.

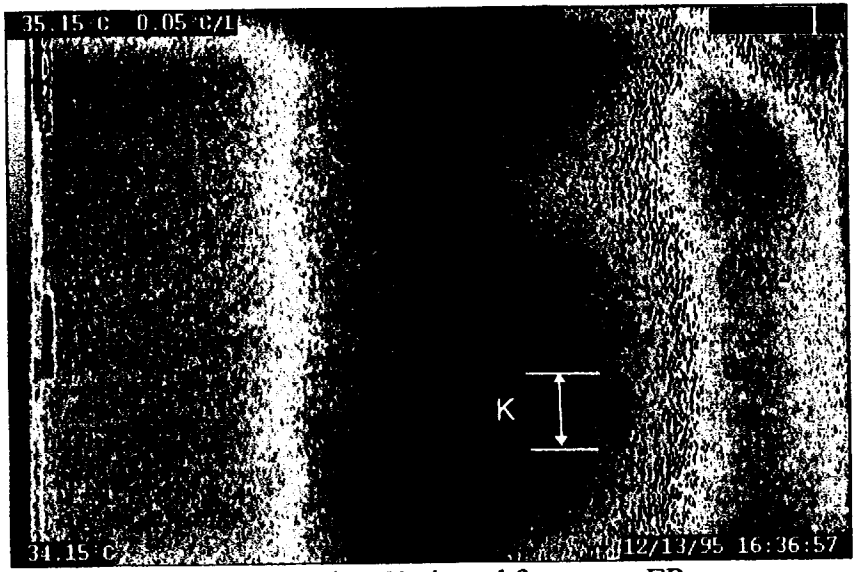

Figure 25. Flaw K viewed from pass ER.

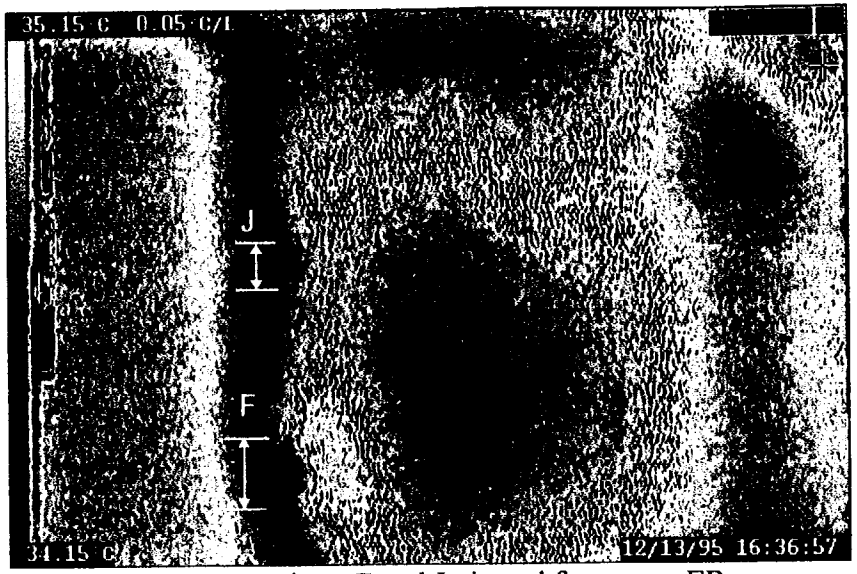

Figure 26. Flaws F and J viewed from pass ER.

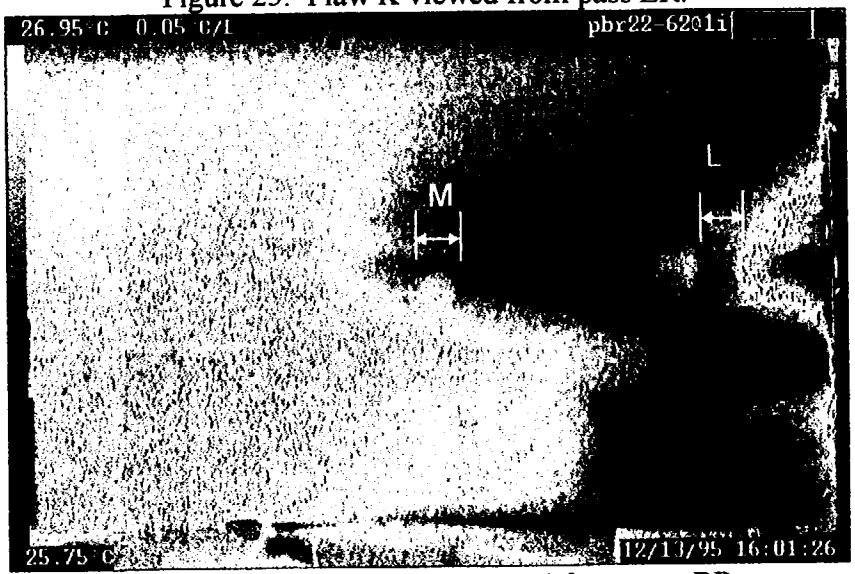

Figure 27. Flaws M and L viewed from pass BR.

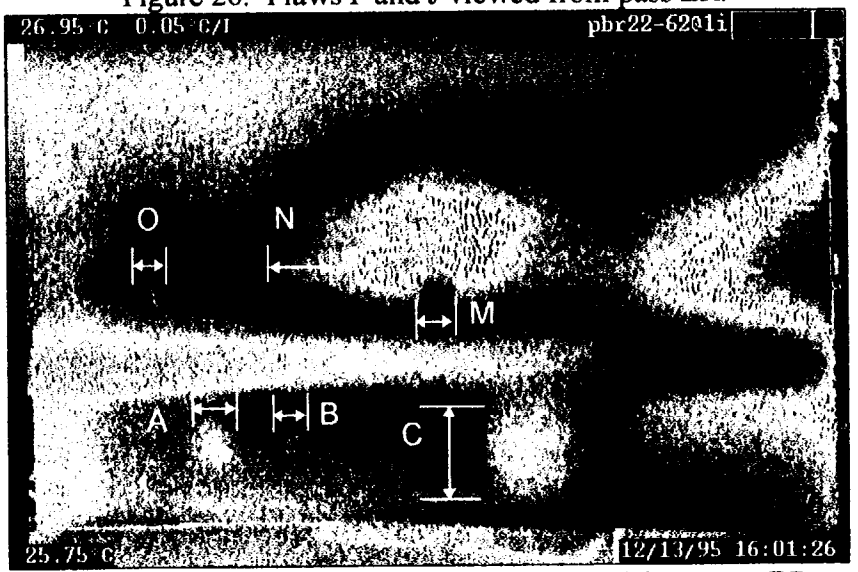

Figure 28. Flaws A, B, C, O, M and N viewed from pass BR.

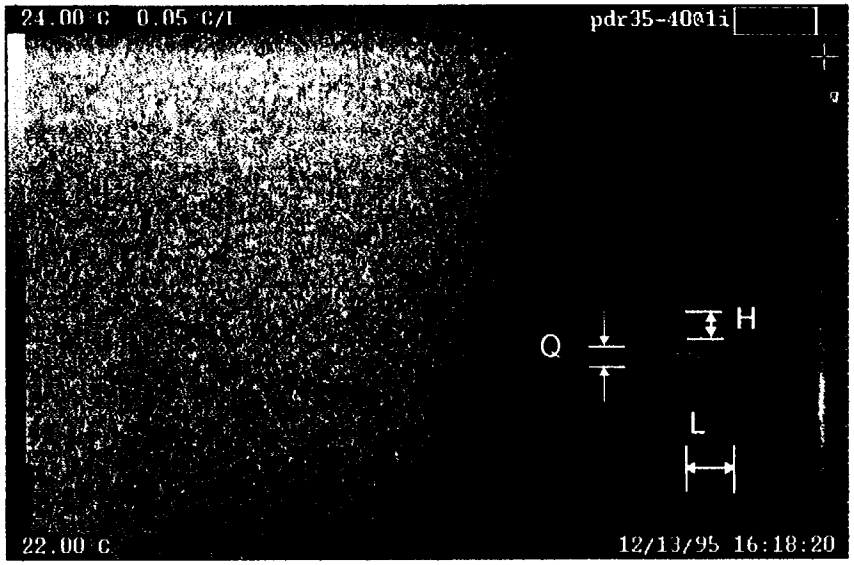

Figure 29. Flaws H, L and Q viewed from pass DR.

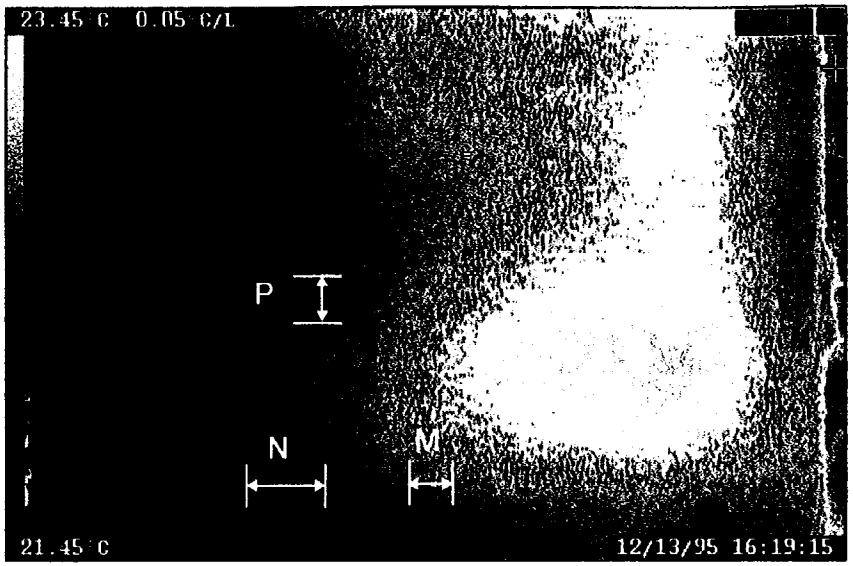

Figure 30. Flaws N, M and P viewed from pass DR.

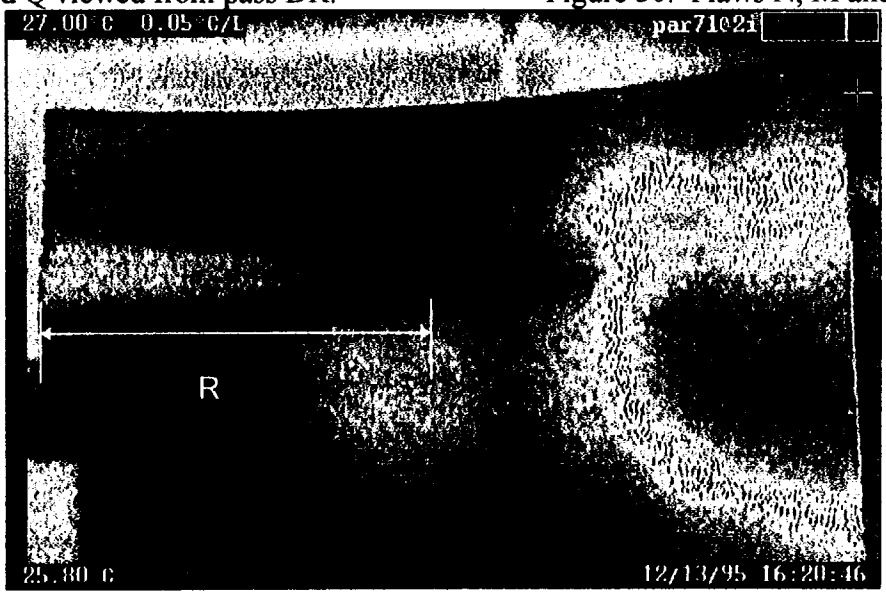

Figure 31. Scan "AR".

5.0 EXTERNAL TANK NOSE CONE

5.1 Non Production Unit 3

The thermographic inspection of the non production unit three (NPU-3) composite nose cone for the space shuttle external tank is described in this section. The NPU-3 was manufactured with embedded flaws (Teflon inserts) to provide a test base and qualification unit for nondestructive evaluation techniques. The purpose of this test was to investigate the potential of the Bales Scientific thermography camera and software. By running the Bales camera along side the Lockheed-Martin thermography system a comparison could be made as to its delectability.

The results presented herein are from the first inspection of the NPU-3 nose cone and were conducted as a "tag along" to the Lockheed-Martin inspection. No attempt was made to optimize the heating of the nose cone or general configuration of the Bales system for these tests.

The NPU-3 nose cone was thermographically mapped in 13 passes. The first four passes (Figure 32) were conducted using a the Lockheed-Martin composite nose cone turntable and A-frame. A 2000 watt heat lamp was positioned on the inside of the inverted nose cone, four inched from its surface, over the area to be scanned. The Bales Scientific thermographic camera was positioned on the outside of the nose cone, 90 degrees down stream of the heat lamp and kept as near to normal with the outer surface of the nose cone as possible.

The spike attachment end was inspected by hand scanning the heat lamps over the outside of the nose cone (Figure 33). Here, the thermographic camera imaged the inside of the nose cone.

The faring region was mapped in seven passes as shown in Figure 34. The heat was again applied by hand using the 2000 W heat lamps, this time on the inside of the faring. The camera was maintained at a position normal to the area of interest at a distance of approximately 55 inches.

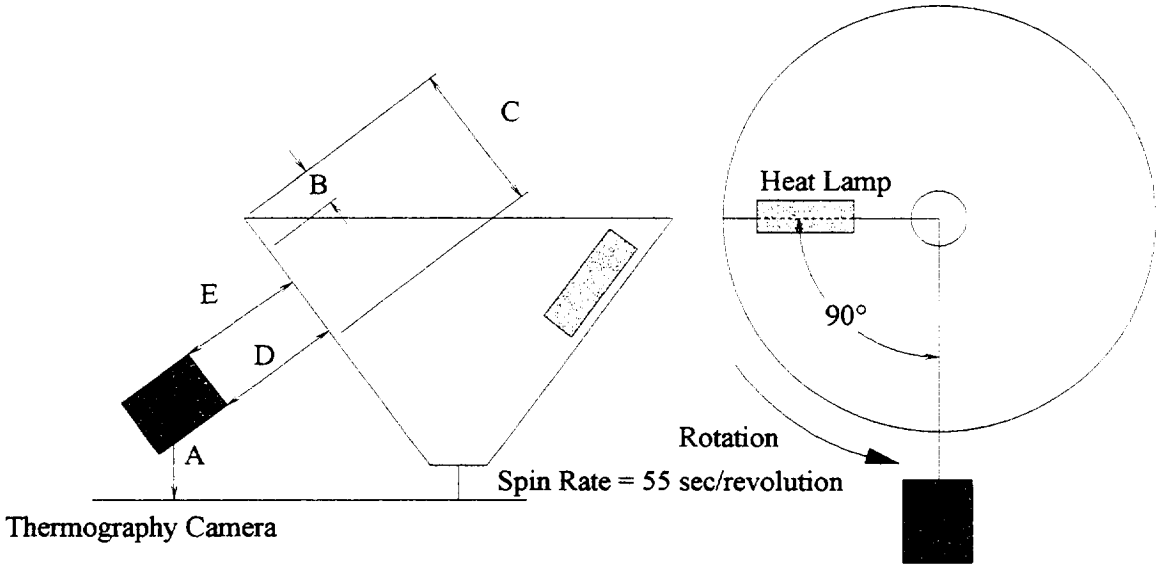

	Dimension (inches)				
Filename	A	B	C	D	E
NP3_A	22	4	16	38	38
NP3_B	19.5	24	36	42	37
NP3_C	36	0	6	28	27
NP3_D	19.5	14	26	43	40

Note: Images taken at 1 second/frame for 60 seconds.

Figure 32. Configuration for pass A through D.

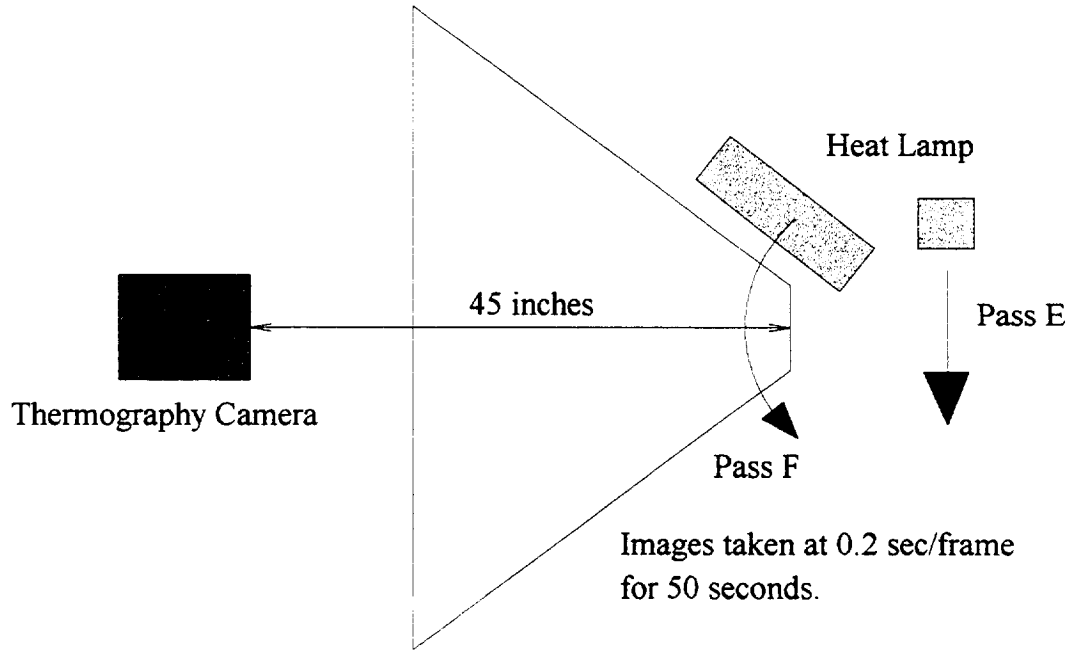

Figure 33. Configuration for passes E and F.

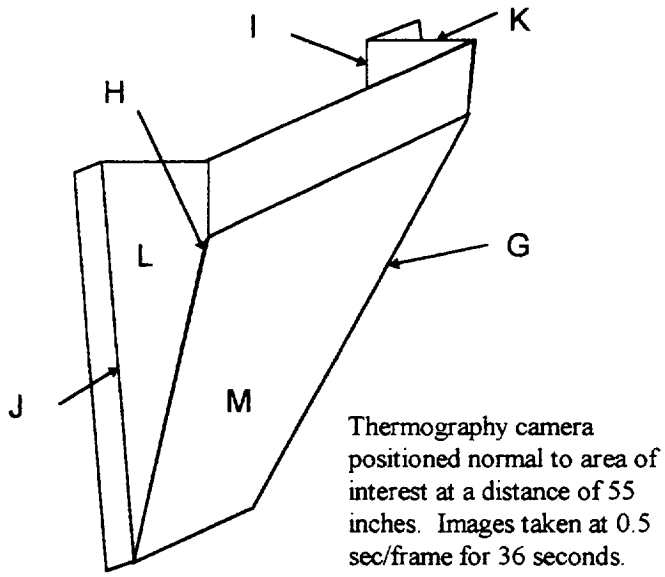

Figure 34. Configuration for passes I through M.

The Bales system was able to capture nearly all of the flaws that the Lockheed-Martin detected. By allowing overlap between scans, flaws could be more easily isolated from background thermal noises caused by variations in the thickness and heating of the nose cone.

Six of the seven flaws imaged during pass A, could also be seen in pass C including flaws A, B, C, E, F and G. During pass B and M, the two inserts located at the end of the faring were detected and labeled flaws H and I. Five flaws were found during the scan of the top portion of the nose cone, labeled J, K, L, M and N. During pass D, flaw "N" was again detected along with the inserts in the corner radius of the faring. These inserts, O, P, Q and R were also visible during the hand scans conducted as passes I and J.

Finally, the defects located in the spike attachment point were imaged during passes E and F. The defects were in such close proximity to each other that it was difficult to distinguish between the individual inserts. This problem was compounded by the extra thickness of material and inability to get the camera in close enough to the region to provide adequate spatial resolution. Figures 56 through 58 clearly show that flaws are present by the highly distorted heat pattern, but identification of individual inserts is difficult.

Overall, the results of this test show that the Bales thermographic inspection system is capable of inspecting the composite nose cone. Work will have to be done though to optimize the heating and field of view of the system to capture all critical flaws with a degree of confidence.

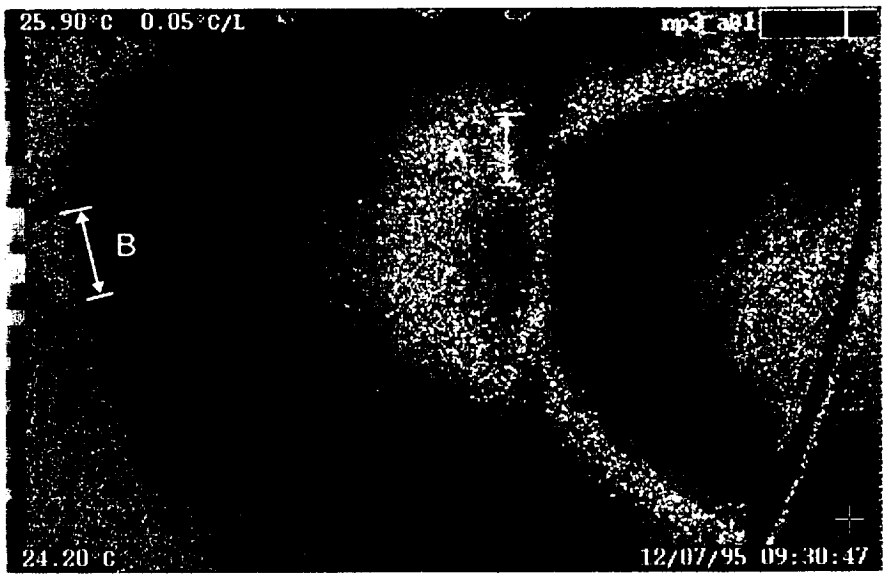

Figure 35. NPU-3, Pass A, Flaws A and B.

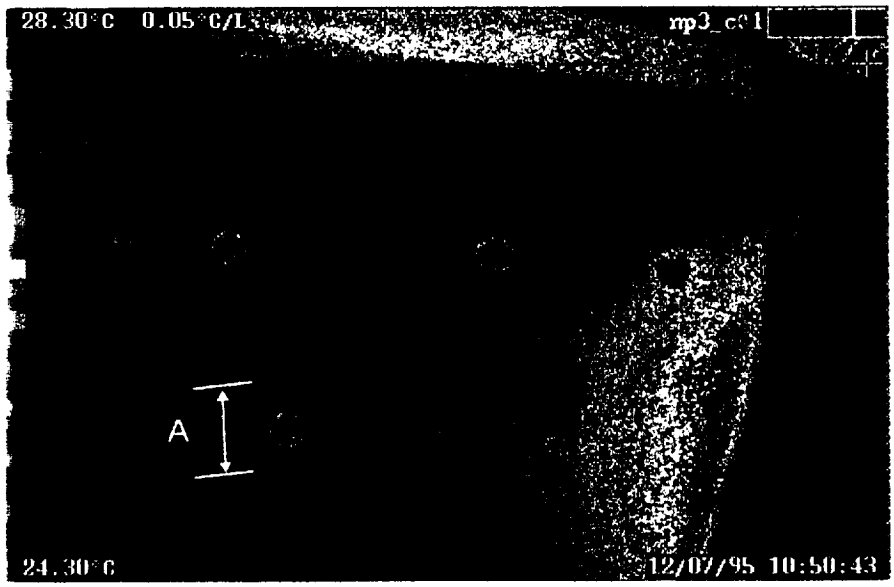

Figure 36. NPU-3, Pass C, Flaw A.

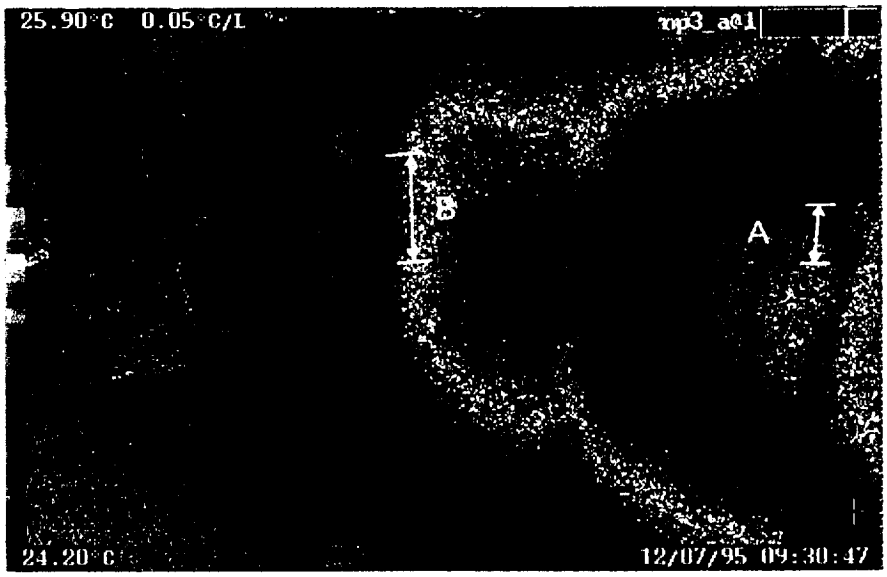

Figure 37. NPU-3, Pass A, Flaws B and A.

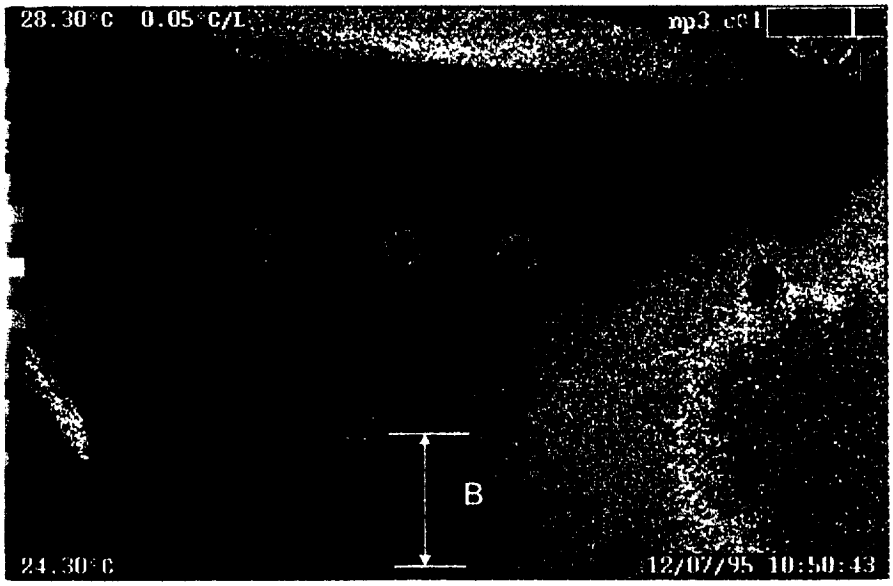

Figure 38. NPU-3, Pass C, Flaw B.

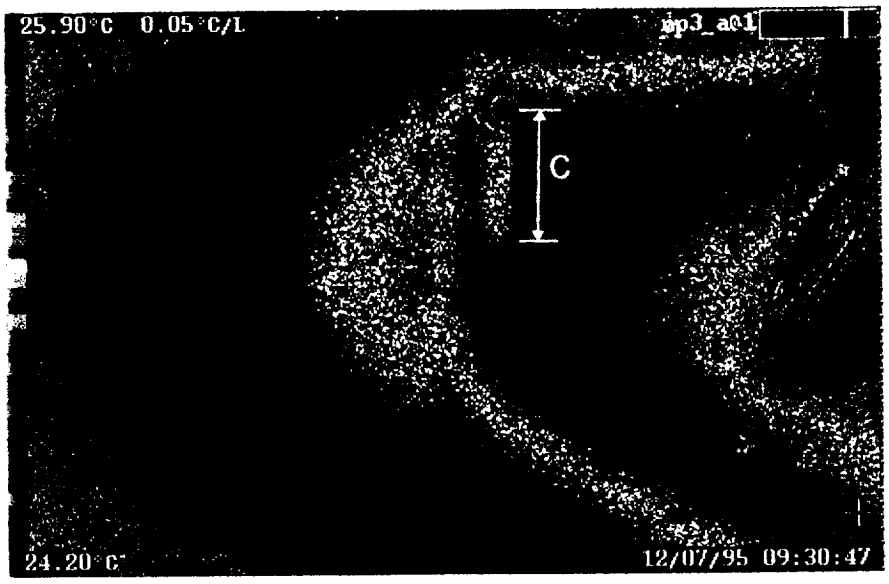

Figure 39. NPU-3, Pass A, Flaw C.

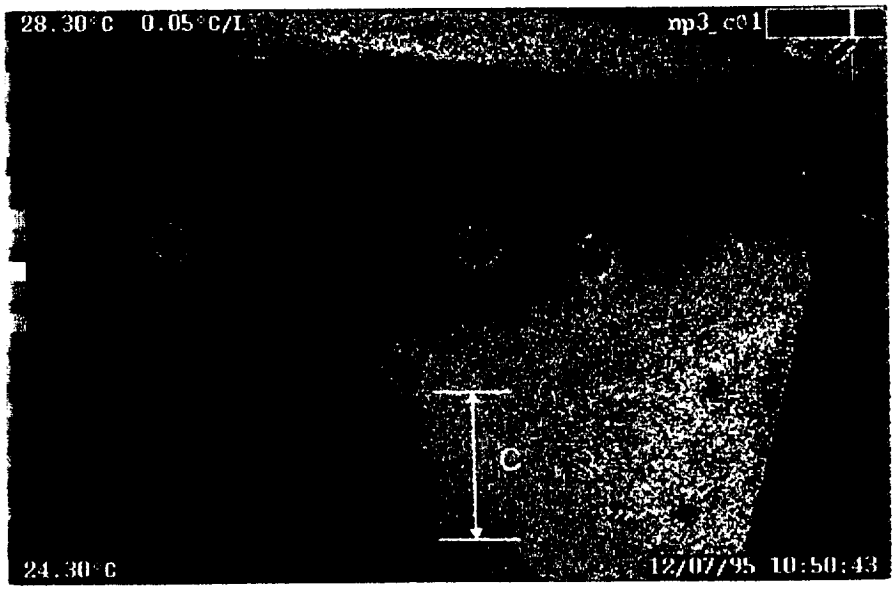

Figure 40. NPU-3, Pass C, Flaw C.

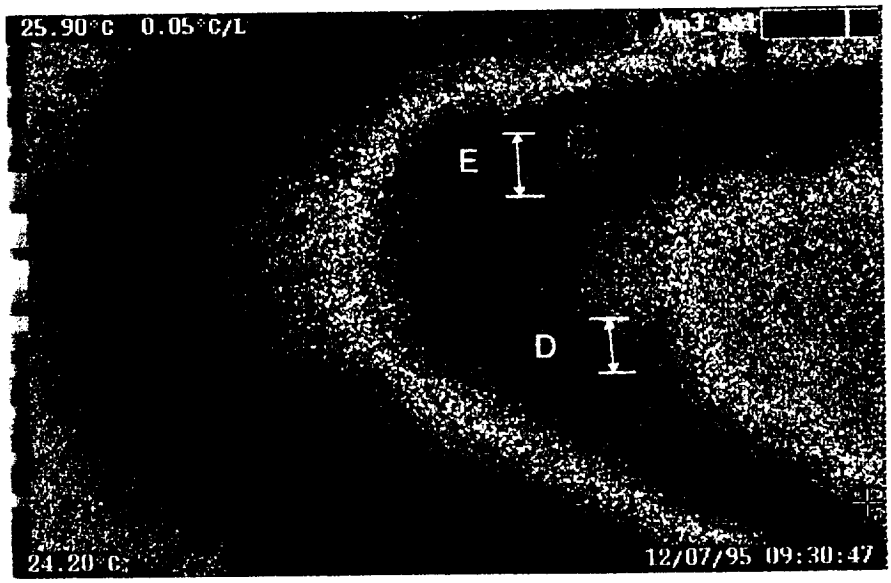

Figure 41. NPU-3, Pass A, Flaws D and E.

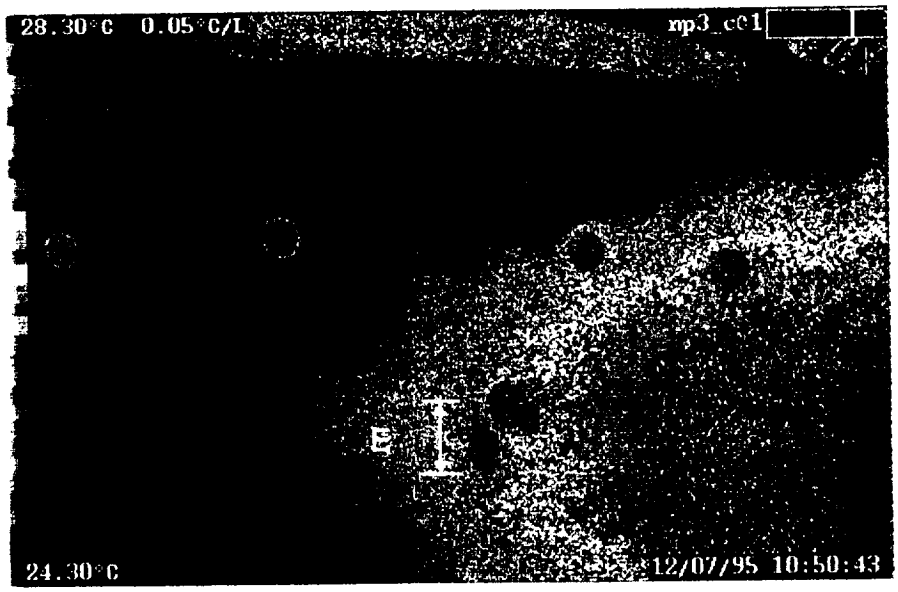

Figure 42. NPU-3, Pass C, Flaw E.

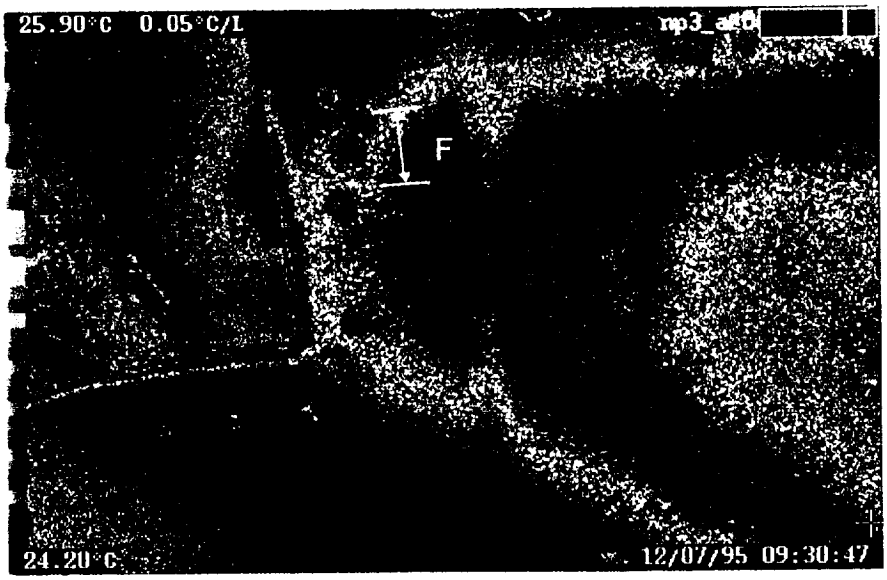

Figure 43. NPU-3, Pass A, Flaw F.

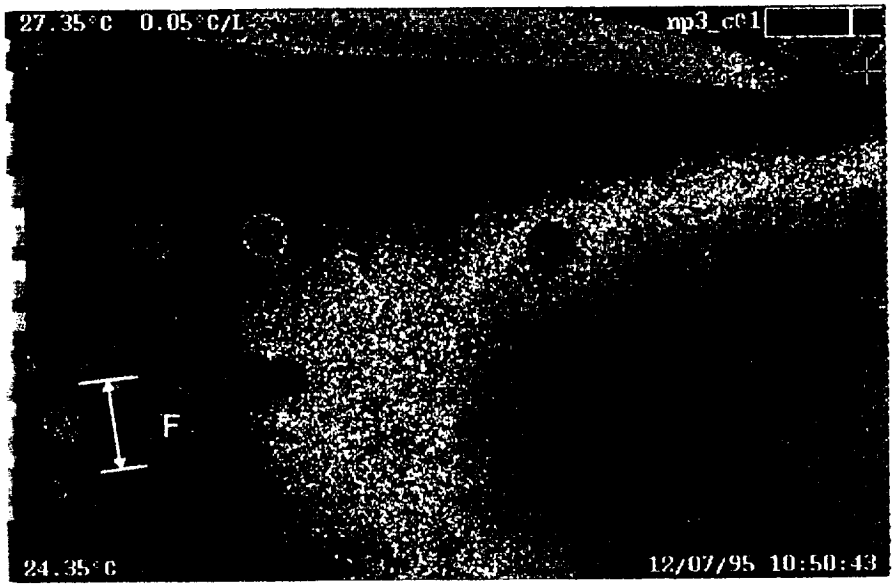

Figure 44. NPU-3, Pass C, Flaw F.

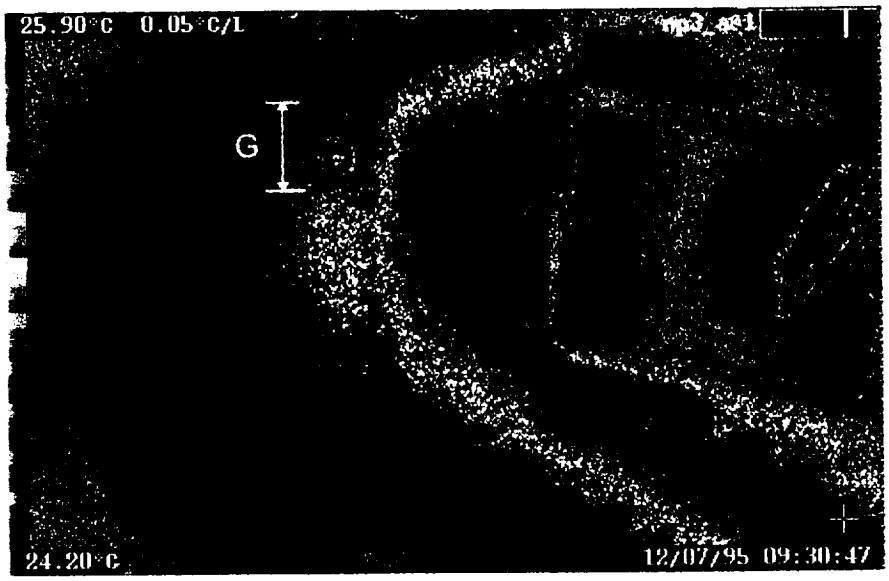

Figure 45. NPU-3, Pass A, Flaw G.

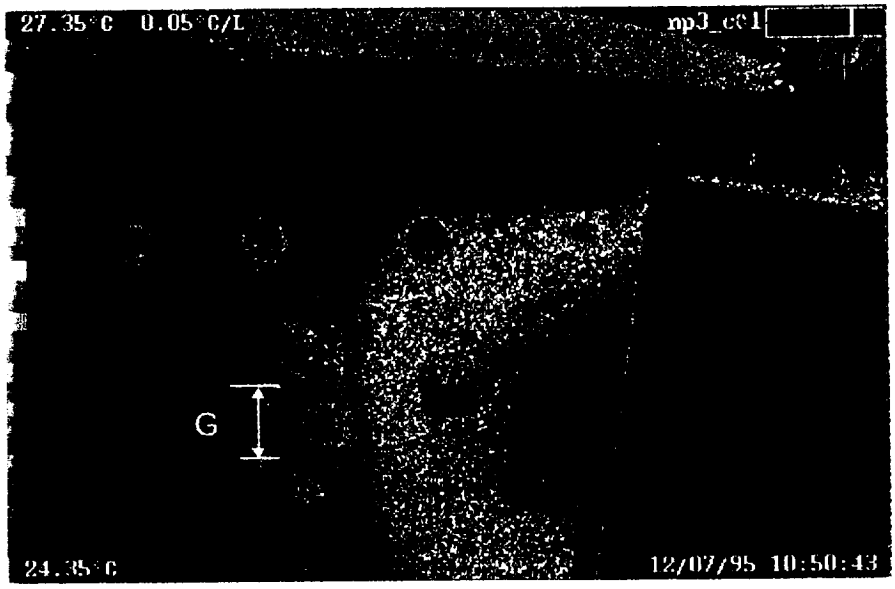

Figure 46. NPU-3, Pass C, Flaw G.

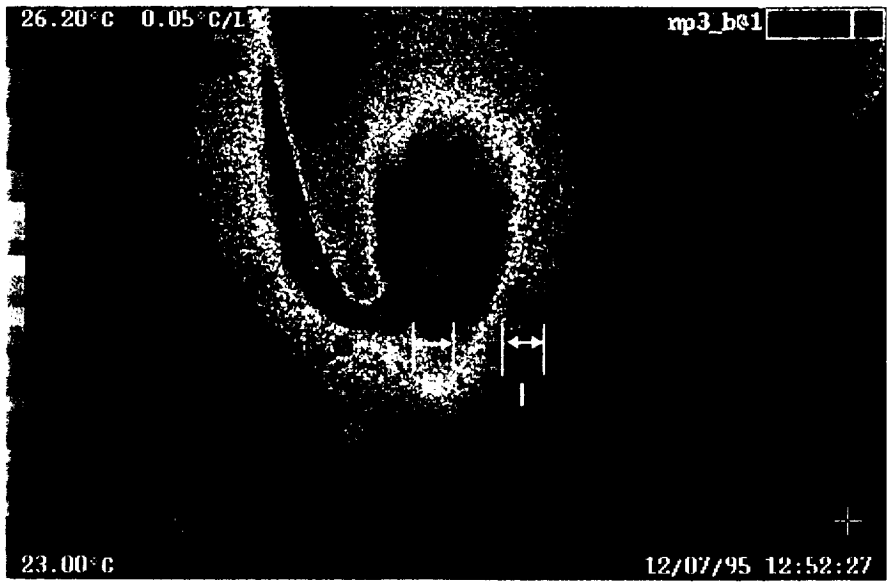

Figure 47. NPU-3, Pass B, Flaws H and I.

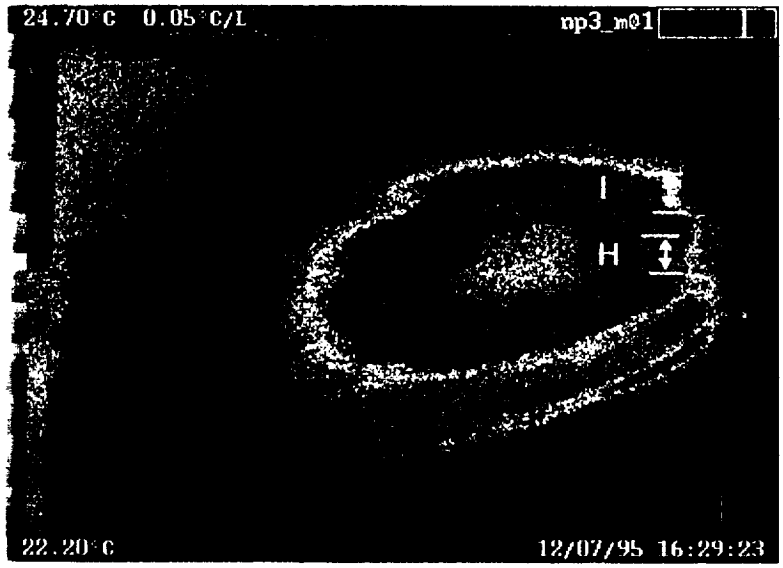

Figure 48. NPU-3, Pass M, Flaws H and I.

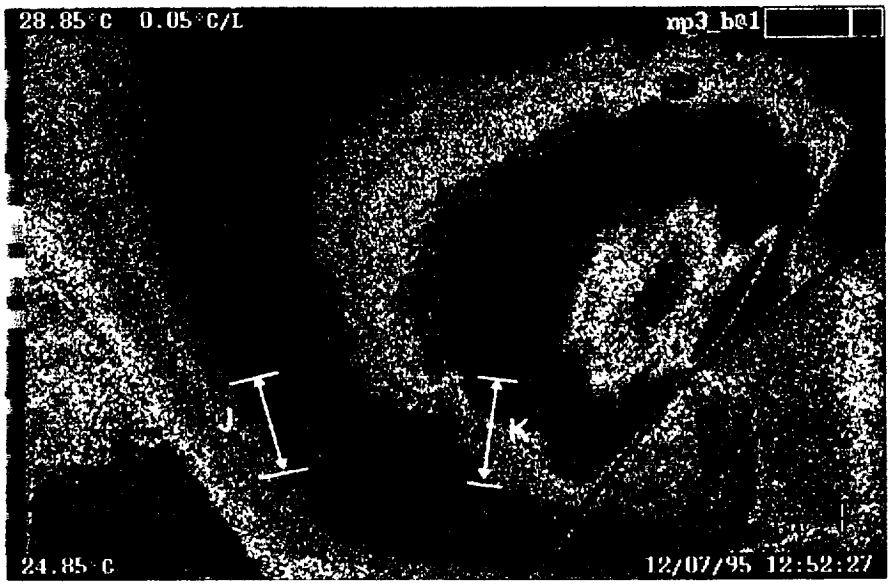

Figure 49. NPU-3, Pass B, Flaws J and K.

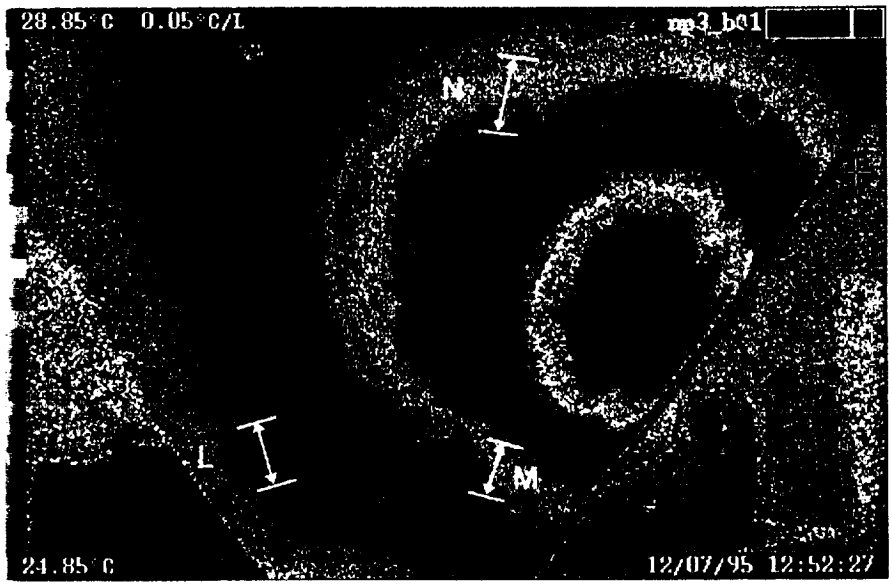

Figure 50. NPU-3, Pass B, Flaws L, M and N.

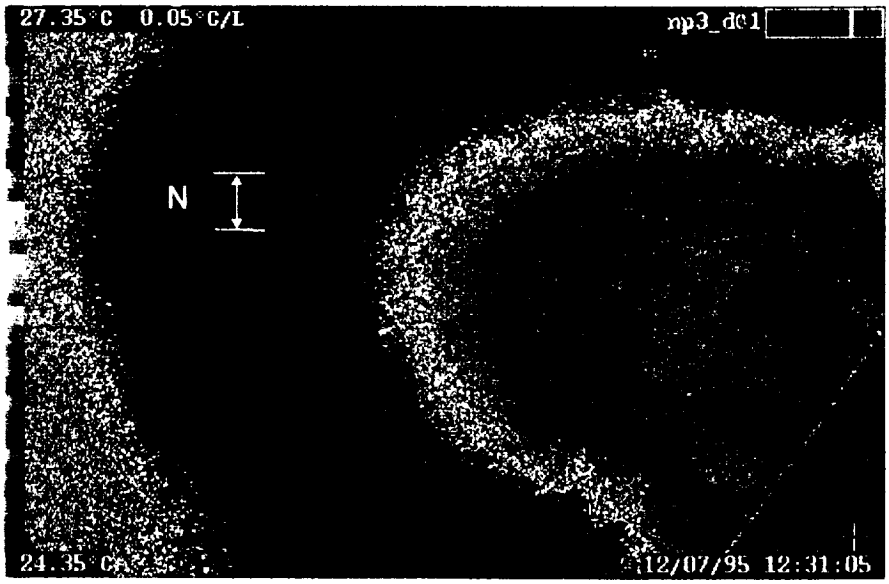

Figure 51. NPU-3, Pass D, Flaw N.

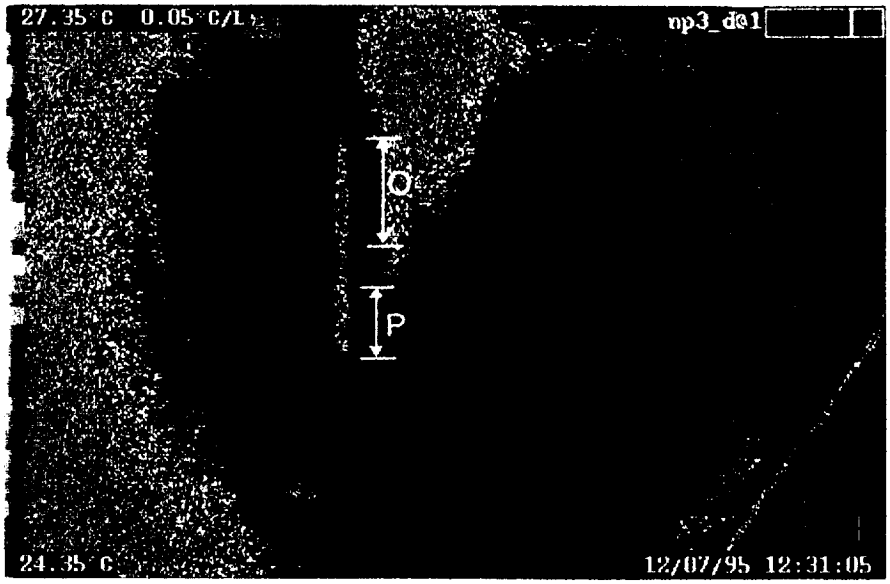

Figure 52. NPU-3, Pass D, Flaws O and P.

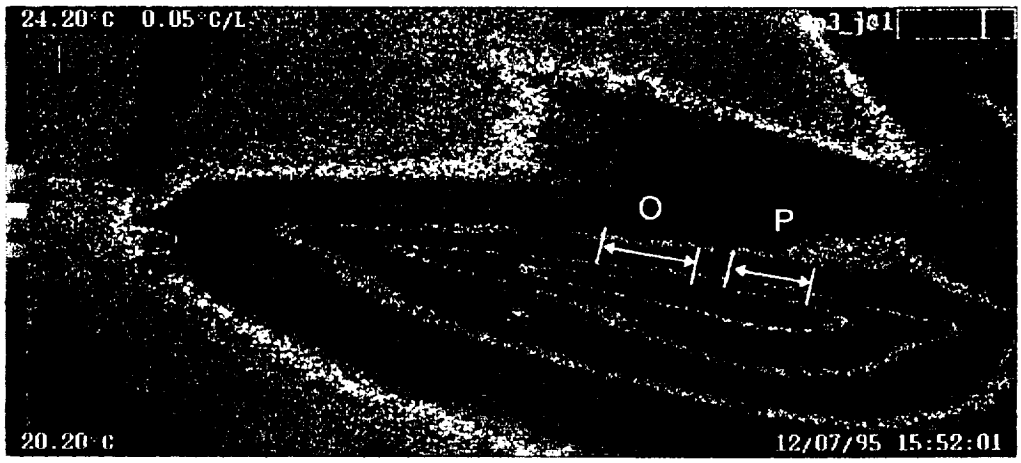

Figure 53. NPU-3, Pass J, Flaws O and P.

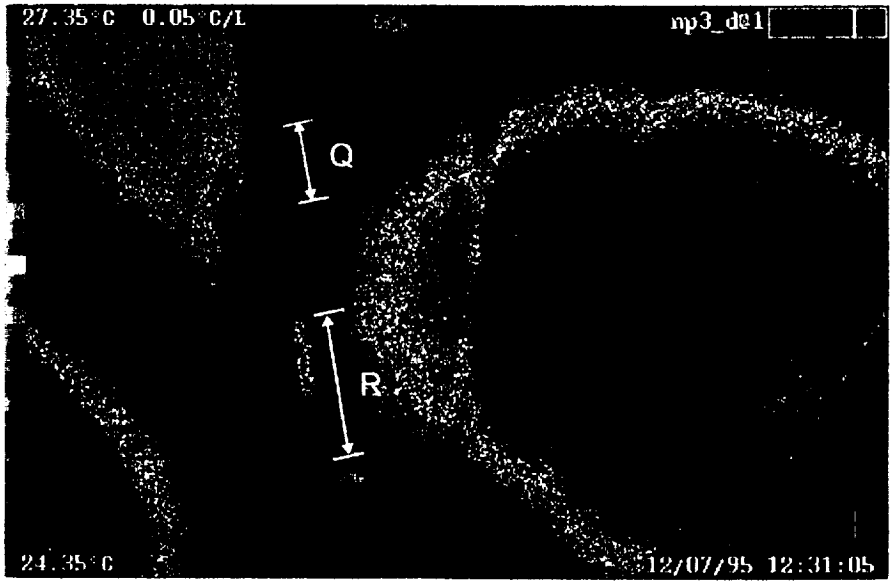

Figure 54. NPU-3, Pass D, Flaws Q and R.

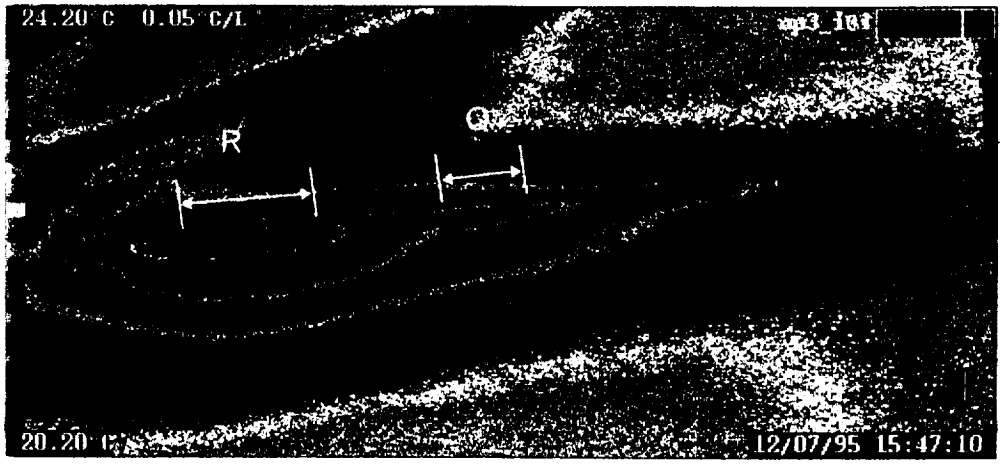

Figure 55. NPU-3, Pass I, Flaws Q and R.

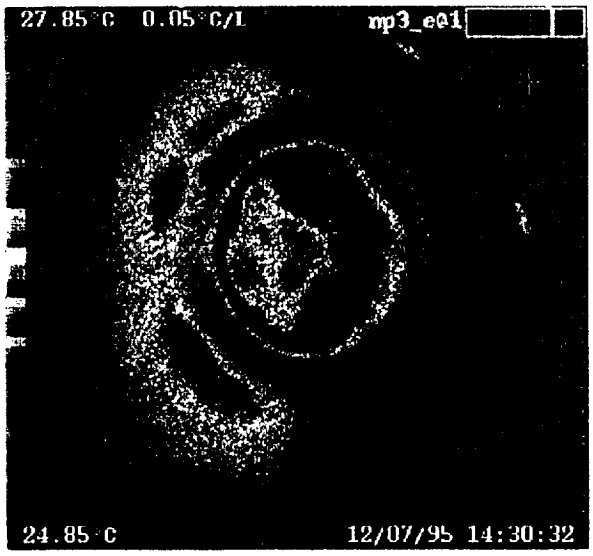

Figure 56. NPU-3, Pass E.

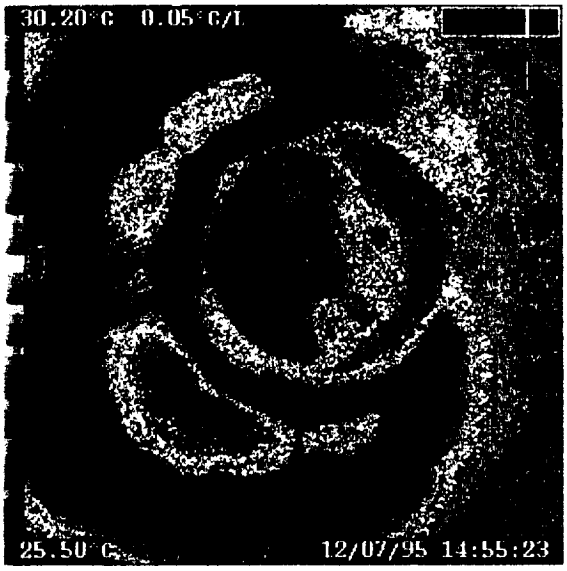

Figure 57. NPU-3, Pass F.

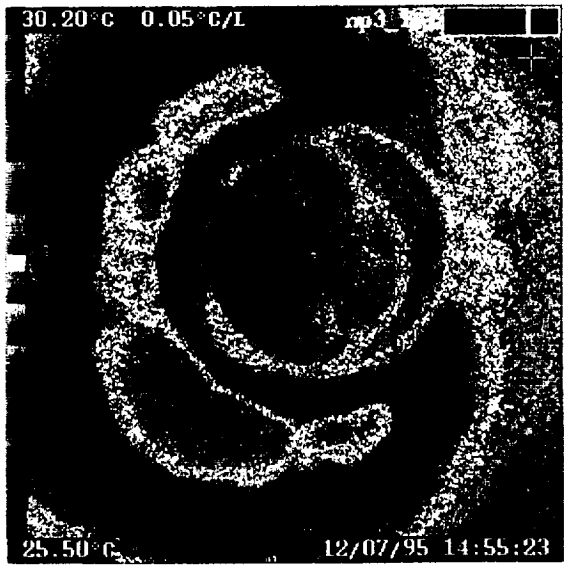

Figure 58. NPU-3, Pass F.

5.2 Flight Unit 1 (Pre machining)

The thermographic inspection of the first flight unit (F1) composite nose cone for the space shuttle external tank is described. The nose cone is in the untrimmed and predrilled state. The thermographic inspection process was qualified through the concurrent inspection of the NPU-3 nose cone, which features embedded critical sized defects (teflon inserts). The results presented herein are from the inspection of the F1 nose cone and were conducted as a "tag along" to the Lockheed-Martin inspection.

The same general procedures and equipment settings as described in Section 5.1 were utilized for the inspection of the F1 nose cone. The only variation between the two tests was that a 1 sec/frame acquisition rate was maintained throughout the entire series of "F1" scans. On the previous tests insufficient time had been given to scan the 24 ply region of the nose cone resulting in an incomplete temperature profile.

All scheduled defects were found during Pass A of the NPU-3 nose cone as shown in the Figures labeled NPU_A5, NPU_A13, NPU_A21, NPU_A28, NPU_A34, and NPU_A52 of Appendix 12.8. A question had arisen during the first test of the NPU-3 unit as to the validity of using teflon inserts for making simulated flaws. To answer this question specimens were cut from a section of a nose cone and impacted at various levels. Section 3.0 of this report demonstrates the sensitivity of thermography to map the effects of the impacts with energies ranging from 3.34 ft-lbs to 18.7 ft-lbs. To determine how well the nose cone qualification procedures would map the impact damage two of the specimens, GR-1 (3.34 ft-lb) and GR-6 (9.22 ft-lb), were clamped to the inside of the access holes of the NPU-3 unit and scanned. Figures NPU_A_IMPACT2 and 5 show that the thermographic inspection procedures are capable of detecting and discriminating between the two impact levels. Also, the magnitude of the indications for the impact specimens is of the same order as the teflon inserts.

The NPU-3 and F1 nose cones were swapped, after successfully locating all the scheduled flaws in the "B" pass of NPU-3, and the F1 unit scanned for defects. No flaws were found during the four passes made around the nose cone except for the seam lines (Figure F1_A and B) and thermocouple leads (Figure F1_C14 and 54).

5.3 Flight Unit 1 (F1) Nose Cone (Post machining)

This section describes the thermographic inspection of the F1 nose cone after being trimmed and drilled. The thermographic inspection process was qualified through the concurrent inspection of the NPU-3 nose cone, which features embedded critical sized defects (teflon inserts). The results presented herein are from the inspection of the F1 nose cone and were conducted again as a "tag along" to the Lockheed-Martin inspection.

The same general procedures and equipment settings as described in the previous two sebsections were utilized for the inspection of the machined F1 nose cone. The only modification to the process was that passes "E" and "F", over the 24 ply spike attach region, were combined into one pass.

After successfully locating all the scheduled flaws in pass "A" of NPU-3, the NPU-3 and F1 nose cones were swapped, and the F1 unit scanned for defects. No defects were found of the size or larger than those described by QA-NDE-001.

A tool had been dropped on the inside of the nose cone during the machining process that left a small visible mark. Special attention was given to Pass "D" since it would overlap the impact site. Based upon the thermographic results, the damage appears to be only superficial. The following figure shows the impact site as a small aberration along a seam line. A hand scan of the region, with higher magnification, also showed no thermal indications of delamination due to the impact. The remainder of the F1 nose cone showed no thermographic indications of damage.

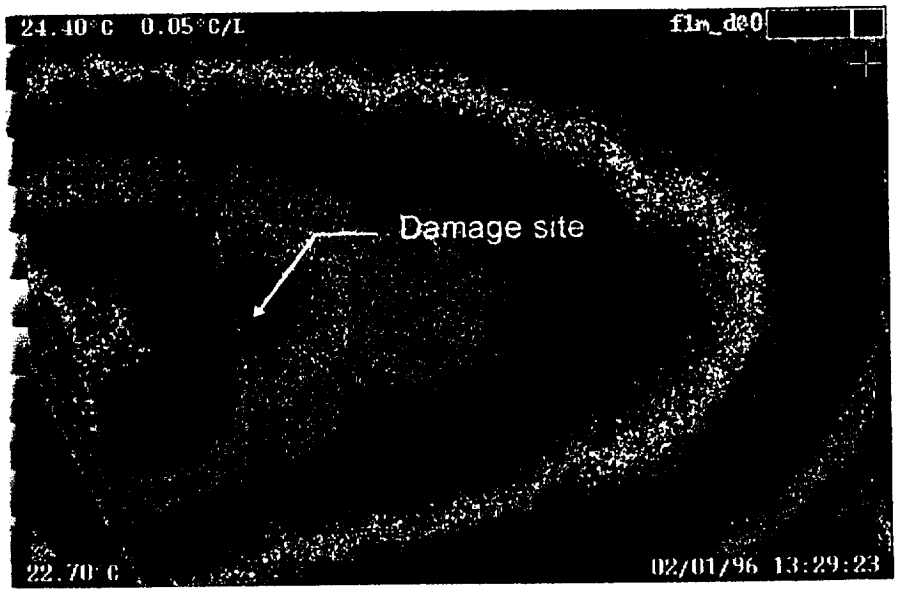

Figure 59. Thermogram of damage on nose cone F1.

6.0 HOT GAS PANELS

Two separate inspections were performed on graphite/polyimide hot gas panels. The first thermographic inspection of 6 graphite/polyimide panels was conducted at a distance of 32 inches during back side heating by two 500 W quartz heat lamps. The lamps were set 15 inches from the back surface of the panel and oriented to provide uniform heating for approximately 20 seconds. Both the tooling (shiny) side and the machined (dull) side of the panels were scanned to help enhance any features that may have been closer to one side of the panel than the other.

The results of the thermography tests before hot gas treatment showed no thermal abnormalities or indications that could be attributed to internal flaws in the panels. In all the thermograms were relatively uniform across the panels during the entire scan for both their front and rear face. The variations shown in the thermograms were simply a result of the heating method and boundary conditions.

A surface feature was found around the top middle hole of panel HG2B (T1-1B HG2) . The hole was scanned at a closer range showing that the flaw, a delamination, did not extend beyond what was visible.

After the hot gas treatment the panels were re-examined to determine the effects that the hot gas tests had on the integrity of the panels. All of the panels except for HG2A (T1-1A HG2) showed no indications except for the small delamination that was already present with the top hole in HG2B. A large delamination was found near machined side of panel HG2A. The flaw was most visible during the machined side scan but could also be seen during the tool side scan with the flaw facing away from the image.

The thermograms are provided in Appendix 12.3.

The second series of IRT tests involved three hot gas panels, post treatment. The thermographic inspection of three graphite/polyimide panels was conducted using a Bales Scientific thermal image processor from a distance of 36 inches during both front and back side heating by 250 W infrared heat lamps. Two lamps were held below and even with the front of the camera for the front surface heating as shown in configuration 1. During back side heating, configuration 2, one lamp was hand scanned at a distance of six inches over the panel surface.

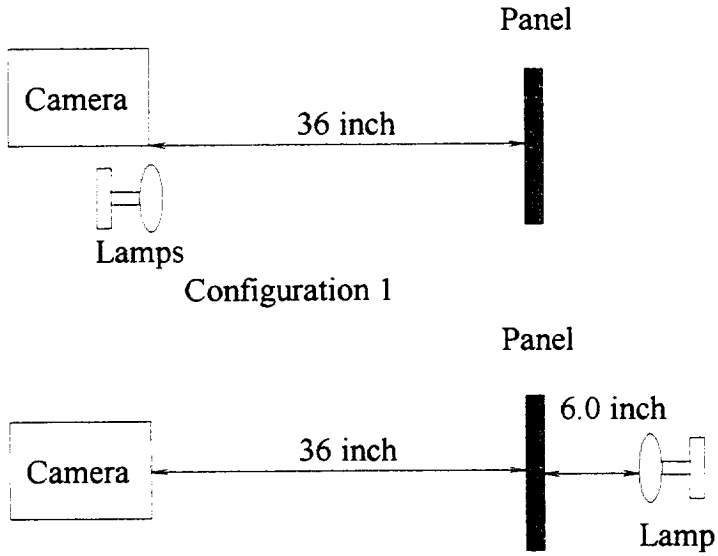

Both the tool and bag side of the panel were inspected. The following table outlines the procedures used for each scan.

Filename HG1, HG2, HG3	Configuration	Side imaged
a	1	tool
b	1	bag
c	2	tool
d	2	bag

HG1: A large delamination covering nearly a third of the panel was visible on the tool side of HG1 as shown in Figure 1a. On the bag side one large (2 to 3 inch diameter) and several small (0.25 to 1 inch) delaminations were found. No new indications were found during back surface heating. Figures 1c and 1d illustrate the presence of the larger delaminations from both sides superimposed upon each other.

HG2: The tool side of the panel featured a large delamination covering almost half of the surface. The thermal image indicated that the visible delamination may be formed from multiple sub-delaminations of varying depths. Image 2a shows a large primary delamination over a secondary region. During heating the primary region became visible first followed by the sub region indicating the possible depth variation. The bag side scan showed only a few small (0.25 to 1 inch) delaminations.

HG3: No abnormal indications could be found on either side of the HG3 panel.

The thermograms for the second series of hot gas panel tests can be found in Appendix 12.4.

7.0 GRAPHITE/EPOXY FATIGUE TEST TUBES

A series of 57 graphite/epoxy tubes were fatigue tested at MSFC as a part of a Summer Faculty Fellowship program. The tubes were inspected before and after being loaded in fatgue using pulse heating (1400 volt power setting) at a distance of 16 inches. The thermograms were captured at a rate of 20 msec/frame. The images provided in this report are all taken at frame 5 (80 msec) after flash.

The ability of the imager to measure damage in the tubes was tested by inflicting, impact damage at the 0 and 180 degree mid-length points (Figure 60).

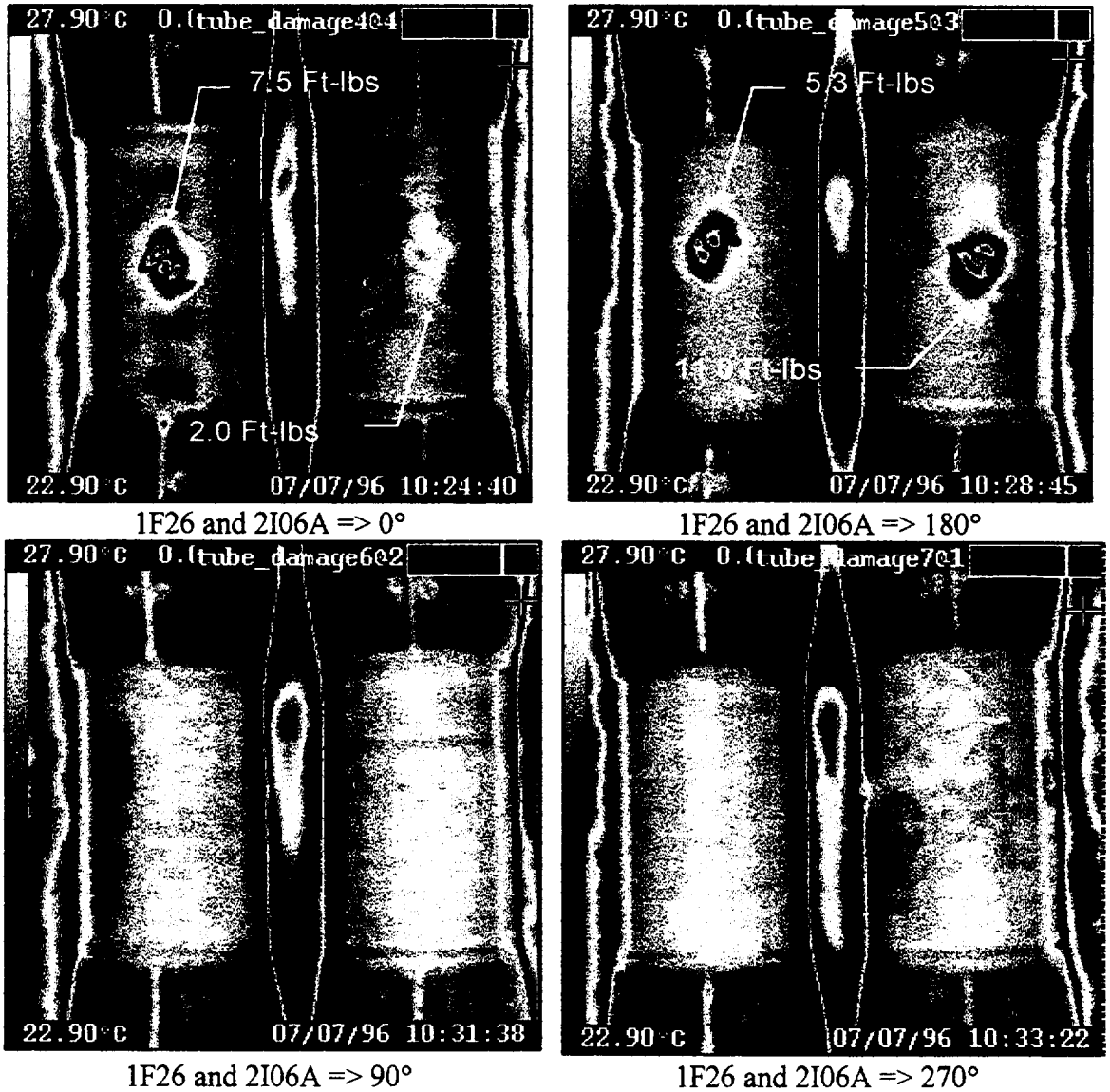

1F26 and 2I06A => 0°

1F26 and 2I06A => 180°

1F26 and 2I06A => 90°

1F26 and 2I06A => 270°

Figure 60. Impact damage in gr/ep tubes.

All but the lowest (2.0 ft-lb) energy impact produced a hole at the impact site. The 2.0 ft-lb impact was barely visible on the surface. The thermal indication from the impact damage relates well with the impat energy, higher impact equating to a larger indication, just as was seen on the graphite/phenolic impact coupons (Section 3.0).

The tubes before fatigue loading are provided in Appendix 12.6. The images are labed by tube set number and the tubes in each set are ordered, as shown in the images, with Table 4.

After fatigue loading (Appendix 12.7) the tubes were re-ordered as shown in Table 5 and new thermograms taken. In most cases, delaminations between the grip and tube could be seen and most of the damage was located at the edge of the grip region.

Tube	Reference number			
1	1-002-13	Standard	5-001-09	
2	20-2-14	20-2-29	20-2-12	
3	10-2-5	9-2-8	9-2-25	
4	20-2-22	9-2-6B	7-2-24	
5	20-2-5	20-2-21	20-2-3	
6	7-2-22	9-2-6A	9-2-23	
7	7-2-218	8-2-24B	9-2-19	
8	20-2-18	10-2-8B	9-2-16	
9	7-2-21A	8-2-24A	8-2-10	
10	10-2-8A	20-2-20A	20-2-20B	
11	7-2-13B	7-2-13A	9-2-11	
12	3-1-11	3-1-12	5-1-7	3-1-23A
13	20-1-31A	5-1-8	20-1-31B	20-1-35
14	3-1-23B	5-1-16	20-1-30B	20-1-34B
15	20-1-22	6-1-26	20-1-30A	20-1-34A
16	20-1-32A	3-1-27	20-1-21	20-1-32B
17	20-1-22A	20-1-32C	5-1-5	20-1-21A

Table 4. Data file of tubes before fatigue loading.

PTube	Reference number			
1	20-2-14	20-2-29	9-2-8	9-2-25
2	20-2-22	9-2-6B	7-2-24	
3	20-2-21	20-2-3	7-2-22	9-2-23
4	8-2-24B	9-2-19	10-2-8A	20-2-20A
5	20-2-18	10-2-8B	9-2-16	7-2-13B
6	7-2-21A	8-2-24A	8-2-10	7-2-13A

Table 5. Data file of tubes post fatigue testing.

8.0 MISCELLANEOUS INSPECTIONS

8.1 X-33 subscale fuel tank

A subscale X33 fuel tank was damaged during removal of its sand mandrel by driving a jack hammer though one end of the hoop section. A thermographic scan was requested to determine the extent of the damage in the impact region and to locate other zones where damage may have been produced during the removal of the mandrel.

The hoop region of the vessel was scanned with a Bales Scientific TIP using interior heating by a hand held hot air gun for thermal excitation. The damaged end of the tank was scanned in fourteen passes, with an approximate field of view of 12 inch by 9 inch, starting at the main impact point. The remaining portion of the hoop section was scanned in eight passes, approximately 22 inch by 14 inch each, starting along the damage axis.

In addition to the hoop scans, the dome regions were examined thermographically. In general, the resolution of the images from the dome ends was not sufficient to locate the size of features expected due to the thickness of the dome region and the inability to get sufficient heat into the material fast enough. Work is in progress to overcome these limitations for future projects.

The thermographic image of the primary damage zone (Figure 61) closely resembled that which could be seen visually. That is, delaminations do not appear to exist beyond the region where the fibers have been damaged.

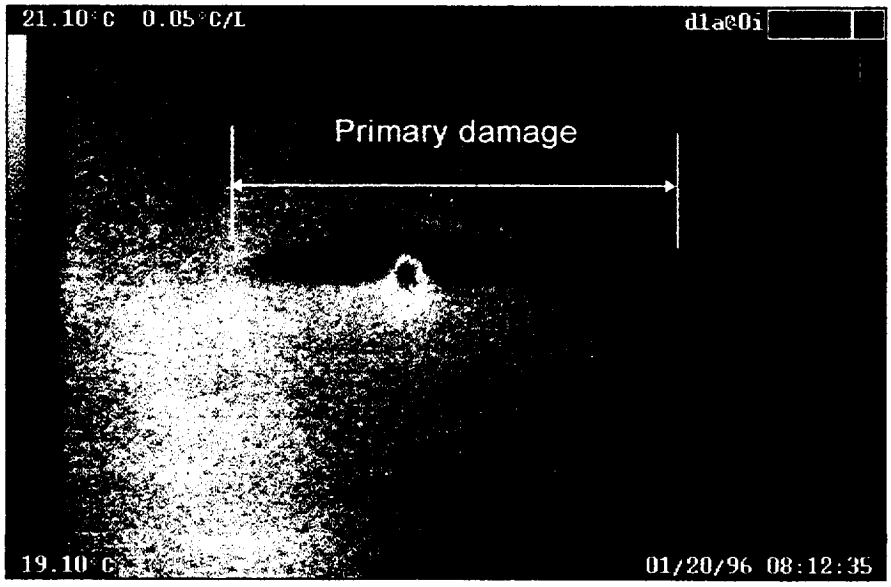

Figure 61. Image D1A of primary damage.

A second damage zone (Figure 62), labeled B in the following figure, was found in region 14 just below a thermocouple mark. The majority of the damage appears to be at the transition between the thick and thin portions of the hoop region and then gradually reduce in magnitude toward the end of the thermocouple mark.

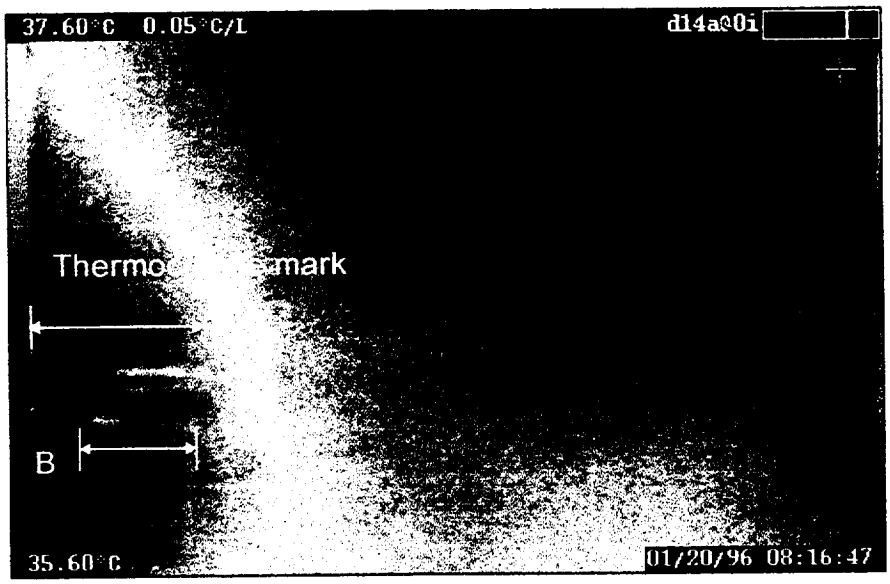

Figure 62. Image D14A of secondary damage zone.

On the opposite end of the tank from the primary damage two small indications (Figures 63, 64 and 65) were found. These indications may be the result of the lay-up procedure, i.e. irregular overlapped layers, or an actual flaw site. Due to the magnitude of the indications it is unexpected that they would cause any structural problems, but have been included in this report for future reference if a problem develops.

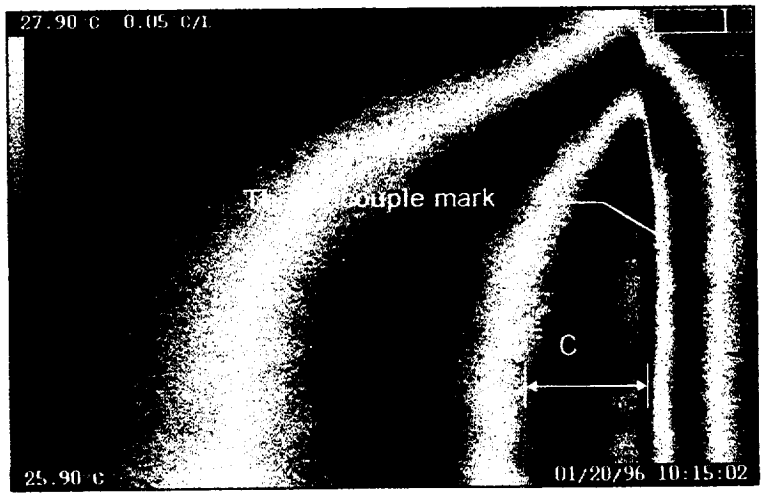

Figure 63. Image E5A for sub-scale tank.

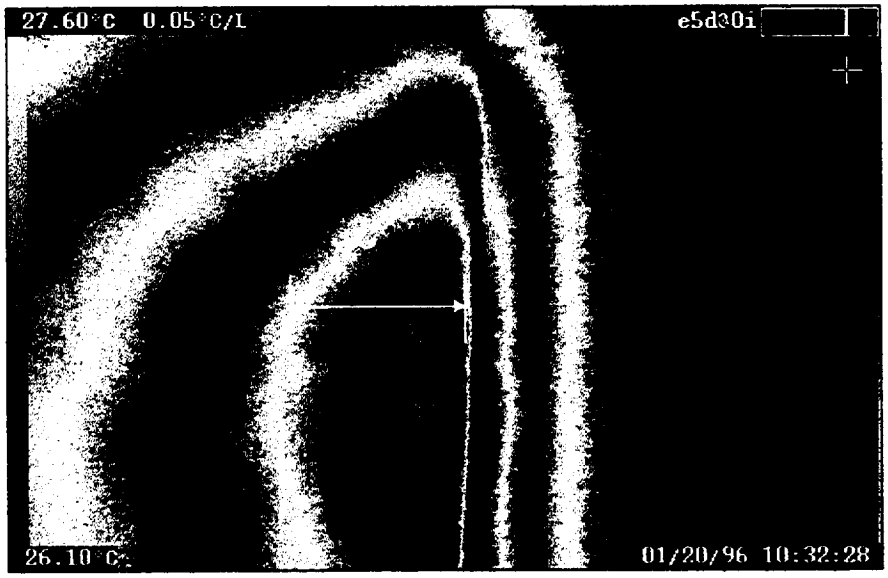

Figure 64. Image E5D.

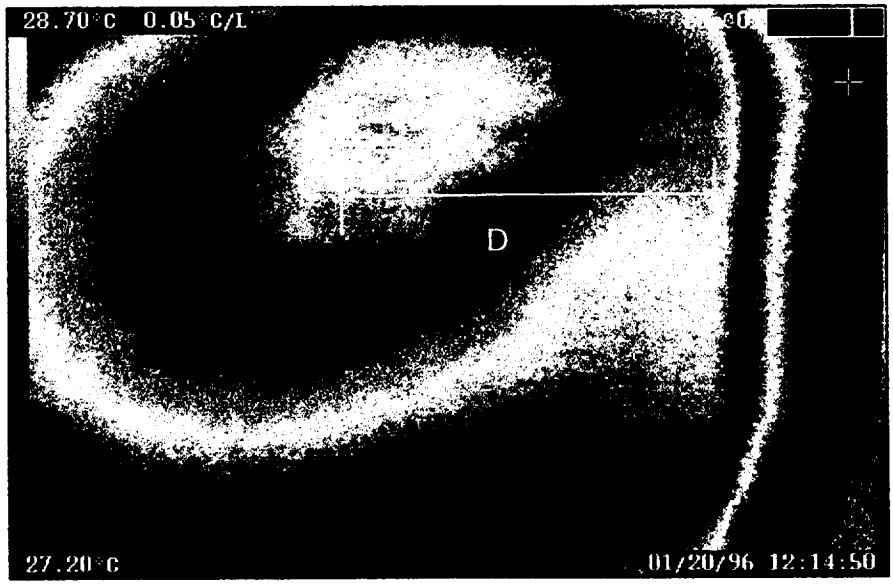

Figure 65. Image E8A.

8.2 Cryogenic feedlines

A thermographic inspection of an IM-7/977-2 (graphite/epoxy) cryogenic feedline flange section has been performed using the Bales Scientific TIP. The feedline was divided into six inspection zones including both front and back side scans of the pipe, flange and transition region. Several heating methods and fields of view were attempted to maximize the resolution of the thermal map. Measurements were made with heat

applied by means of a hot air gun or a 500 W lamp to both the viewing and opposite sides and of the feedline. The feedline was cooled between each thermal scan by placing it on a standard box fan until its thermal profile was uniform.

The thermal scans showed no abnormal indications in the flange or transition region for any of the heating methods or fields of view. Three indications were found on the pipe region though, labeled "A", "B" and "C" in Figure 66. Surface features could possibly explain indications "B" and "C", as there were ripples in the laminate in those regions. The rectangular shape in the center of the pipe region could not be seen visually. Unless this is a feature of the lay-up process, indication "A" may be something that warrants further analysis.

All of the indications were much weaker during the scan of the inside of the pipe as shown in Figure 67. Note that indications "B" and "C" show up as faint diagonal bands oriented down and to the right while indication "A" appears as a light region in the center of the image. Whatever is creating these indications must be closer to the outside of the flange since they appear brighter and more defined on the outside scan (Figure 66).

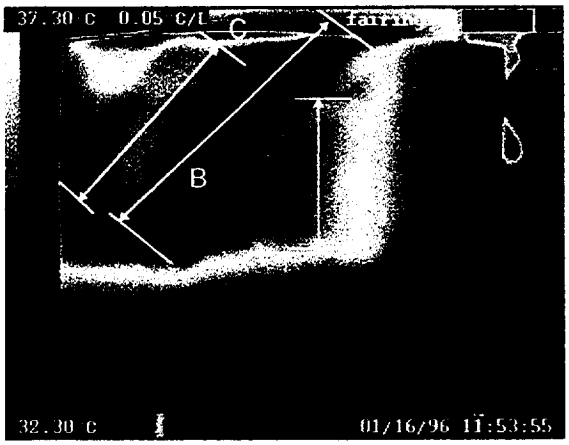

Figure 66. Outside of flange.

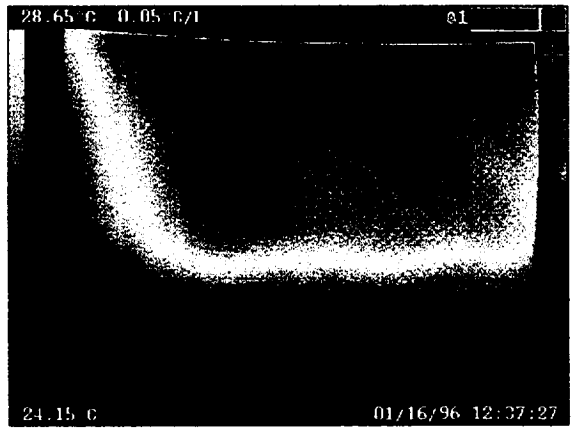

Figure 67. Inside of flange.

8.3 Silicon carbide/silicon carbide disks.

Three sets of silicon carbide/silicon carbide blisks were inspected with the Bales TIP system using front face (camera side) pulse heating. The pulse amplitude was set at 1400 volts and the image processor configured to scan at 20 msec per frame (50 frames/sec). The thermograms from each can be found in Appendix 12.1.

Series 1 A linear indication or abnormality was found on the back side of disk 1. The indication was colder than the rest of the disk and lasted for about 7 frames (140 msec). No visible defect could be seen on the surface of the disk to match the thermogram. The remaining views of the disks showed no abnormal indications other than the dimpled surface finish.

Series 2 Both sides of the disks were inspected with the Bales TIP system using front face (camera side) pulse heating. The pulse amplitude was set at 1400 volts and the image processor configured to scan at 20 msec per frame (50 frames/sec).

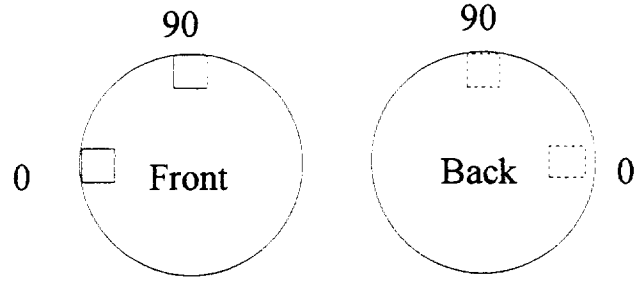

Many thermal features could be found on both sides of the disks. The abnormal regions showed up as hot compared to the remaining disk. In most instances these regions were found to terminate at a surface delamination.

Series3 Both sides of the disks were inspected with the Bales TIP system using front face (camera side) pulse heating at a distance of 32 inches. The pulse amplitude was set at 1400 volts and the image processor configured to scan at 20 msec per frame (50 frames/sec).

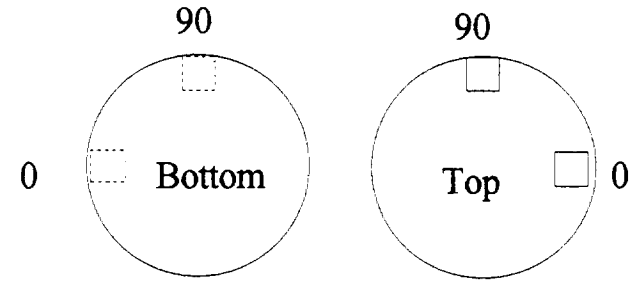

8.4 Graphite/Epoxy Channel For Space Station.

A graphite/epoxy channel was inspected using pulse heating with the Bales Scientific TIP. One end of the channel had a region of suscpected porocity. A digital filter was applied to the fifth image from each end of the bar.

0	0	0	0	0	0	0
0	2	2	2	2	2	0
0	2	0	0	0	2	0
0	2	0	10	0	2	0
0	2	0	0	0	2	0
0	2	2	2	2	2	0
0	0	0	0	0	0	0

Table 6. Digital filter for graphite/epoxy spar.

Defective end

Good end

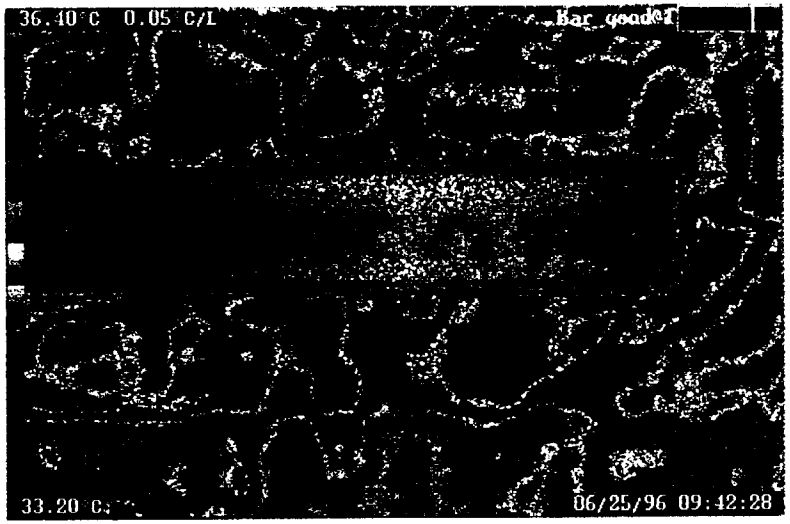

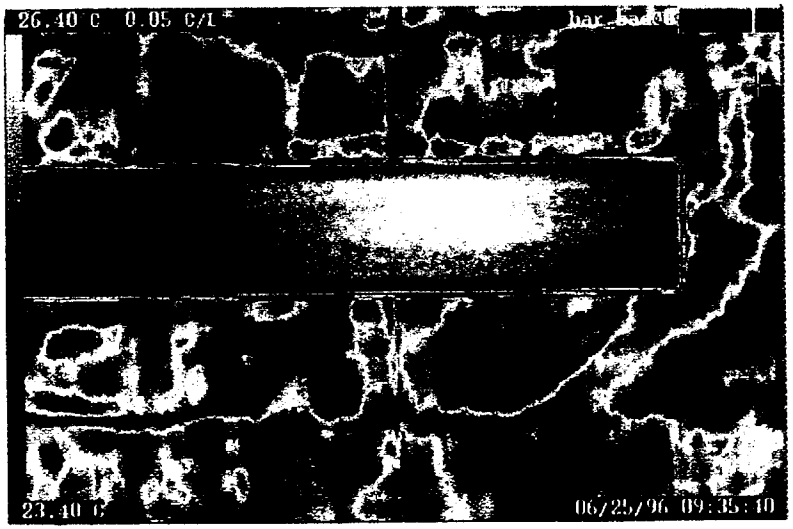

Figure 68 Thermograms of graphite/epoxy spar..

8.5 GRAPHITE/EPOXY PLATES AND HONEYCOMB PANELS (NASA JSC)

A series of eleven graphite/epoxy Nomex honeycomb panels and a single monolithic panel was supplied by the Johnson Space Center in Houston for IRT inspection at MSFC. Two test panels were supplied with known defects including Teflon inserts for the monolithic panels and a combination of separator film insets, insufficient cobond adhesive and release agent for the honeycomb panel (Figure 69 and 70). The panels were imaged with the Bales TIP system using front face (camera side) pulse heating at a distance of 32 inches with as power setting of 1400 volts. The images were scanned at 20 msec per frame (50 frames/sec) and acrilic lamp shields were placed in front of the lamps to block the post flash glare from the parts surface. The ten honeycomb panel thermograms are given in Appendix 12.2. The estimated sizes for each thermal indication is given in Table 7 on page 55.

Indication	Indicated size	Panel
A	1/4	2b
B	1/2	
C	3/4	
D	1 1/4	
E	1/2	3t
F	1/4	
G	1 1/2	
H	1/4	3b
I	1/4	
J	3/4	
K	1 1/2	
L	1	
M	1 1/2	4t
N	1/4	
O	1	
P	3/4	4b
Q	3/4	
R	1/4	
S	1/2	
T	1/2	
U	1 1/4	
V	1/2	
W	1	5t
X	1	
Y	1/4	
Z	1 1/4	
AA	1/4	5b
AB	1/4	
AC	3/4	

Indication	Indicated size	Panel
AD	3/4	6b
AE	3/4	
AF	1	7t
AG	1/2	
AH	1/4	
AI	1	
AJ	3/4	
AK	1 1/4	7b
AL	1 1/4	8t
AM	1/4	
AN	3/4	
AO	1 1/2	
AP	1	8b
AQ	1/2	
AR	1/4	
AS	1/4	
AT	3/4	
AU	1 3/4?	
AV	3/4	
AW	1 1/4	
AX	1 1/4	9b
AY	1/4	
AZ	3/4	
BA	3/4	10t
BB	1/4	
BC	3/4	
BD	1/2	
BE	1/4	10b
BF	1	
BG	1	

Table 7. Estimated flaw sizes for honeycomb panels.

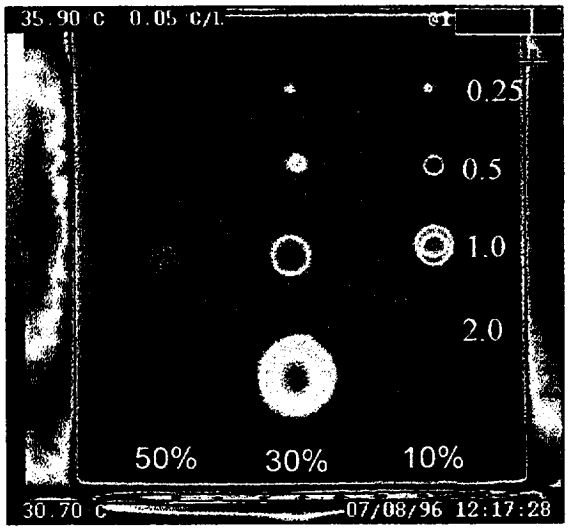

Back side

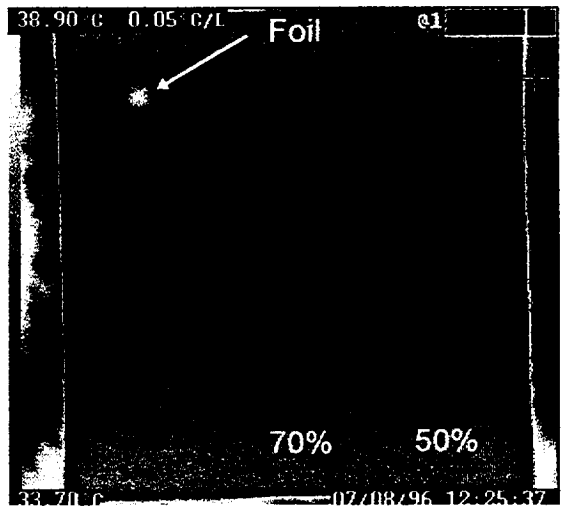

Front side

XX% indicates depth of teflon tape

Figure 69. Monolithic panel from JSC.

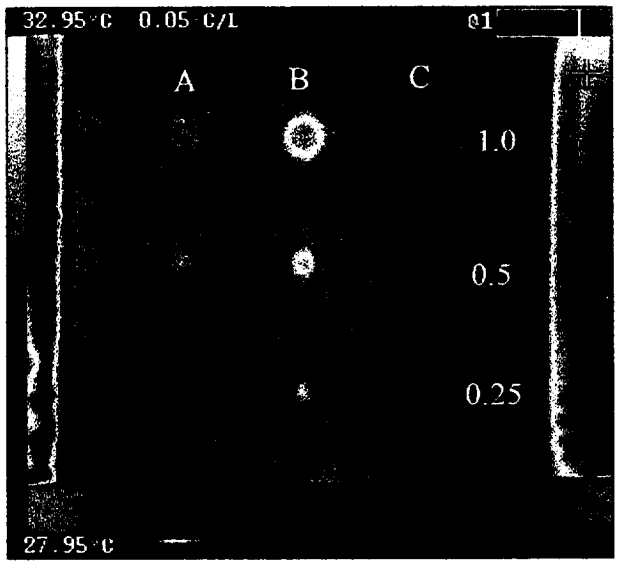

Calibration panel (back)

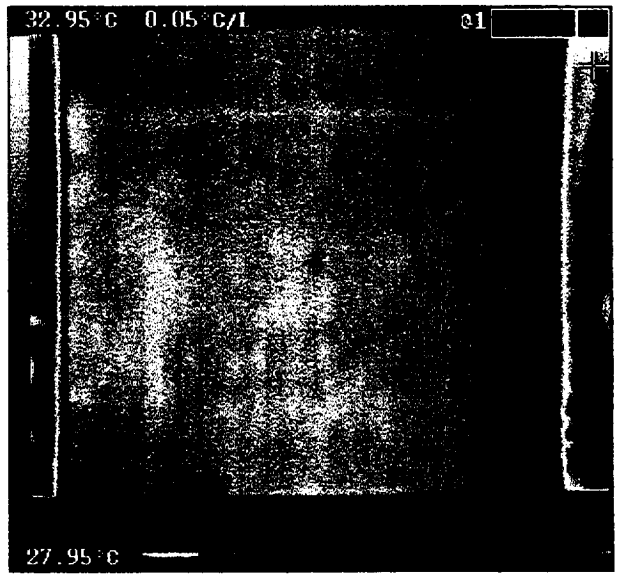

Calibration panel (front)

A = Adhesive removed and separator film inserted
B = Adhesive removed
C = Release agent applied between adhesive and core

Figure 70. Honeycomb panel from JSC.

9.0 18 INCH DIAMETER GRAPHITE/EPOXY PRESSURE VESSEL

An eighteen inch diameter graphite/epoxy vessel was inspected utilizing the Bales Thermographic camera and flash hood. The top polar boss of the vessel was marked at 45 degree intervals for reference (Figure 71). Zero degree was established at the visible wrinkle in the hoop fibers and the vessel was rotated counterclockwise for each of the subsequent measurements.

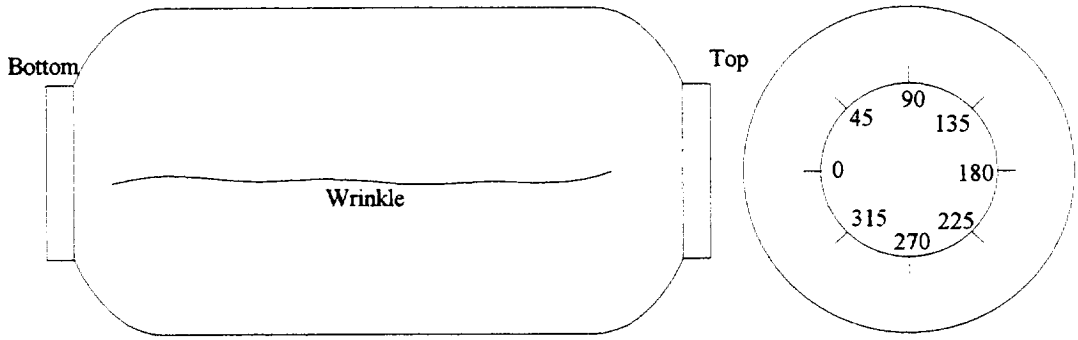

Figure 71. Vessel orientation.

Three image sequences were taken to complete the thermal map of the vessel. First the hoop region was scanned in eight segments by positioning the vessel horizontally on a table and pulse heating with the Bales Spectral Hood (Figure 72). The dome regions of the vessel were also scanned in eight segments. Here, the vessel was oriented 45 degree to the front face of the hood so that the dome was facing the camera.

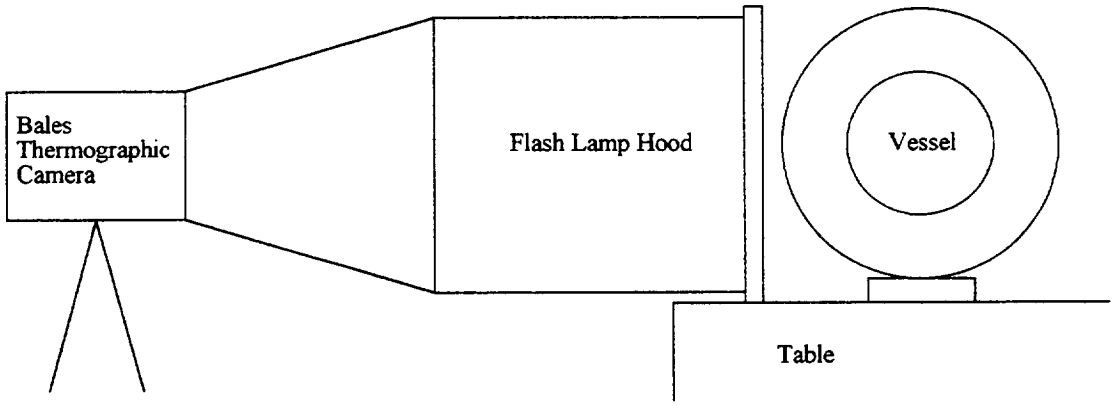

Figure 72. Physical arrangement.

The spectral hood utilizes two high intensity quartz flash lamps to provide a controlled heat pulse to a structure. The inside of the hood is mirrored to help generate a uniform heat wave. The amplitude of the heat pulse was established by way of a 1400 volt pulse from the powered unit. Images were acquired at 20 msec per frame as the vessel cooled down after the flash.

The twenty four thermographic images shown in Appendix 12.9 were all taken 60 msec after the flash lamps were pulsed. Due to the "repeat" feature used for the false color map of these images it is not possible to directly tell directly if one region is hotter than another. Temperature relationships were determined by viewing each image in a "normal" mode. The "normal" mode images were not printed since they contain a great deal of over and under range temperature vales which do not plot well.

Many small features were found during the thermographic testing. Most of these features were found to be "surface" marks attributed to the vessel was "bagged" during manufacture and as such not a serious structural problem. For example, the 0° hoop image had a strong indication in the center of the hoop region which turned out to be a "rough" tape mark. The mark changed the local emissivity of the vessel and showed up as a slightly higher temperature. Many of the small wrinkles, overlapping and tape marks in the dome regions also showed up in the thermographic images. Four indications stood out from the rest though, two on the hoop and two on the dome region. A summary of these finding follows.

Indication 1. 0° hoop

Visible as a large and deep surface wrinkle.
Persisted for over 400 msec after pulse heating as a hot region.
May be due to low consolidation or a void below the surface.

Indication 2. 270° hoop.

Visible as the edge of a tape seam.
Persisted for 200 msec as a hot region.
Possibly due to edge effect of tape seam.

Indication 3. 180° Top

Visible as large surface wrinkle.
Persisted for 300 msec as a hot region.
May be a small linear void or resin pocket under wrinkle.

Indication 4. 225° bottom

Visible as a small surface crater.
Persisted for 200 msec as a hot region surrounding a cold region.

10.0 DESIGN OF A 2000 W INFRARED HEAT LAMP

One of the problems encountered when testing the inter tank panels was that the two 500 W shop lamps did not cover a large enough area to allow for uniform heating over the region of interest. Starting with the lamp design used by Lockheed-Martin (Carl Bouvier) a 20 inch long heat lamp was designed and built to help eliminate this problem in the future. Two 1000 W infrared quartz heat lamps were mounted in an aluminum frame, housed in a fiberglass box. The unit is powered by 3 phase, 220V.

The unit was not operational at the time of the writing of this report due to the lamp holders still being on backorder.

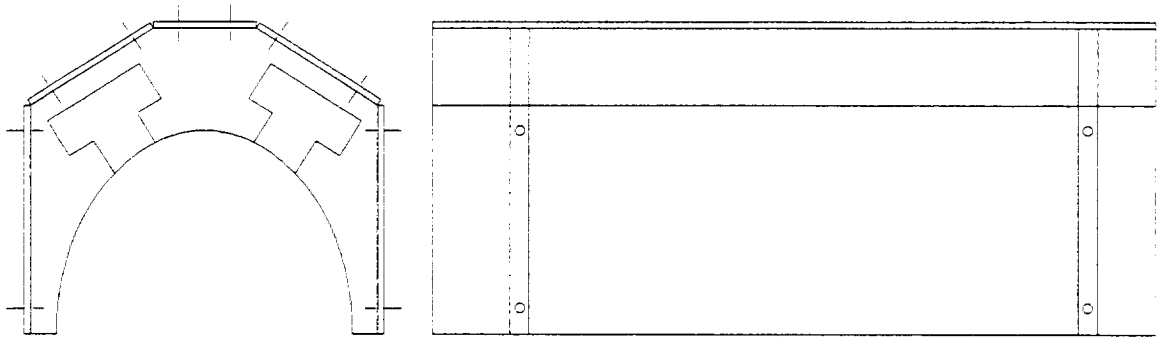

Figure 73. Heat lamp.

11.0 BINARY IMAGE CONVERSION (BIC) SOFTWARE

Software has been developed to convert the UNIX (Bales thermographic system) formatted images to DOS-ASCII formatted matrices for use in post image analysis. This will allow statistical and neural network analysis of the thermograms to be conducted. The software and results from preliminary statiatical and/or neural network analysis will be included in the final report.

12.0 APPENDIX

12.1 SILICON CARBIDE/SILICON CARBIDE BLISKS

12.1.1 Silicon Carbide Blisks

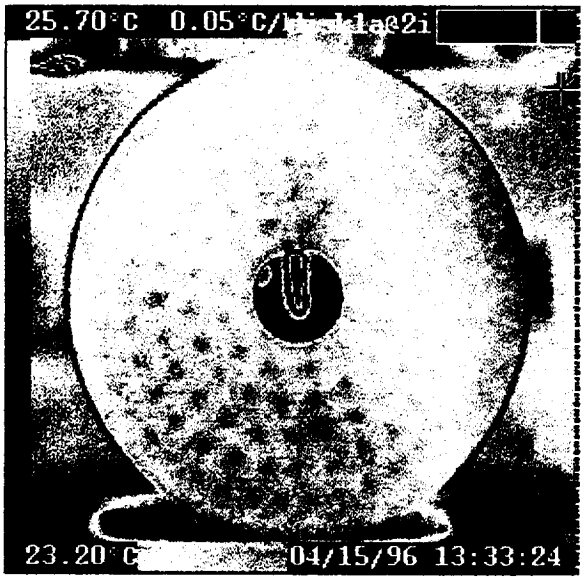

Disk1 (Front)

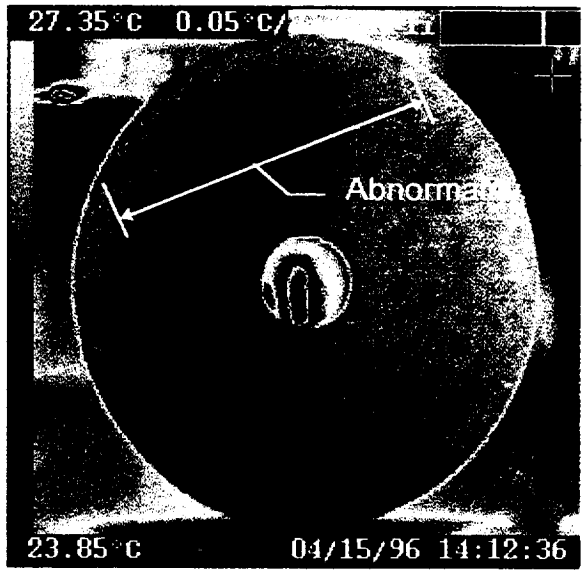

Disk1 (Back)

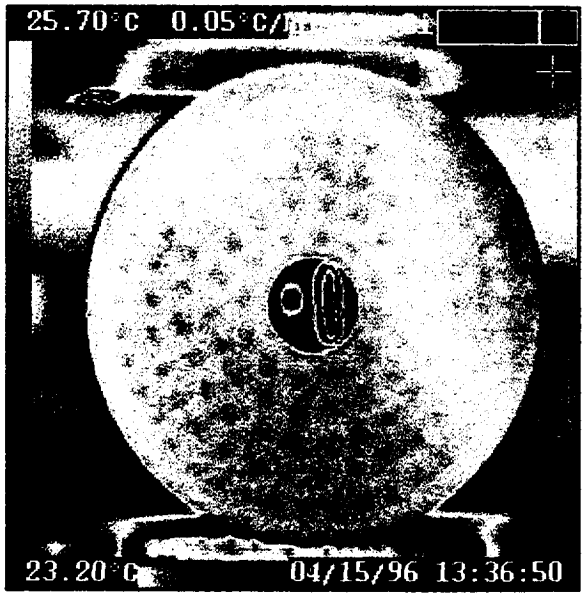

Disk2 (Front)

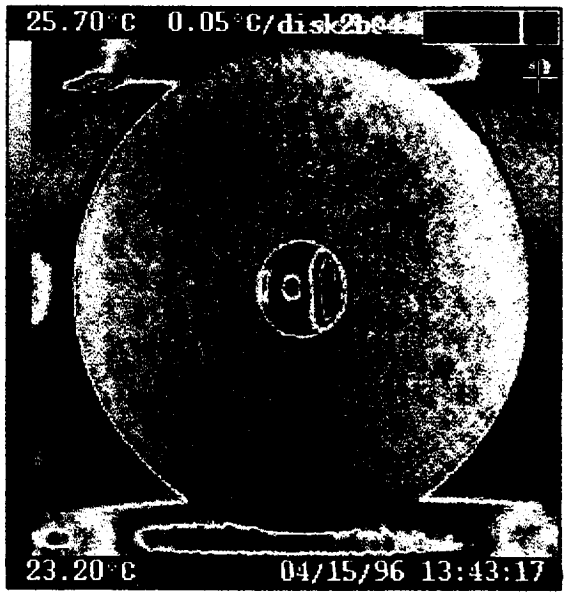

Disk2 (Back)

12.1.2 Blisks 958, 959,974

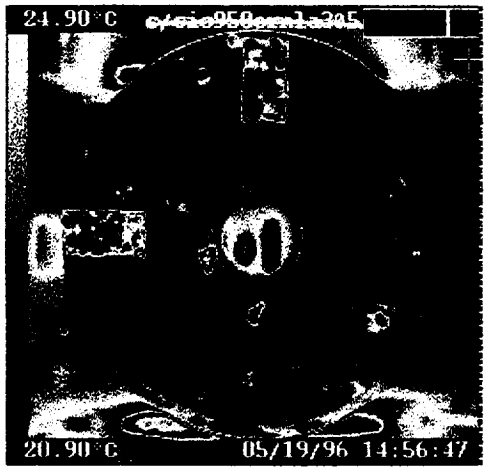

Disk 958 (front)

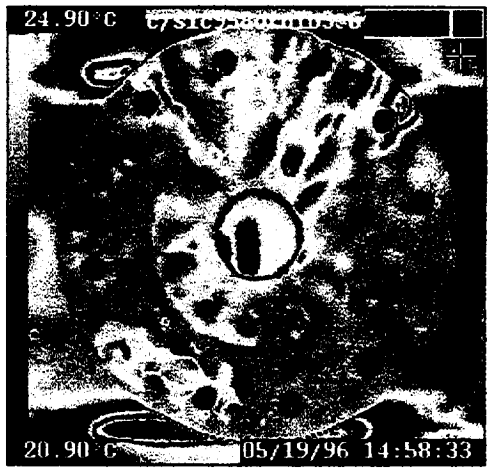

Disk 958 (back)

Disk 958 (front)

Disk 958 (back)

Disk 974 (front)

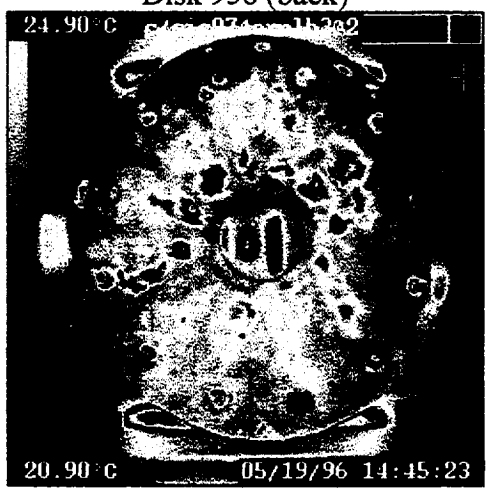

Disk 974 (back)

12.1.3 Blisks 1017, 1032

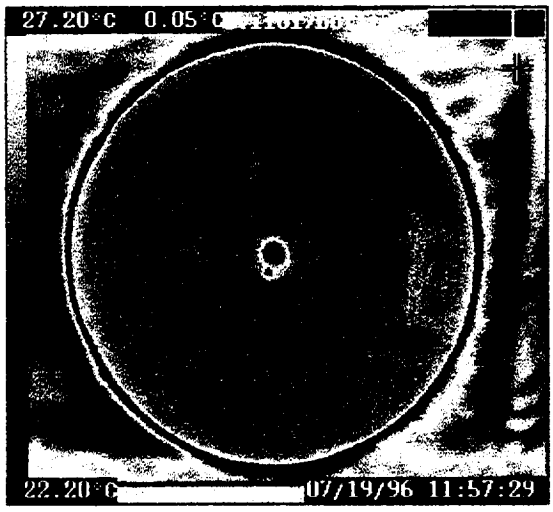

CVI 1017 bottom (260 msec)

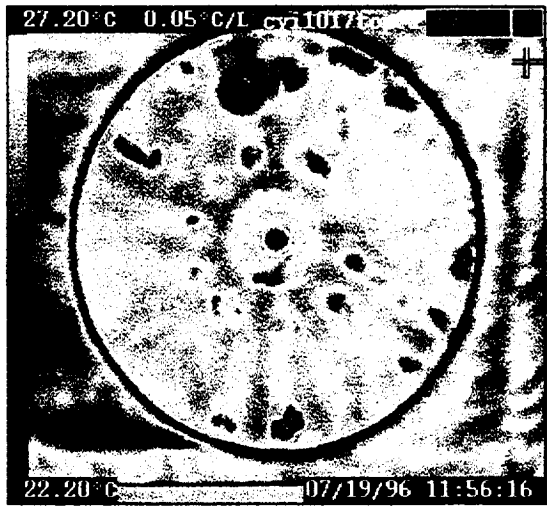

CVI 1017 top (260 msec)

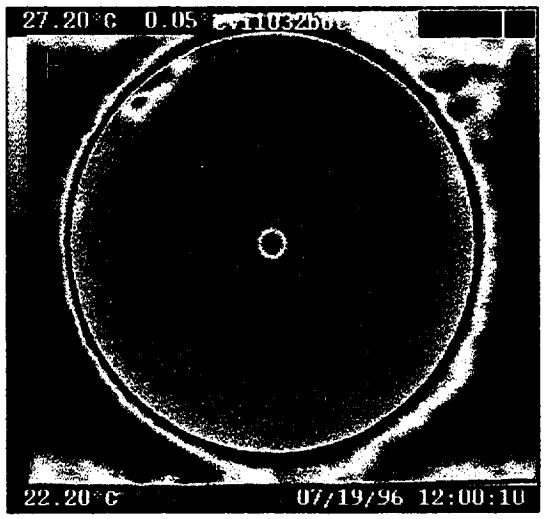

CVI 1032 bottom (260 msec)

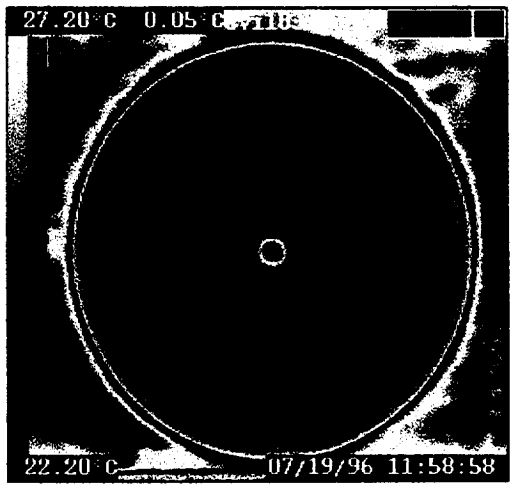

CVI 1032 top (260 msec)

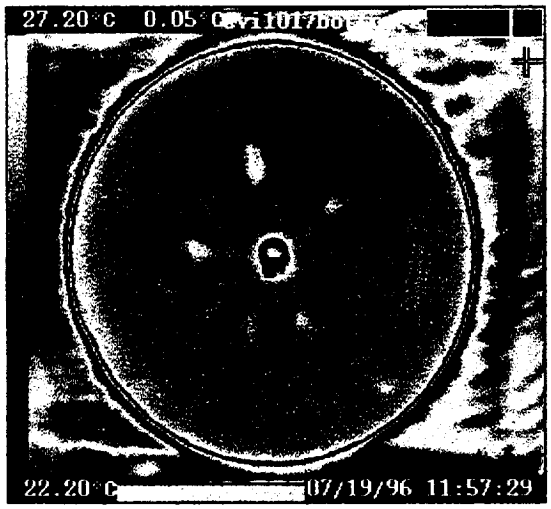

CVI 1017 bottom (60 msec)

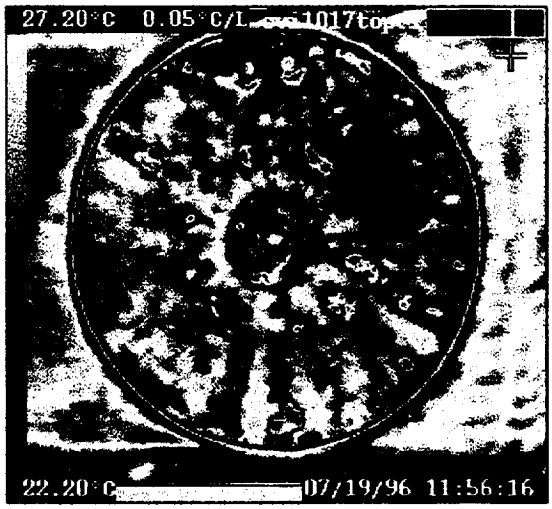

CVI 1017 top (60 msec)

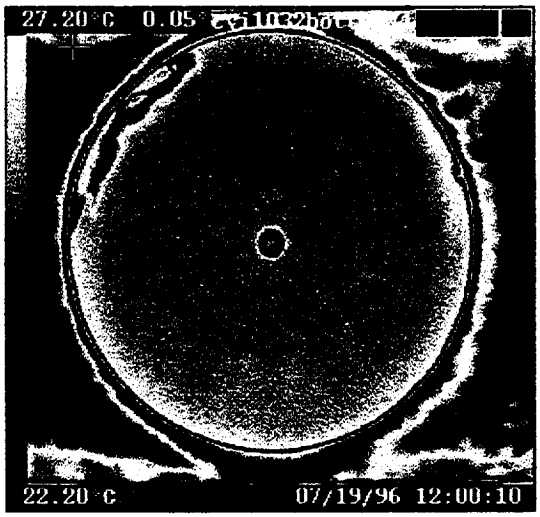

CVI 1032 bottom (60 msec)

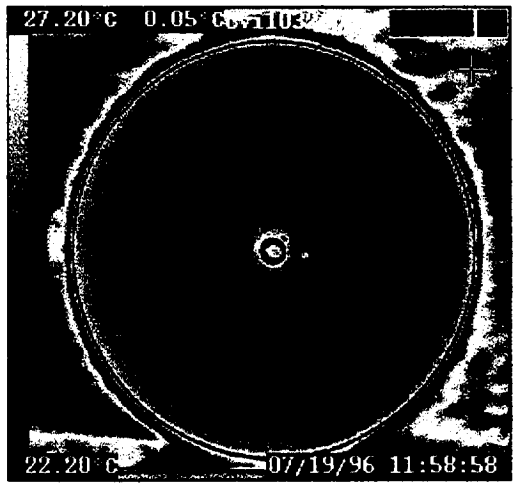

CVI 1032 top (60 msec)

12.2 GRAPHITE/EPOXY PLATES AND HONEYCOMB PANELS (JSC)

Panel 1

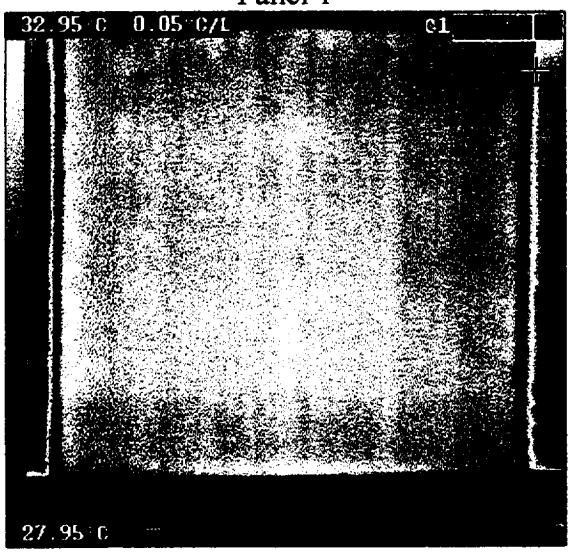

Panel 2

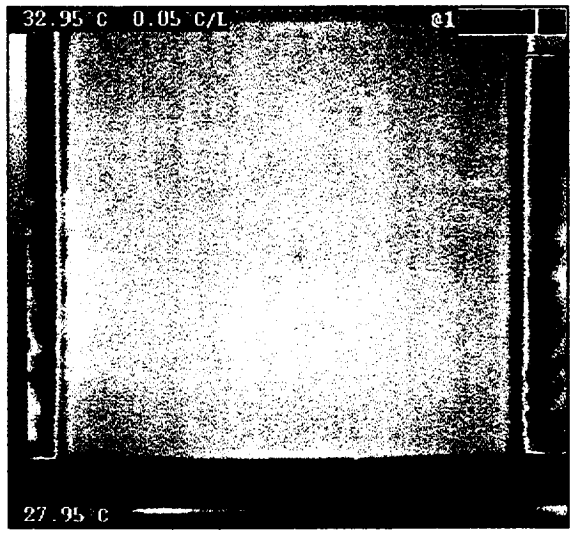

---

fold line

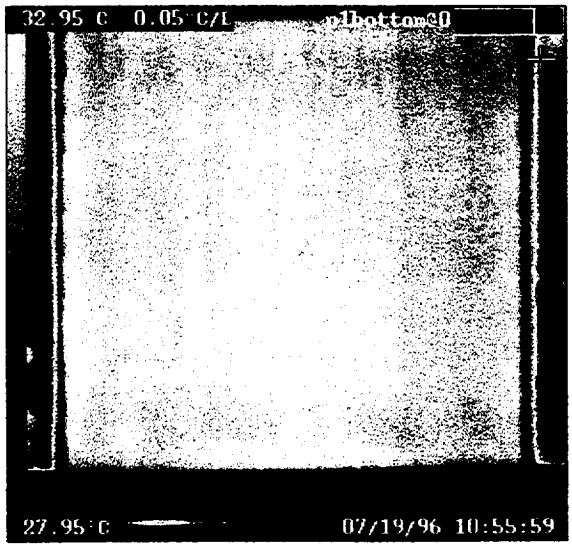

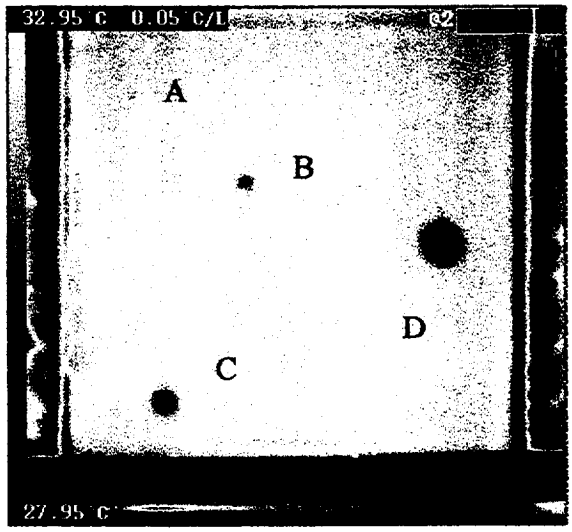

Panel 3

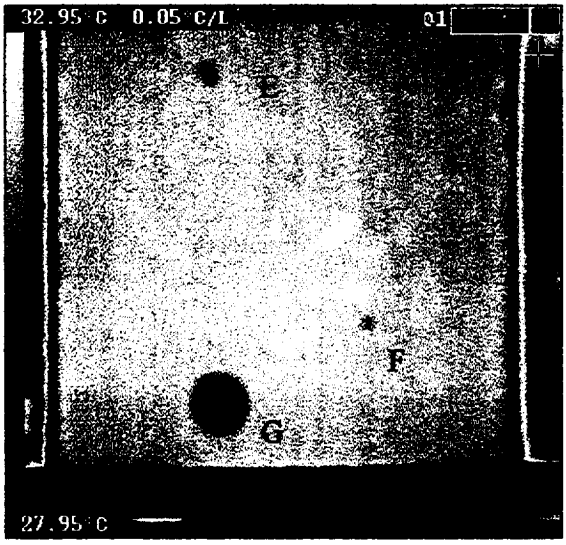

Panel 4

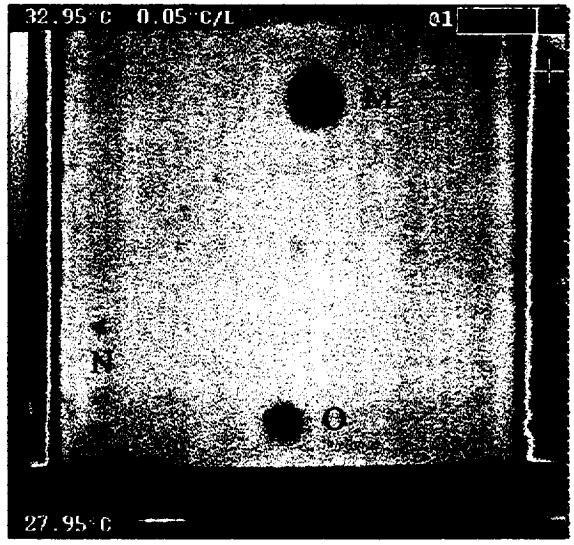

---

fold line

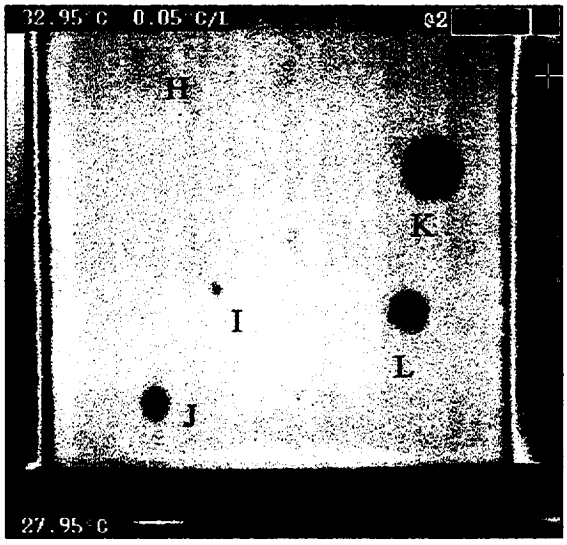

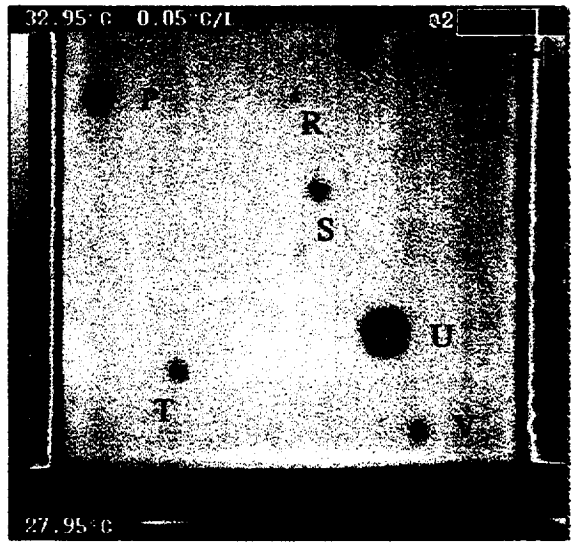

Panel 5

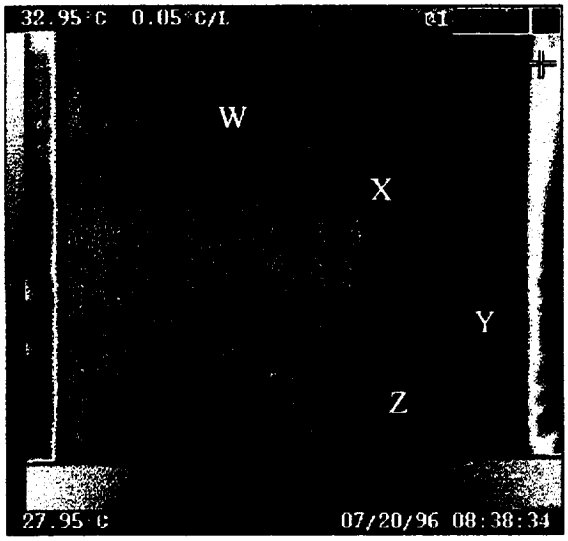

Panel 6

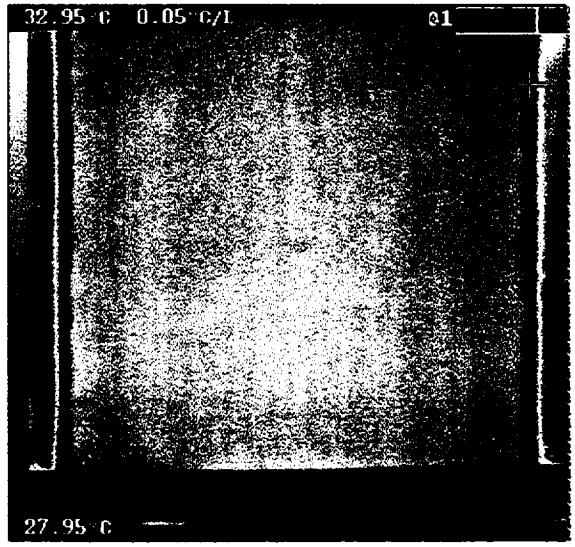

---

fold line

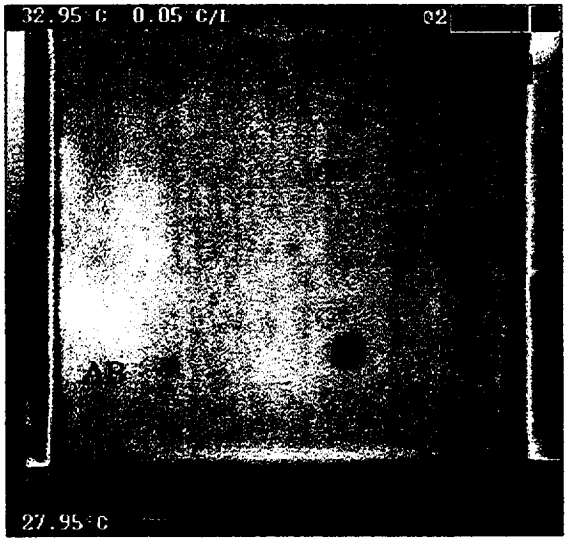

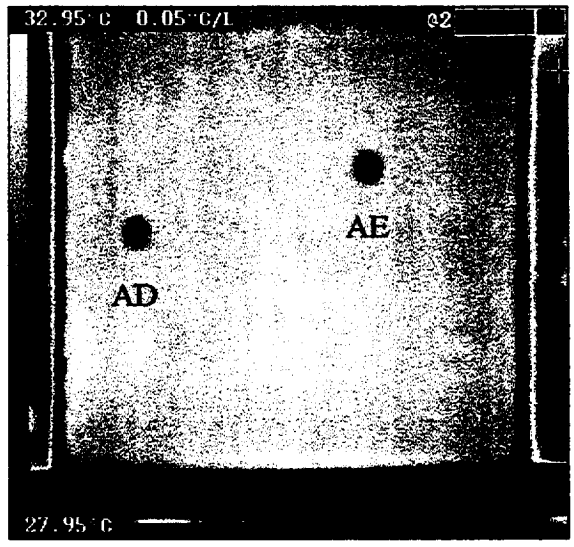

Panel 7

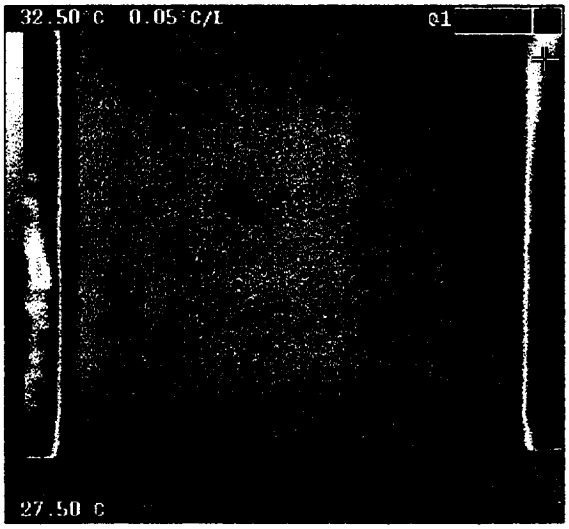

Panel 8

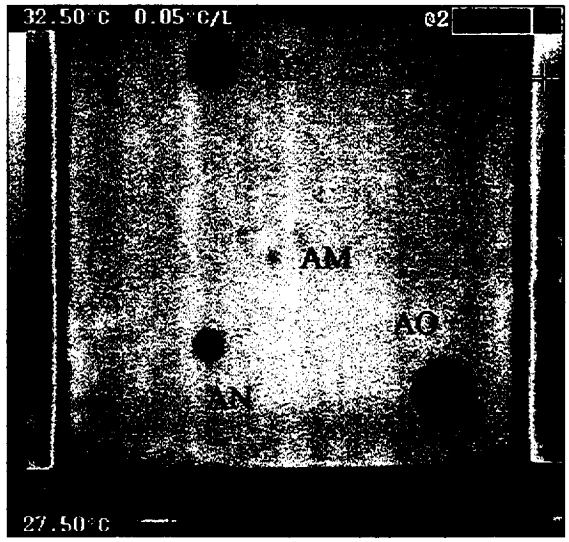

---

fold line

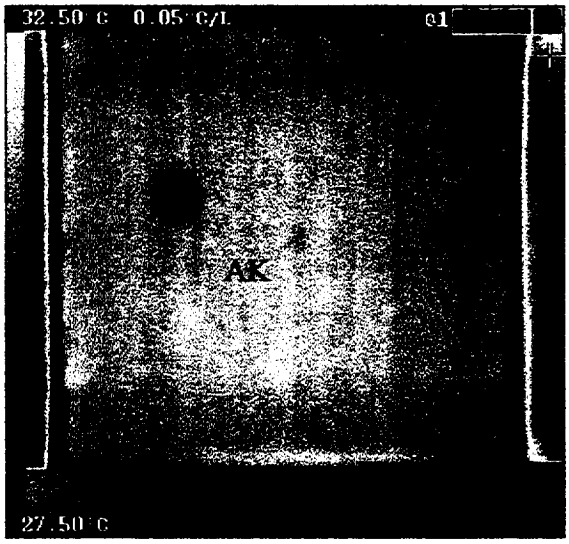

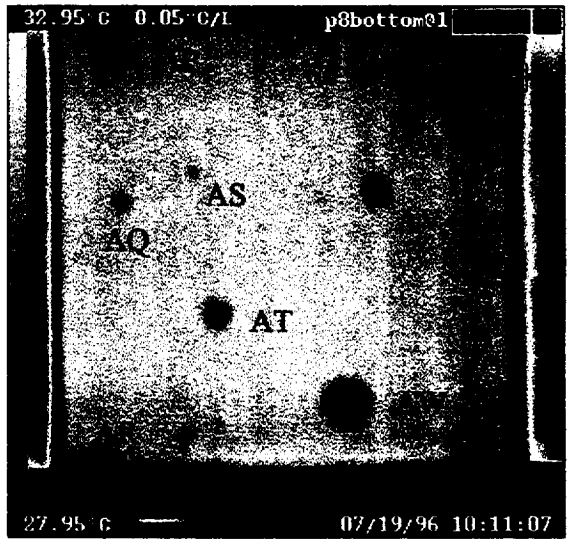

Panel 9

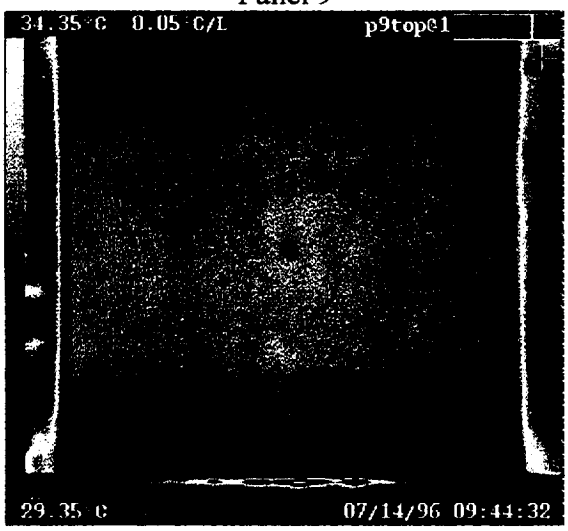

Panel 10

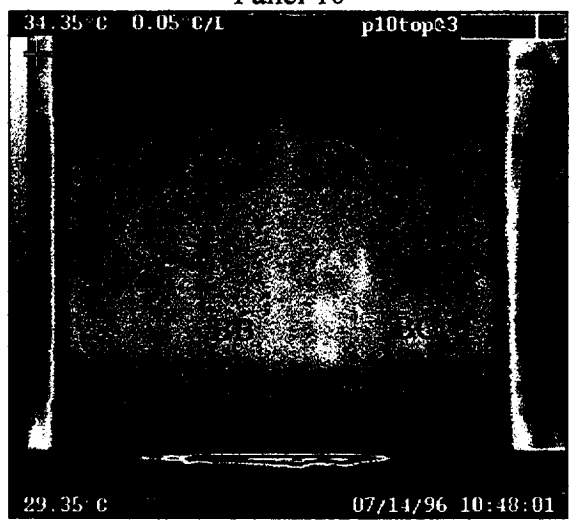

---

fold line

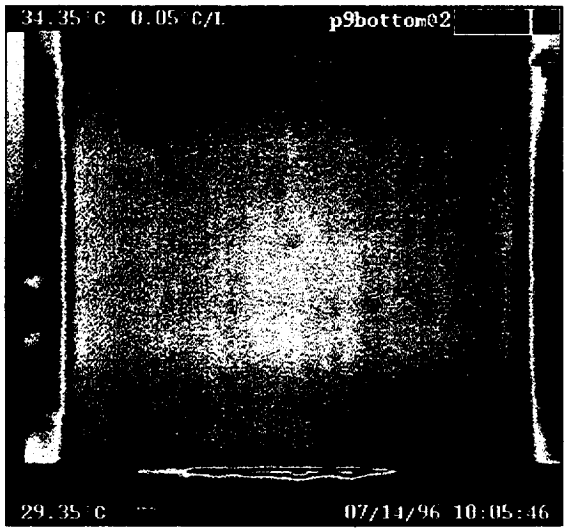

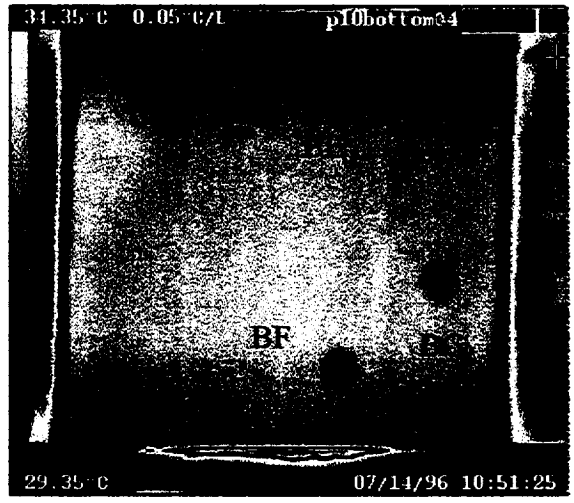

12.3 GRAPHITE/POLYIMIDE HOT GAS PANELS

REFRENCE CONDITION THERMOGRAMS

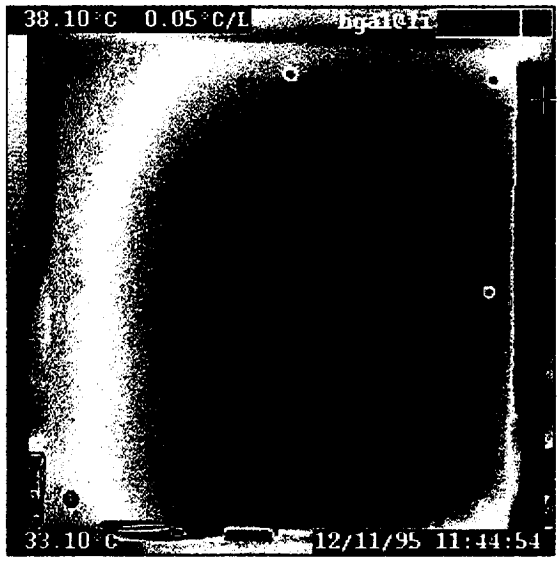

HGA1

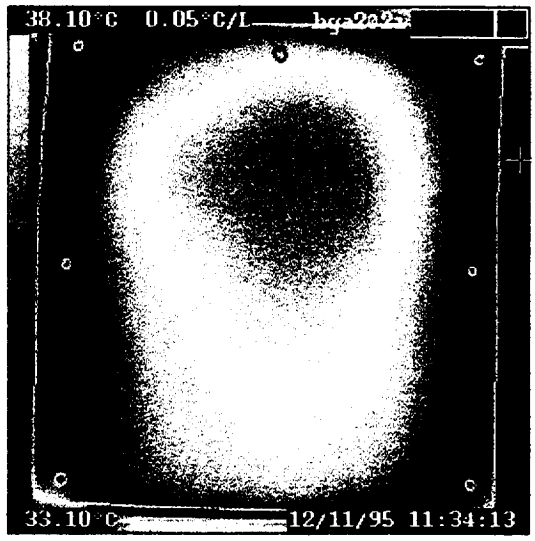

HGA2

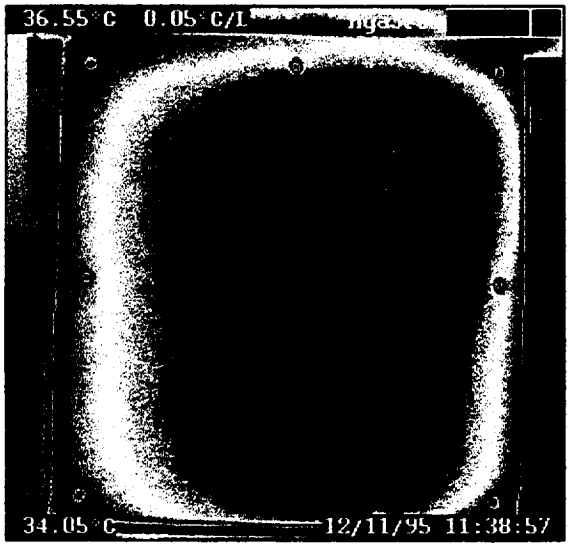

HGA3

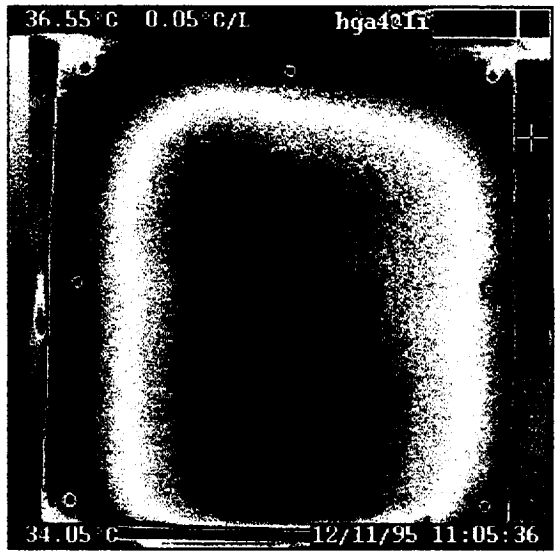

HGA4

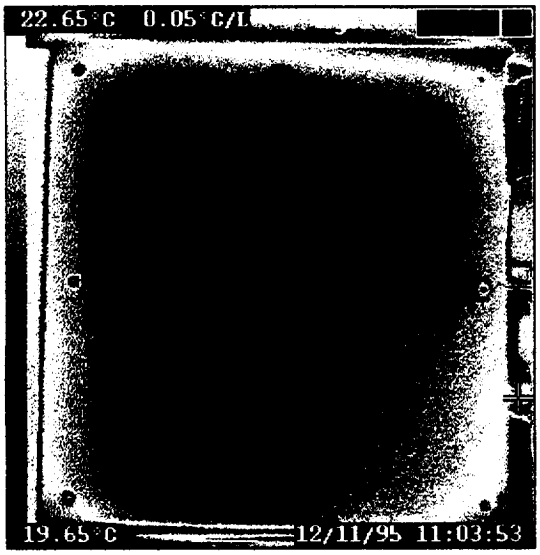

HGB1

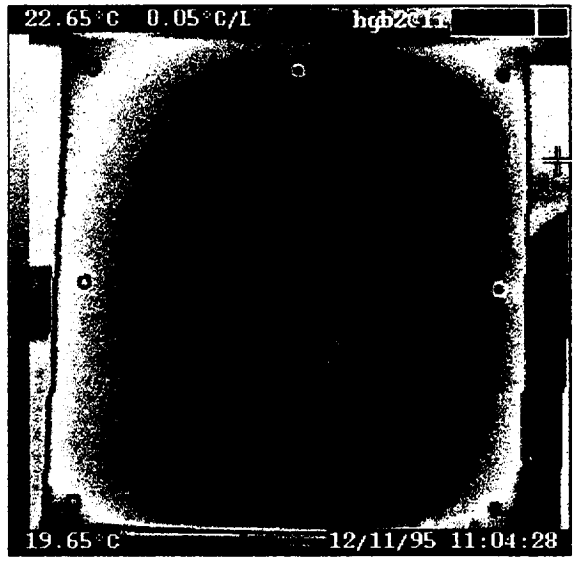

HGB2

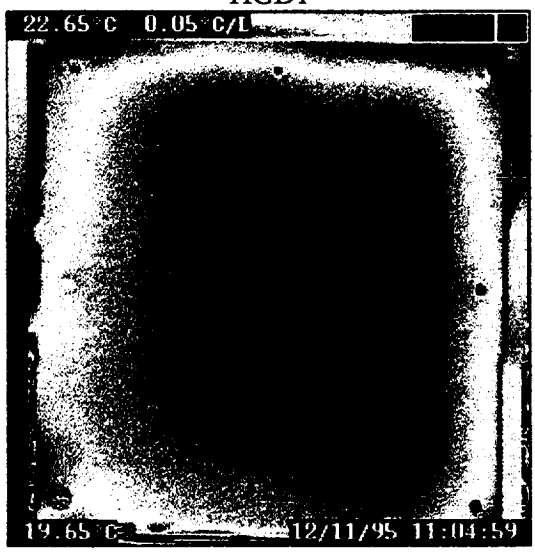

HGB3

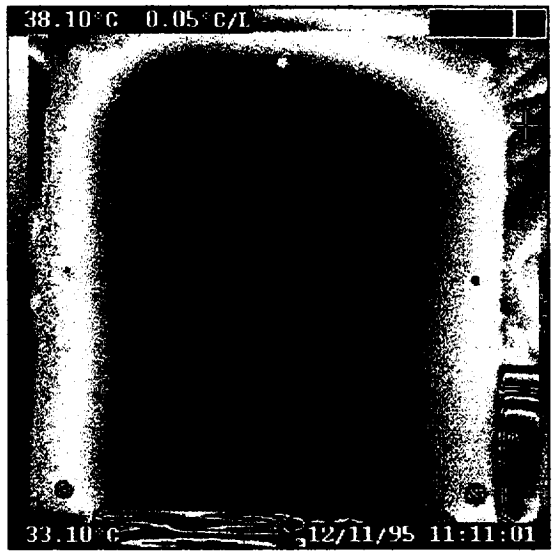

HGB4

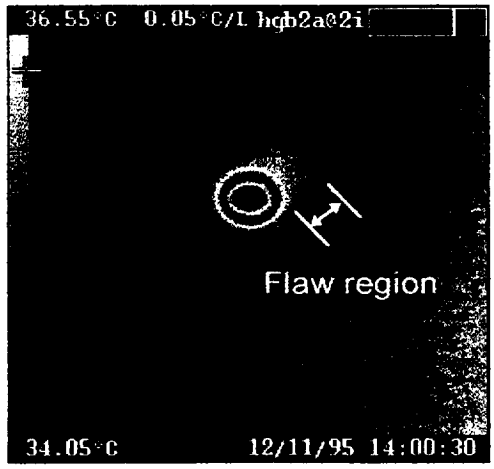

HGB2 flawed hole

POST HOT GAS TREATMENT

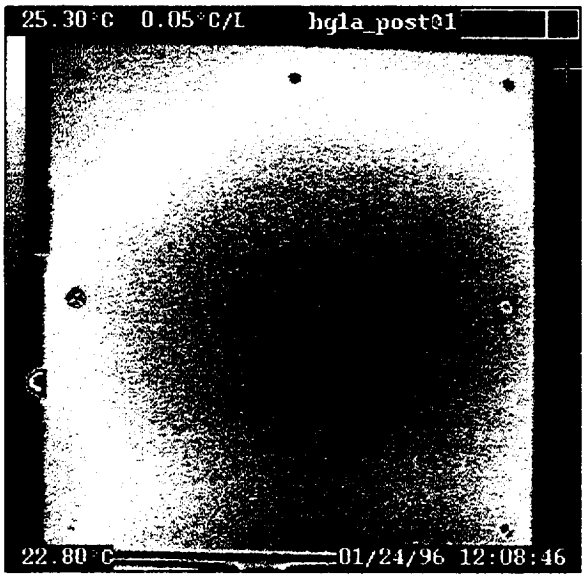

HG1A_POST

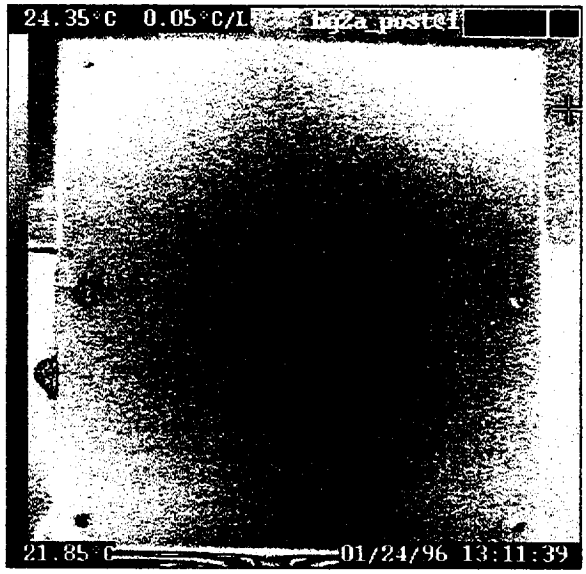

HG2A_POST

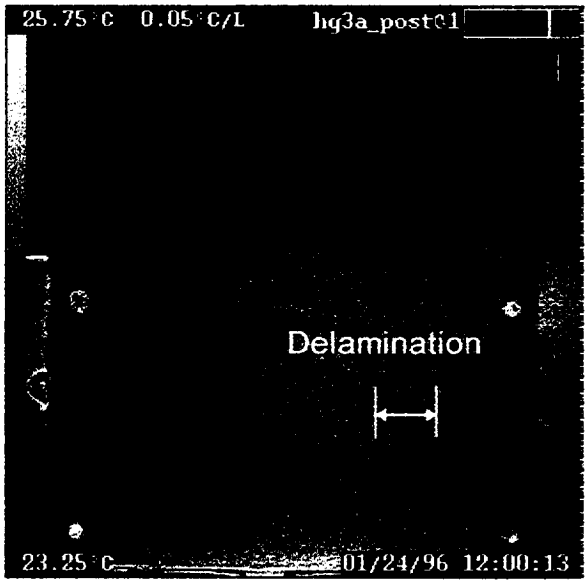

HG3A_POST

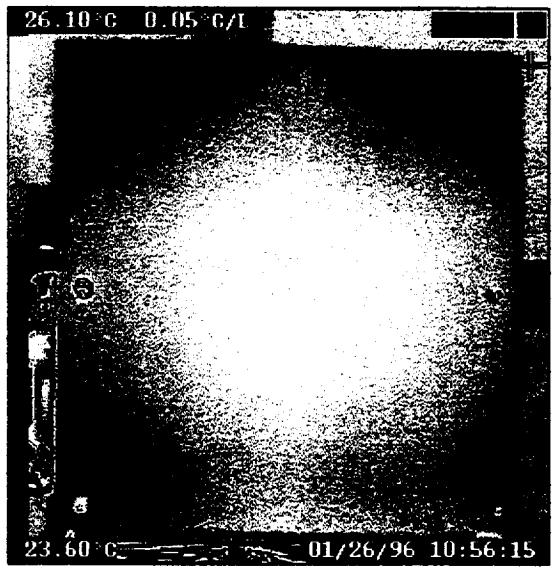

HG4A_POST

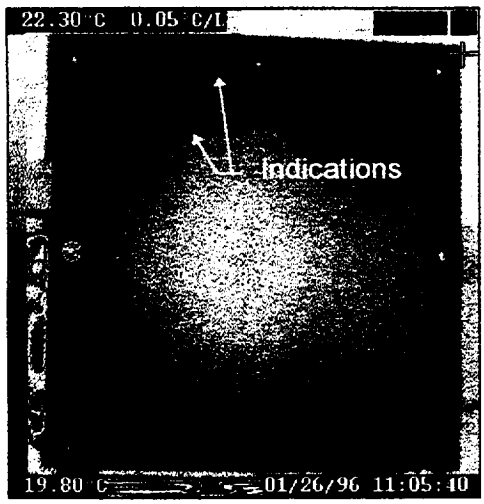

HG1B_POST

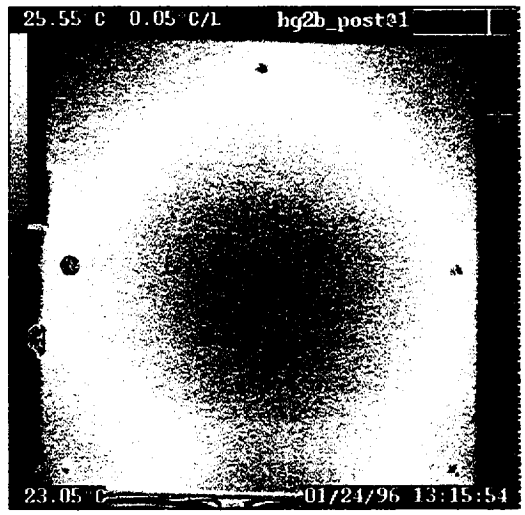

HG2B_POST

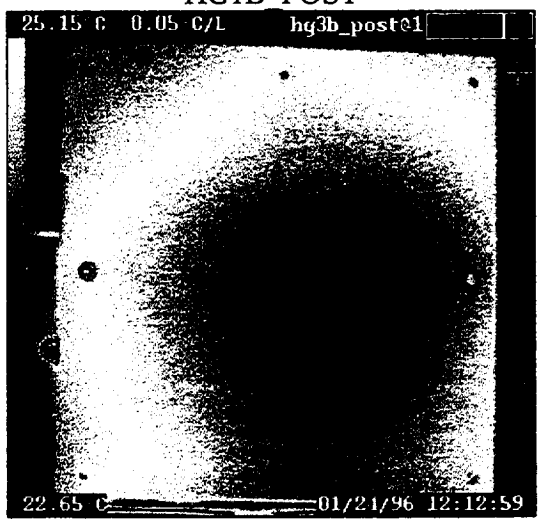

HG3B_POST

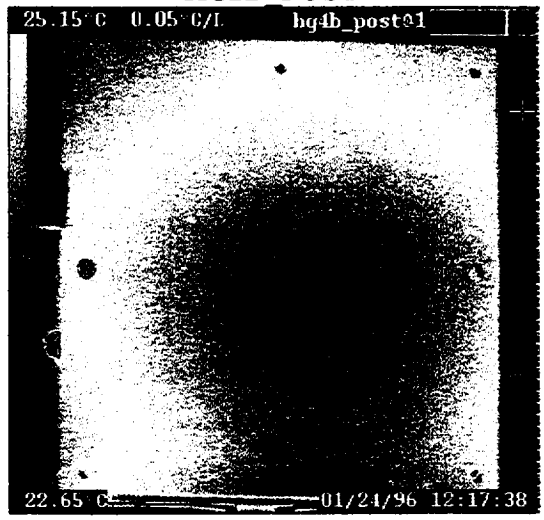

HG4B_POST

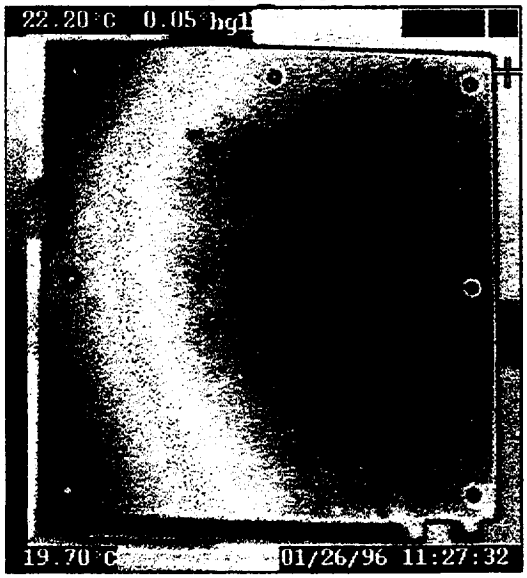

HG1B_POST_51

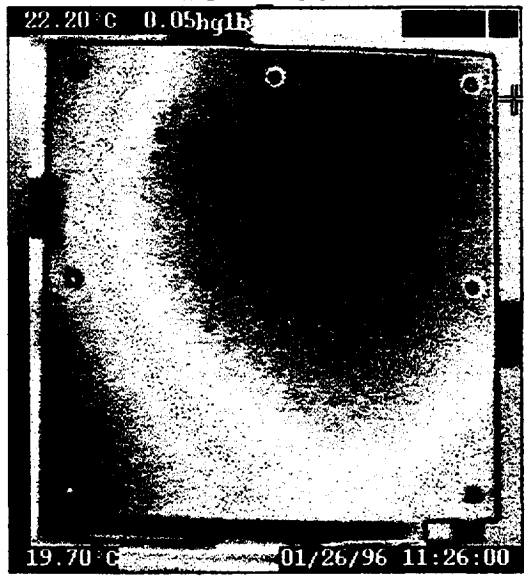

HG1B_POST_104

12.4 GRAPHITE/POLYIMIDE HOT GAS PANELS (FF1-HG1 THROUGH FF1-HG3)

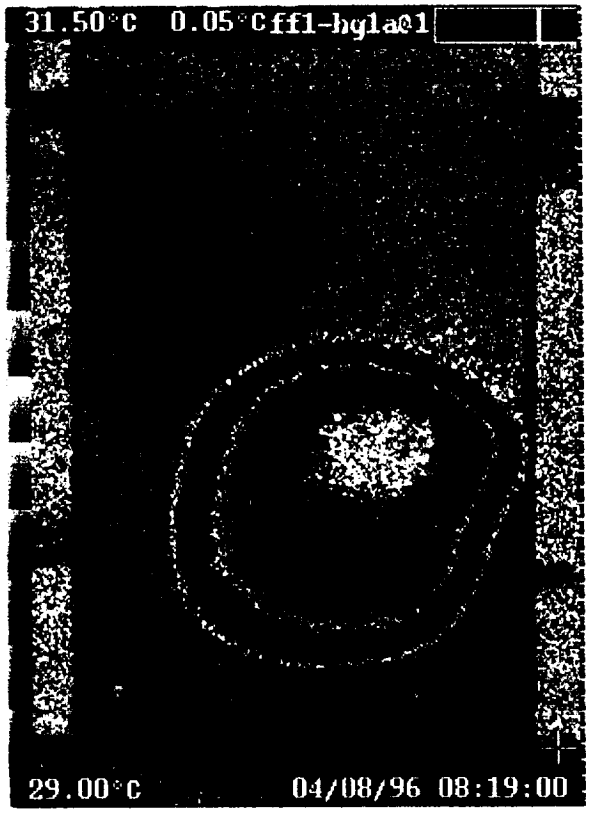

(1a) Tool side

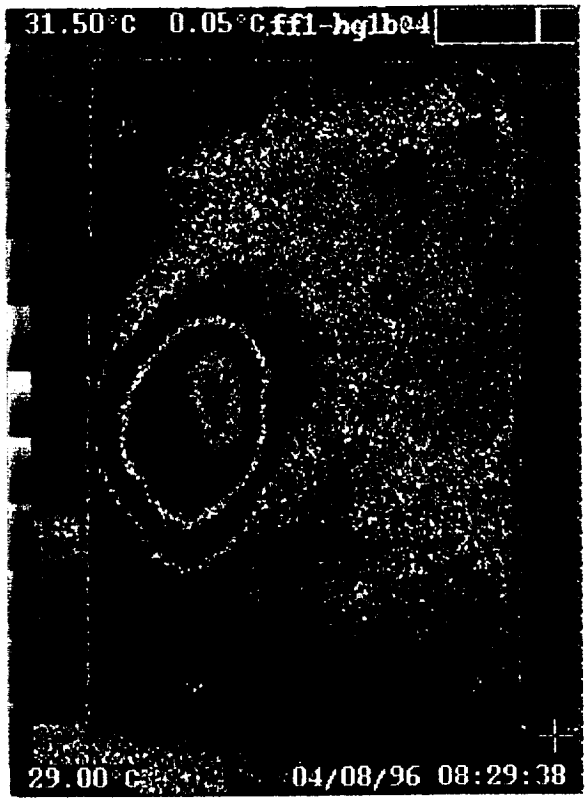

(1b) Bag side

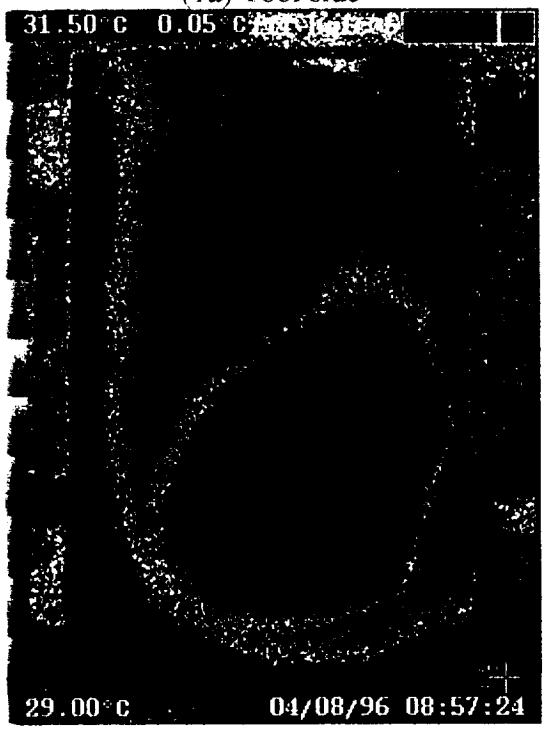

(1c) Tool side

(1b) Bag side

(2a) Tool side

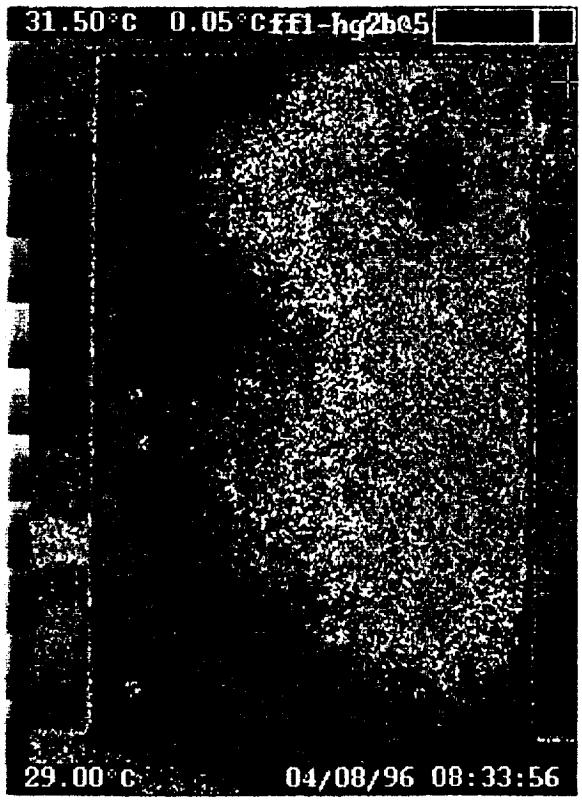

(2b) Bag side

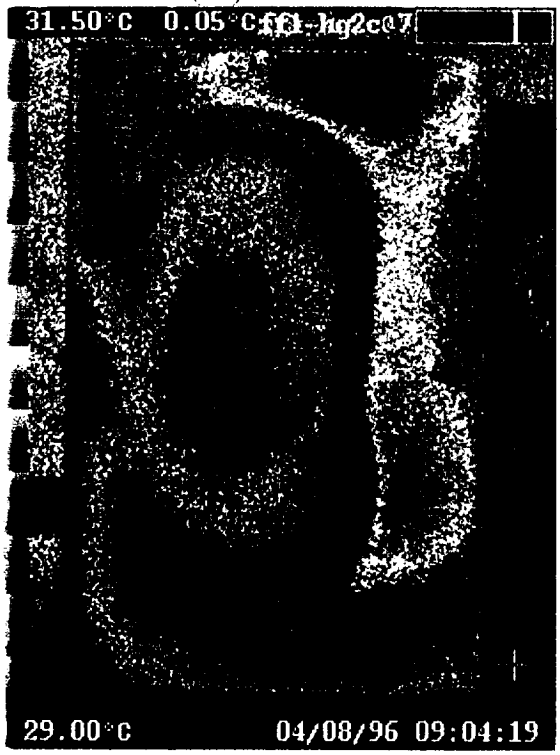

(2c) Tool side

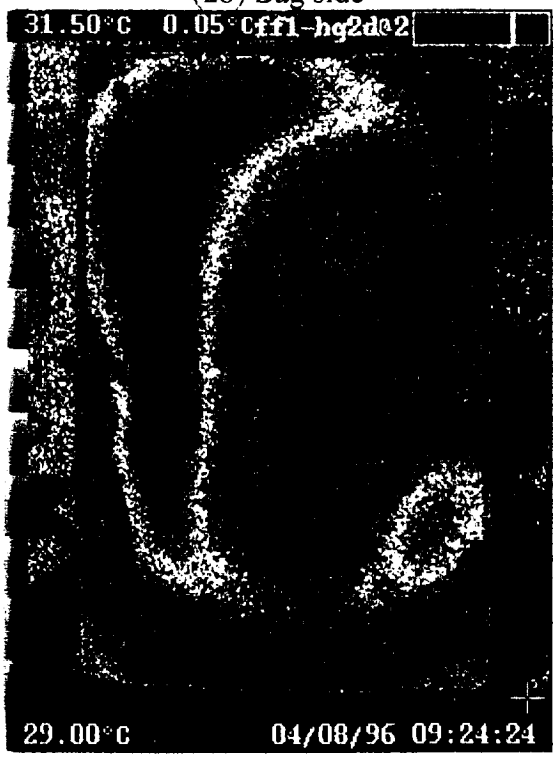

(2d) Bag side

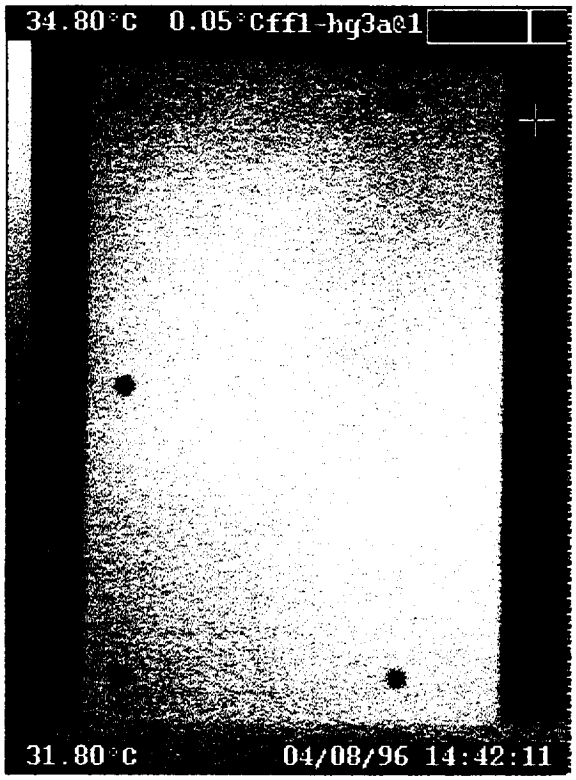

(3a) Tool side

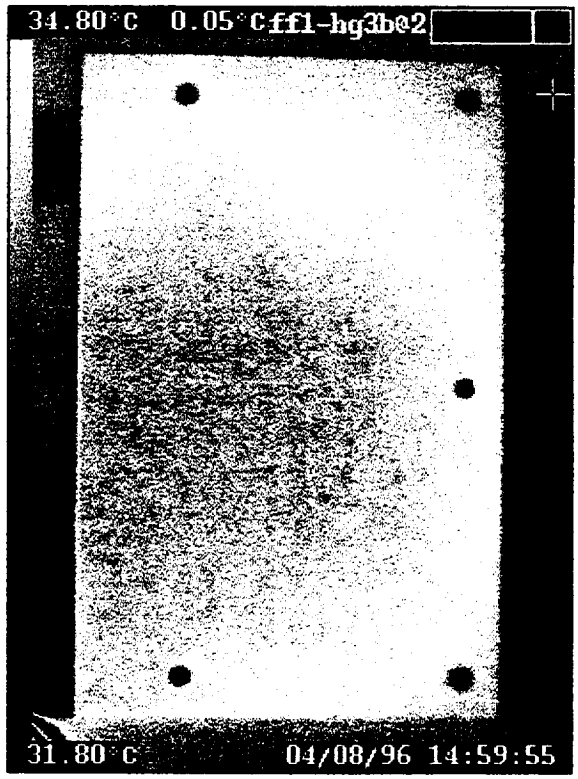

(3b) Bag side

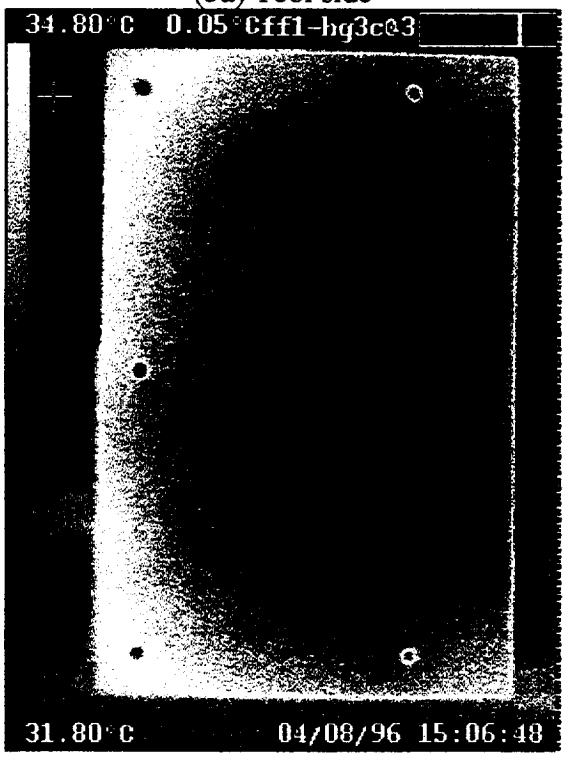

(3a) Tool side

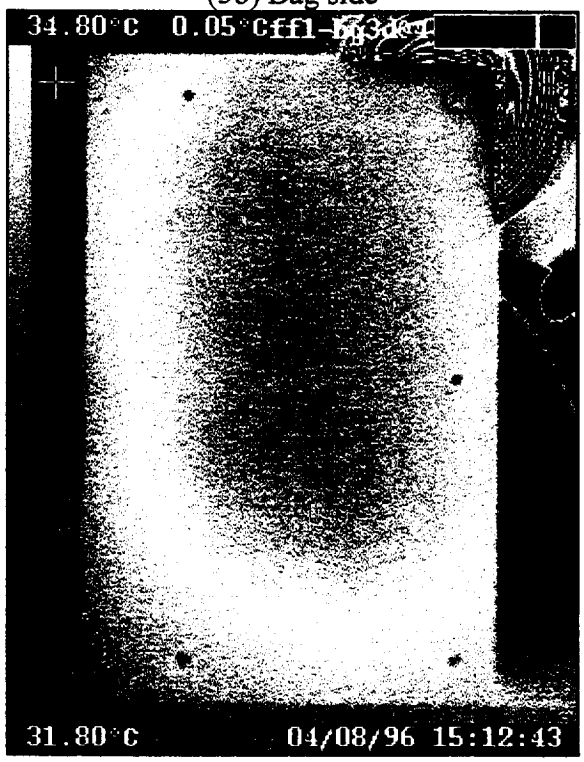

(3b) Bag side

12.5 INTER TANK PANELS

12.5.1 Panel 2

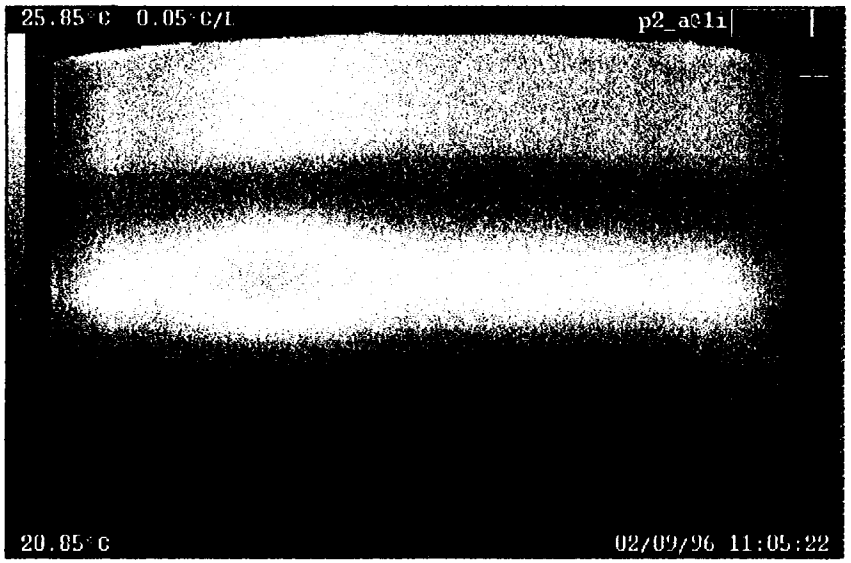

Pass A, Front

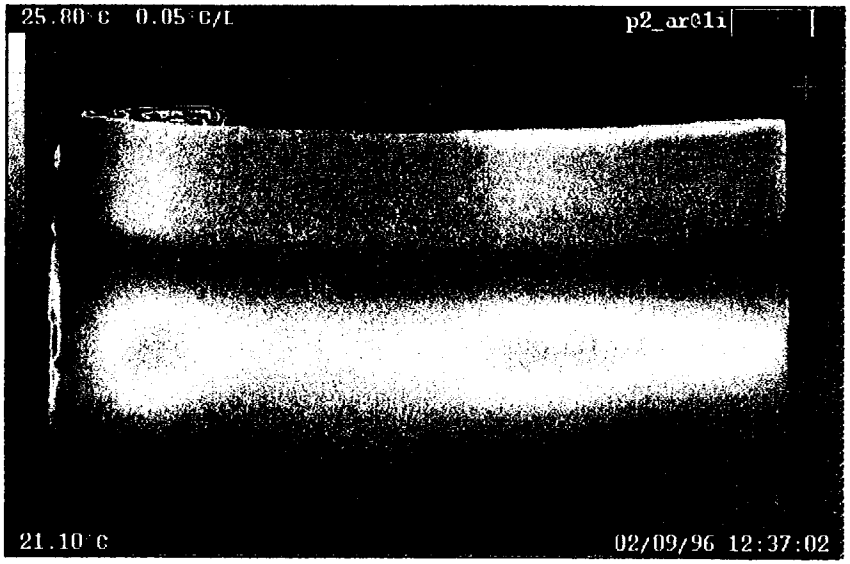

Pass A, Back

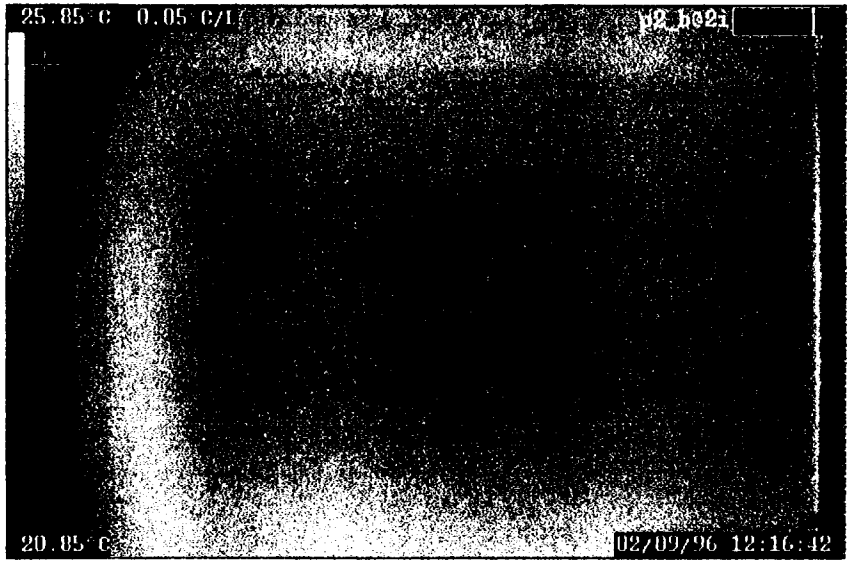

Pass B, Front

Pass B, Back

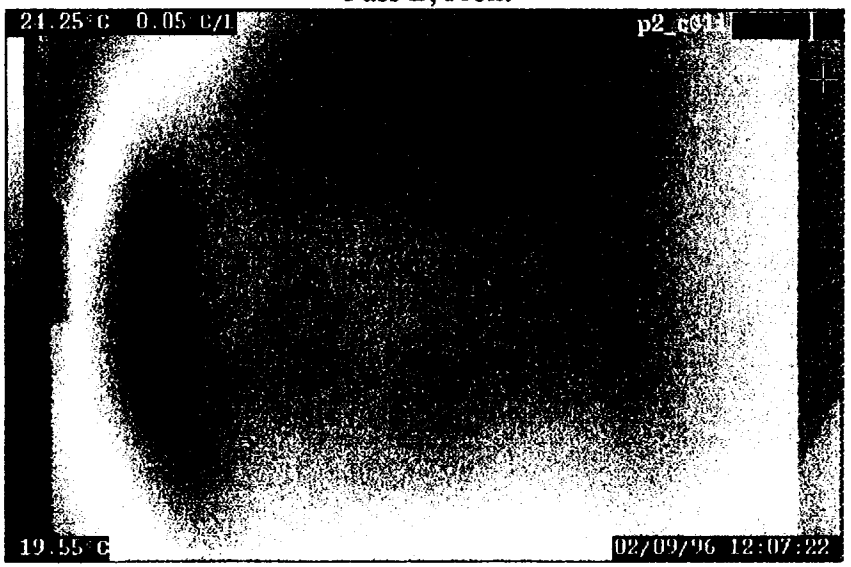

Pass C, Front

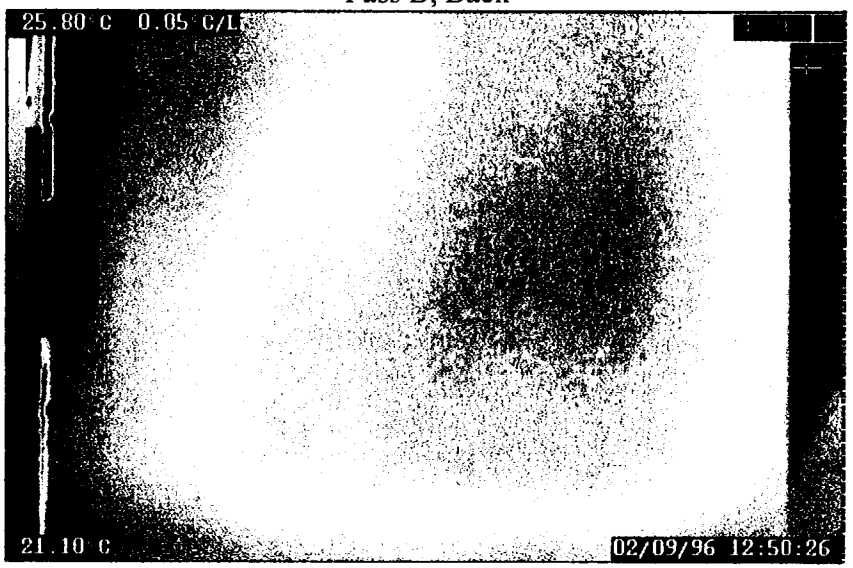

Pass C, Back

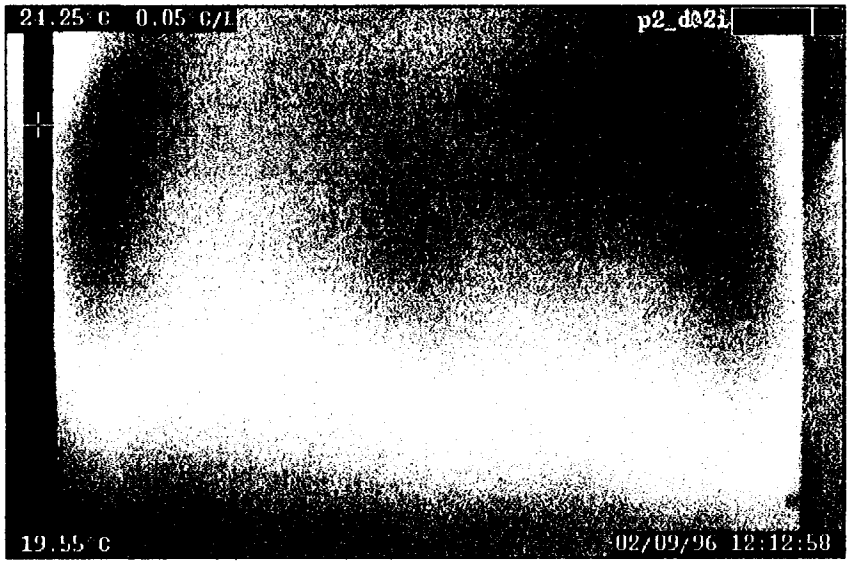

Pass D, Front

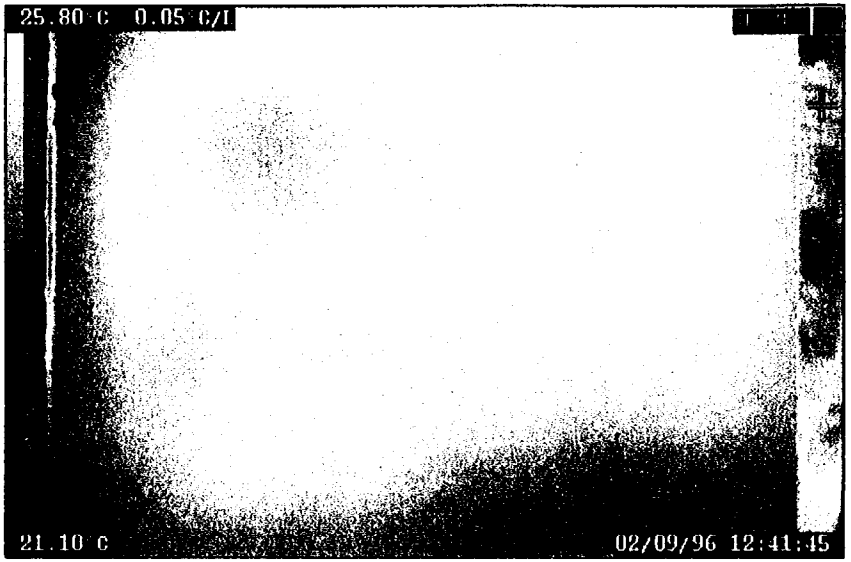

Pass D, Back

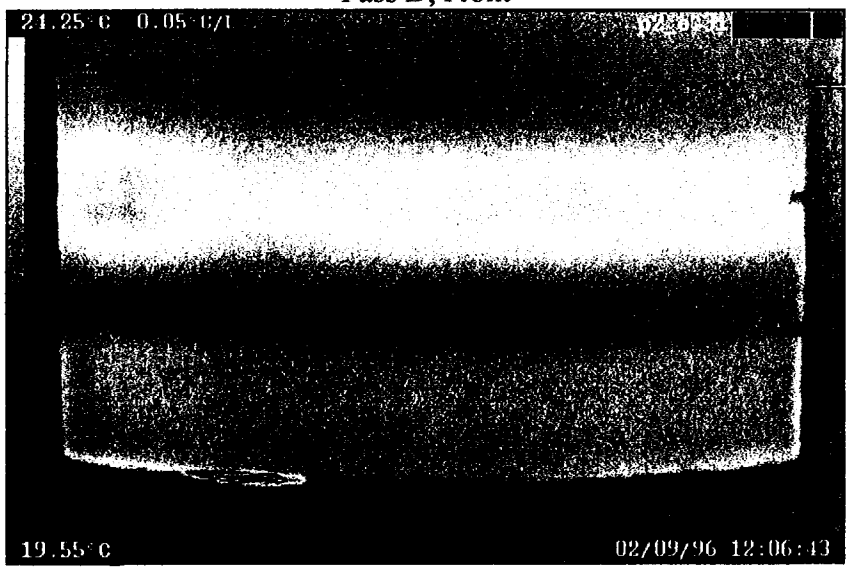

Pass E, Front

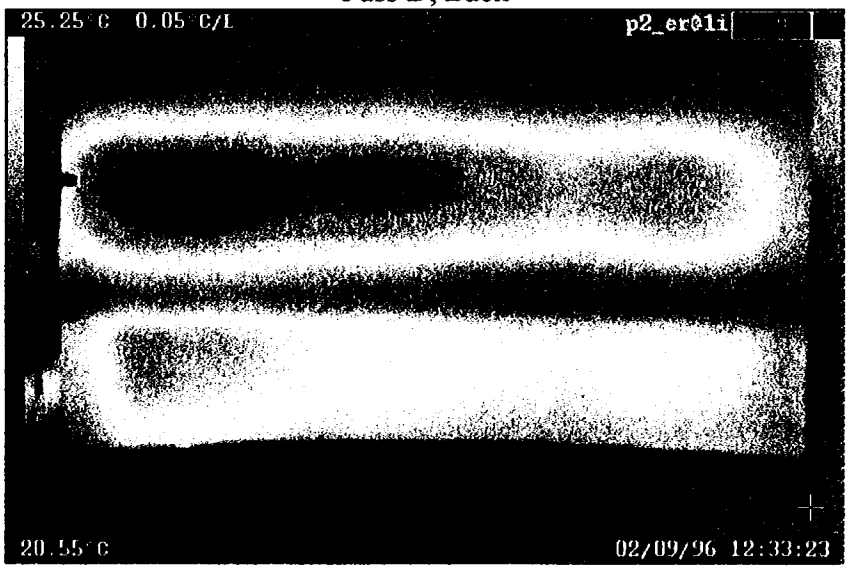

Pass E, Back

12.5.2 Panel 3

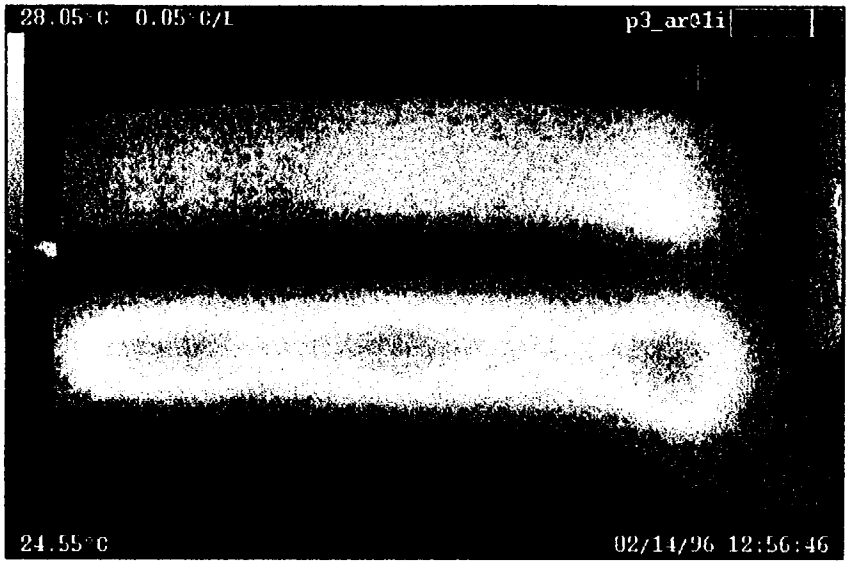

Pass A, Front

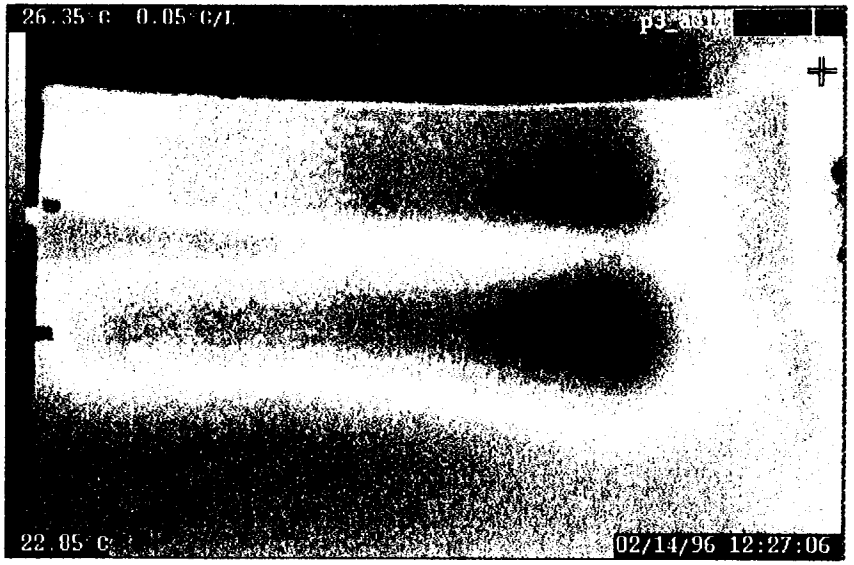

Pass A, Back

Pass B, Front

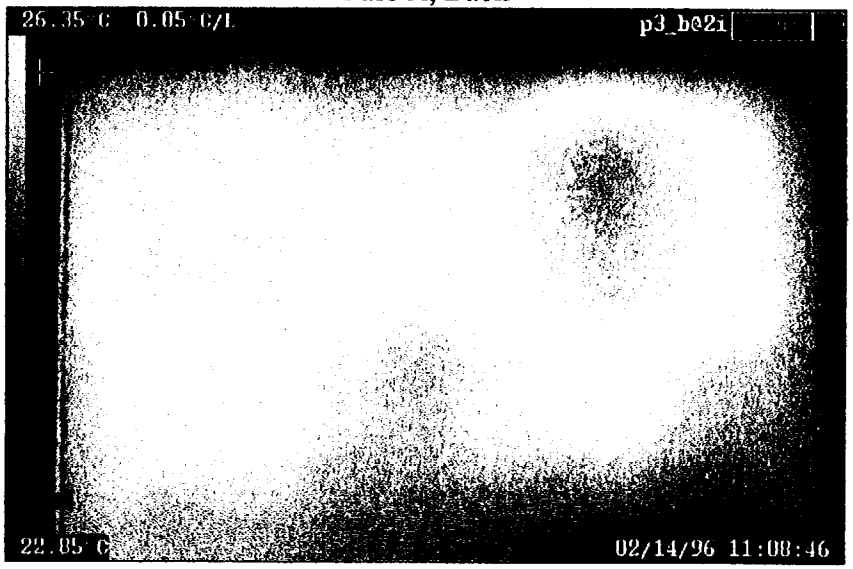

Pass B, Back

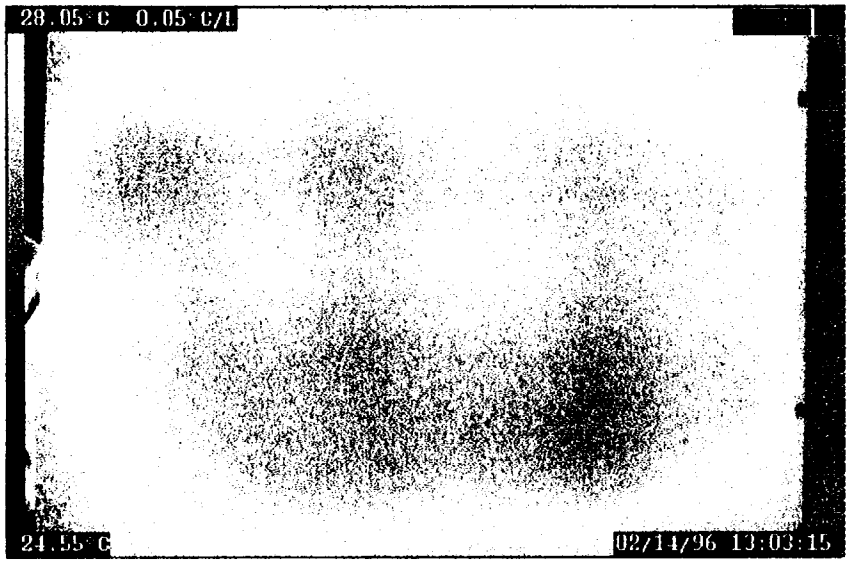

Pass C, Front

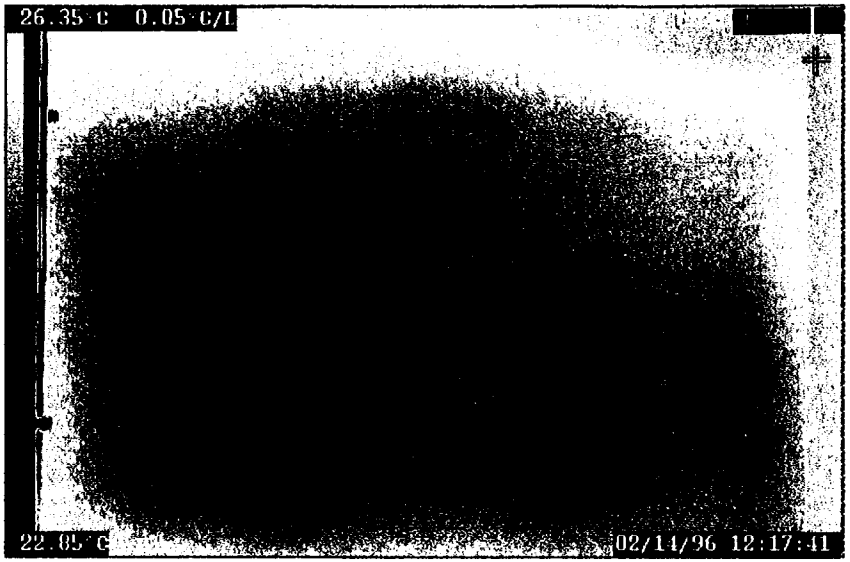

Pass C, Back

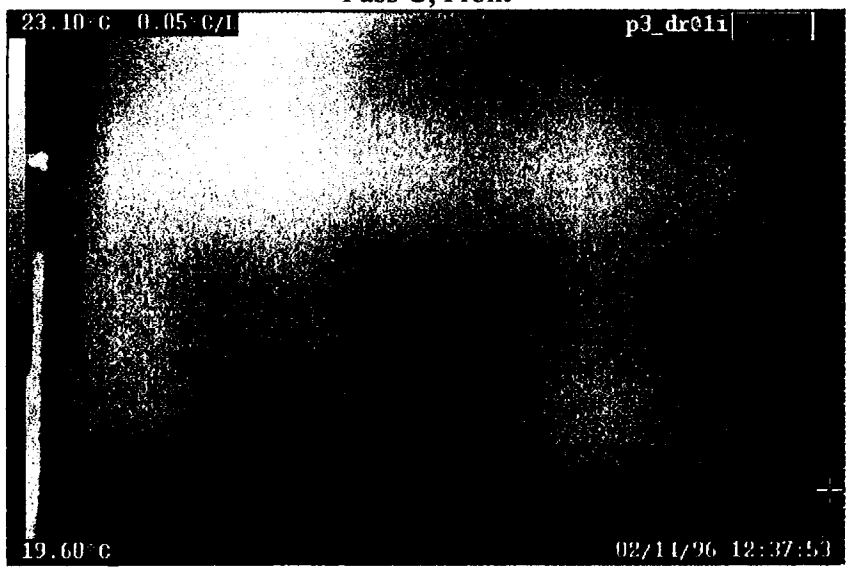

Pass D, Front

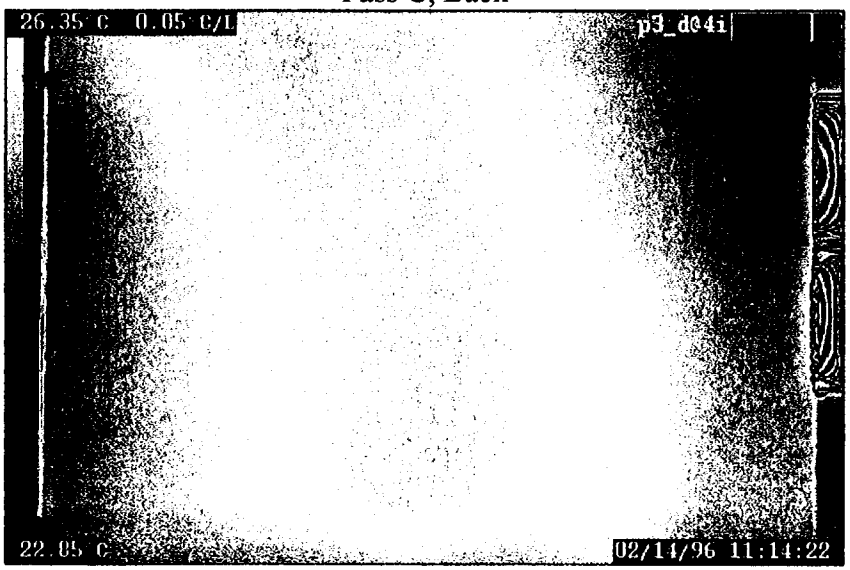

Pass D, Back

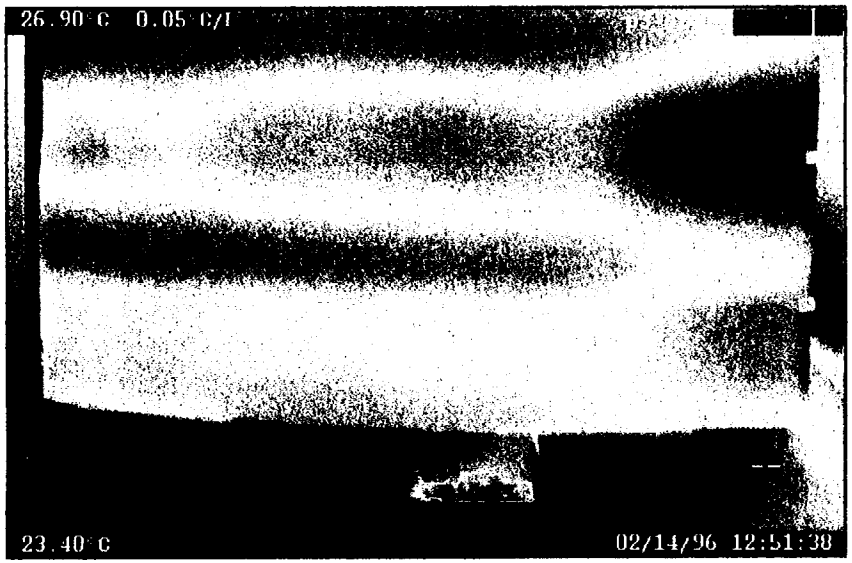

Pass E, Front

Pass E, Back

12.5.3 Panel 4

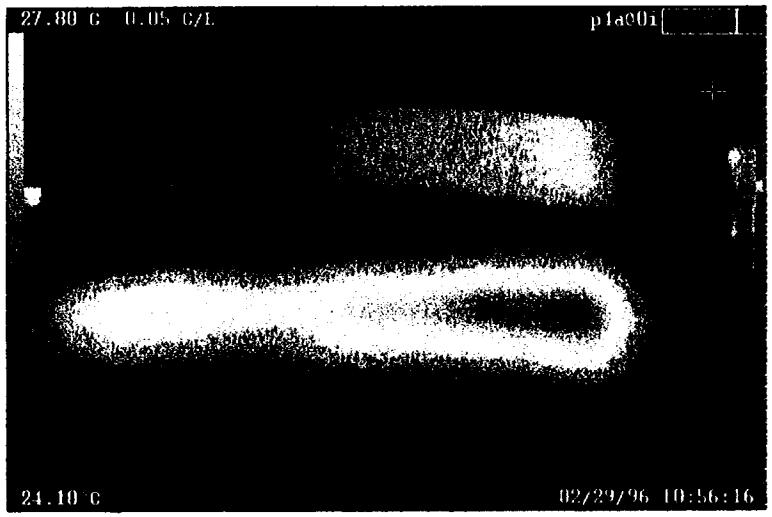

Inter Tank 4 Region A (Outside)

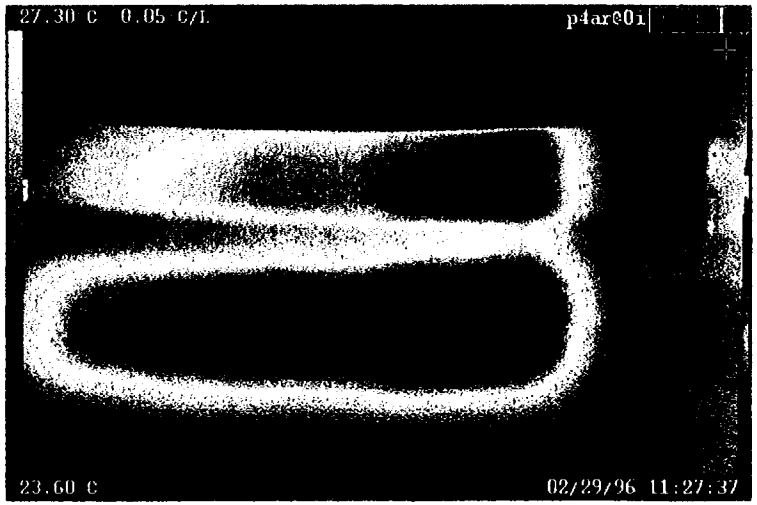

Inter Tank 4 Region A (Inside)

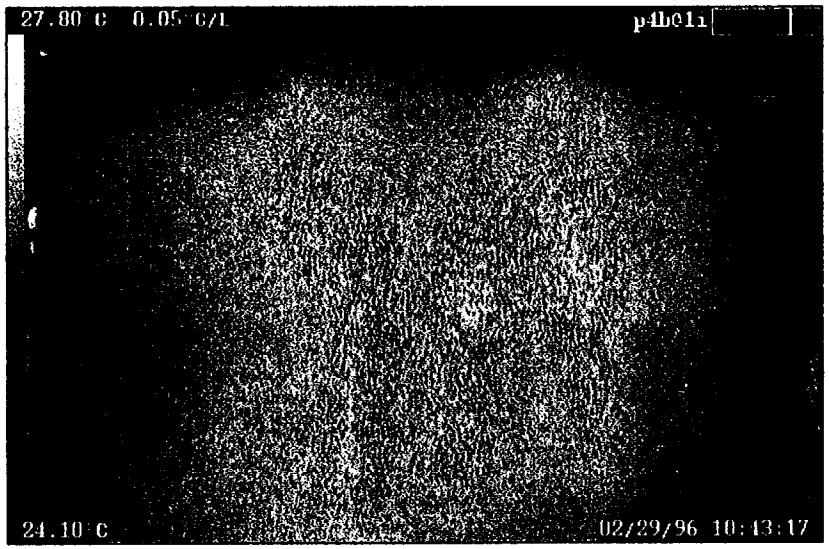

Inter Tank 4 Region B (Outside)

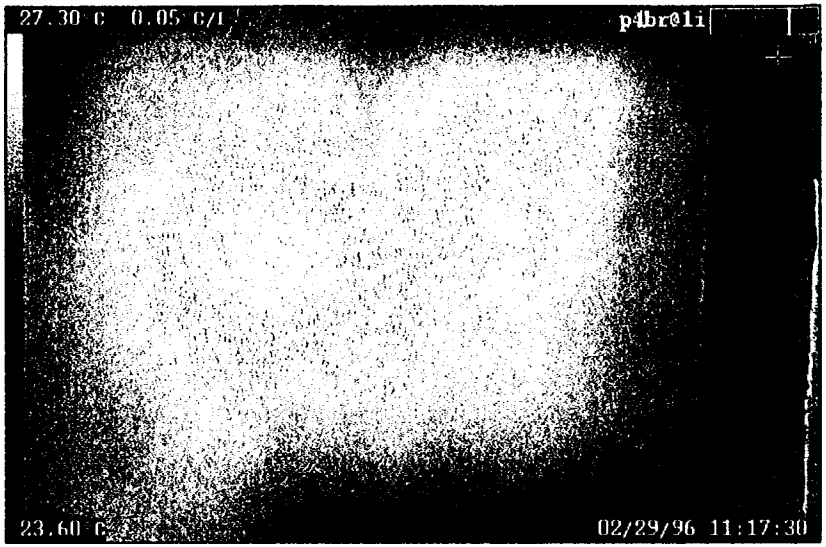

Inter Tank 4 Region B (Inside)

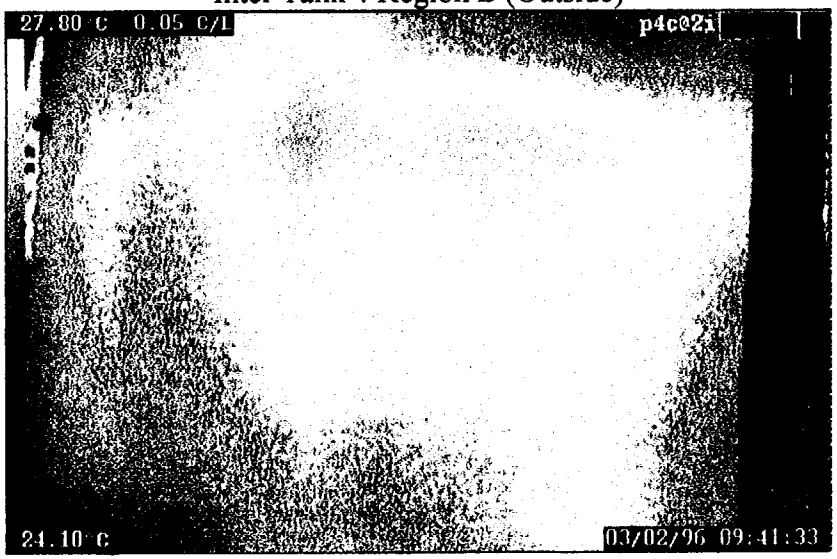

Inter Tank 4 Region C (Outside)

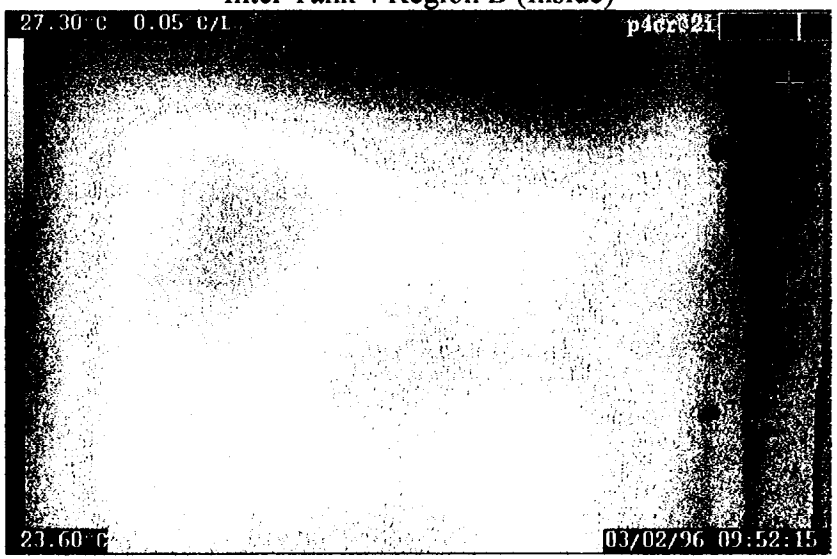

Inter Tank 4 Region C (Inside)

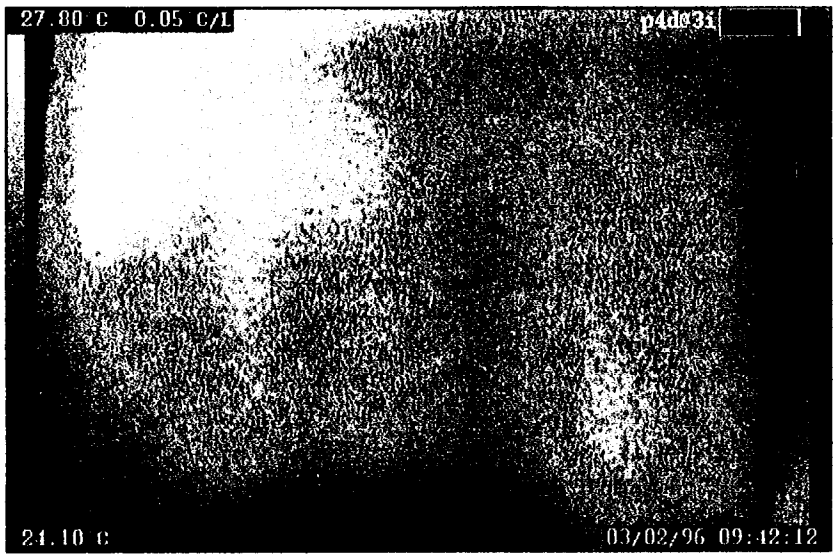

Inter Tank 4 Region D (Outside)

Inter Tank 4 Region D (Inside)

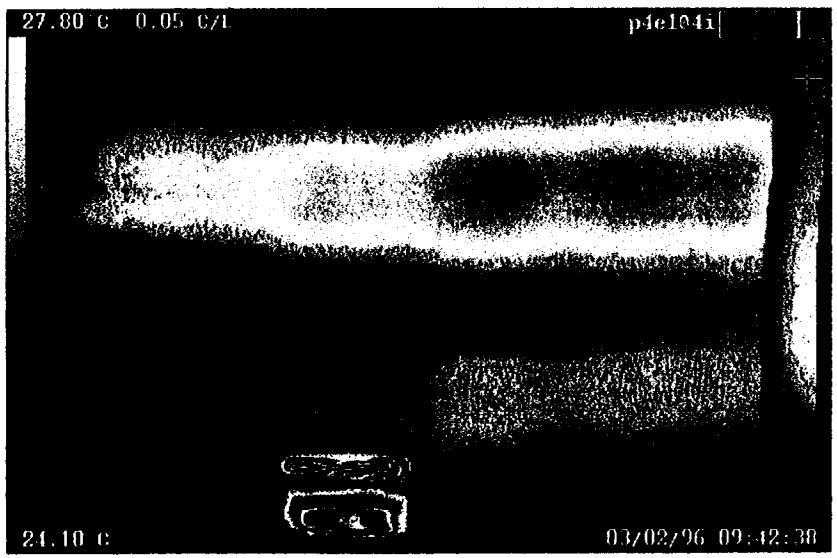

Inter Tank 4 Region E (Outside)

Inter Tank 4 Region E (Inside)

12.5.4 Panel 5

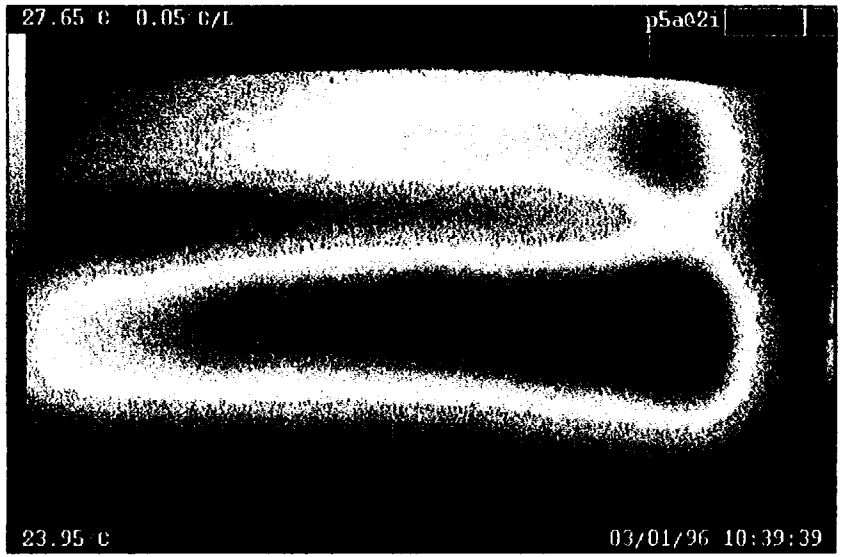

Inter Tank 5 Region A (Outside)

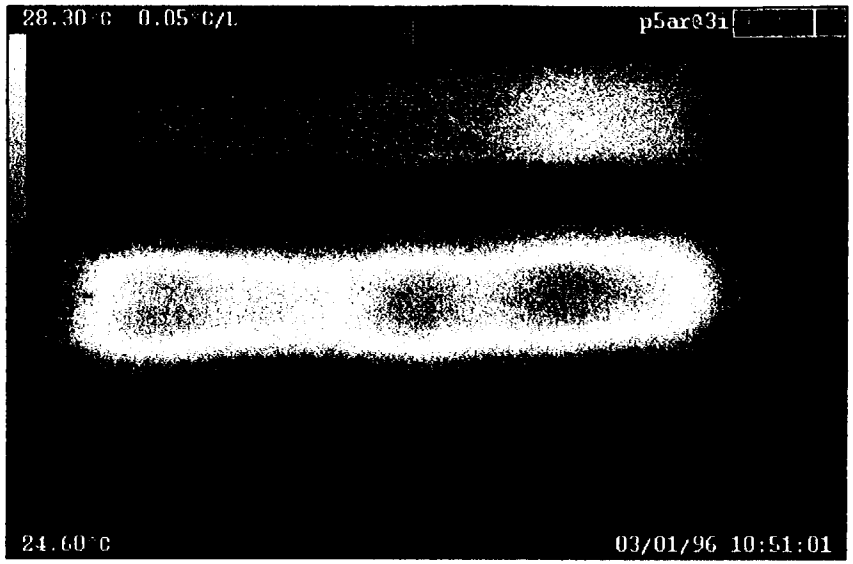

Inter Tank 5 Region A (Inside)

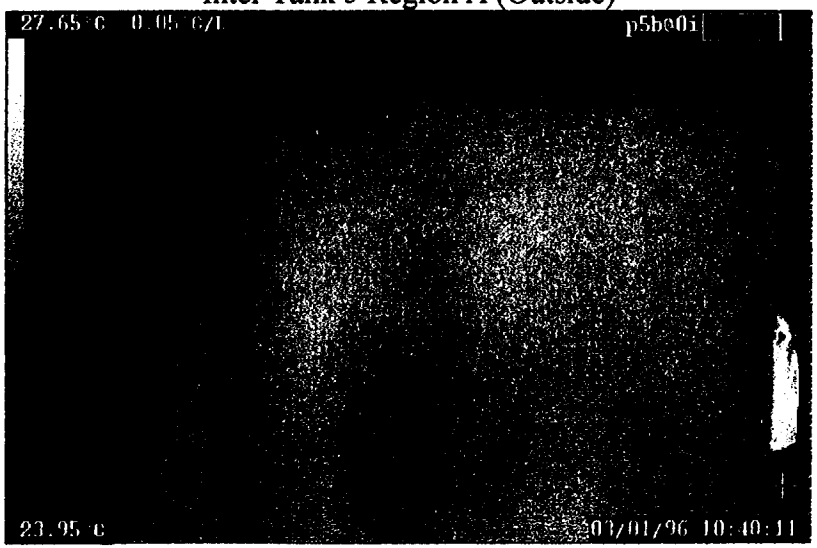

Inter Tank 5 Region B (Outside)

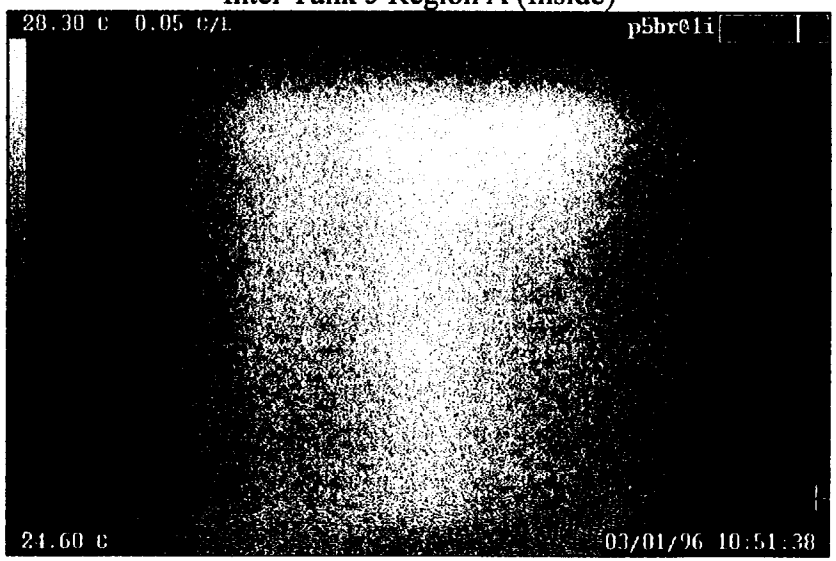

Inter Tank 5 Region B (Inside)

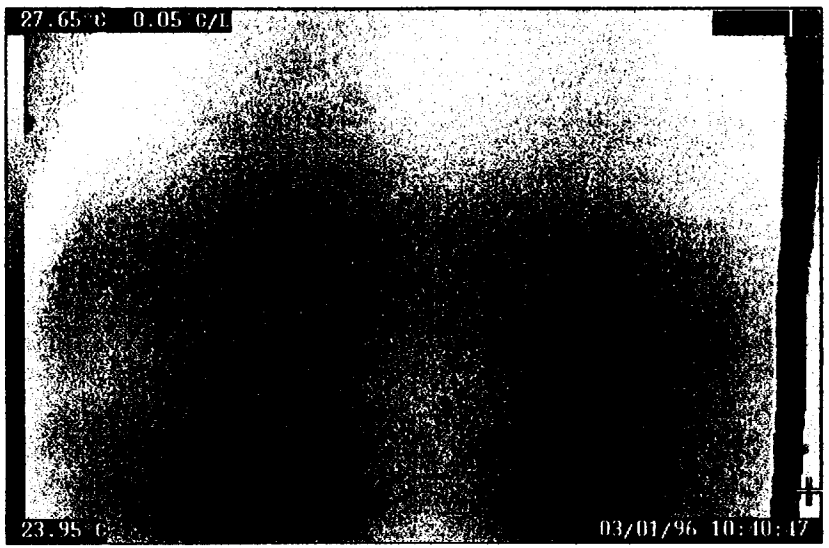

Inter Tank 5 Region C (Outside)

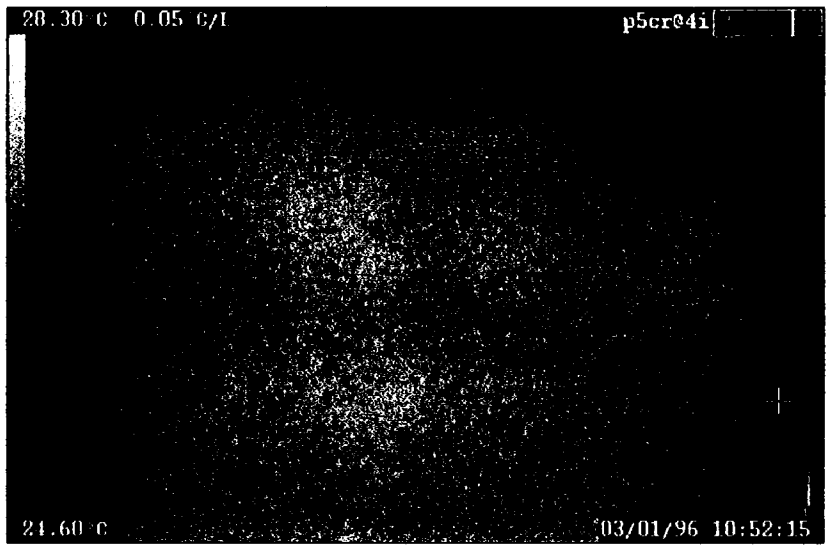

Inter Tank 5 Region C (Inside)

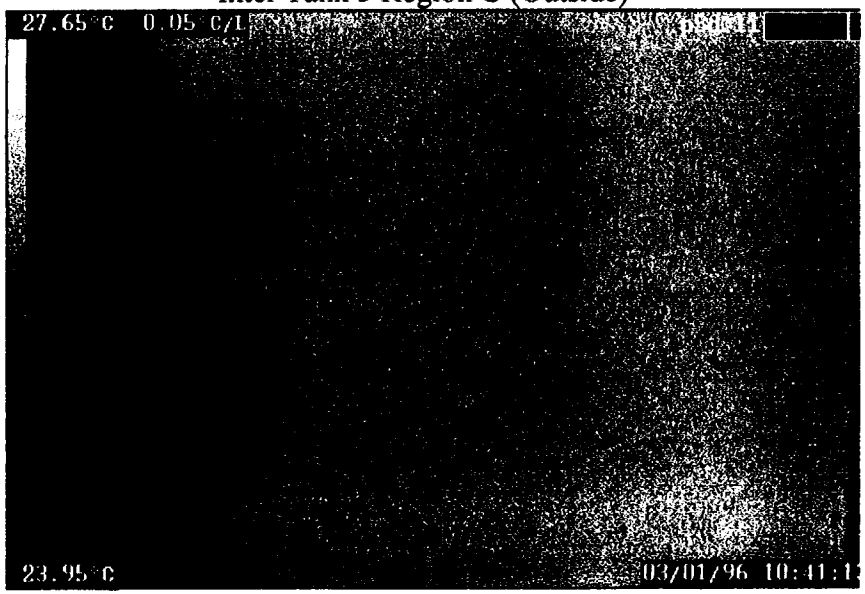

Inter Tank 5 Region D (Outside)

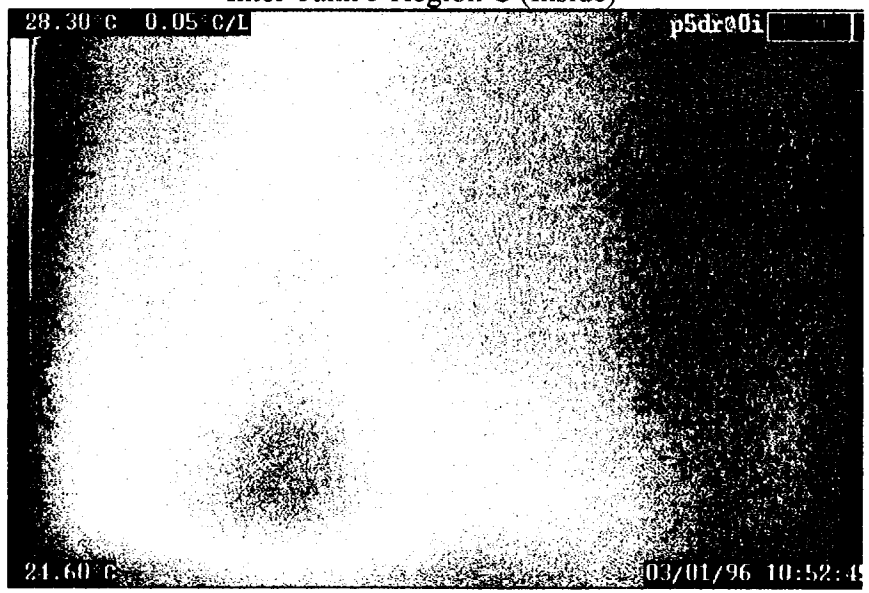

Inter Tank 5 Region D (Inside)

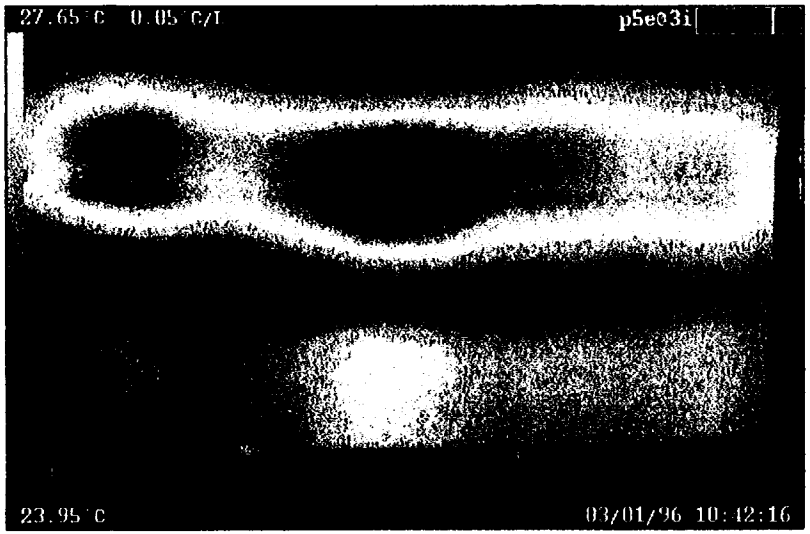

Inter Tank 5 Region E (Outside)

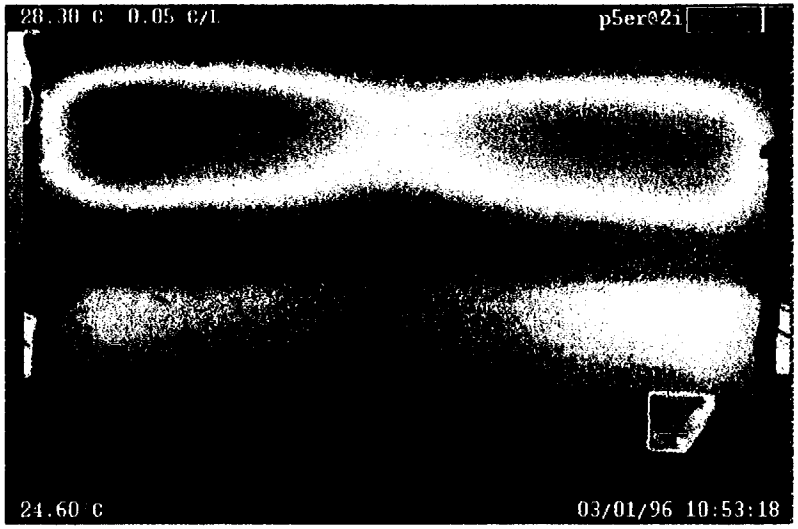

Inter Tank 5 Region E (Inside)

12.5.5 Panel 6

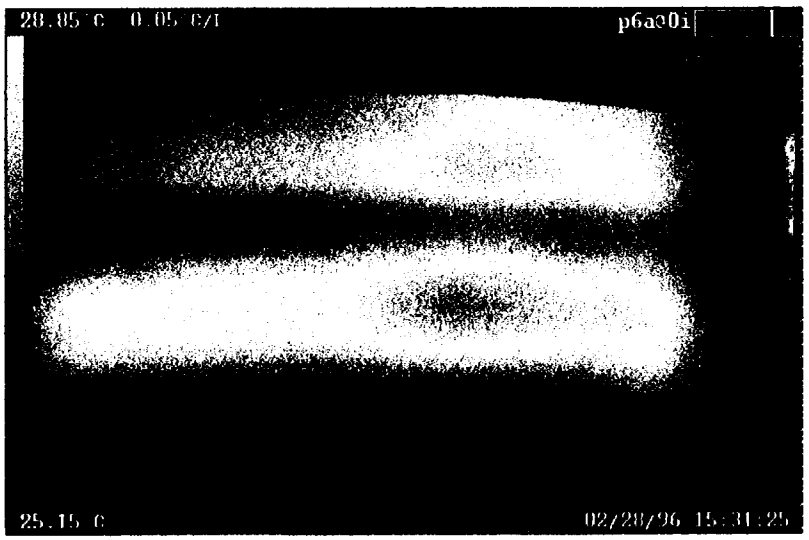

Inter Tank 6 Region A (Outside)

Inter Tank 6 Region A (Inside)

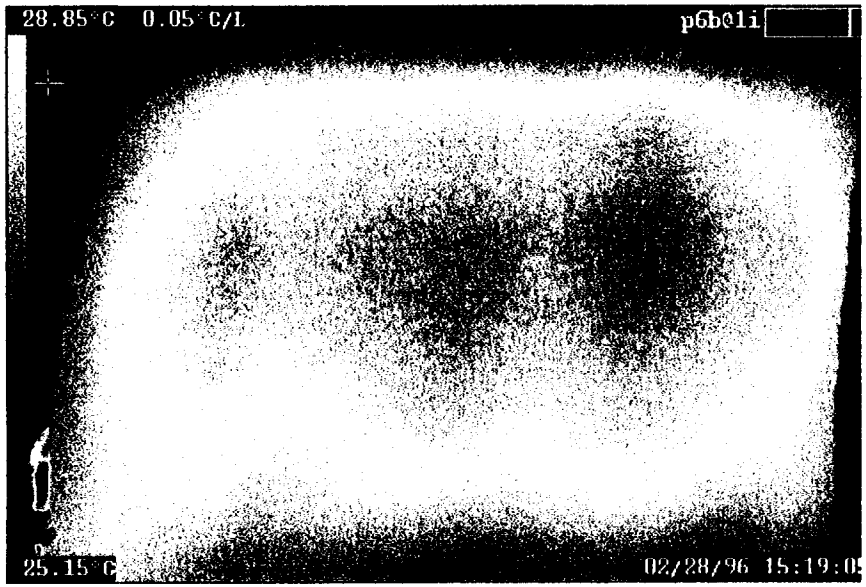

Inter Tank 6 Region B (Outside)

Inter Tank 6 Region B (Inside)

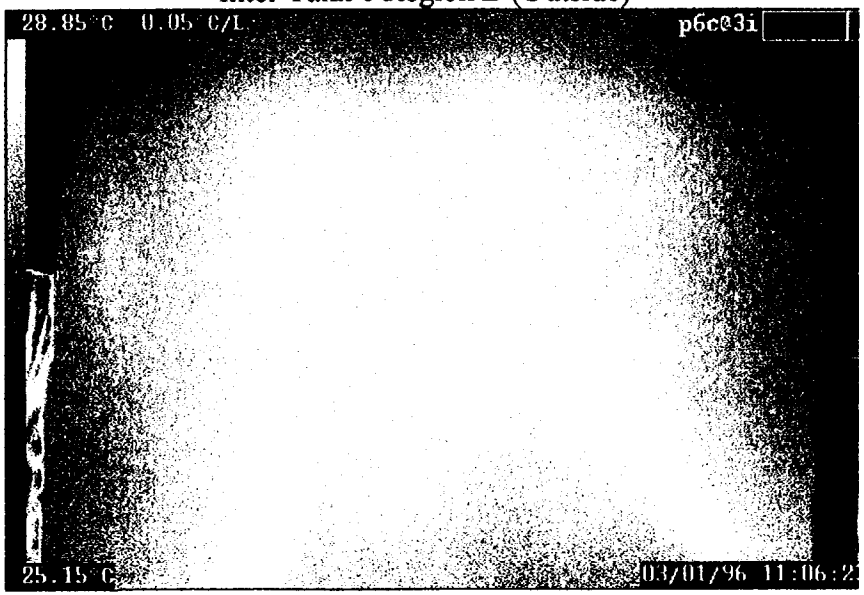

Inter Tank 6 Region C (Outside)

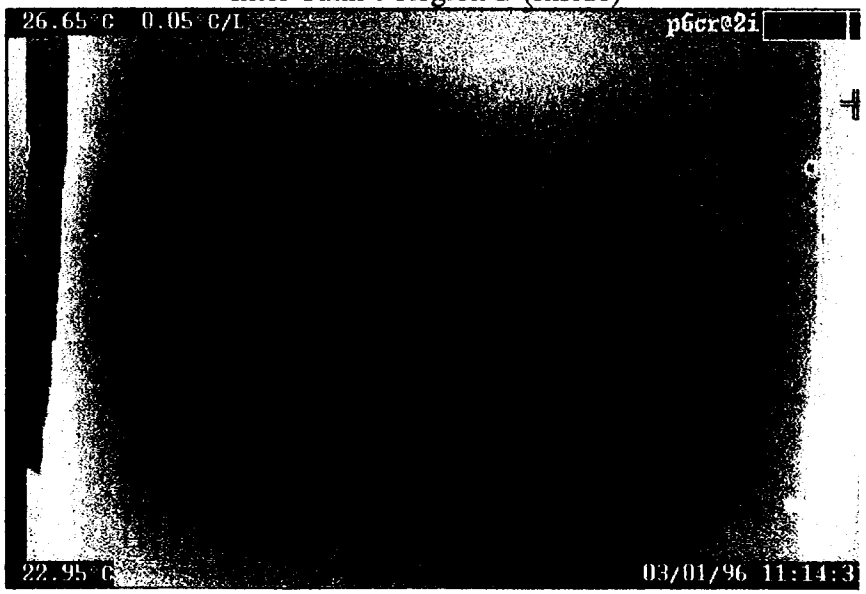

Inter Tank 6 Region C (Inside)

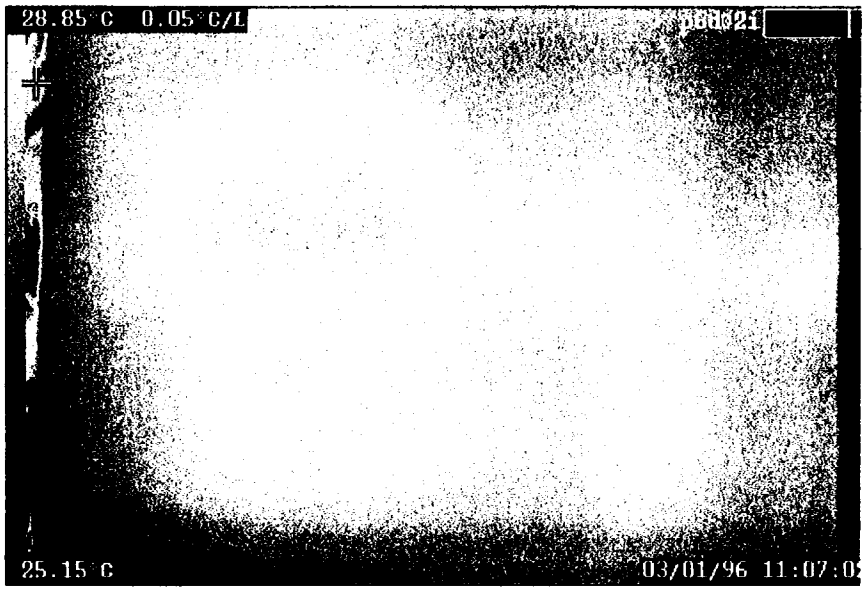

Inter Tank 6 Region D (Outside)

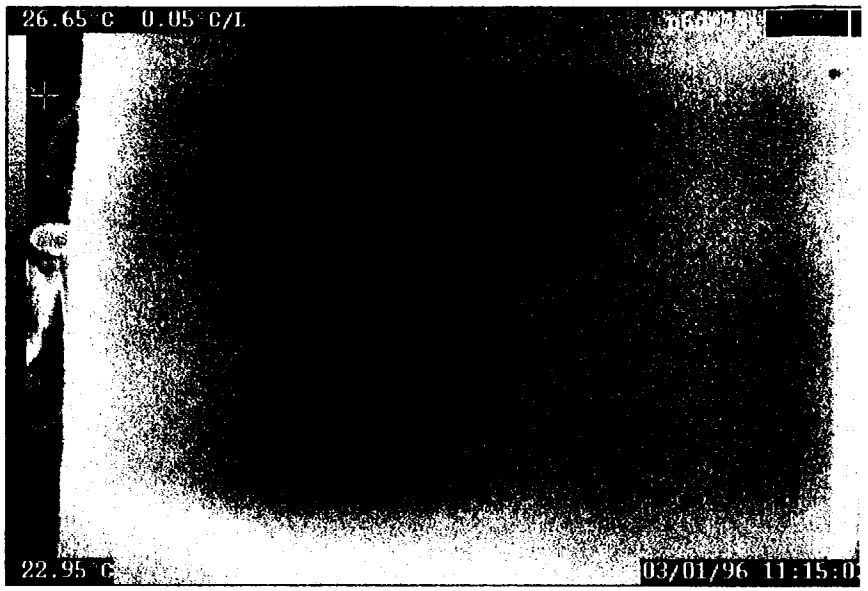

Inter Tank 6 Region D (Inside)

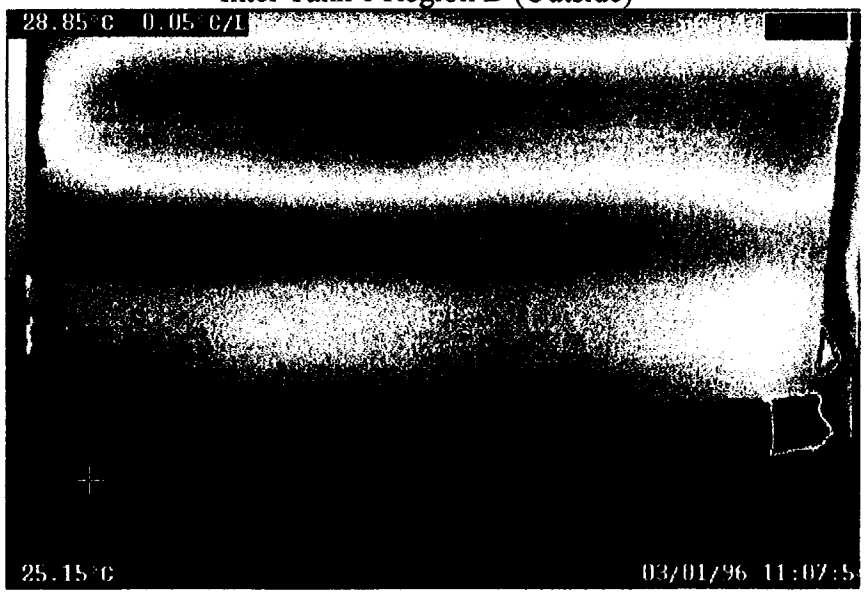

Inter Tank 6 Region E (Outside)

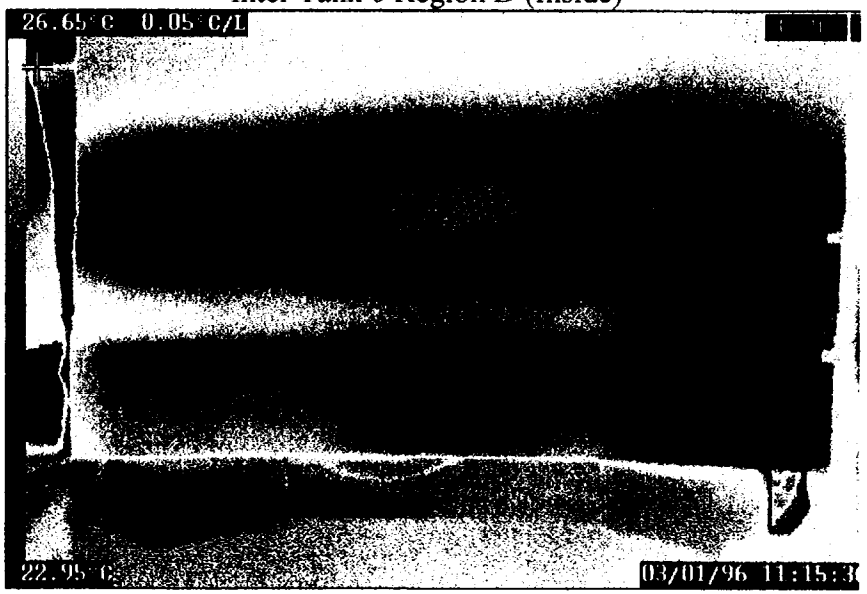

Inter Tank 6 Region E (Inside)

12.5.6 Panel 7

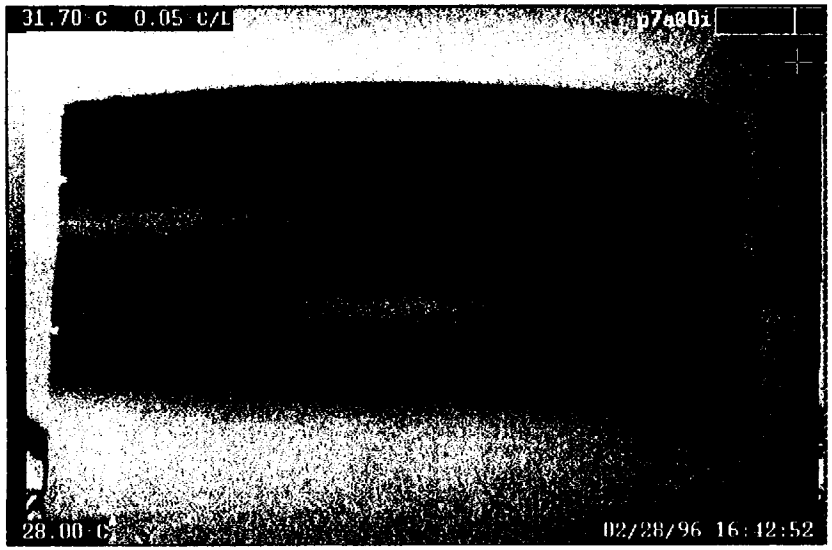

Inter Tank 7 Region A (Outside)

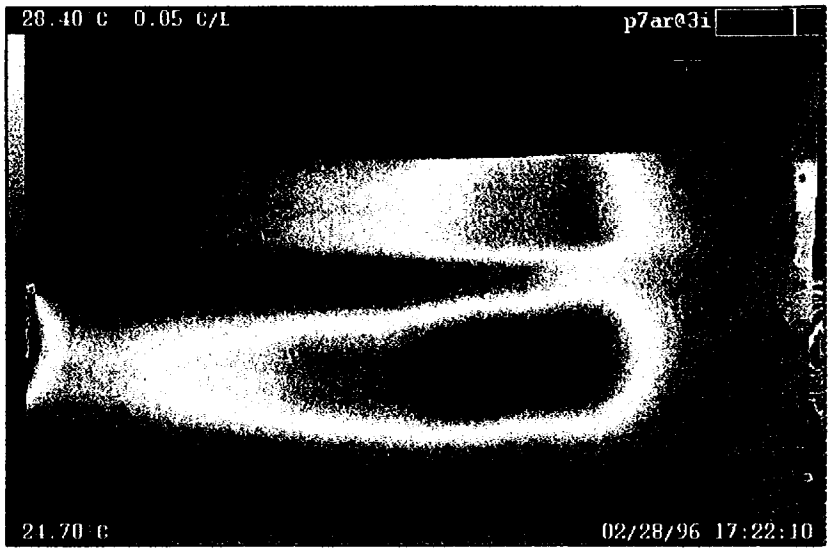

Inter Tank 7 Region A (Inside)

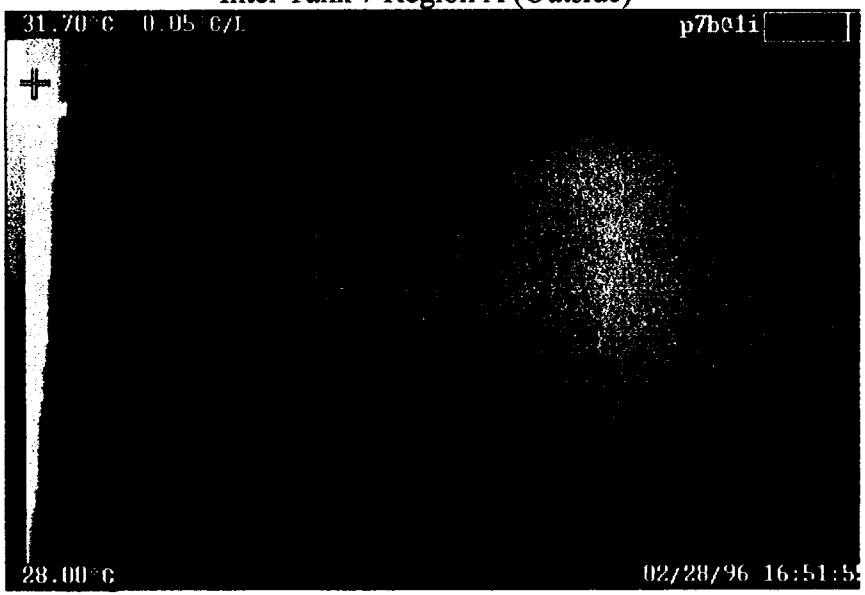

Inter Tank 7 Region B (Outside)

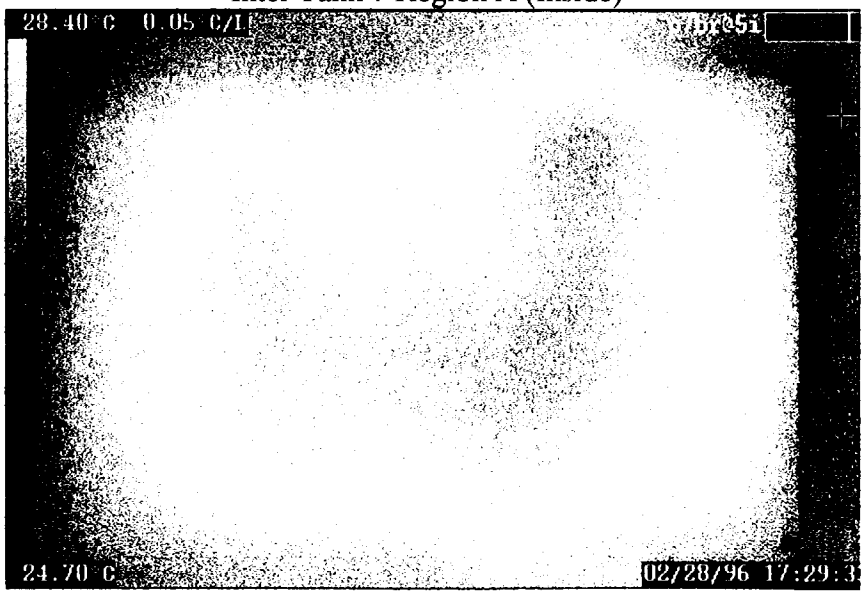

Inter Tank 7 Region B (Inside)

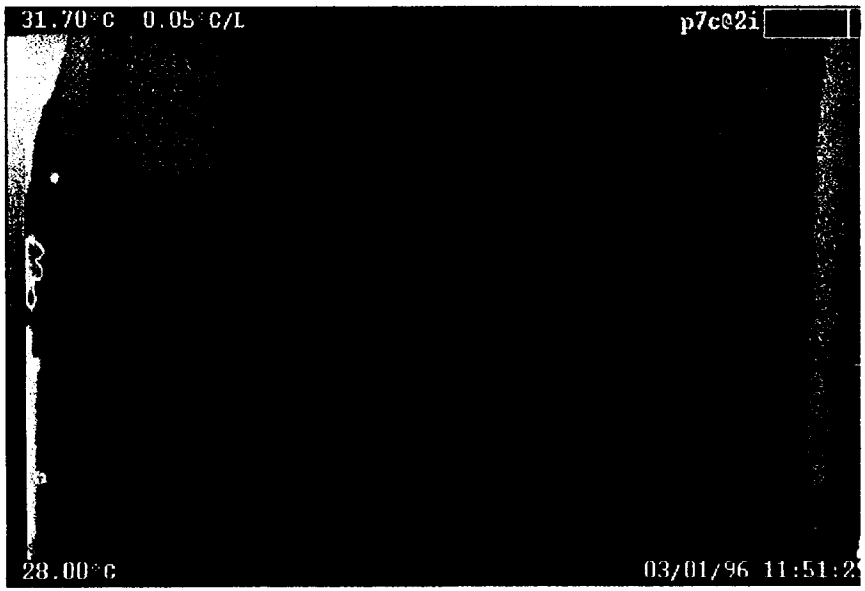

Inter Tank 7 Region C (Outside)

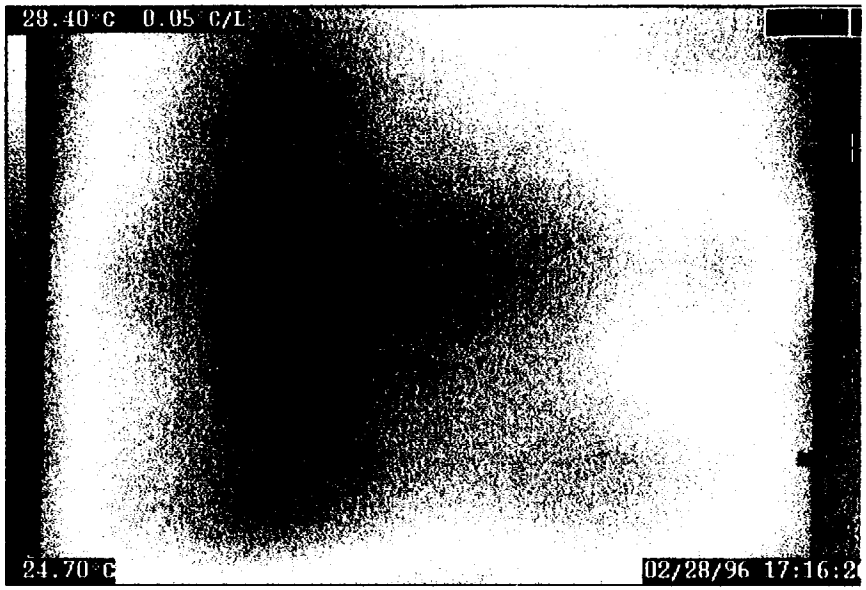

Inter Tank 7 Region C (Inside)

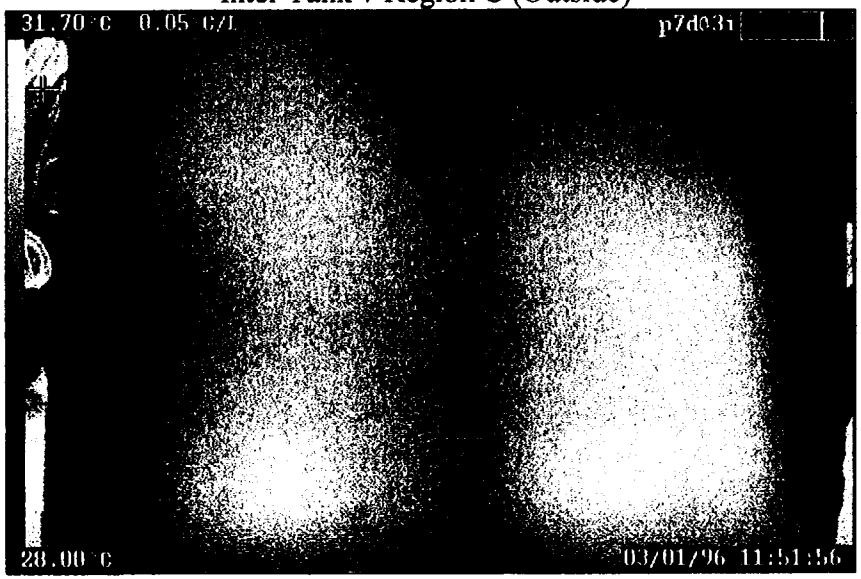

Inter Tank 7 Region D (Outside)

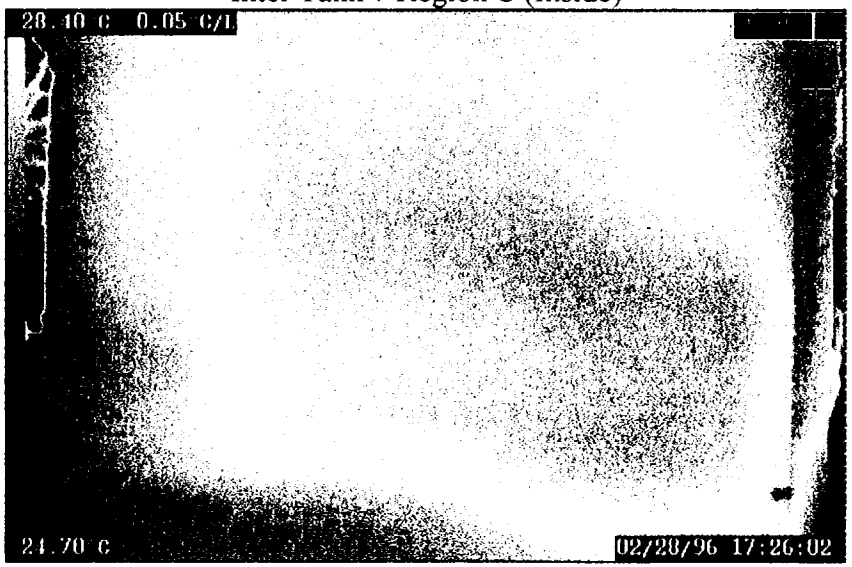

Inter Tank 7 Region D (Inside)

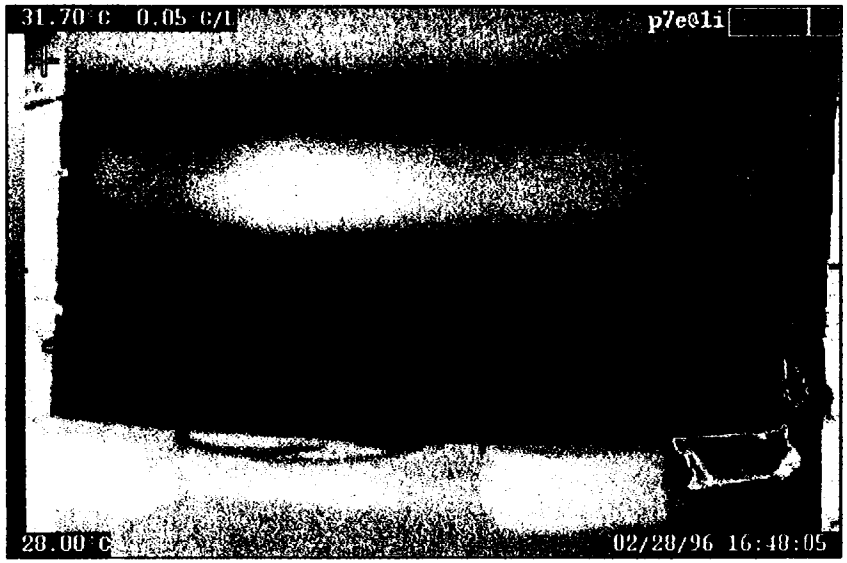

Inter Tank 7 Region E (Outside)

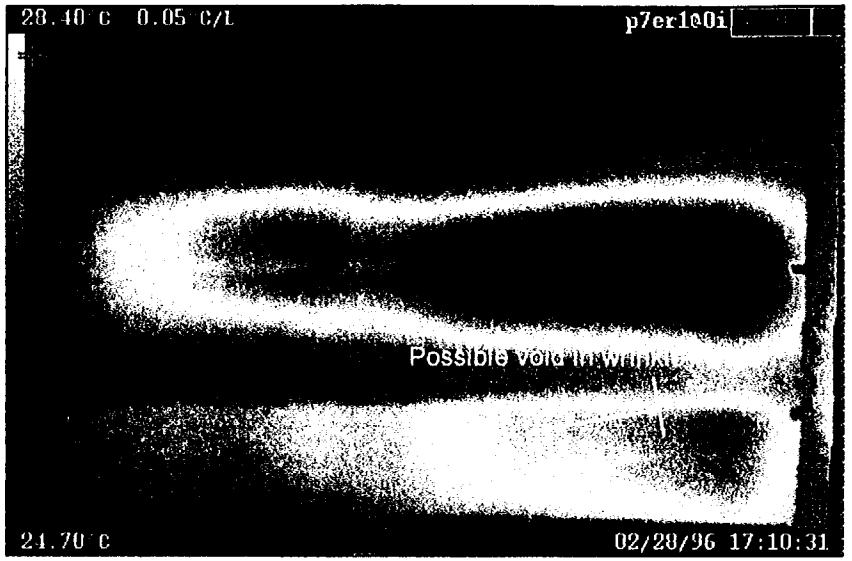

Inter Tank 7 Region E (Inside)

Inter Tank 7 Region A (Outside)

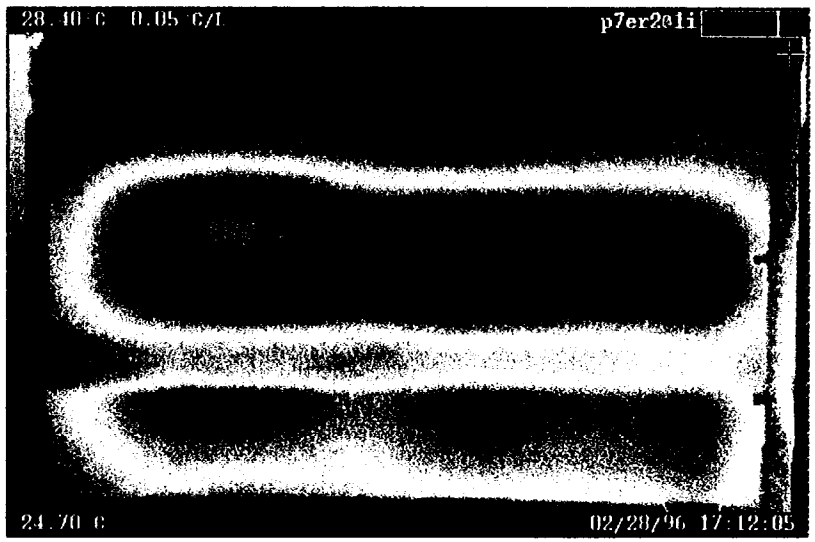

Inter Tank 7 Region E (Inside)

12.5.7 Panel 8

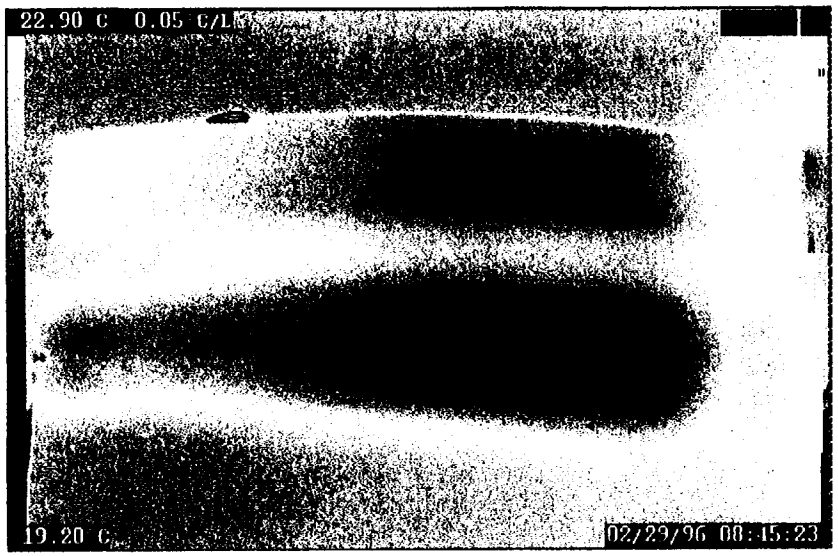

Inter Tank 8 Region A (Outside)

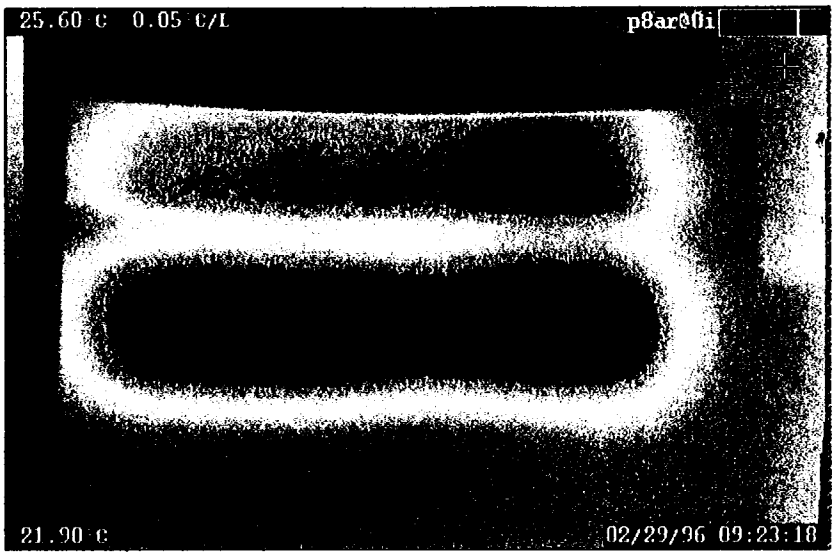

Inter Tank 8 Region A (Inside)

Inter Tank 8 Region B (Outside)

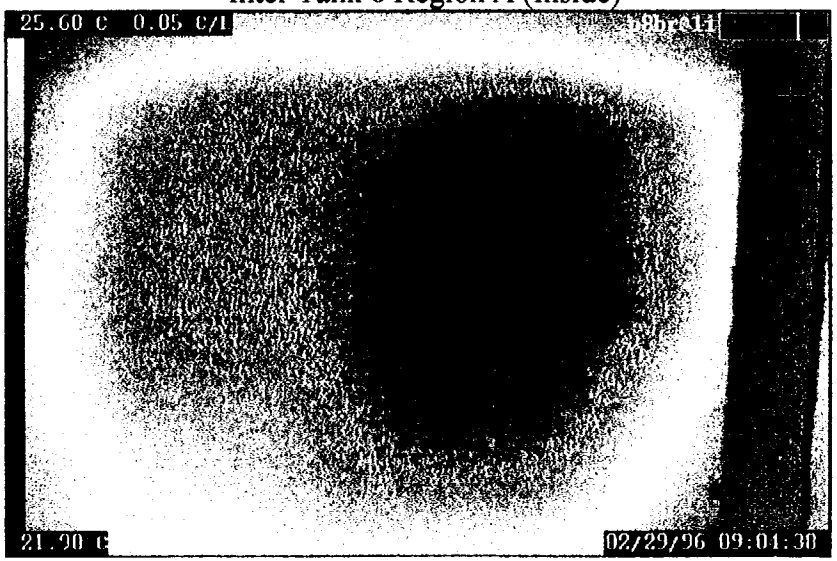

Inter Tank 8 Region B (Inside)

Inter Tank 8 Region C (Outside)

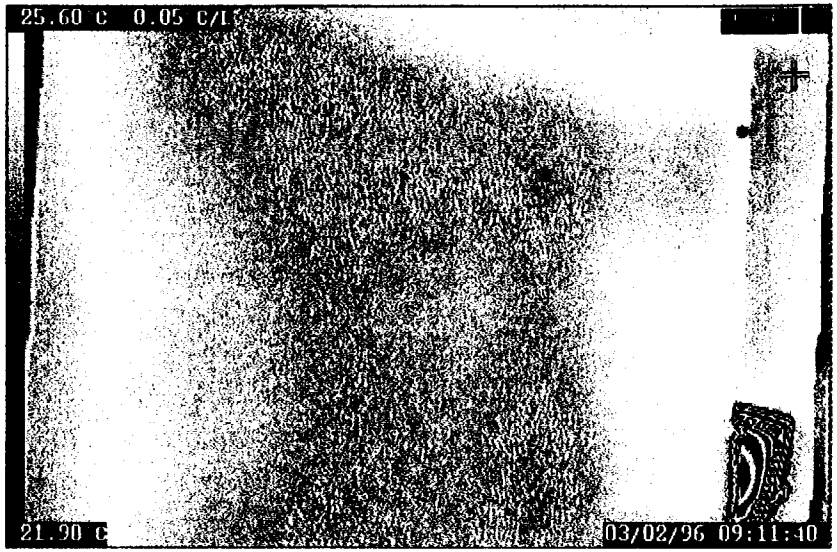

Inter Tank 8 Region C (Inside)

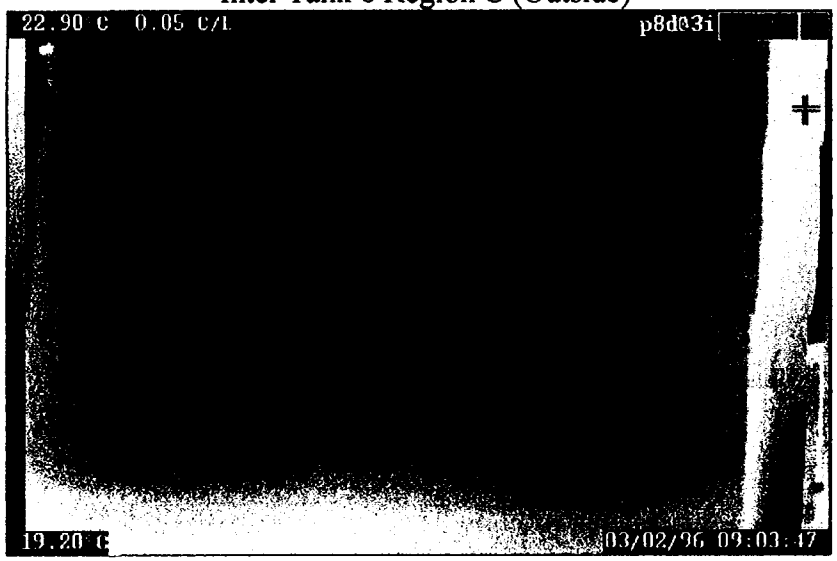

Inter Tank 8 Region D (Outside)

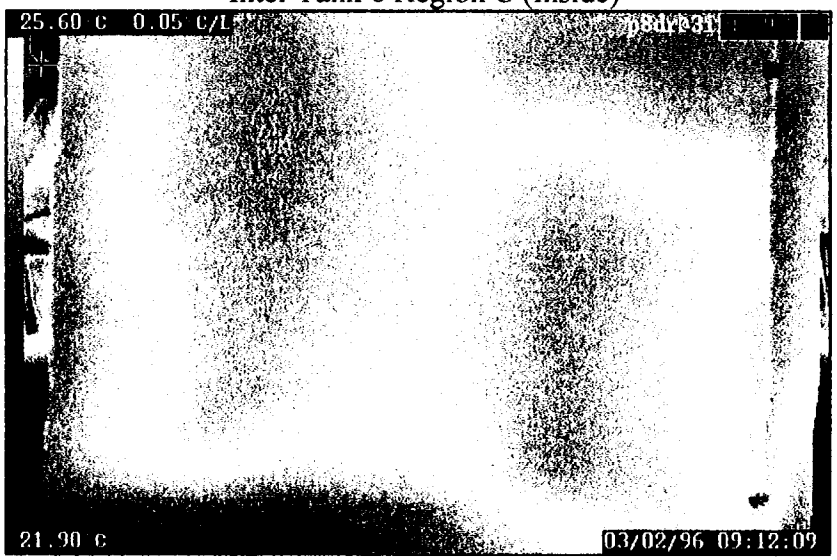

Inter Tank 8 Region D (Inside)

Inter Tank 8 Region E (Outside)

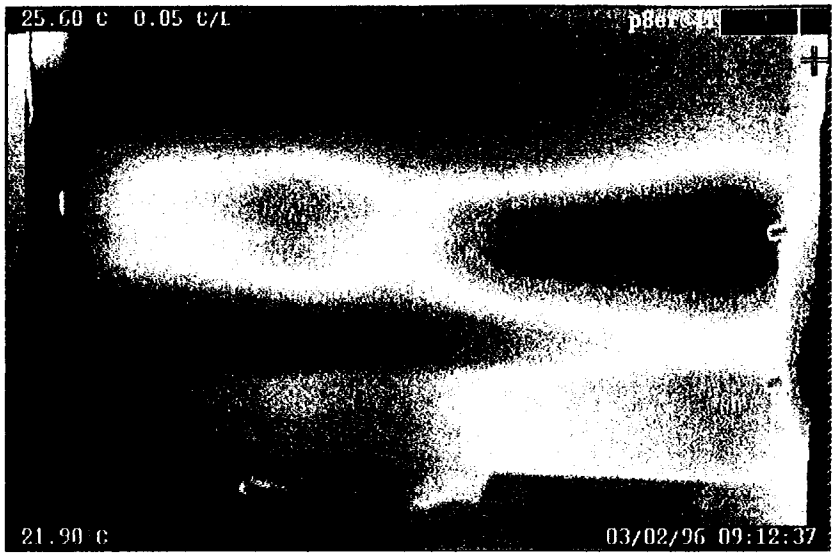

Inter Tank 8 Region E (Inside)

12.5.8 Panel 9

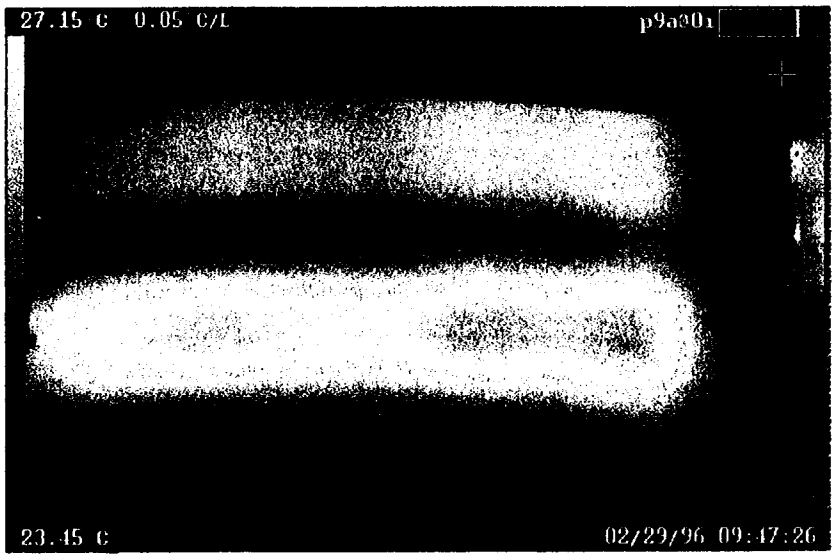

Inter Tank 9 Region A (Outside)

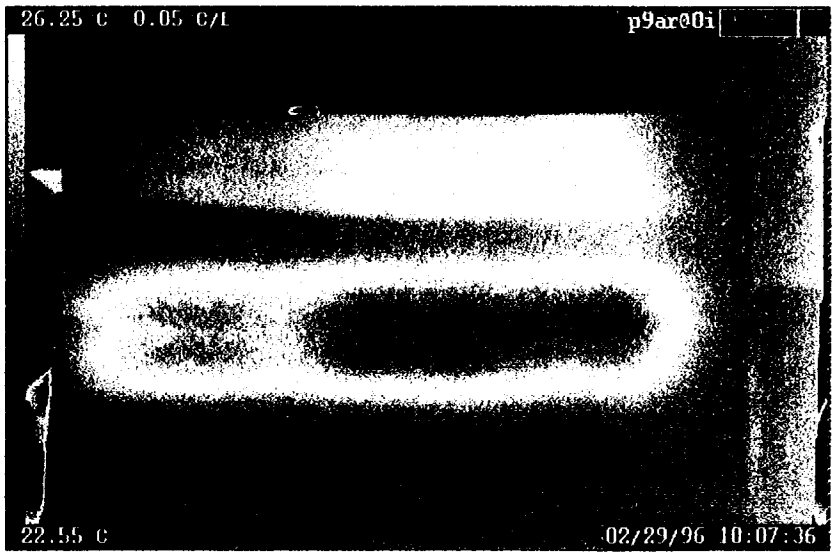

Inter Tank 9 Region A (Inside)

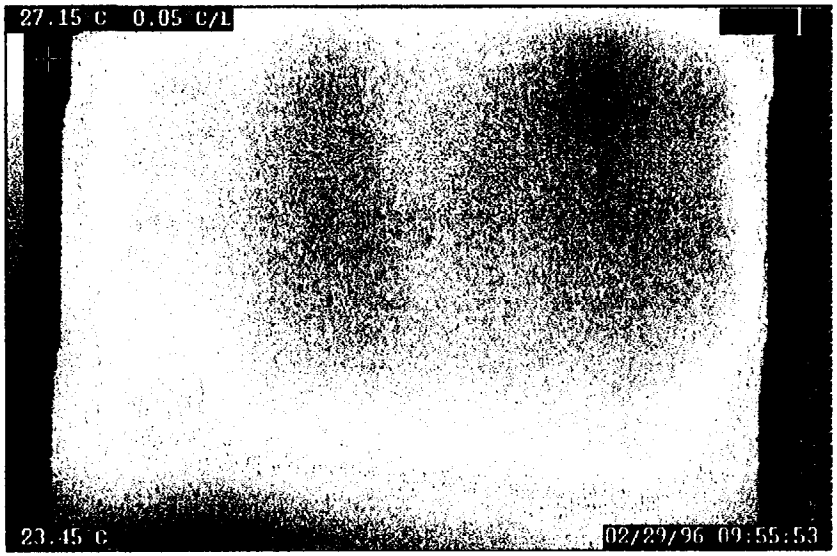

Inter Tank 9 Region B (Outside)

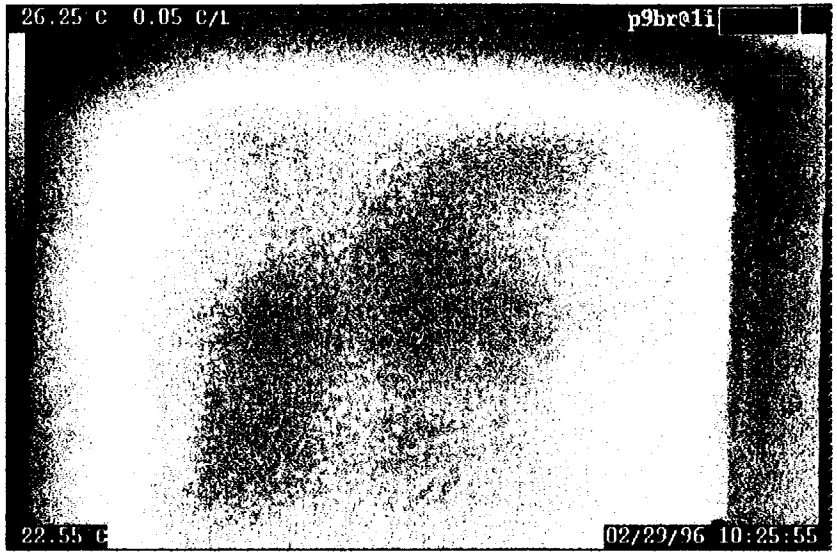

Inter Tank 9 Region B (Inside)

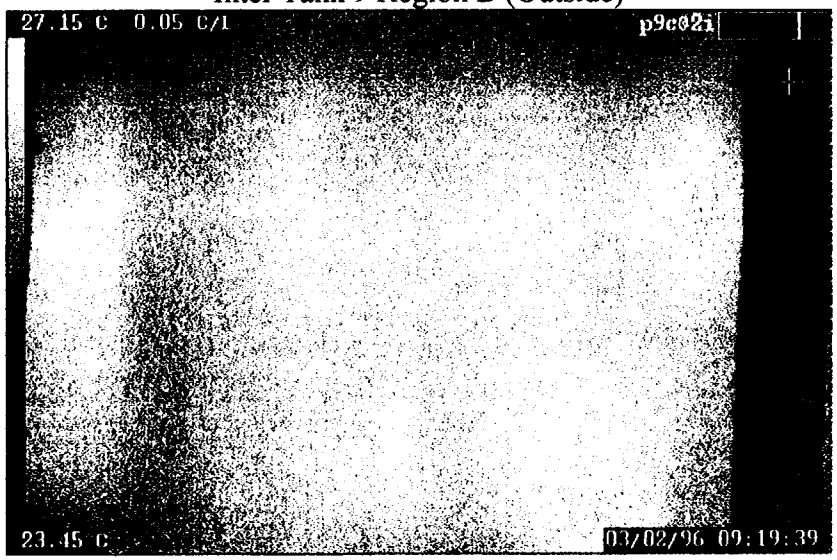

Inter Tank 9 Region C (Outside)

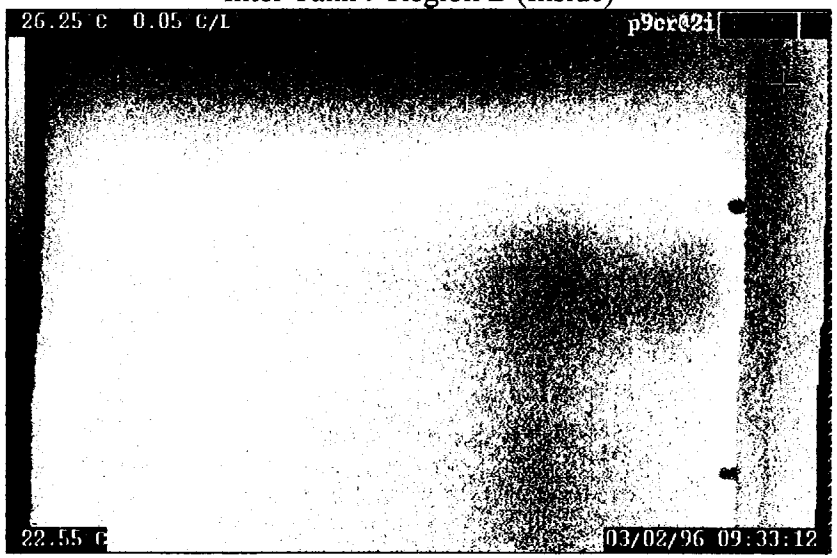

Inter Tank 9 Region C (Inside)

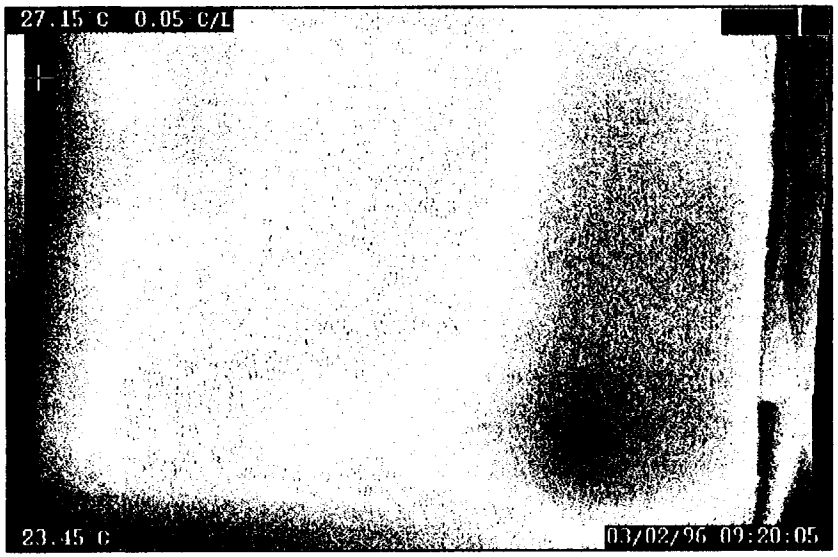

Inter Tank 9 Region D (Outside)

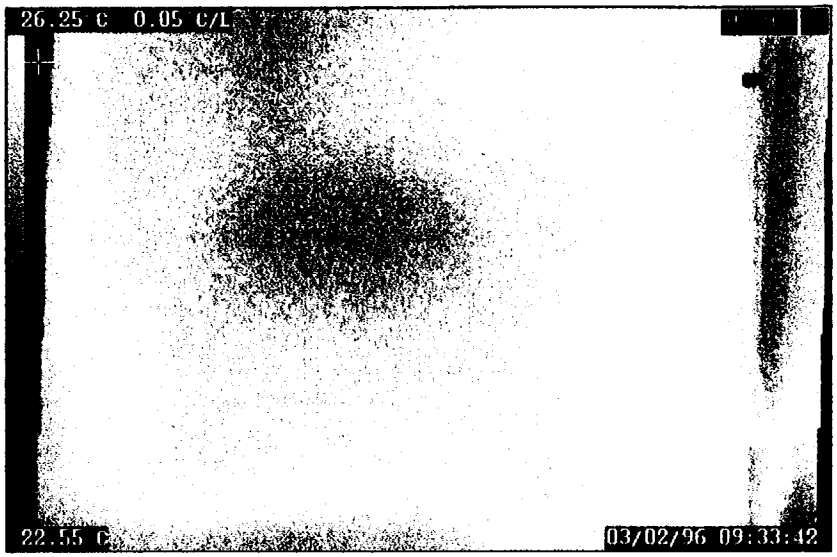

Inter Tank 9 Region D (Inside)

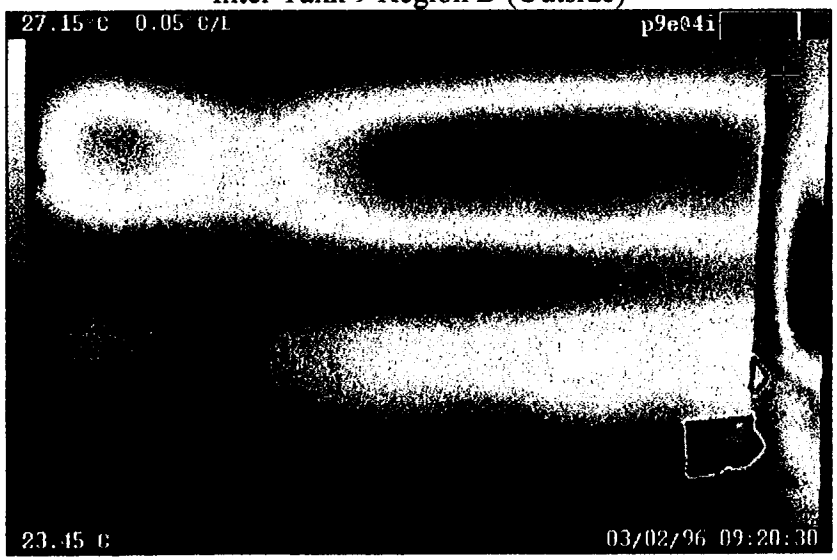

Inter Tank 9 Region E (Outside)

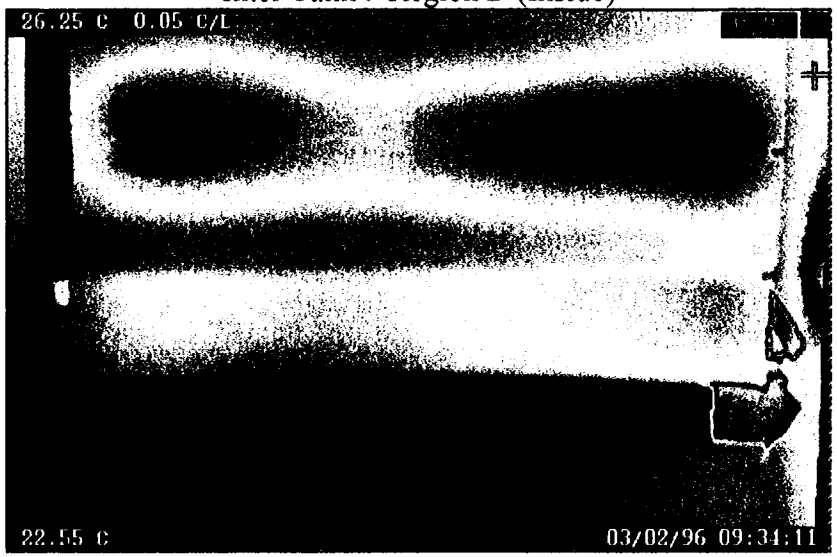

Inter Tank 9 Region E (Inside)

12.6 GRAPHITE/EPOXY TUBES (Before fatigue testing)

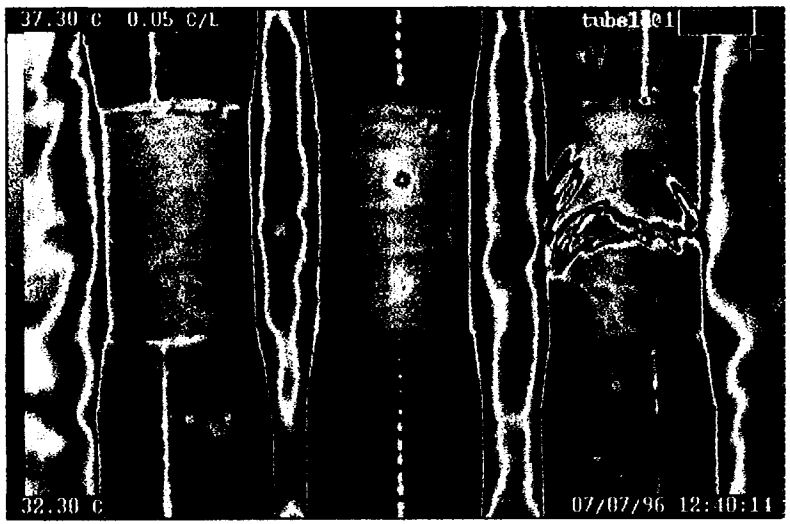

Tube 1a => 0°

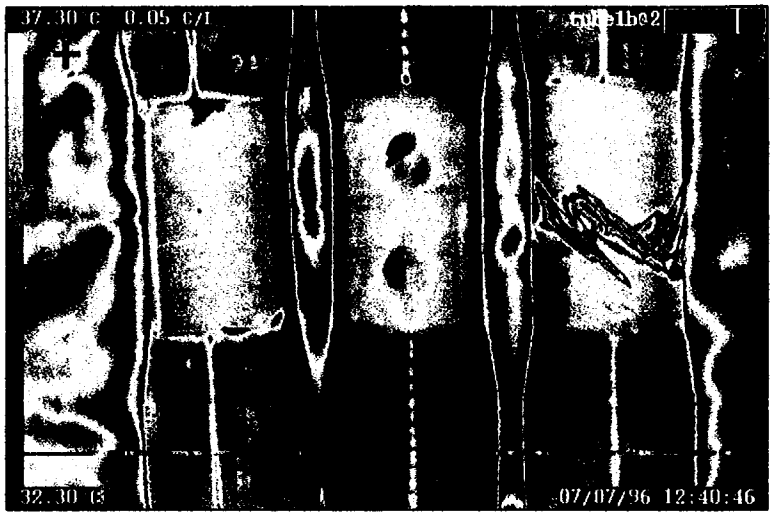

Tube 1b => 90°

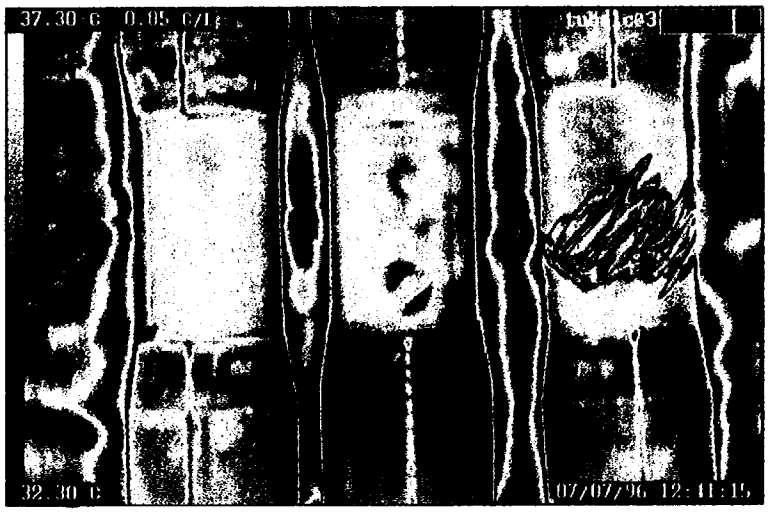

Tube 1c => 180°

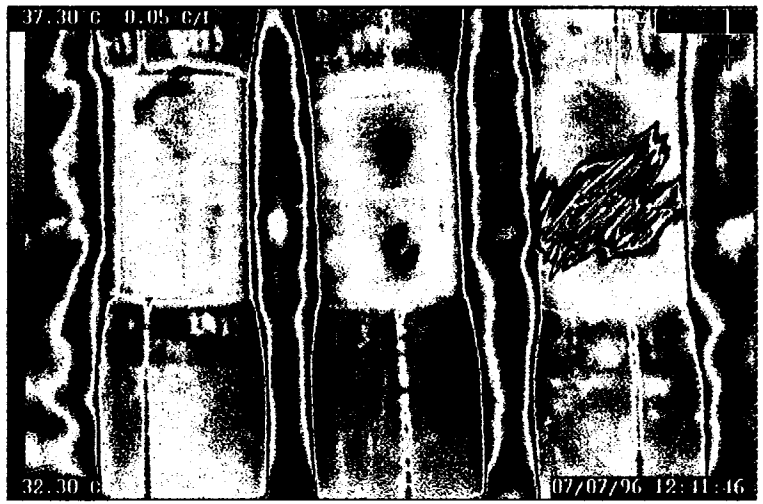

Tube 1d => 270°

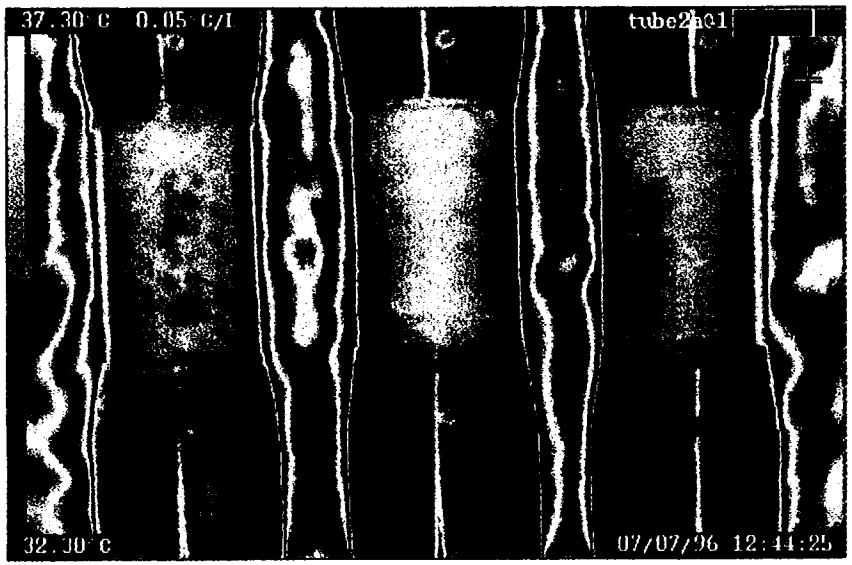

Tube 2a => 0°

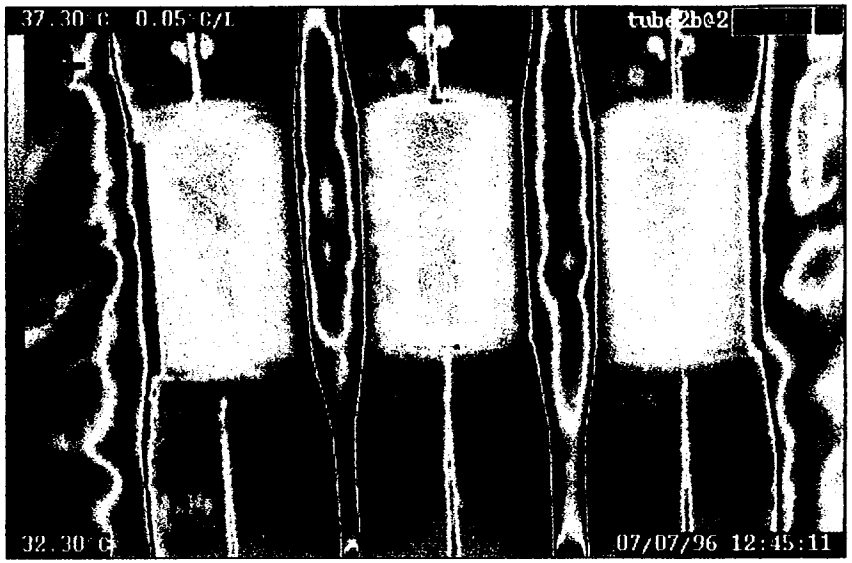

Tube 2b => 90°

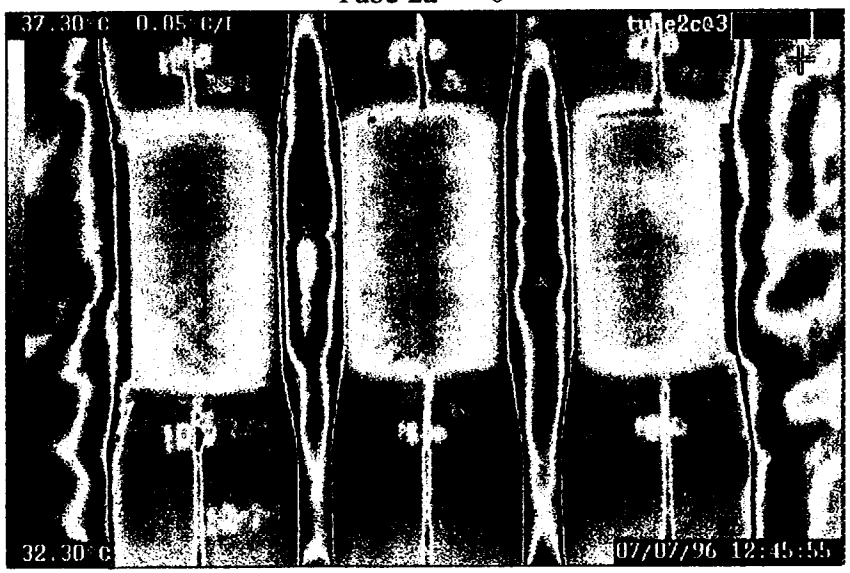

Tube 2c => 180°

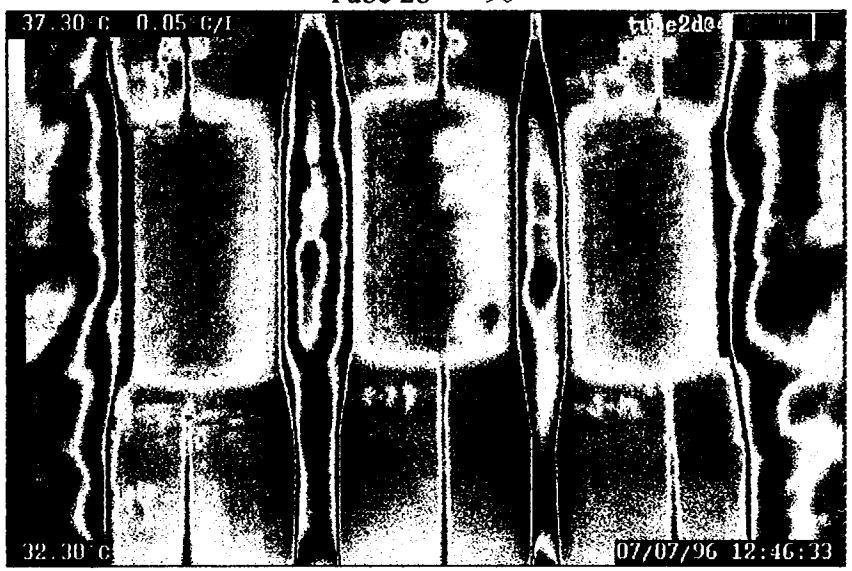

Tube 2d => 270°

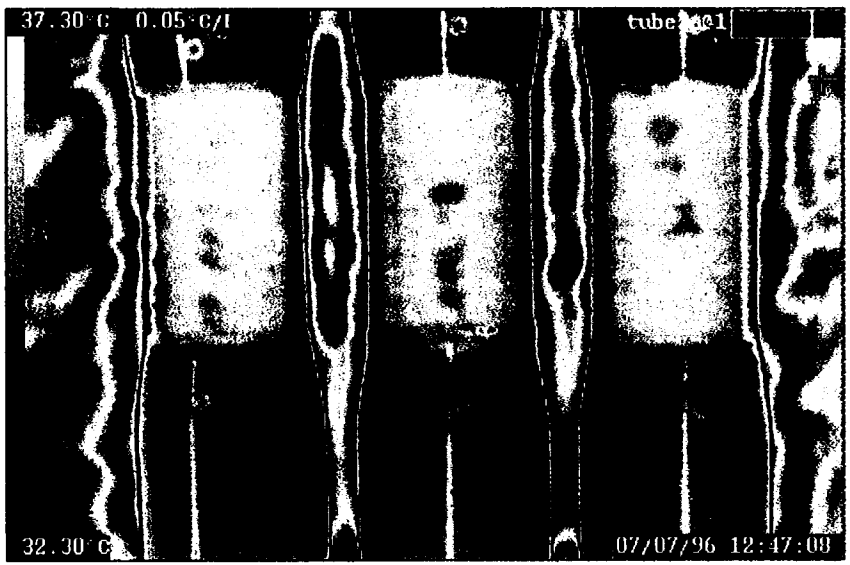

Tube 3a => 0°

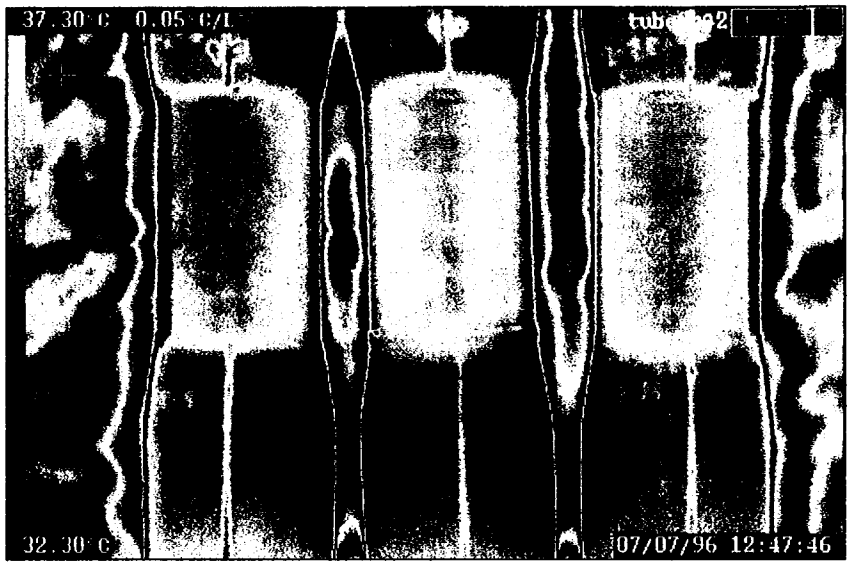

Tube 3b => 90°

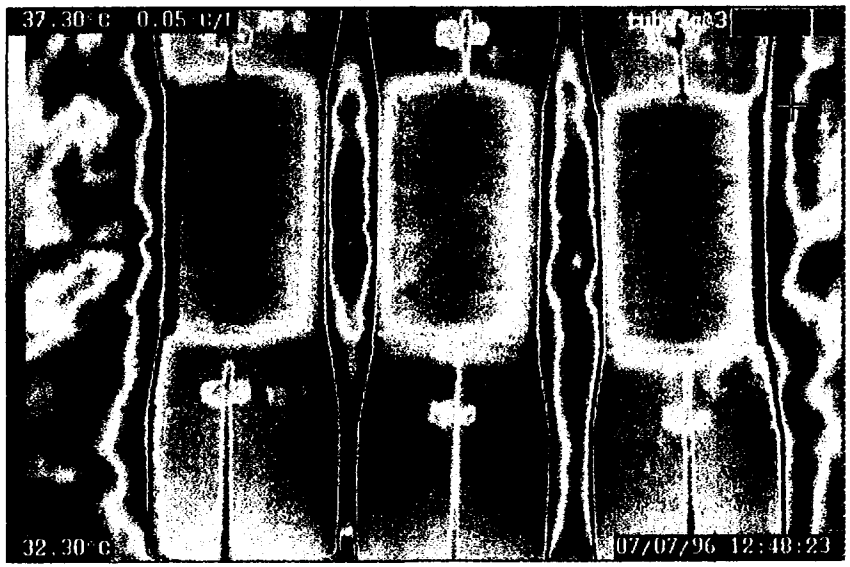

Tube 3c => 180°

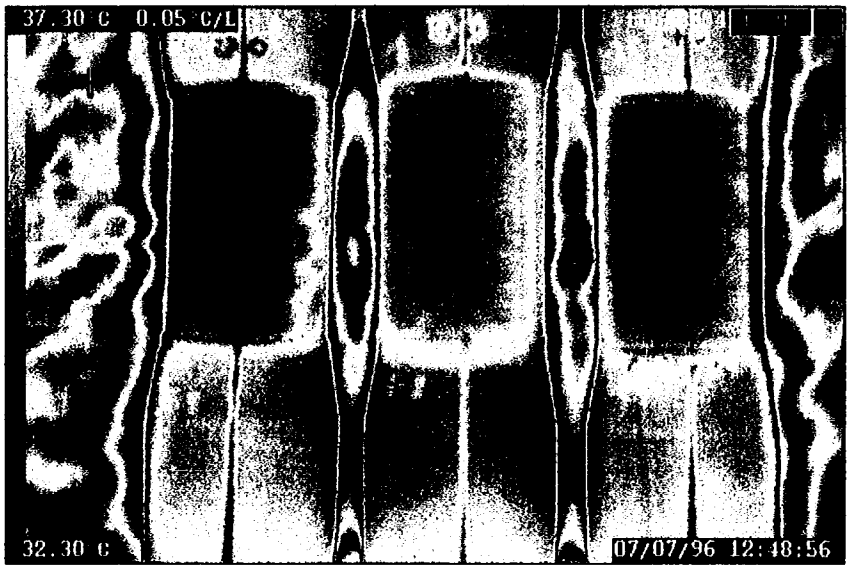

Tube 3d => 270°

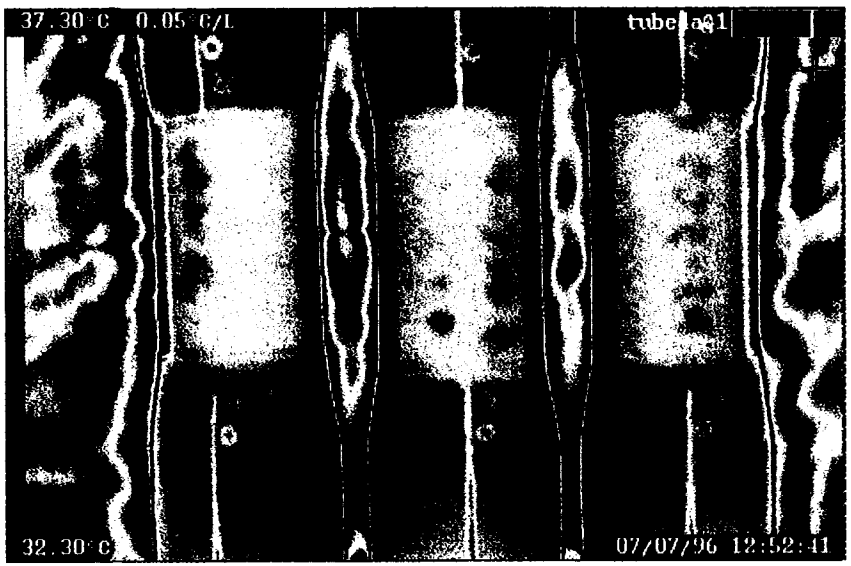

Tube 4a => 0°

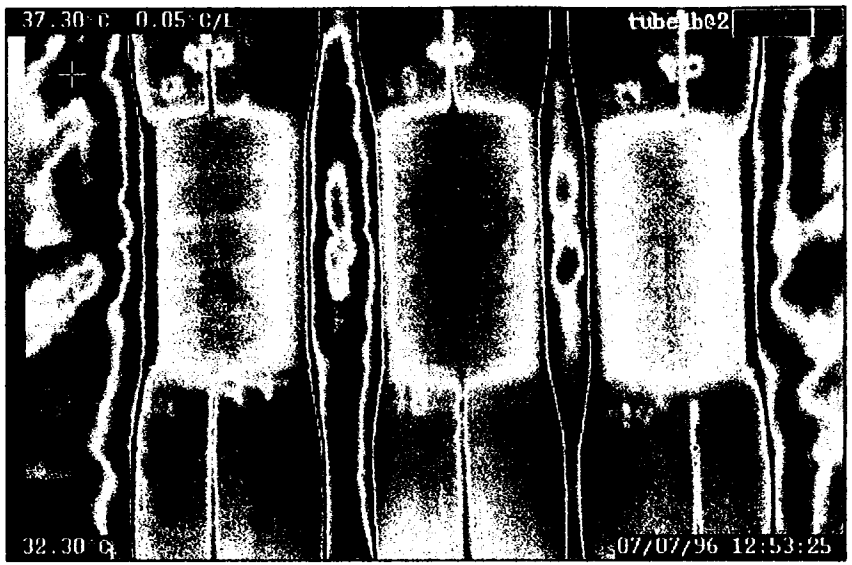

Tube 4b => 90°

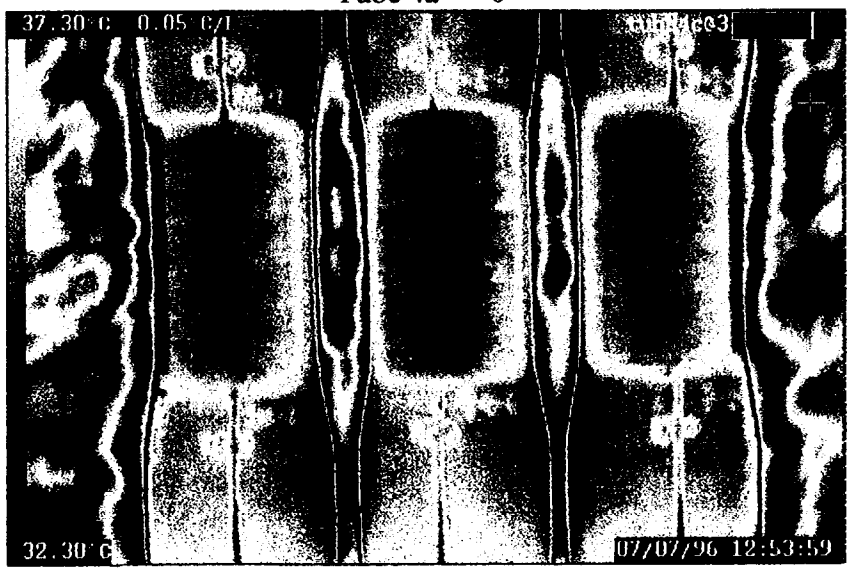

Tube 4c => 180°

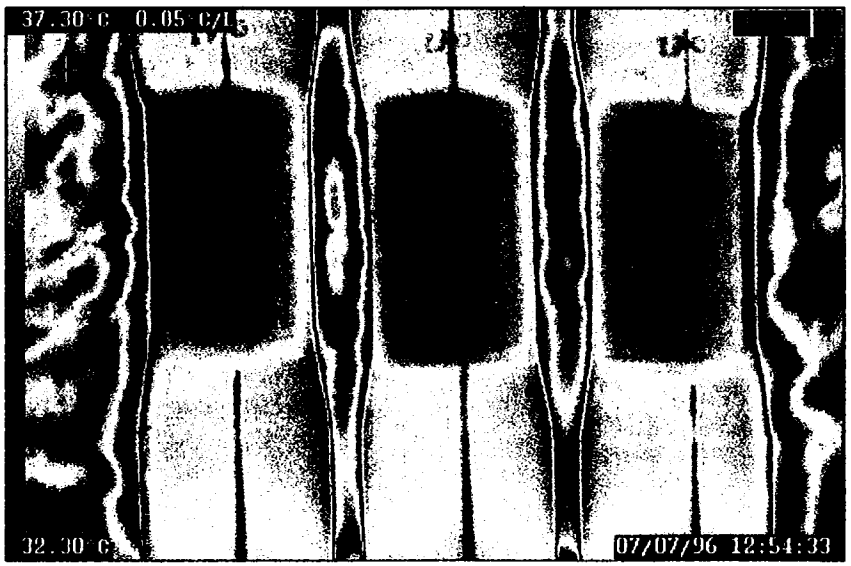

Tube 4d => 270°

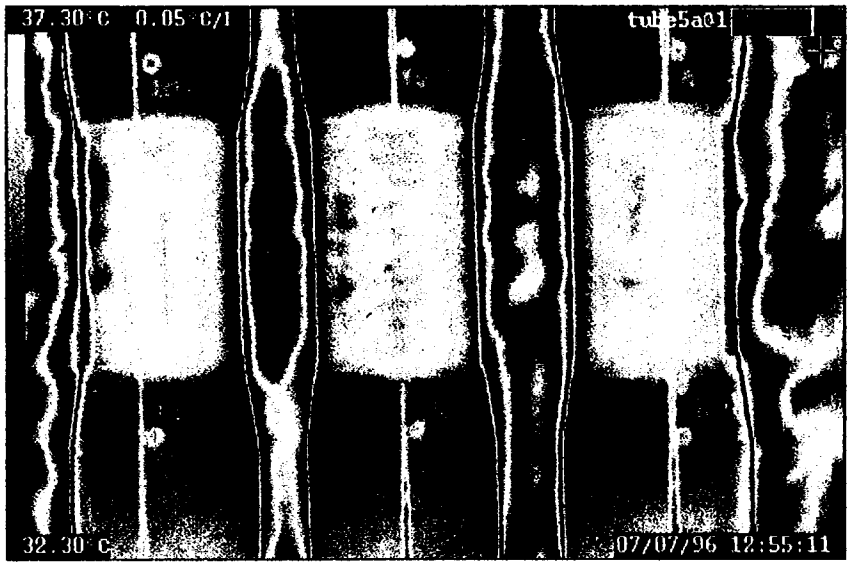

Tube 5a => 0°

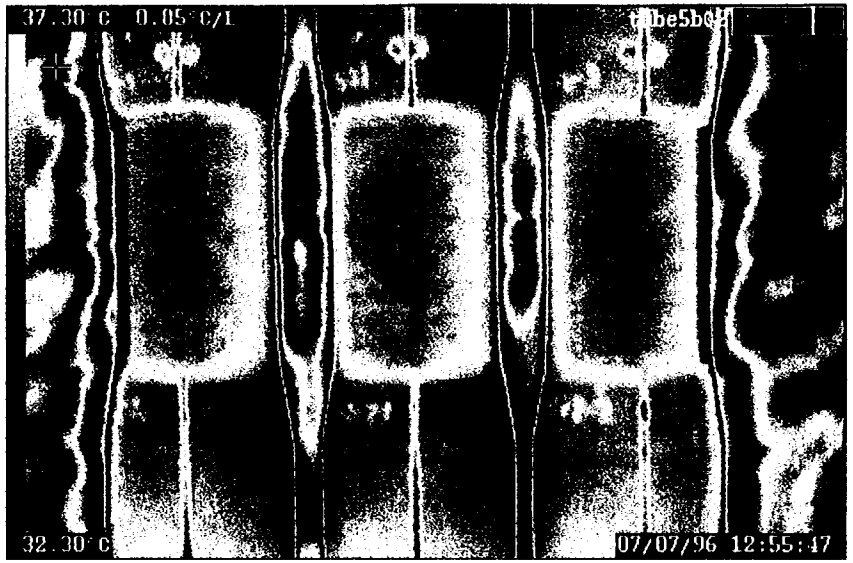

Tube 5b => 90°

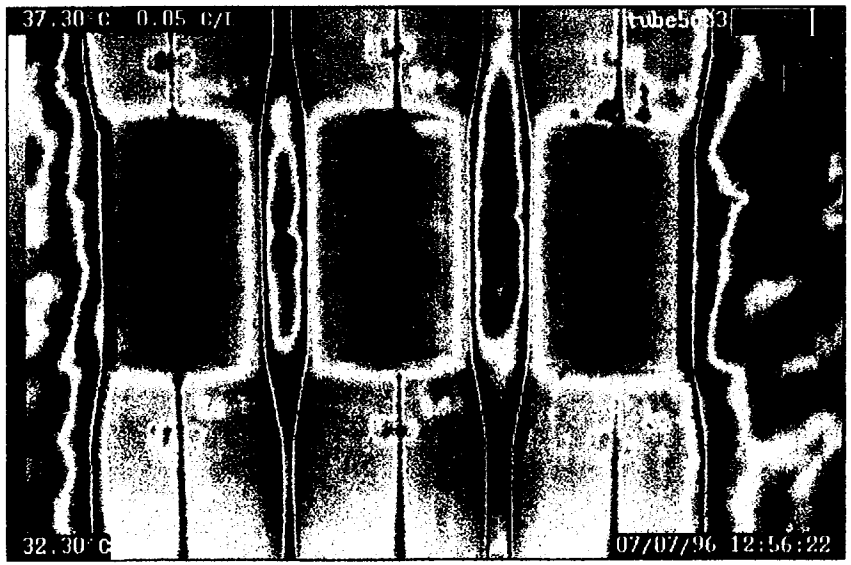

Tube 5c => 180°

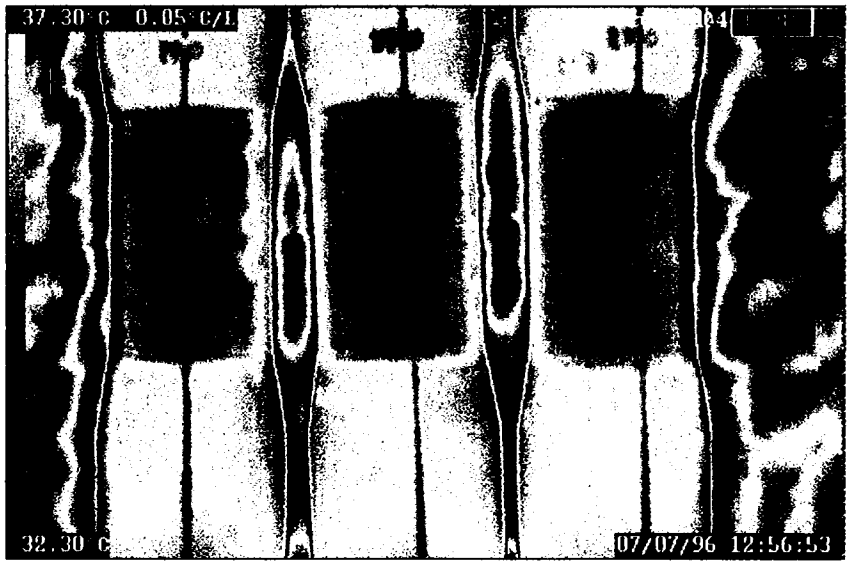

Tube 5d => 270°

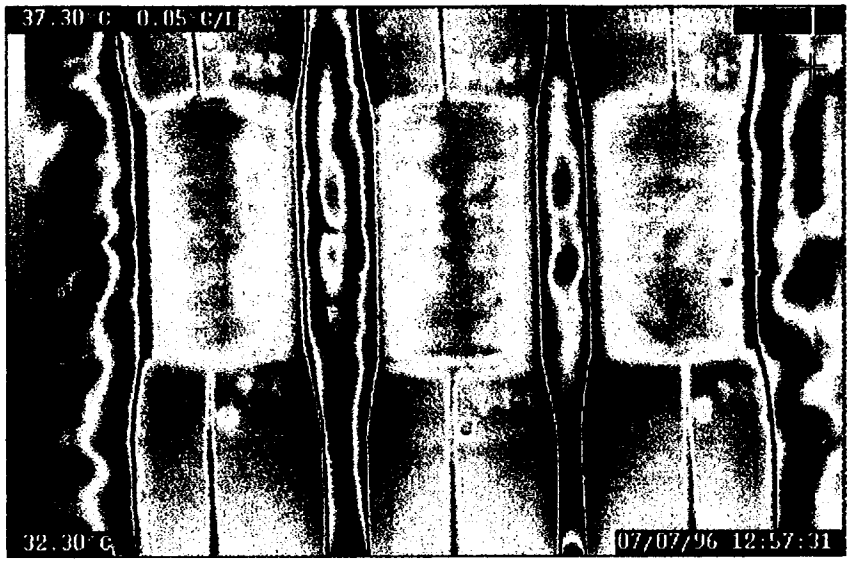

Tube 6a => 0°

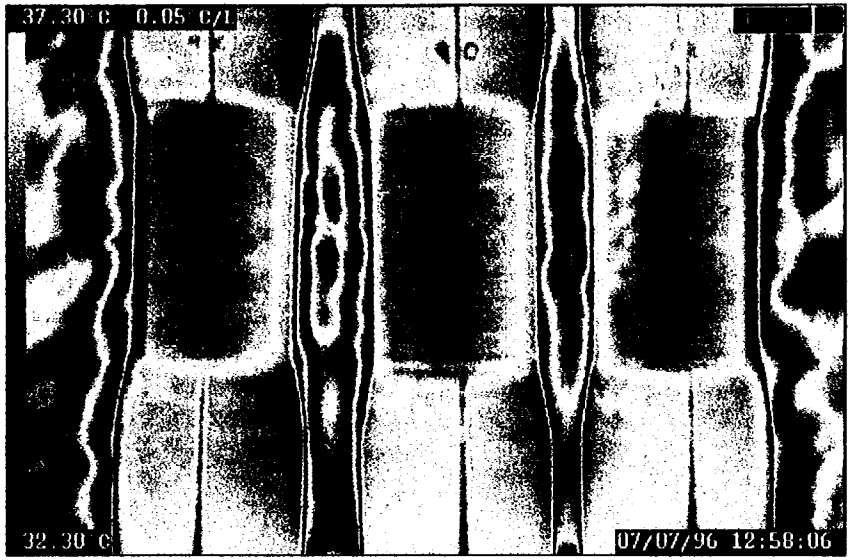

Tube 6b => 90°

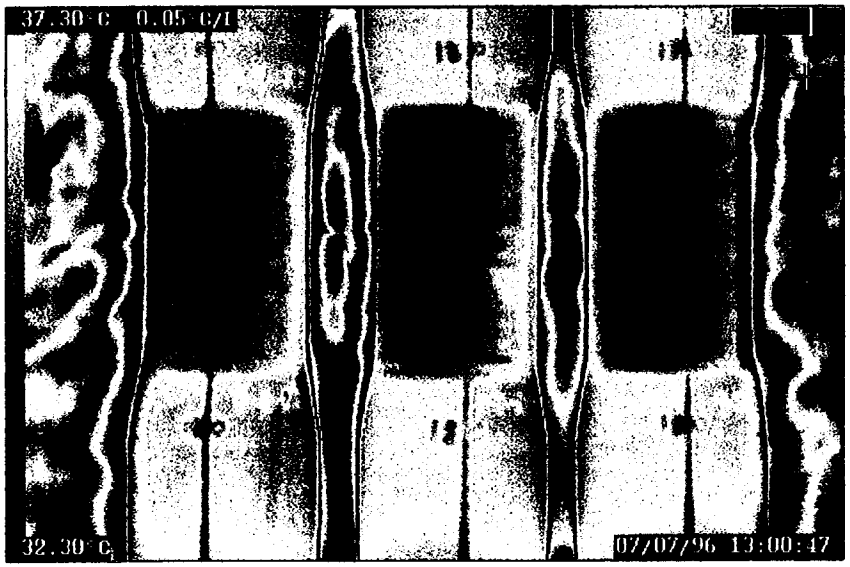

Tube 6c => 180°

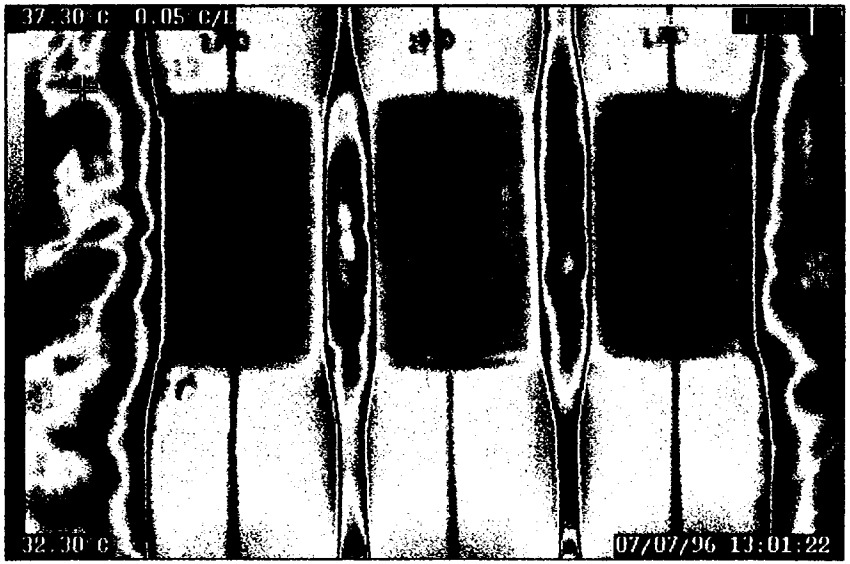

Tube 6d => 270°

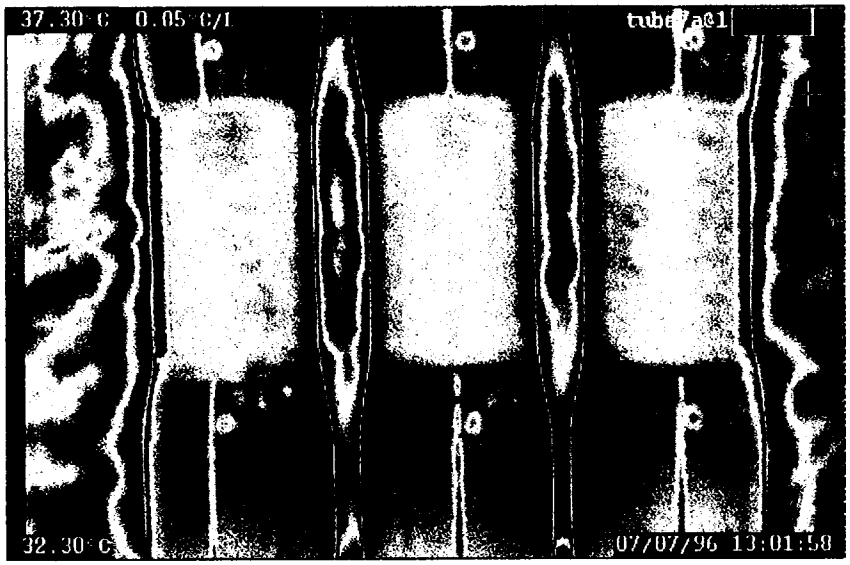

Tube 7a => 0°

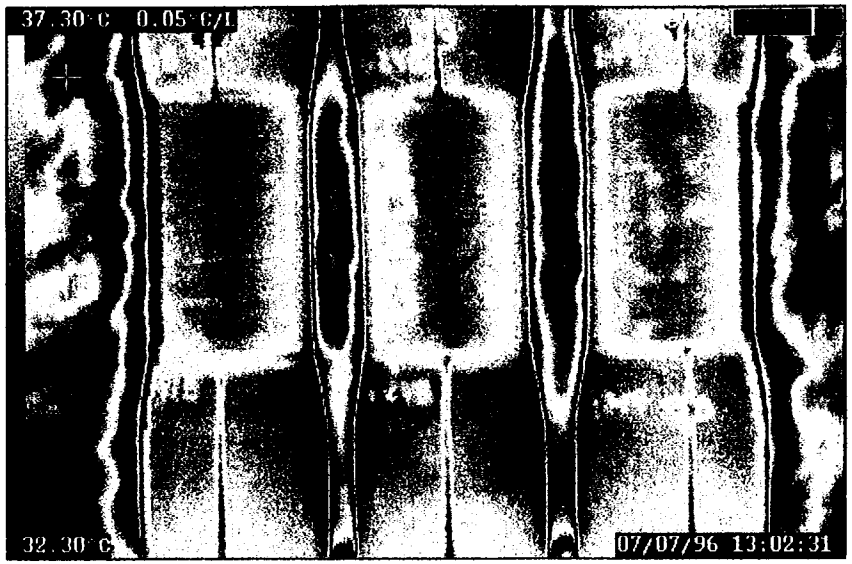

Tube 7b => 90°

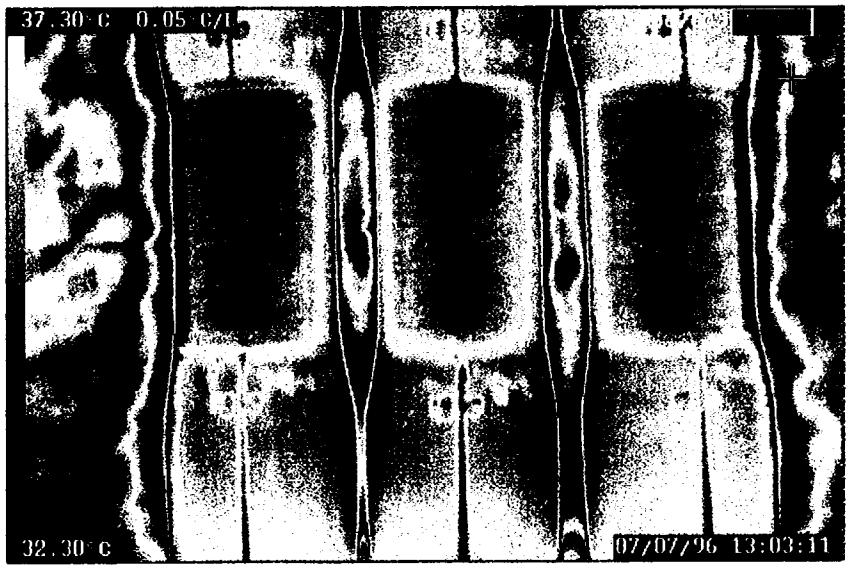

Tube 7c => 180°

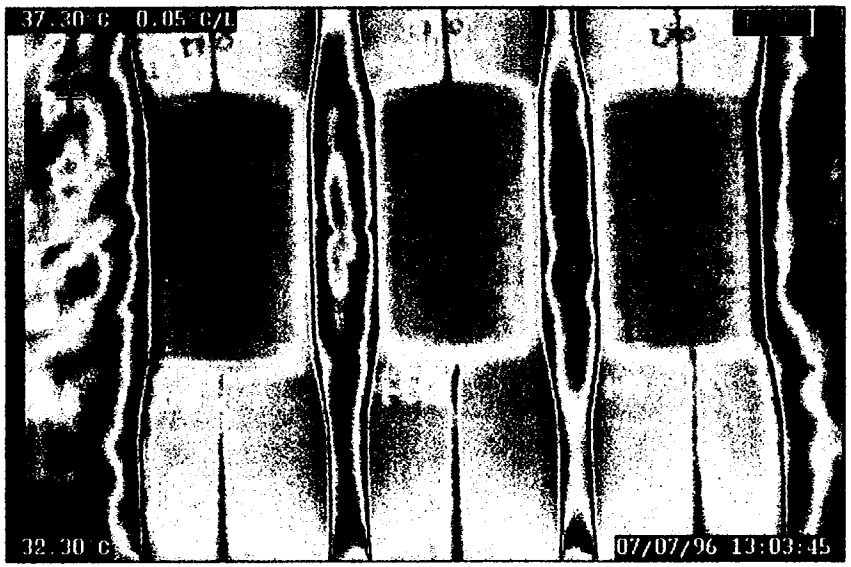

Tube 7d => 270°

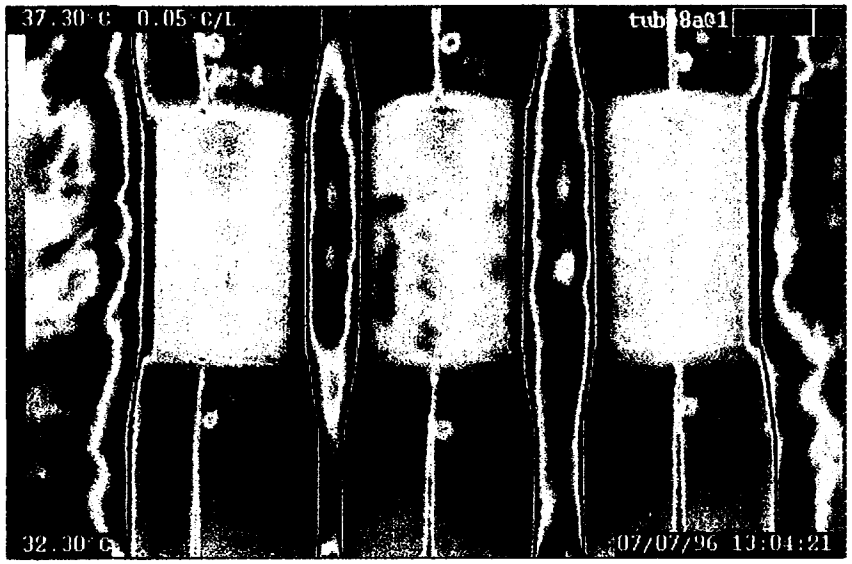

Tube 8a => 0°

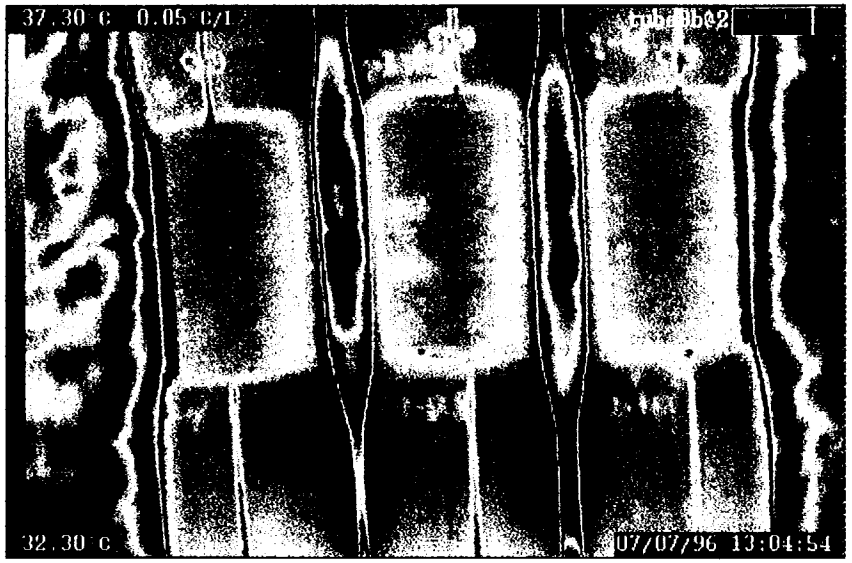

Tube 8b => 90°

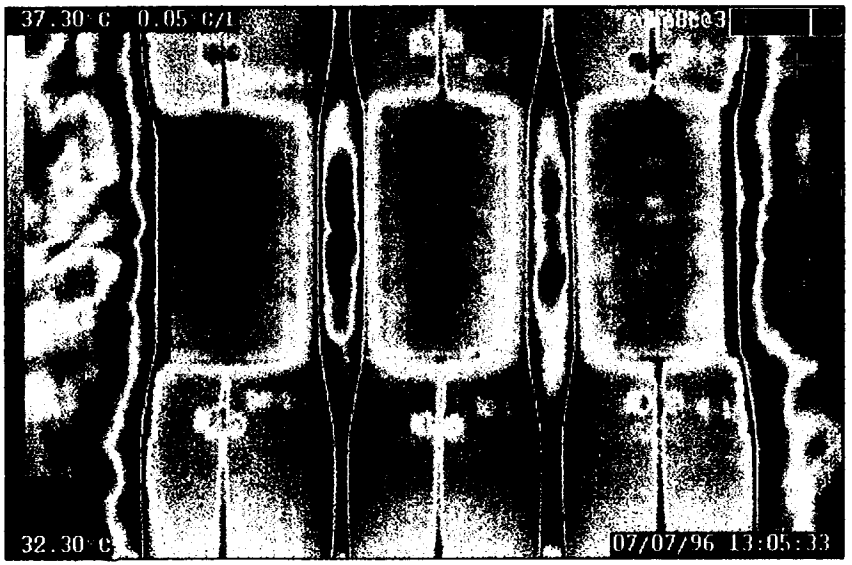

Tube 8c => 180°

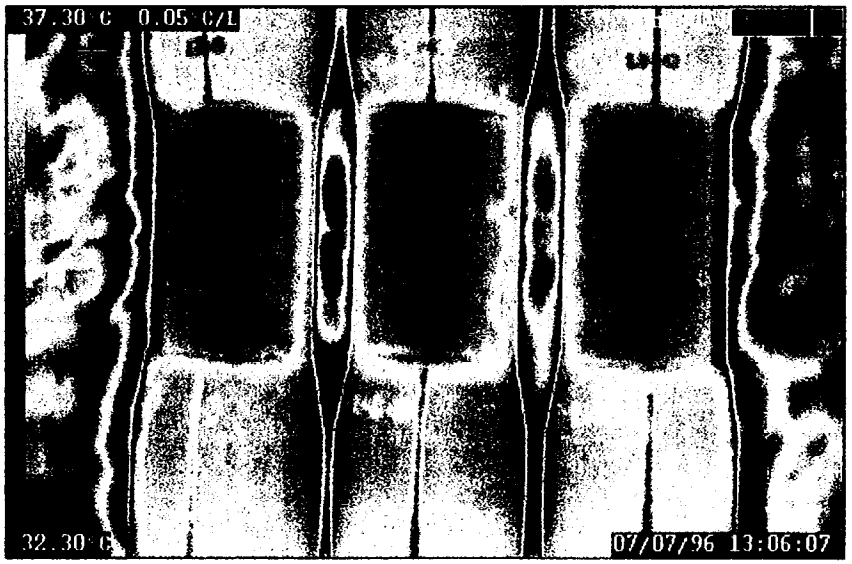

Tube 8d => 270°

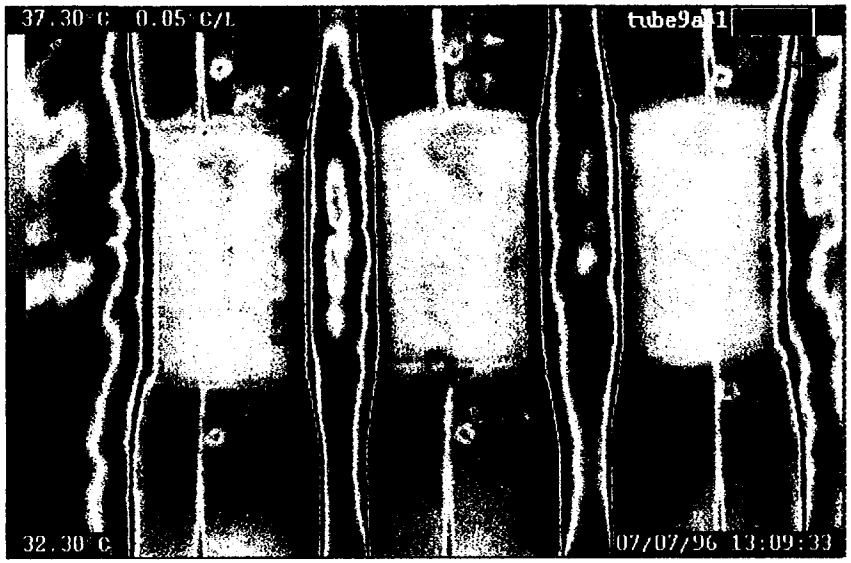

Tube 9a => 0°

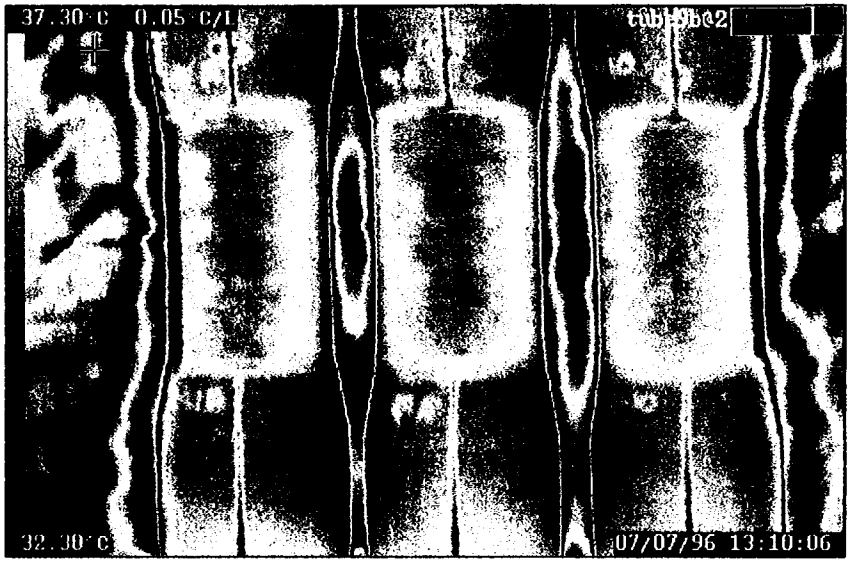

Tube 9b => 90°

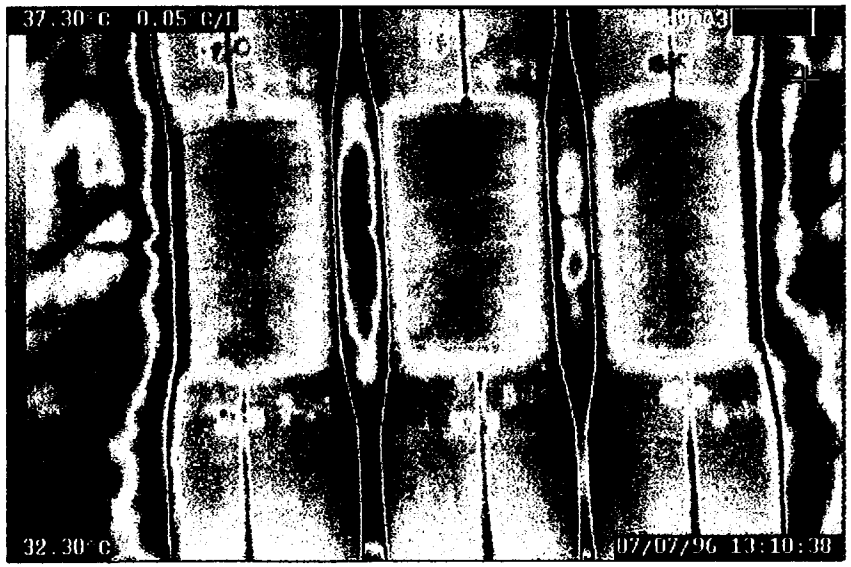

Tube 9c => 180°

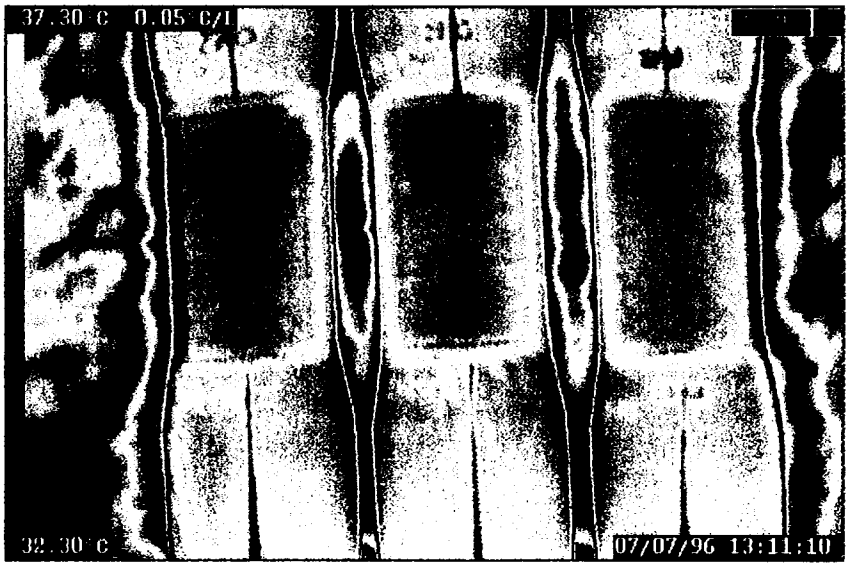

Tube 9d => 270°

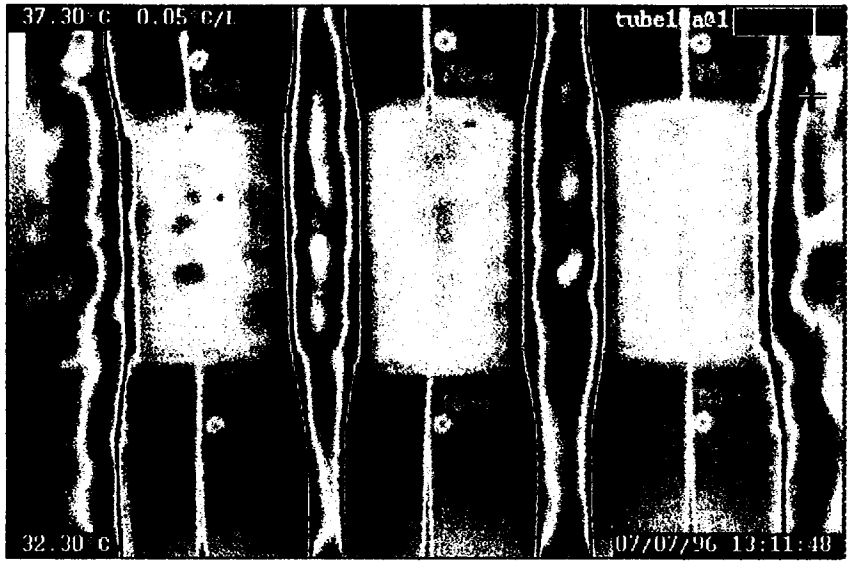

Tube 10a => 0°

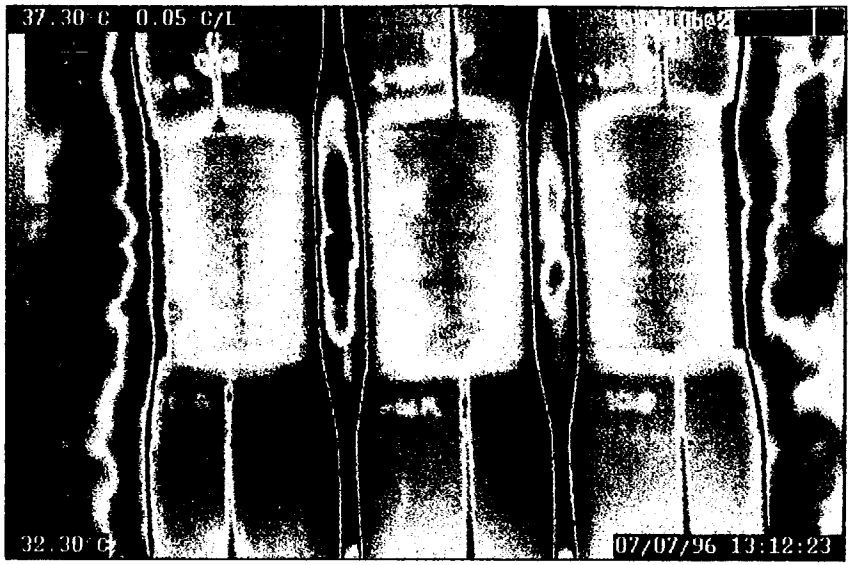

Tube 10b => 90°

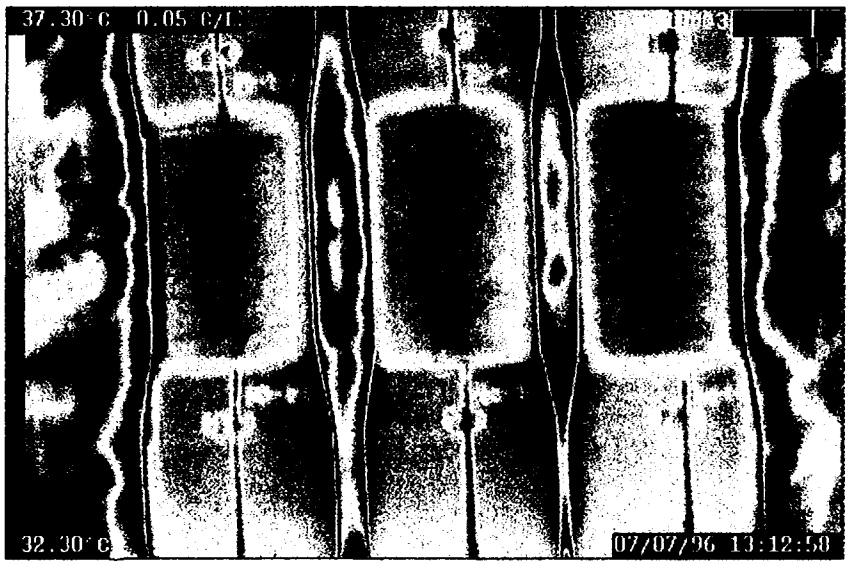

Tube 10c => 180°

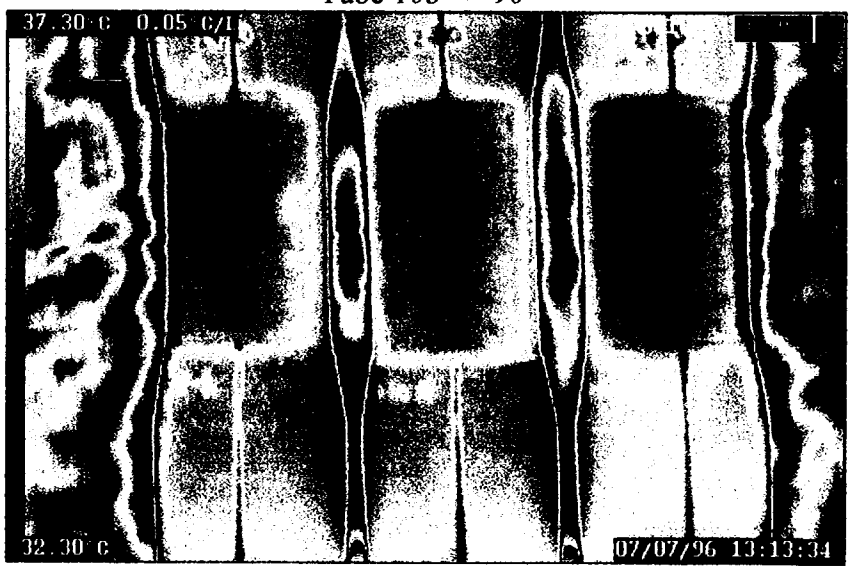

Tube 10d => 270°

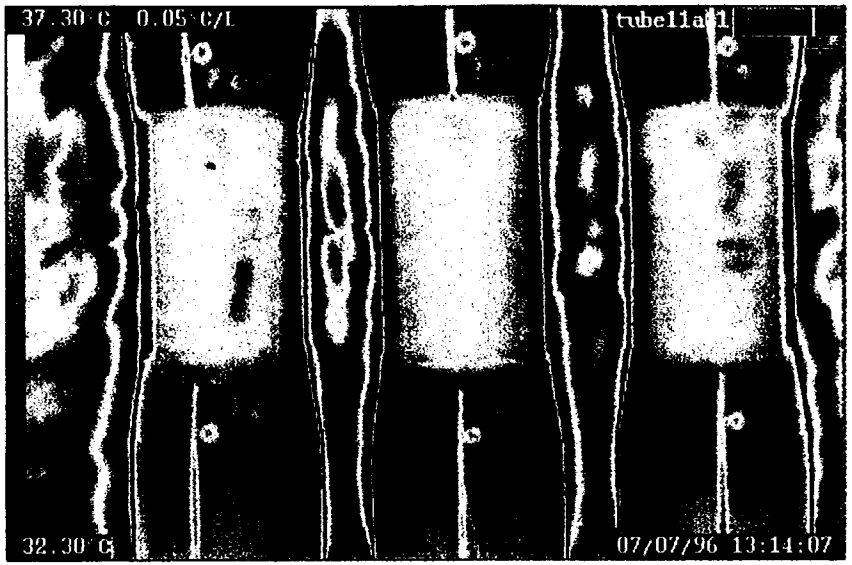

Tube 11a => 0°

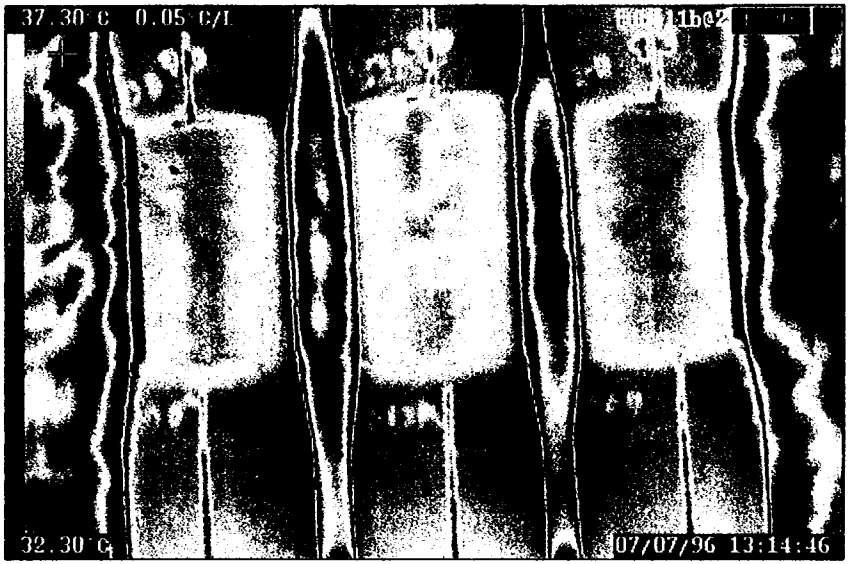

Tube 11b => 90°

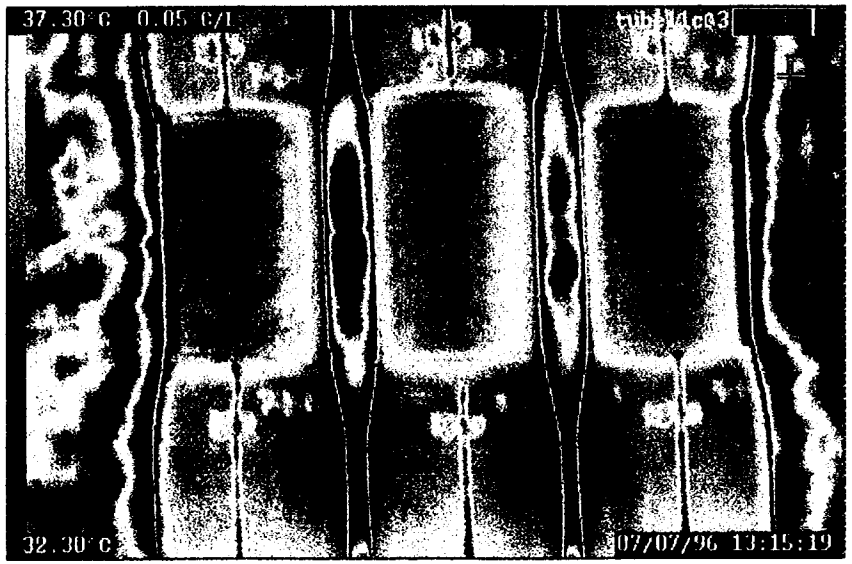

Tube 11c => 180°

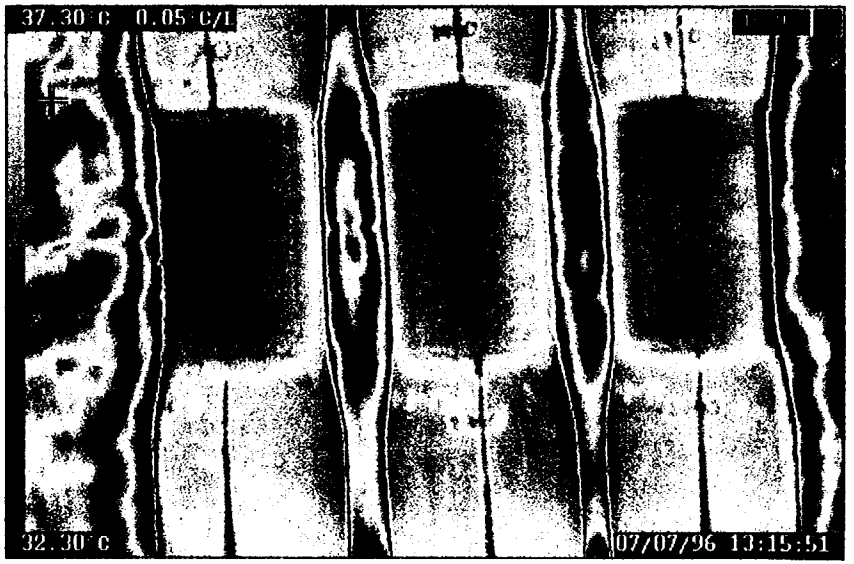

Tube 11d => 270°

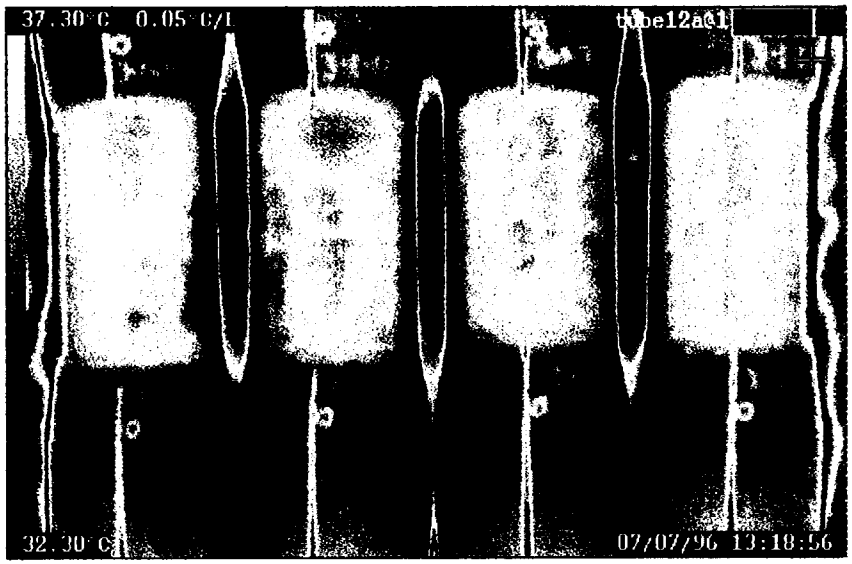

Tube 12a => 0°

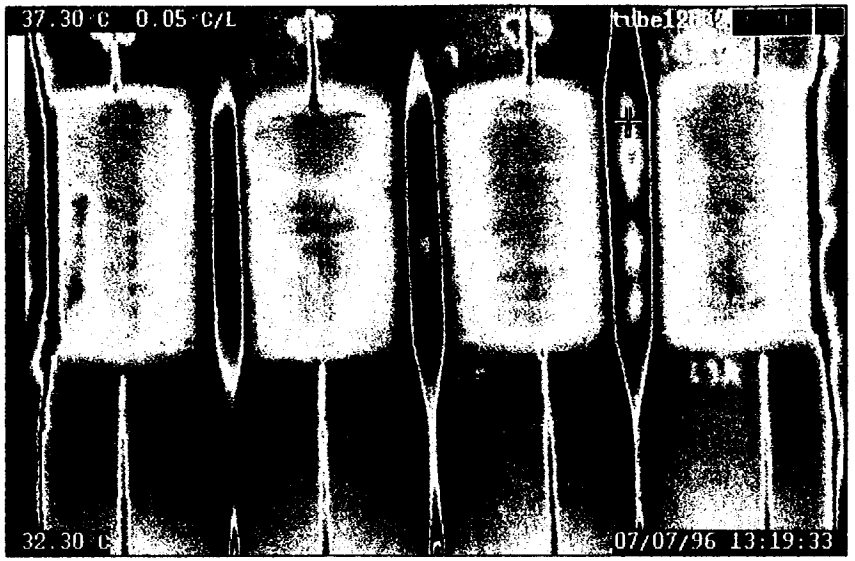

Tube 12b => 90°

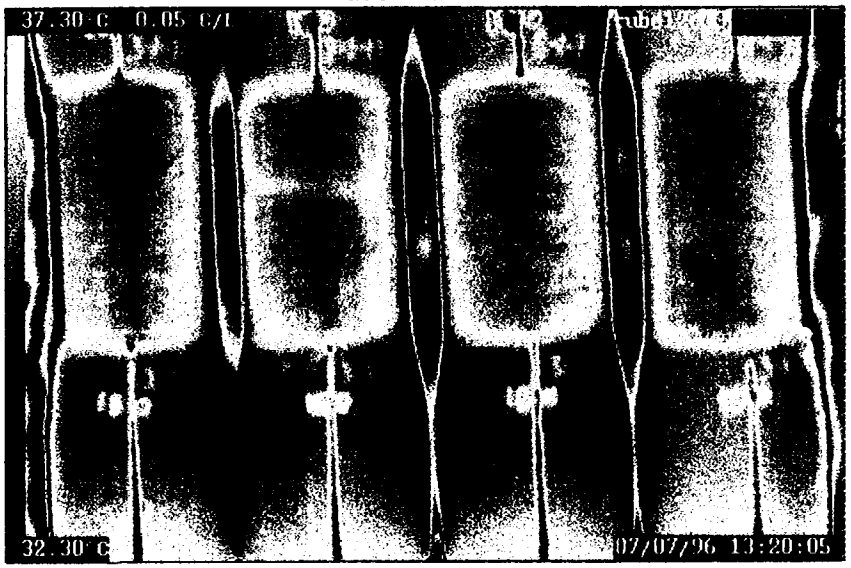

Tube 12c => 180°

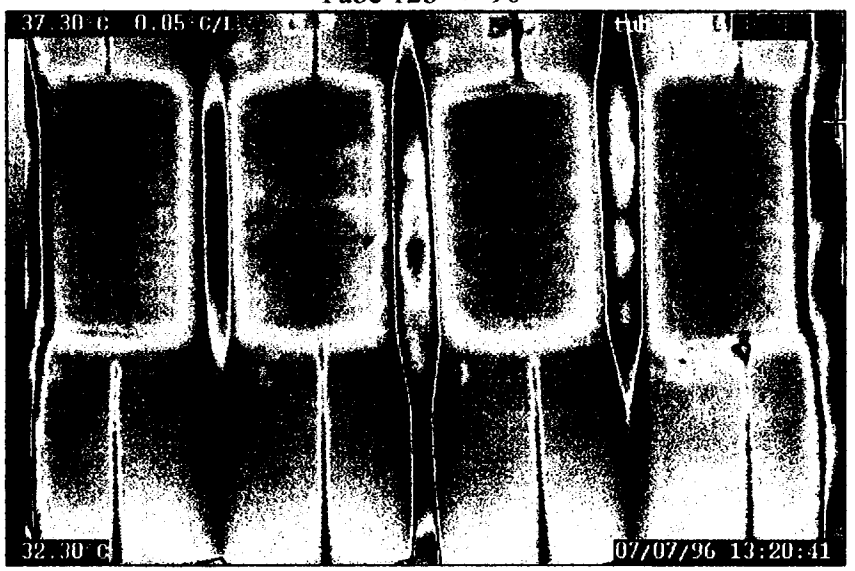

Tube 12d => 270°

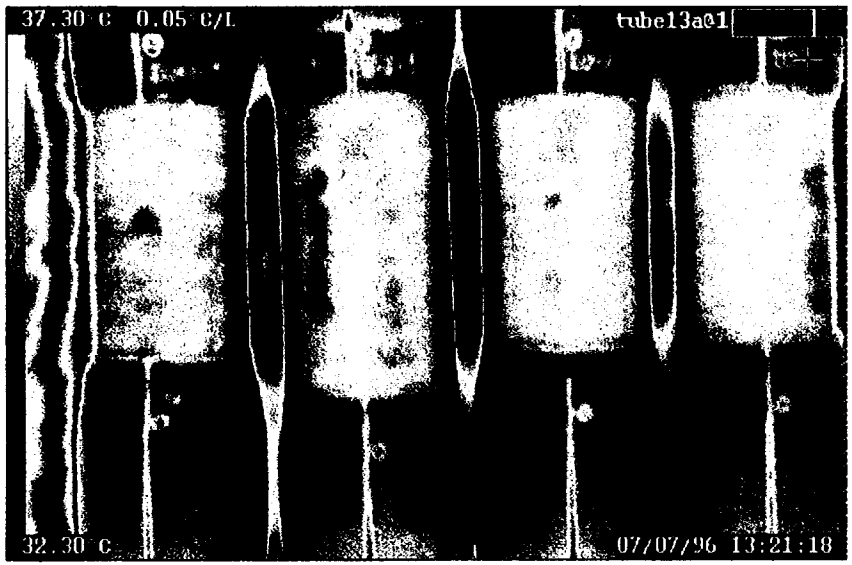

Tube 13a => 0°

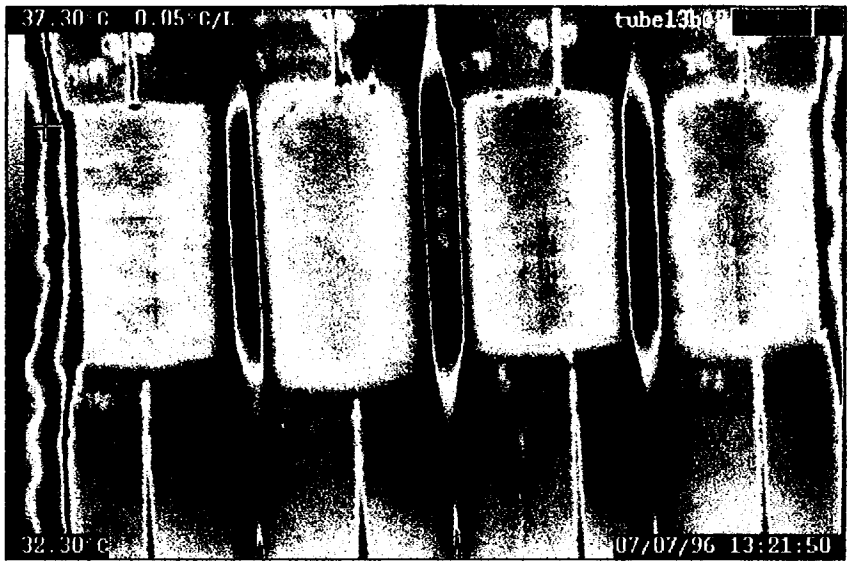

Tube 13b => 90°

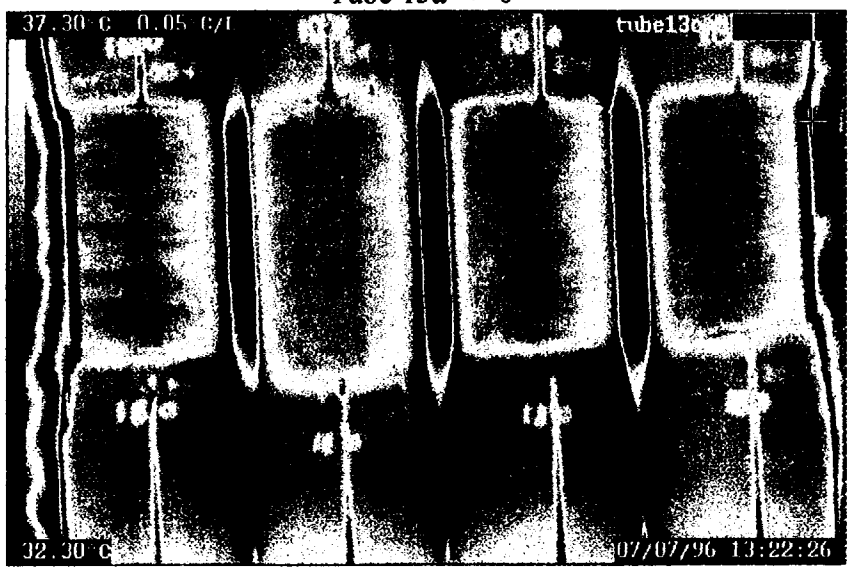

Tube 13c => 180°

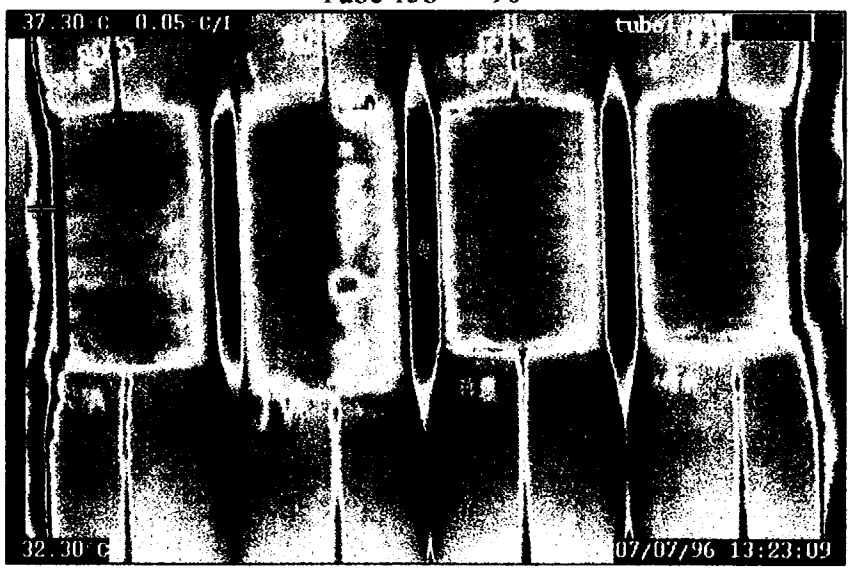

Tube 13d => 270°

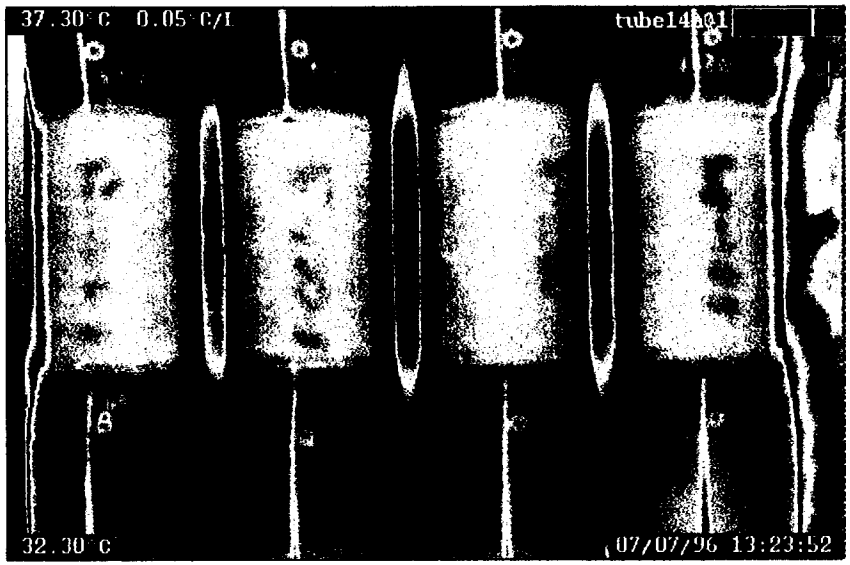

Tube 14b => 90°

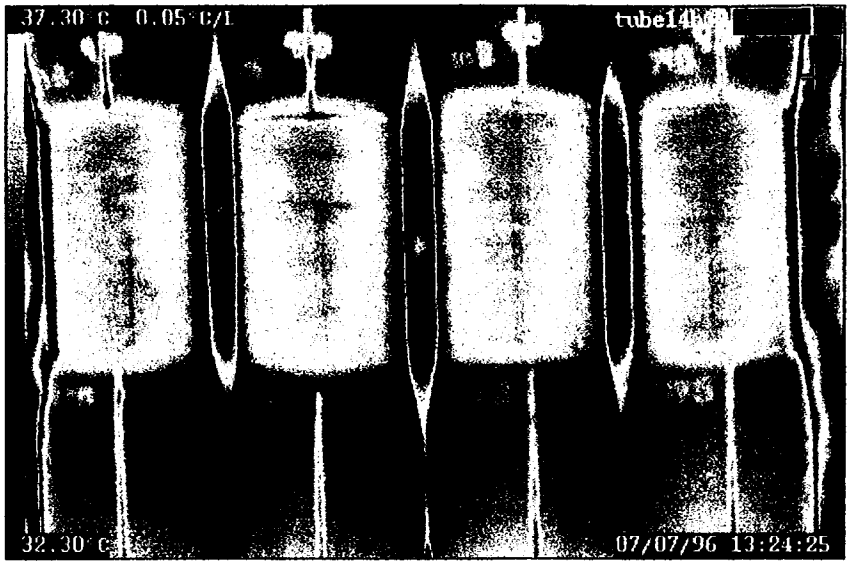

Tube 14a => 0°

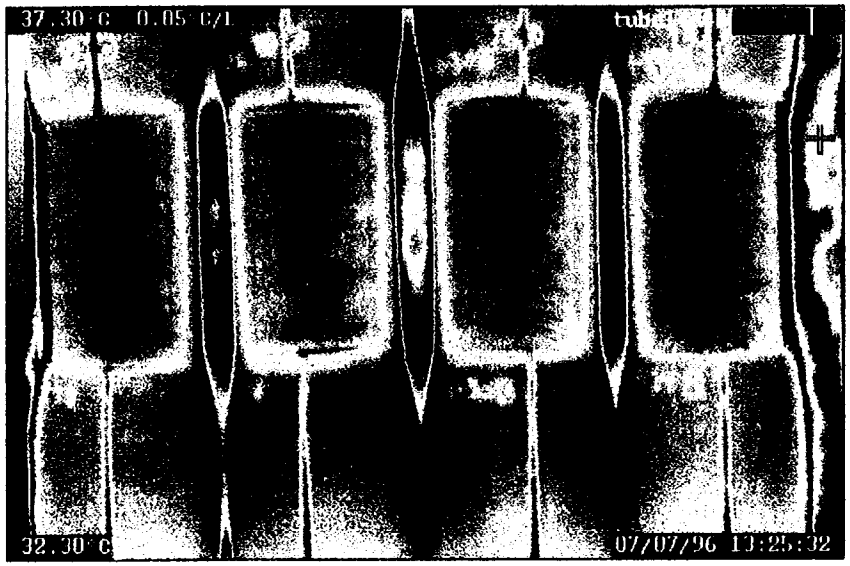

Tube 14d => 270°

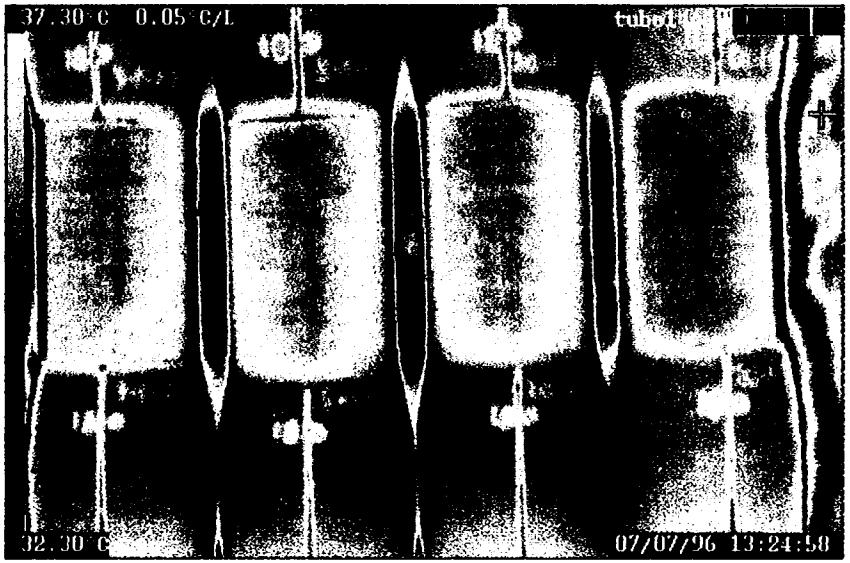

Tube 14c => 180°

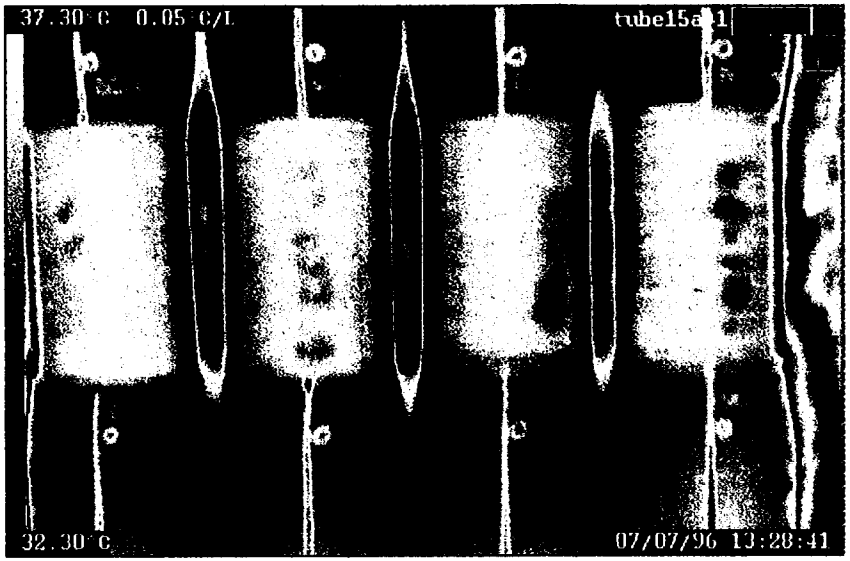

Tube 15a => 0°

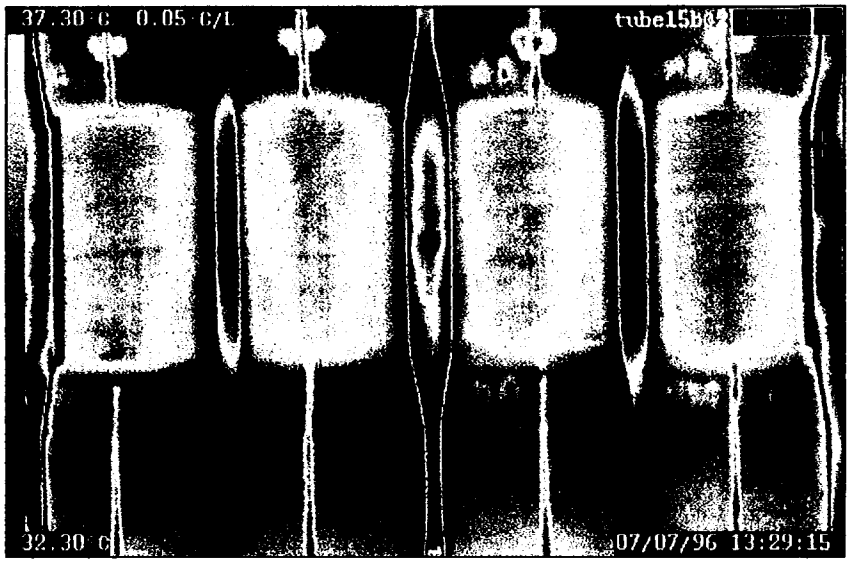

Tube 15b => 90°

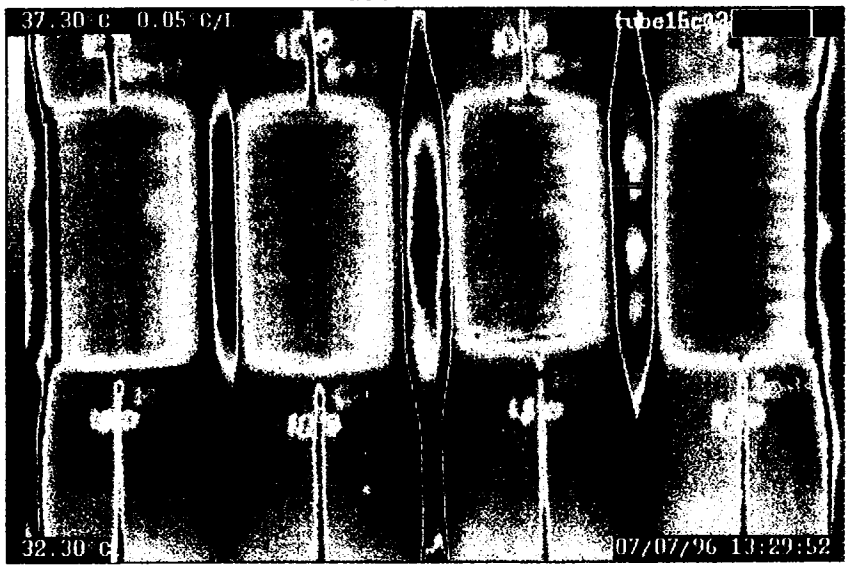

Tube 15c => 180°

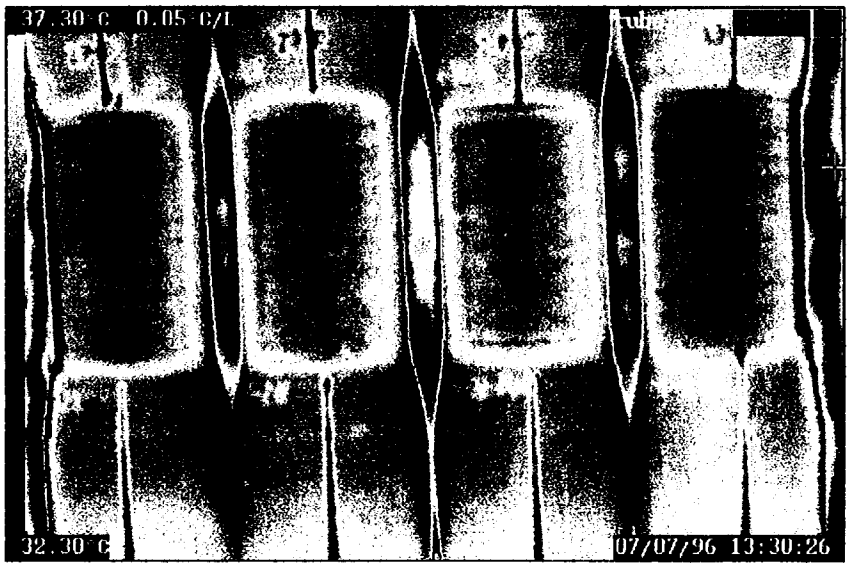

Tube 15d => 270°

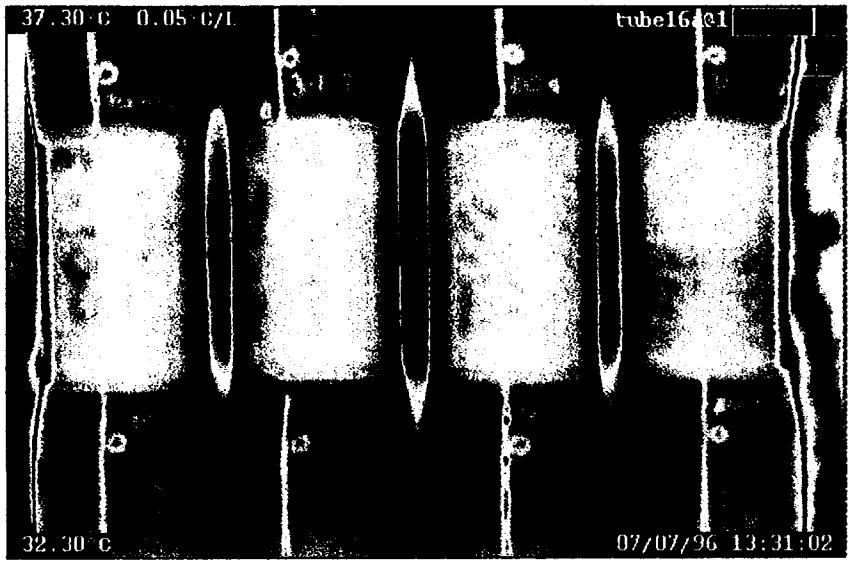

Tube 16a => 0°

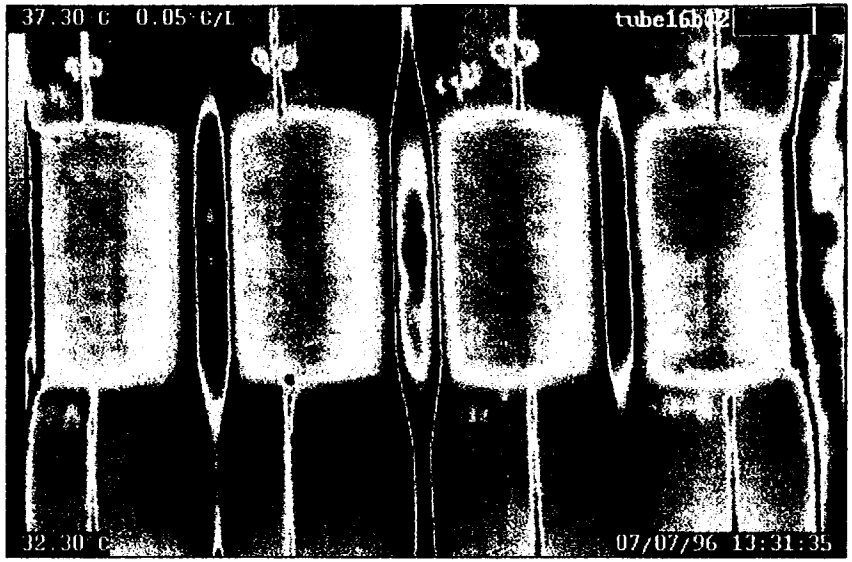

Tube 16b => 90°

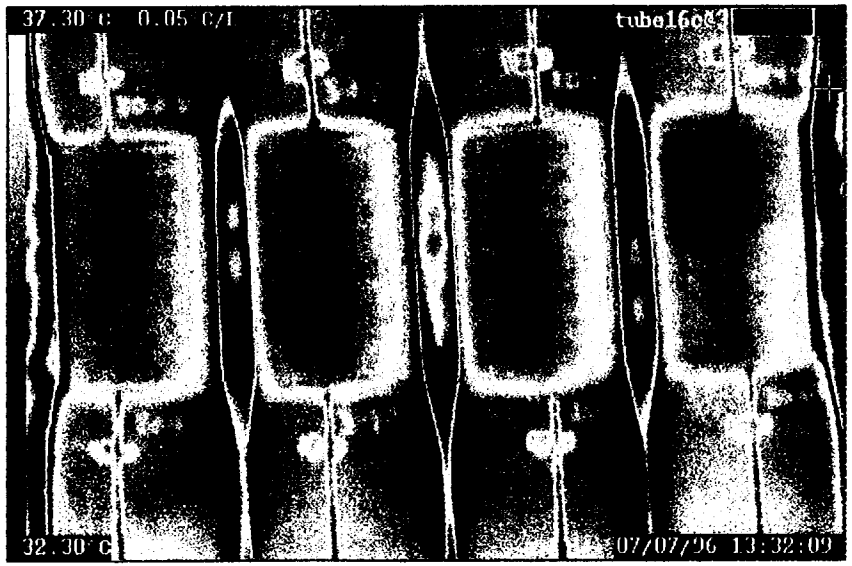

Tube 16c => 180°

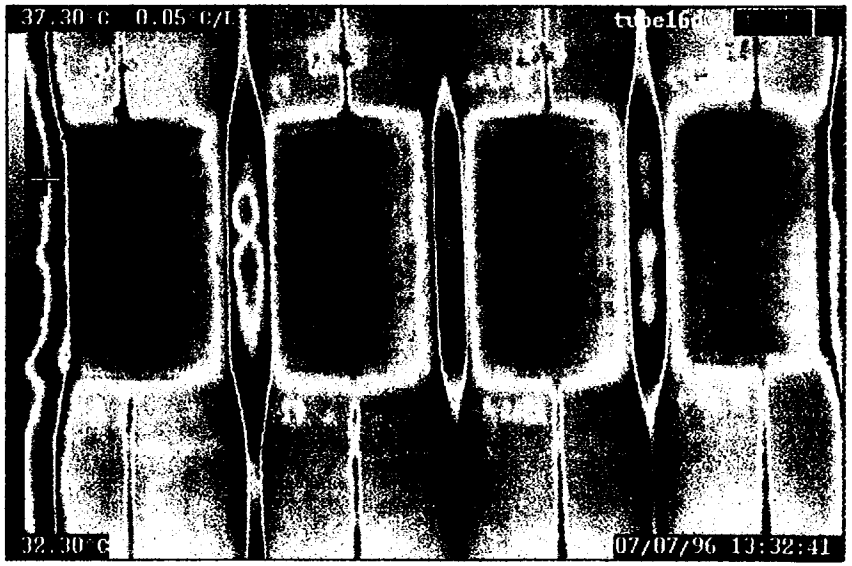

Tube 16d => 270°

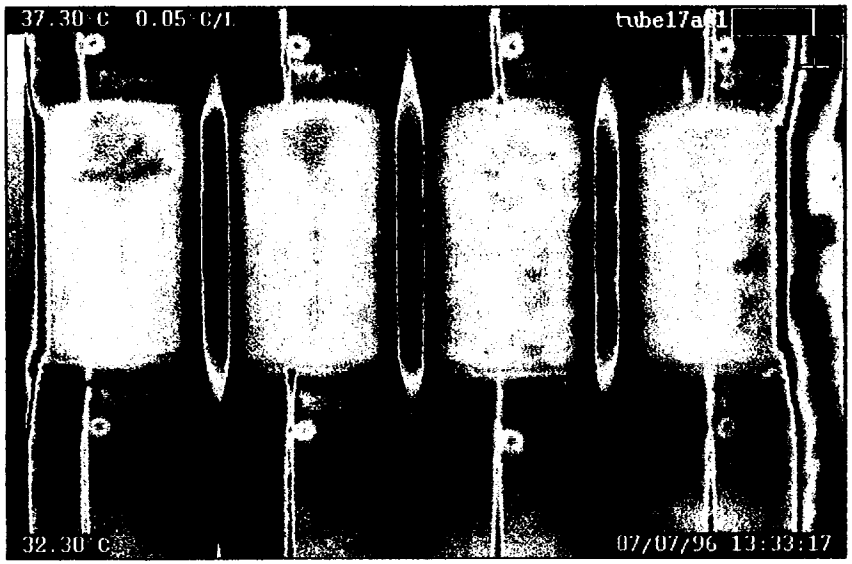

Tube 17a => 0°

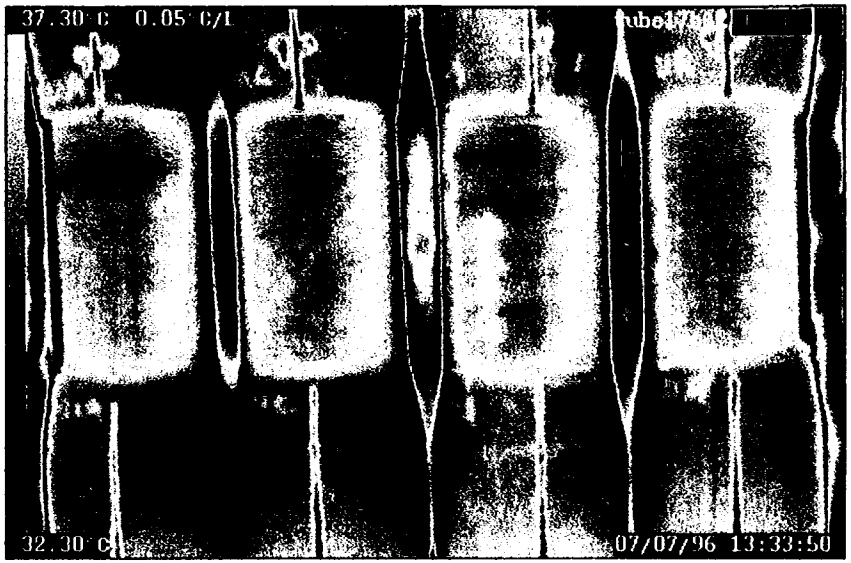

Tube 17b => 90°

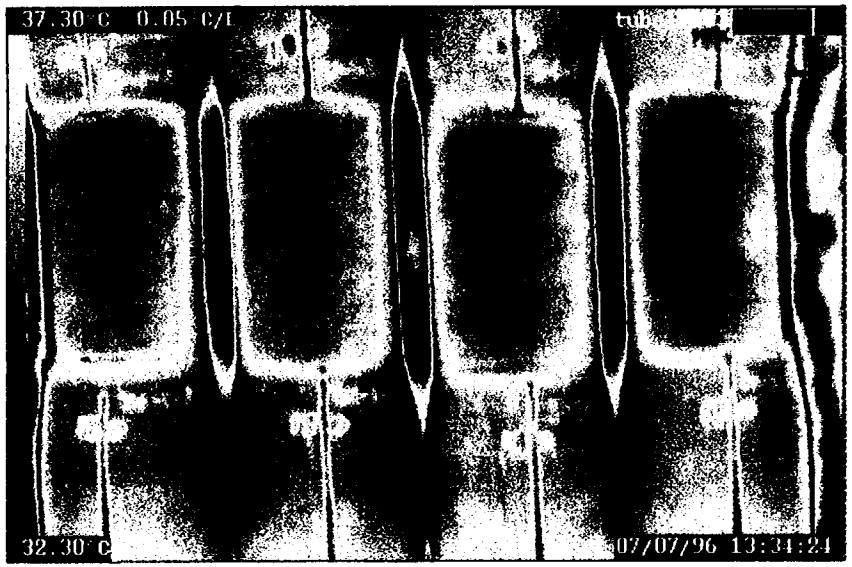

Tube 17c => 180°

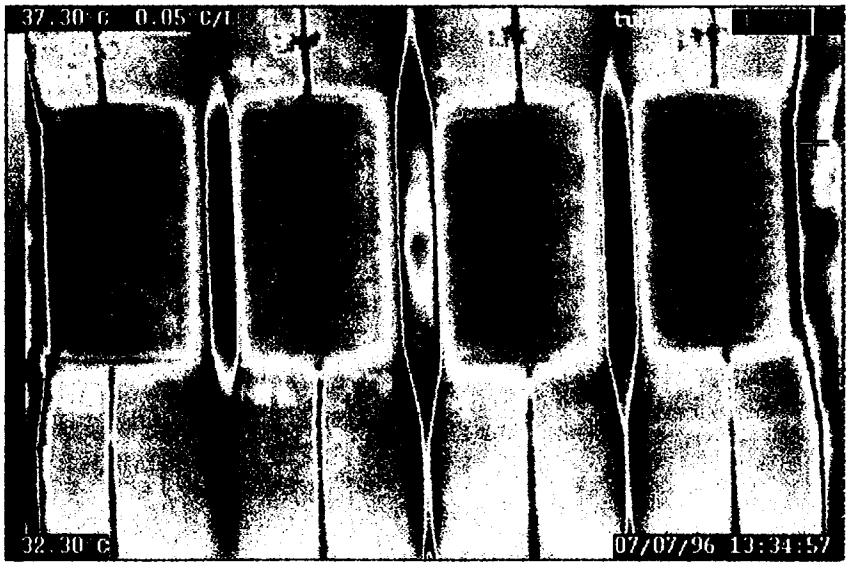

Tube 17d => 270°

12.7 GRAPHITE/EPOXY TUBES (Post fatigue testing)

Ptube 1 (0°)

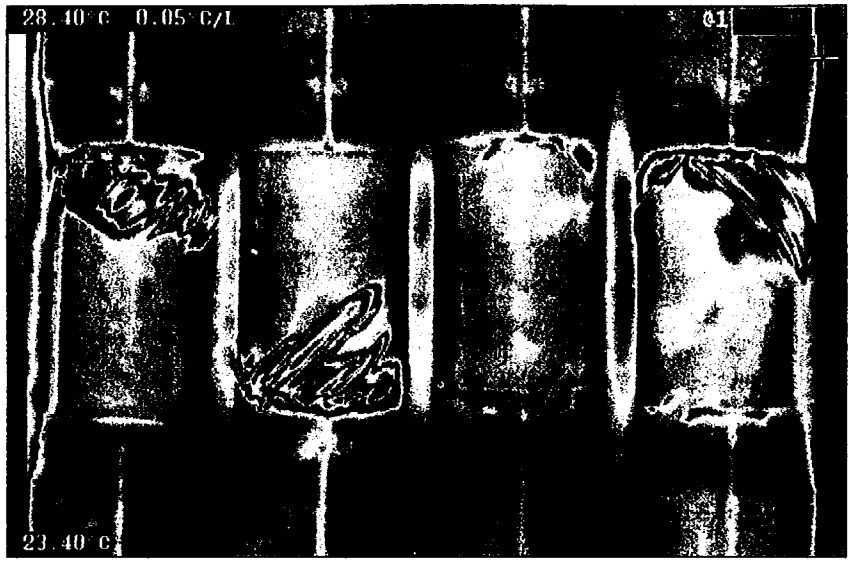

Ptube 1 (90°)

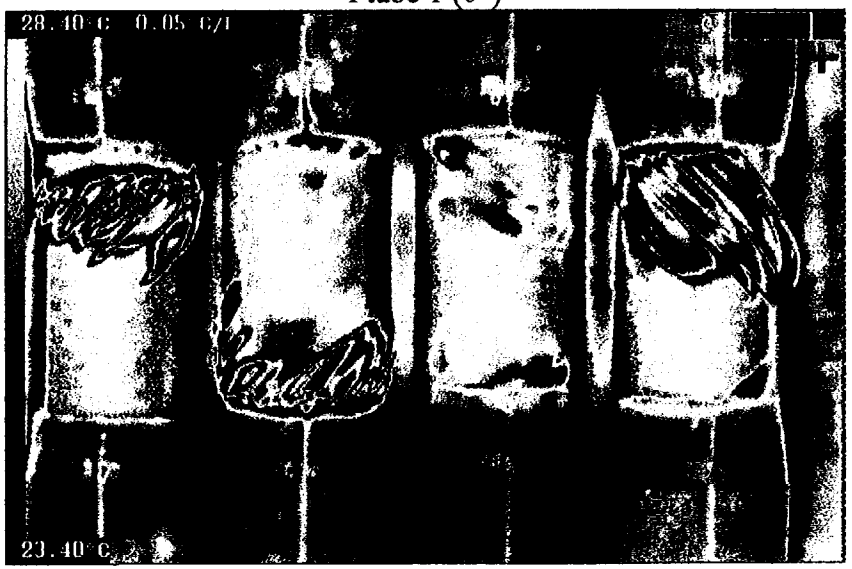

Ptube 1 (180°)

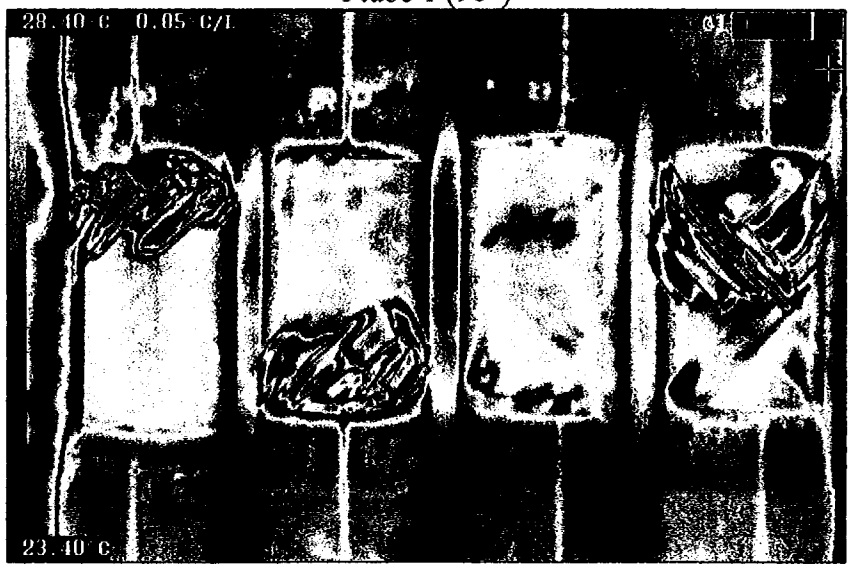

Ptube 1 (270°)

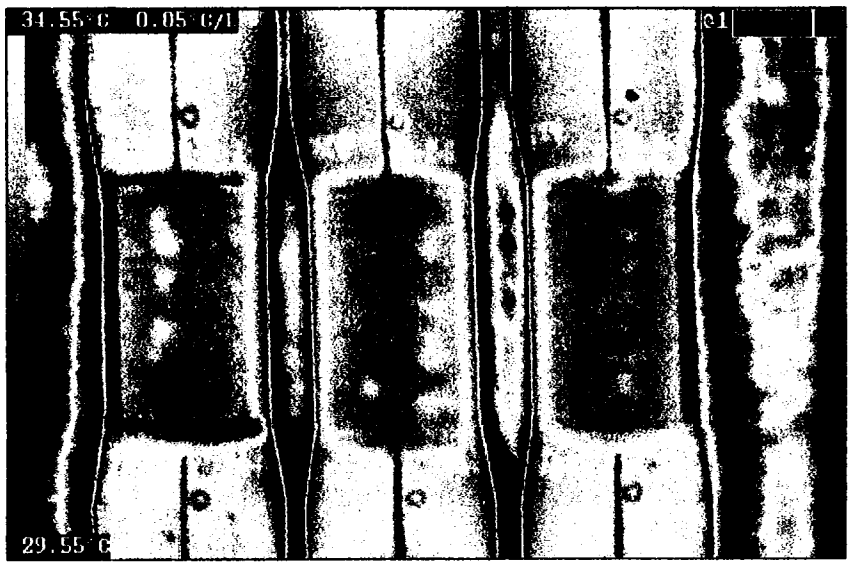

Ptube 2 (0°)

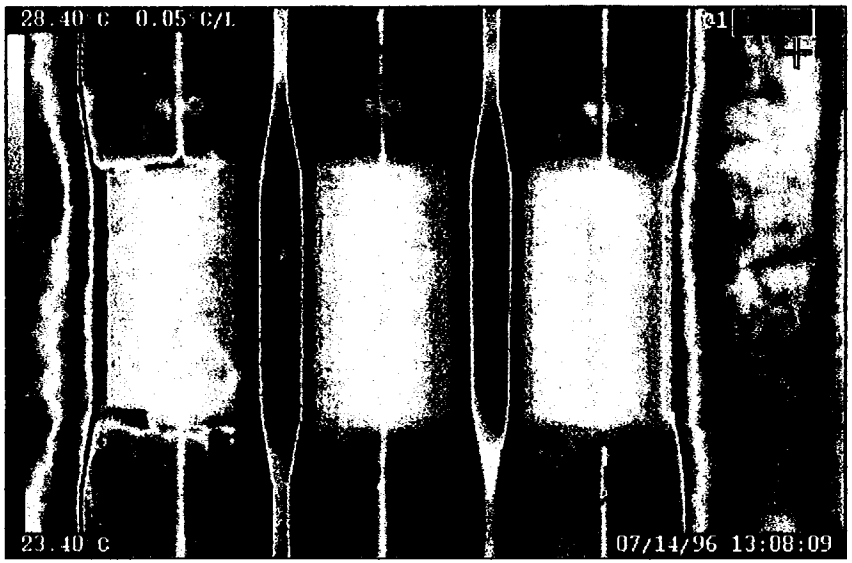

Ptube 2 (90°)

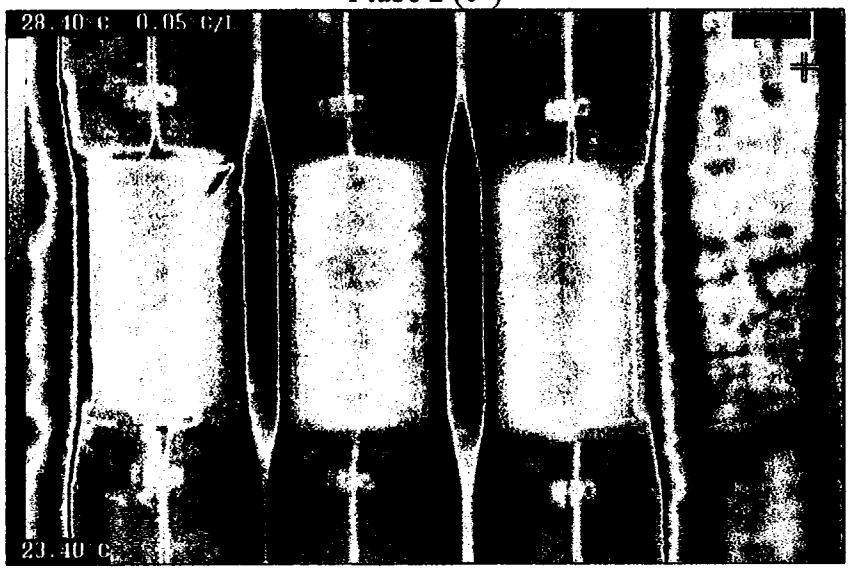

Ptube 2 (180°)

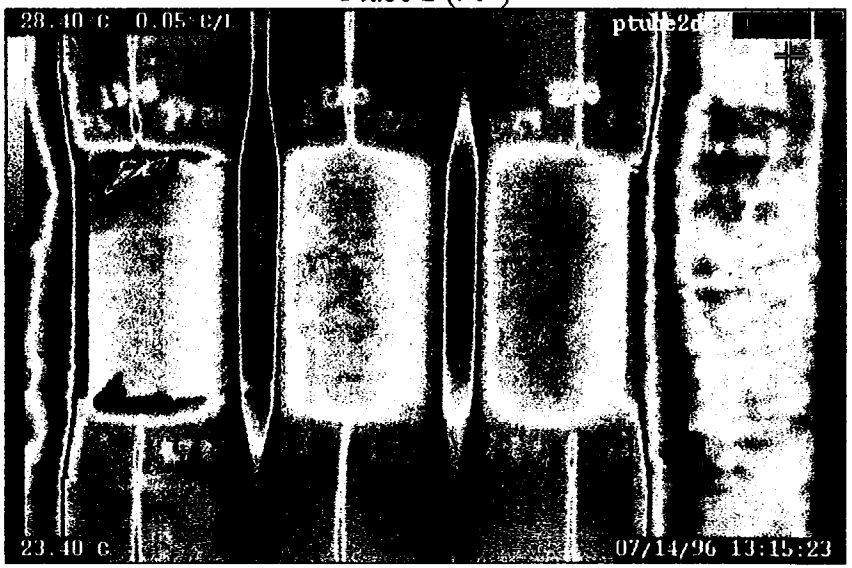

Ptube 2 (270°)

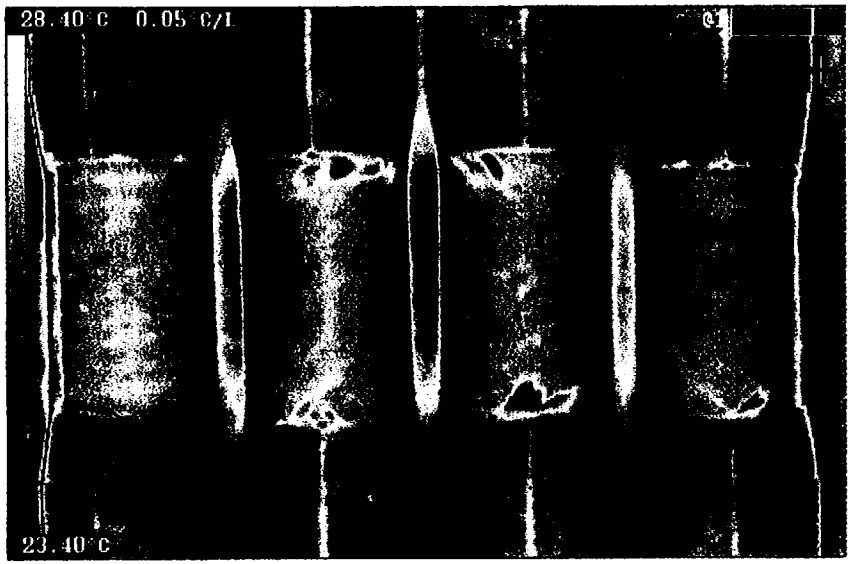

Ptube 3 (0°)

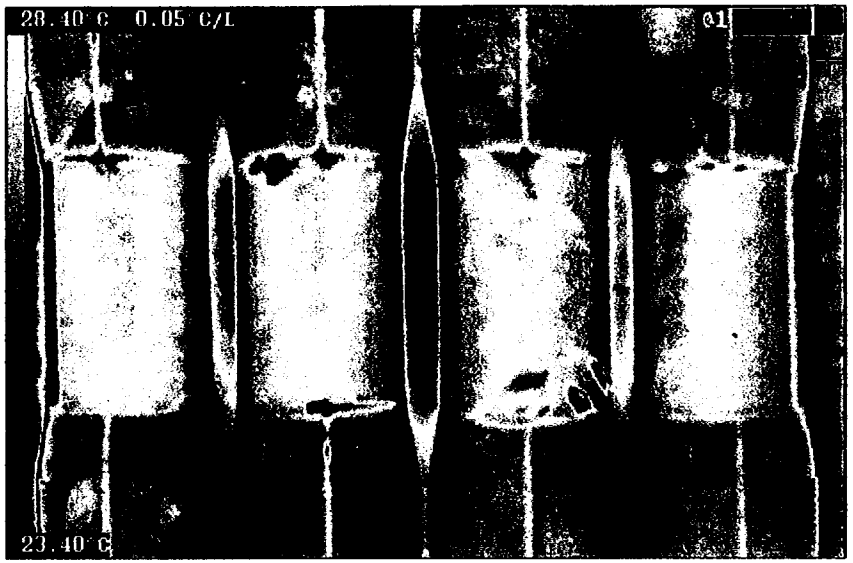

Ptube 3 (90°)

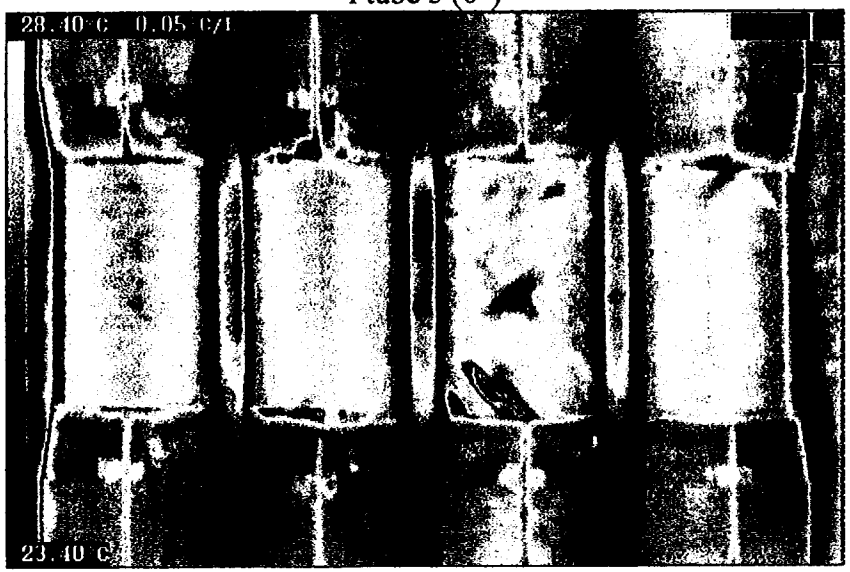

Ptube 3 (180°)

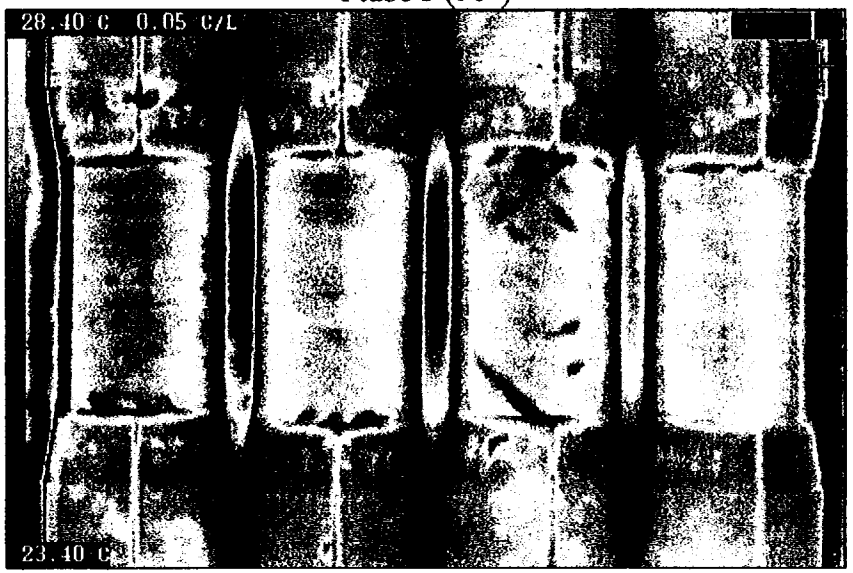

Ptube 3 (270°)

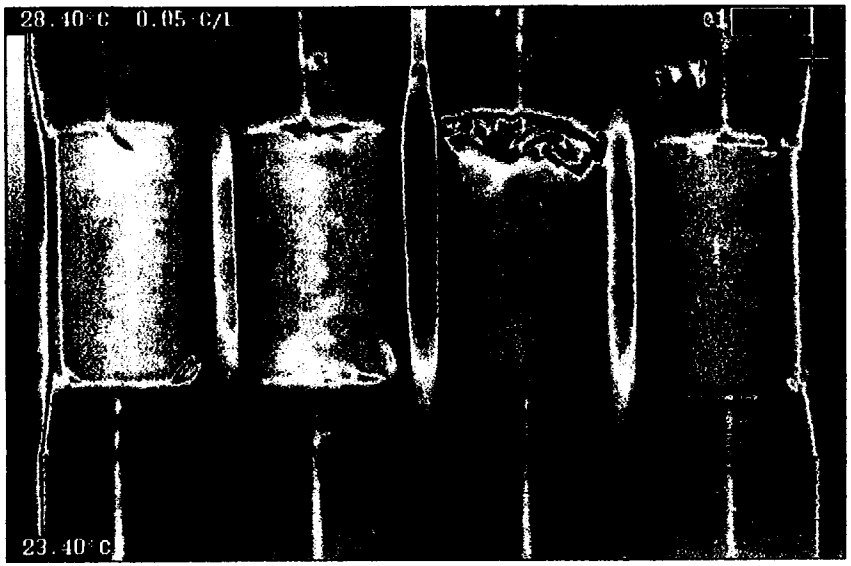

Ptube 4 (0°)

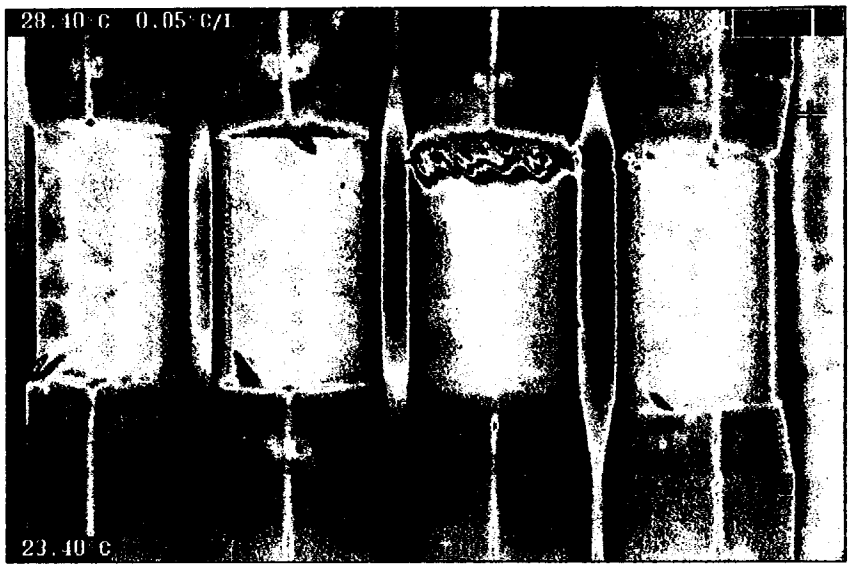

Ptube 4 (90°)

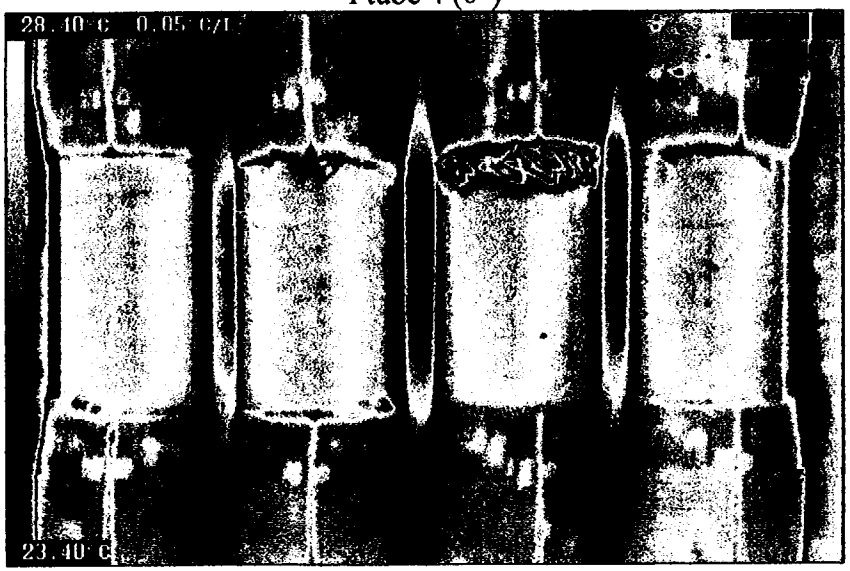

Ptube 4 (180°)

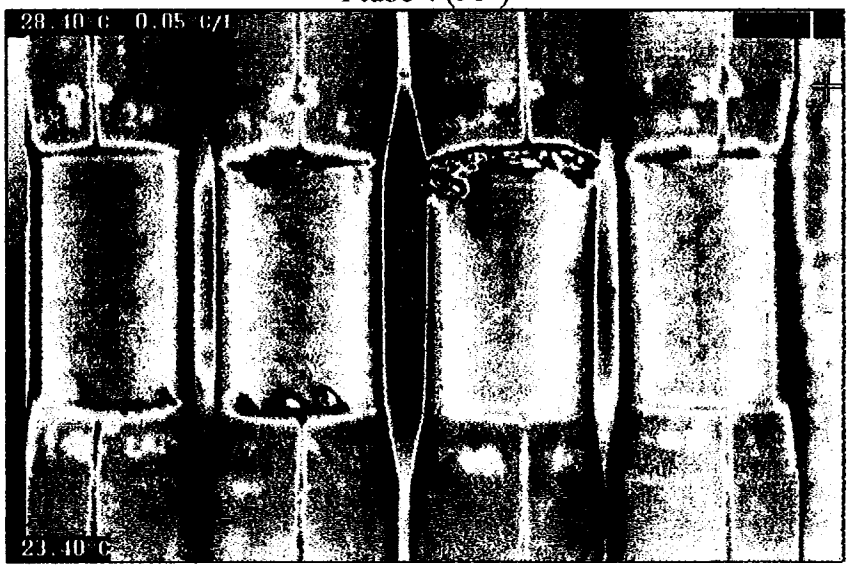

Ptube 4 (270°)

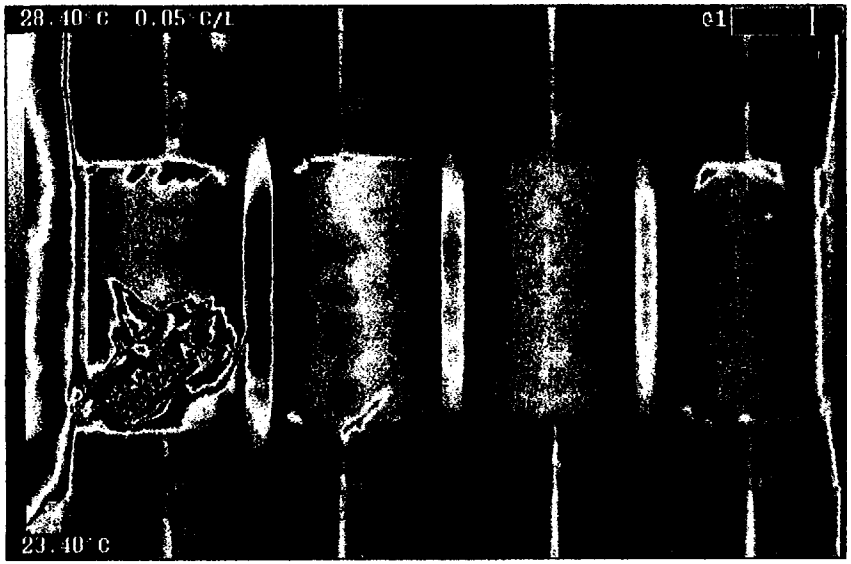

Ptube 5 (0°)

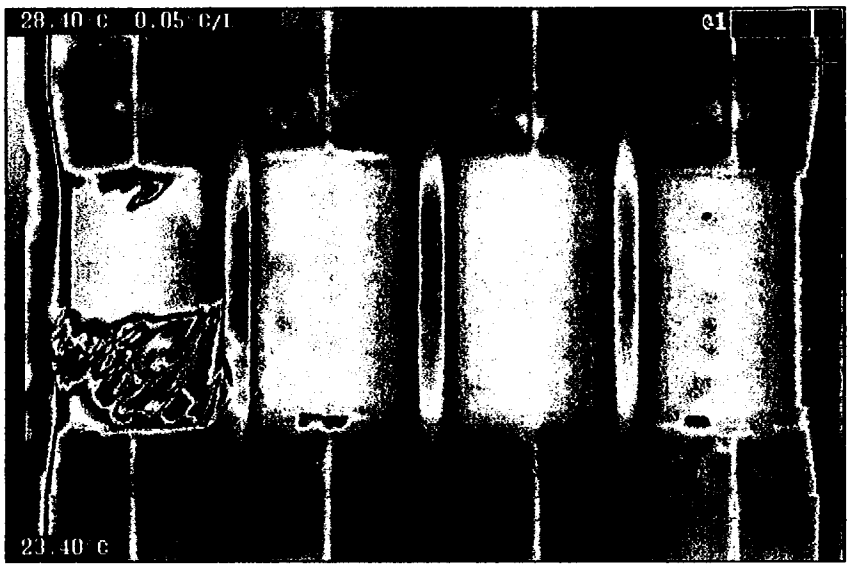

Ptube 5 (90°)

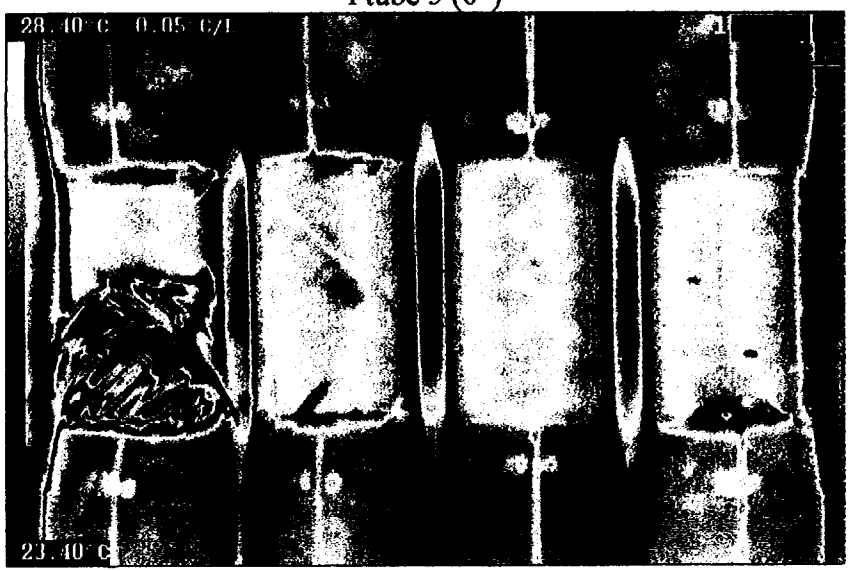

Ptube 5 (180°)

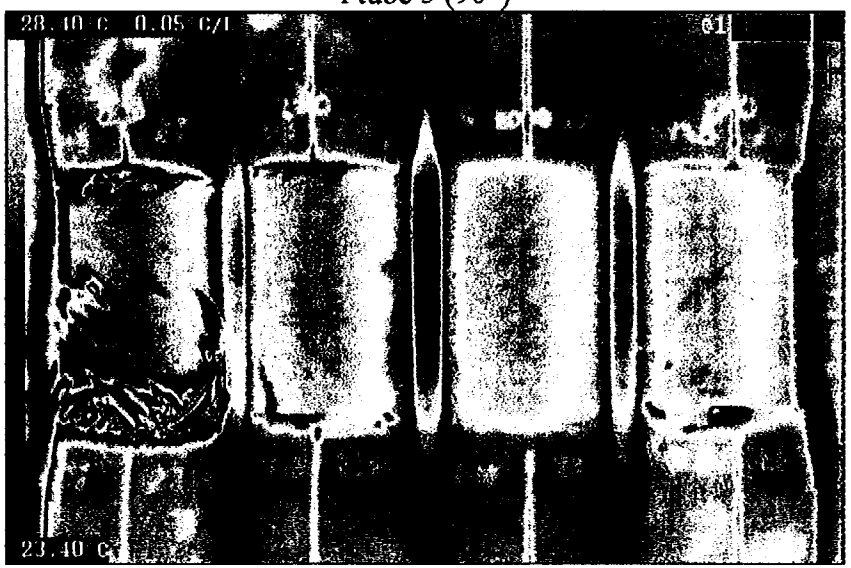

Ptube 5 (270°)

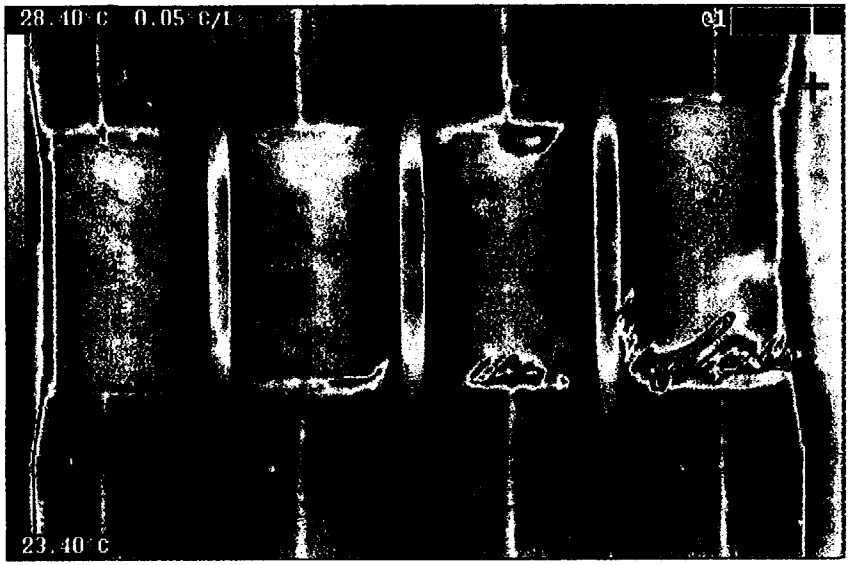

Ptube 6 (0°)

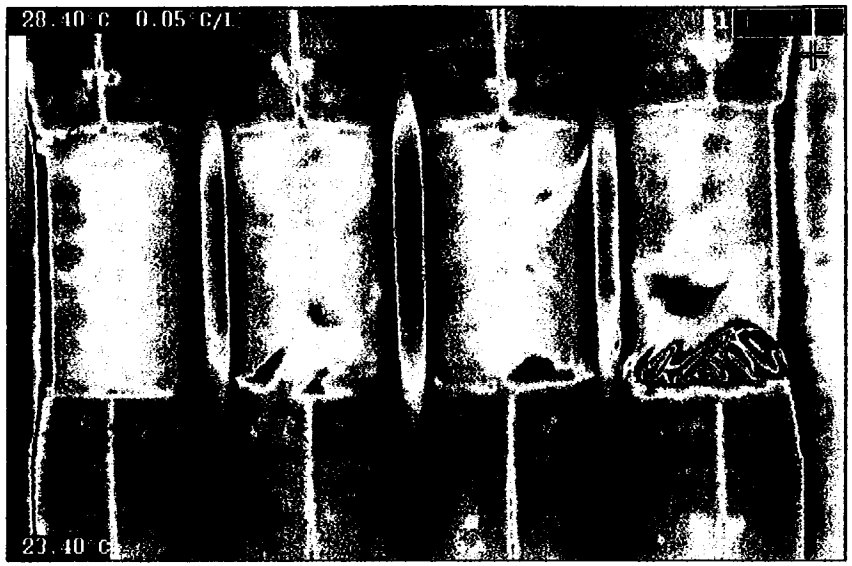

Ptube 6 (90°)

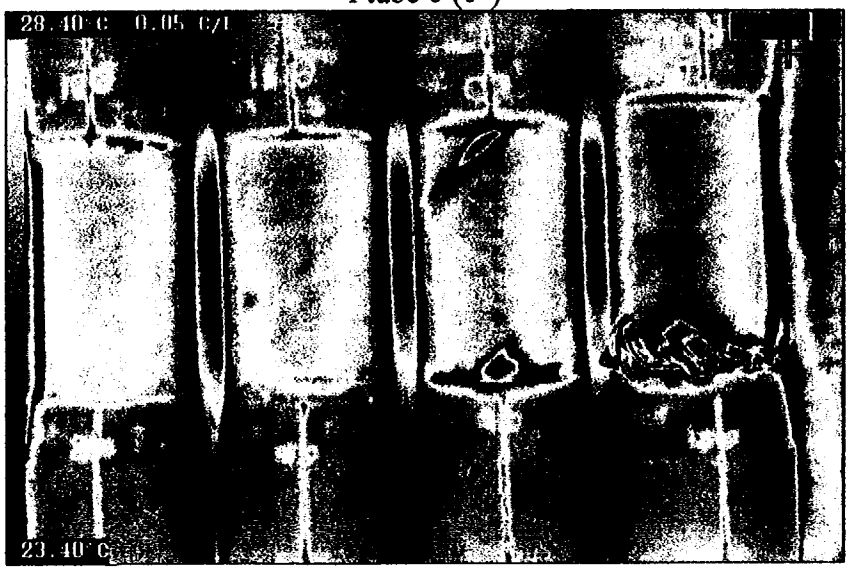

Ptube 6 (180°)

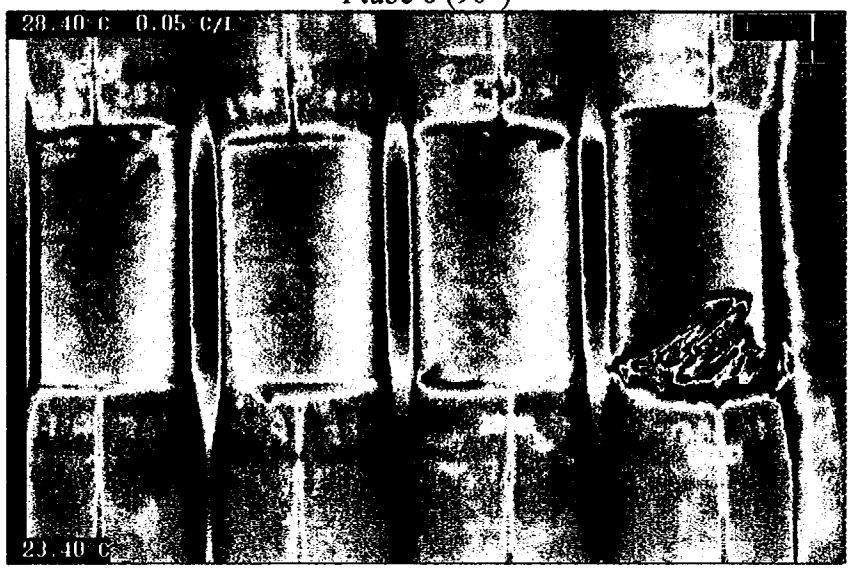

Ptube 6 (270°)

12.8 F1 GRAPHITE/PHENOLIC NOSE CONE

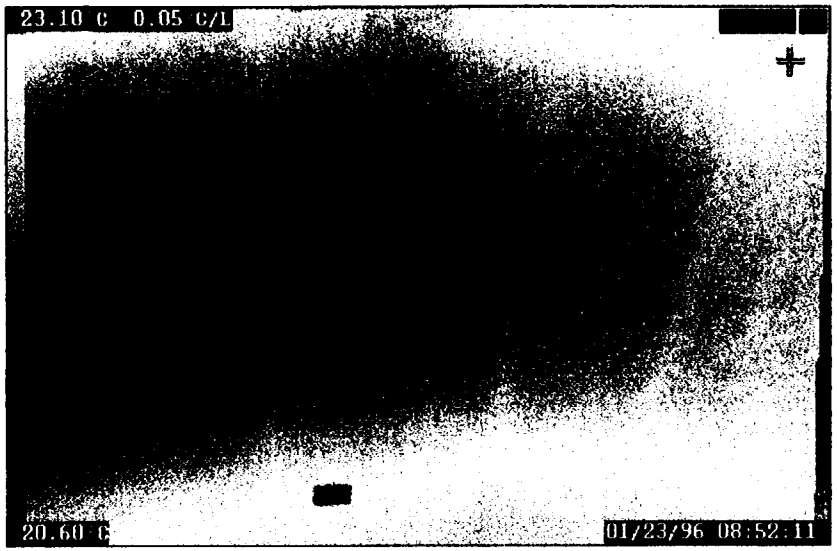

F1_A

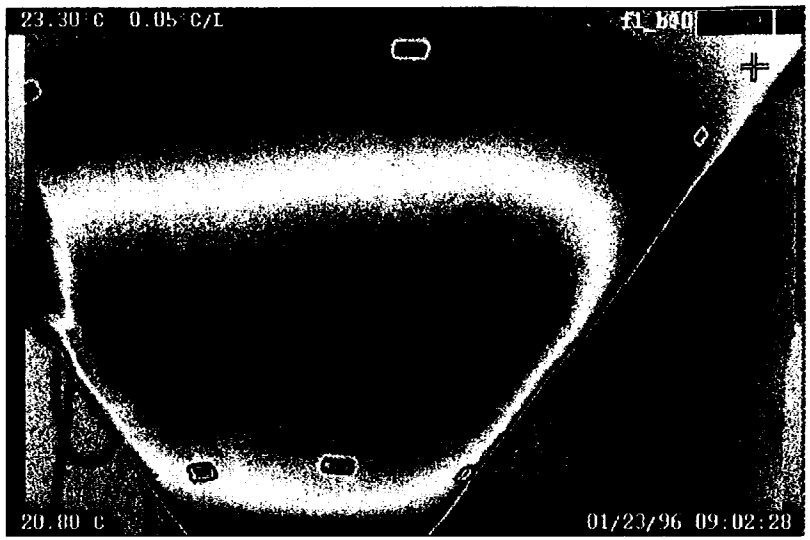

F1_B

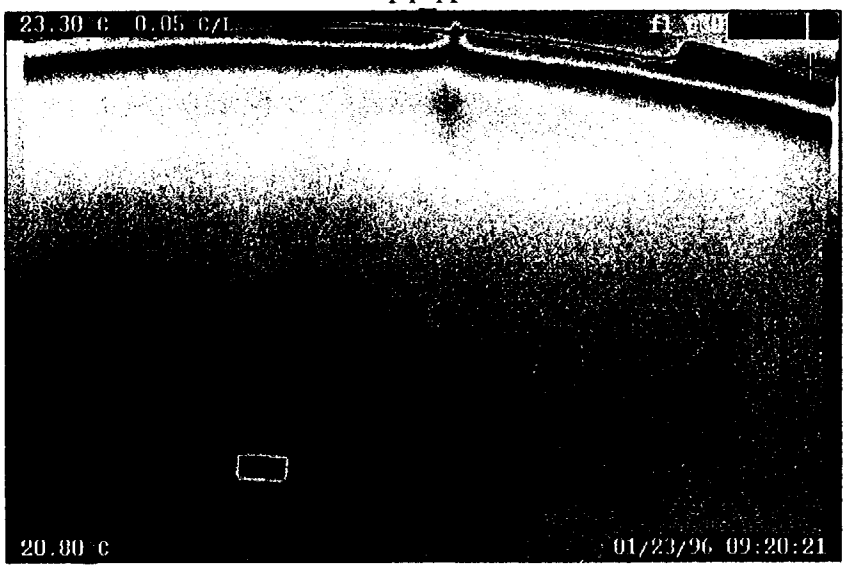

F1_C14

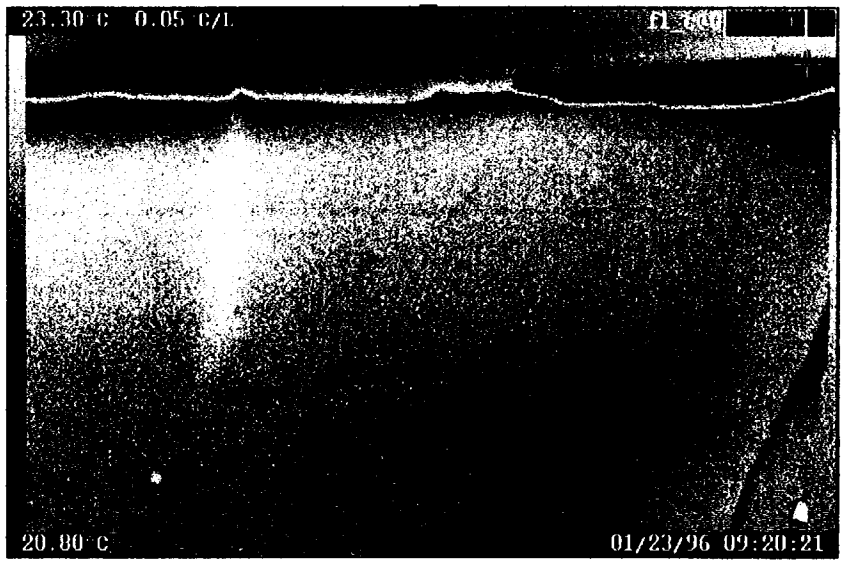

F1_C54

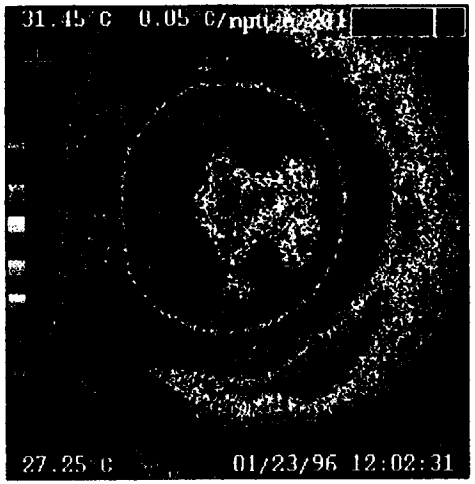

NPU_E_F

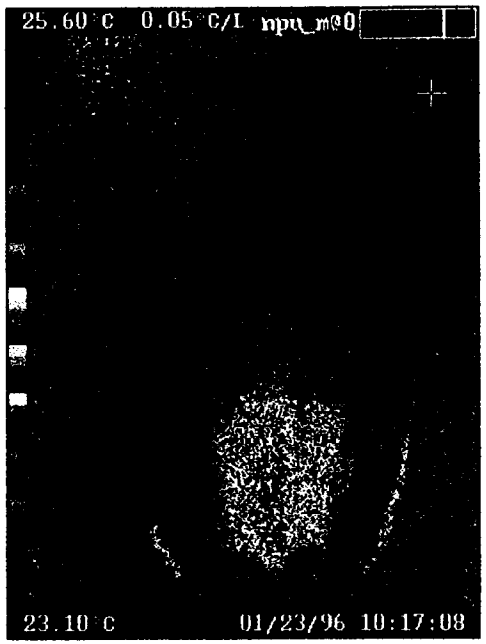

NPU_M

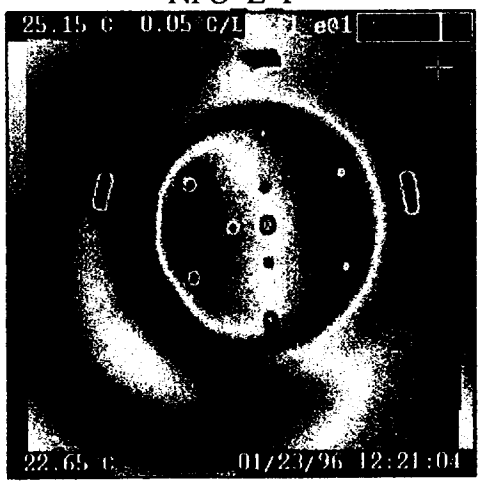

F1_E

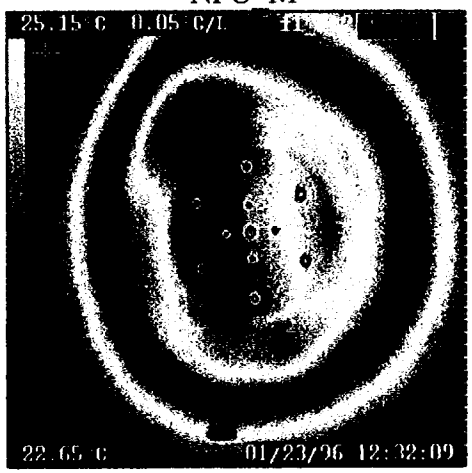

F1_F

F1_G

F1_H

F1_I

F1_J

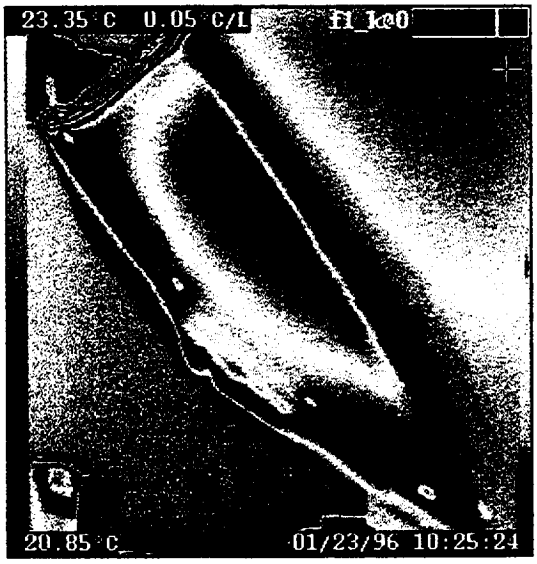
23.35 C 0.05 C/L f1_k@0
20.85 C
01/23/96 10:25:24

F1_K

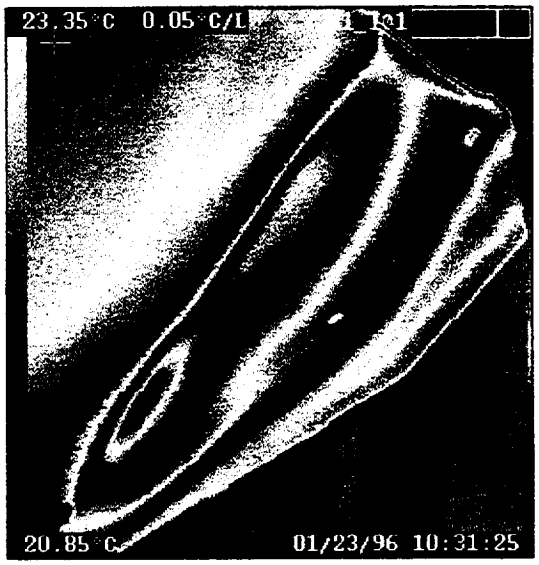
23.35 C 0.05 C/L
20.85 C
01/23/96 10:31:25

F1_L


25.15 C 0.05 C/L f1_m@0
22.65 C
01/23/96 11:23:54

F1_M

12.9 18 INCH DIAMETER GRAPHITE/EPOXY PRESSURE VESSEL

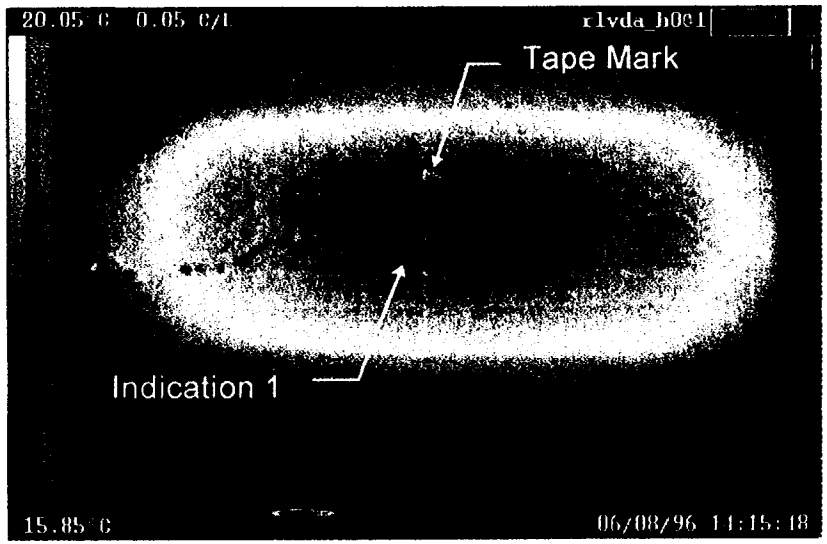

0° Hoop

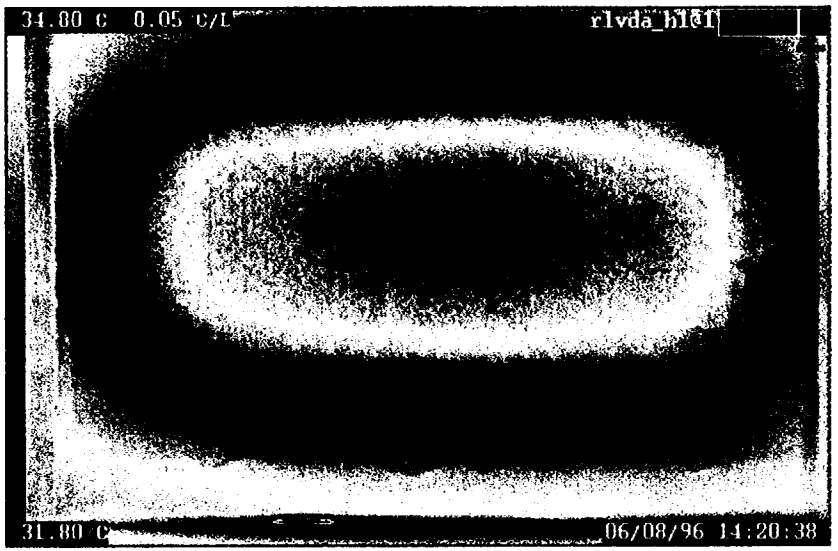

45° Hoop

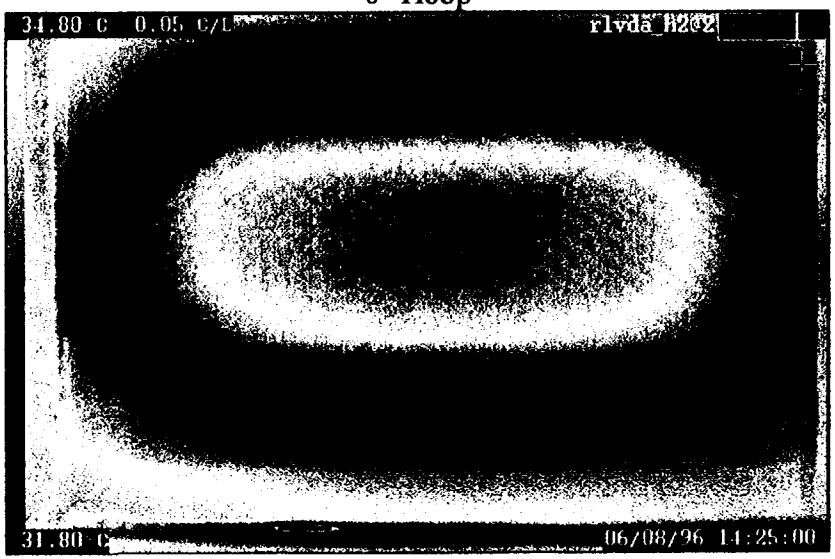

90° Hoop

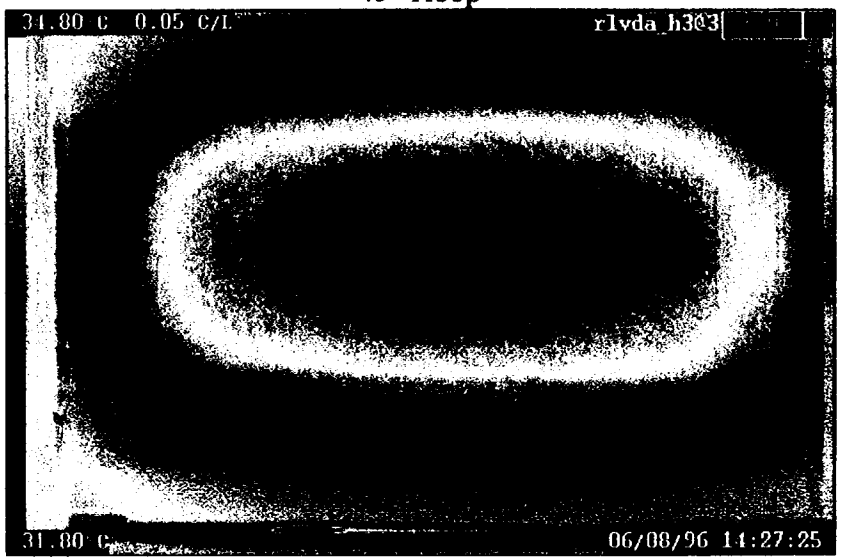

135° Hoop

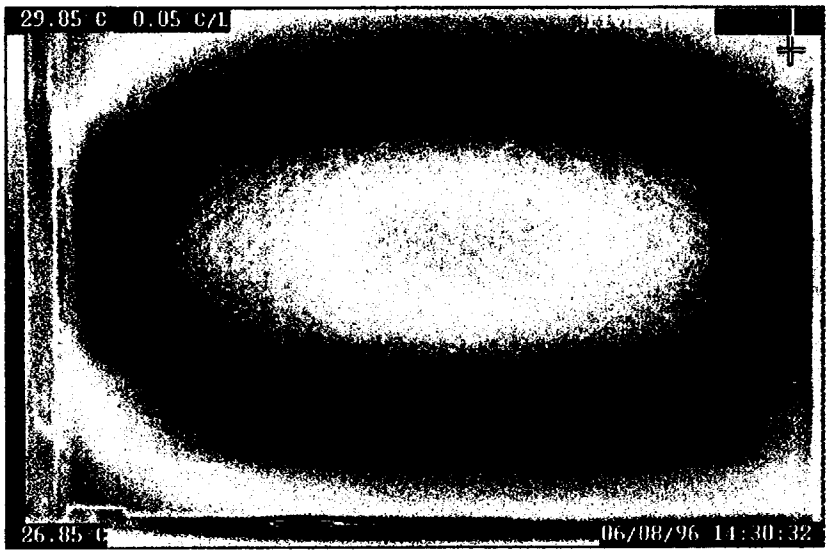

180° Hoop

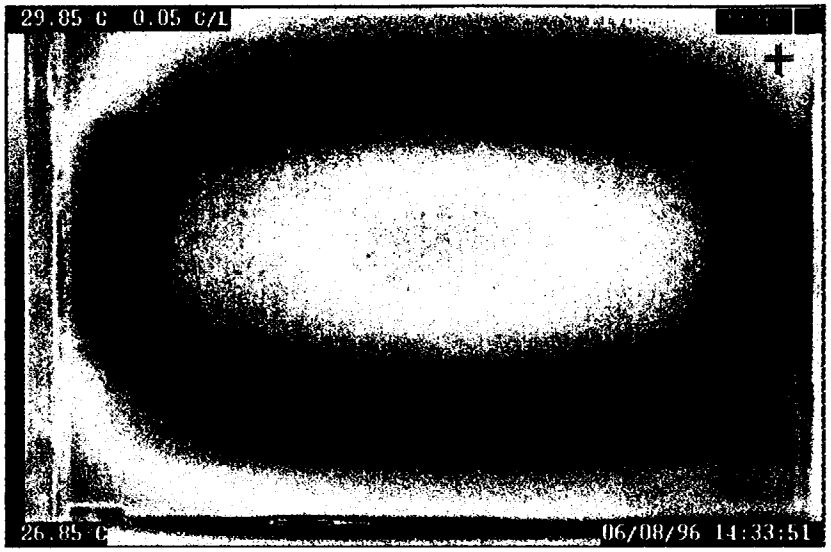

225° Hoop

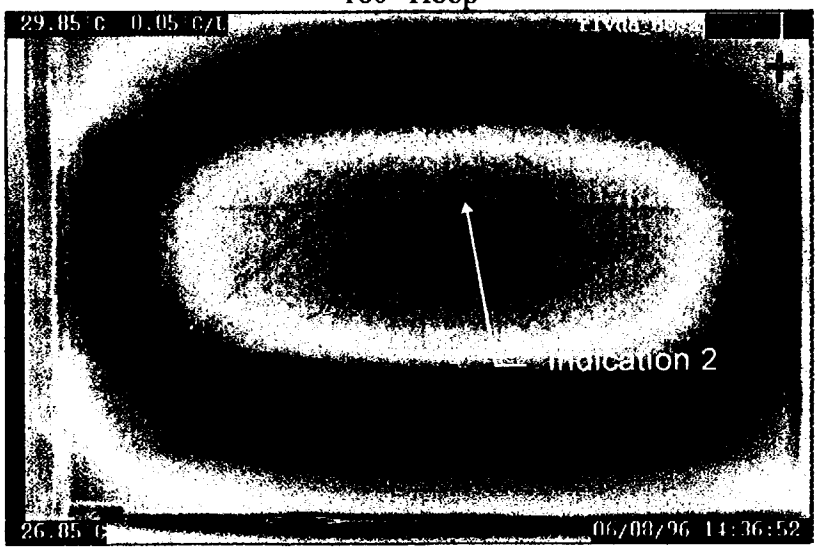

270° Hoop

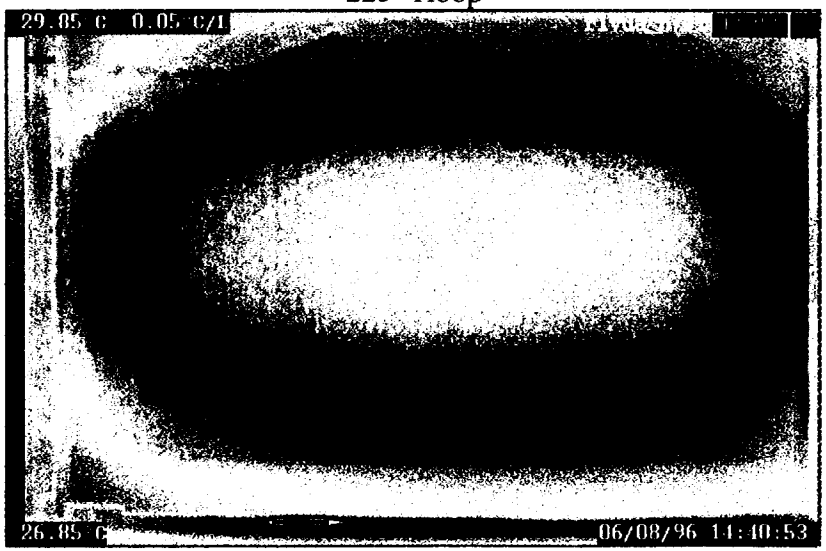

315° Hoop

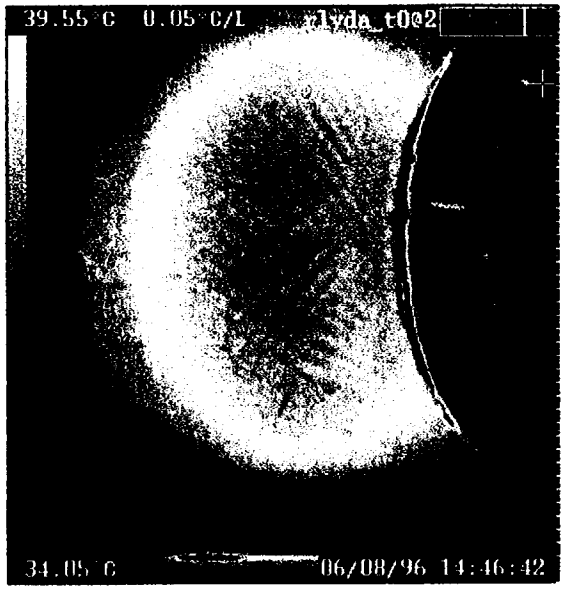

0° Top

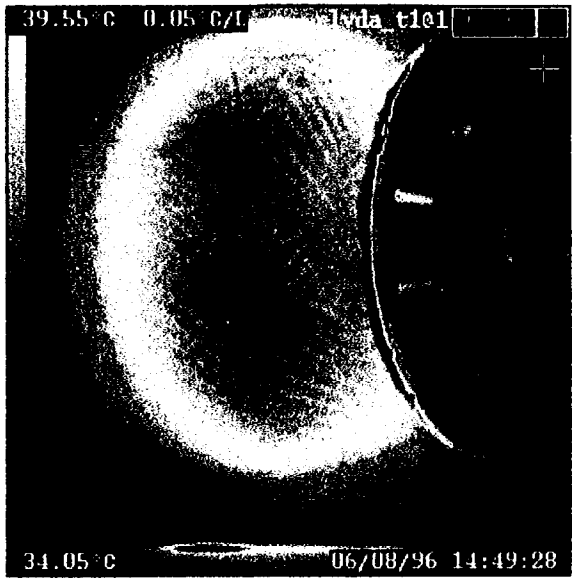

45° Top

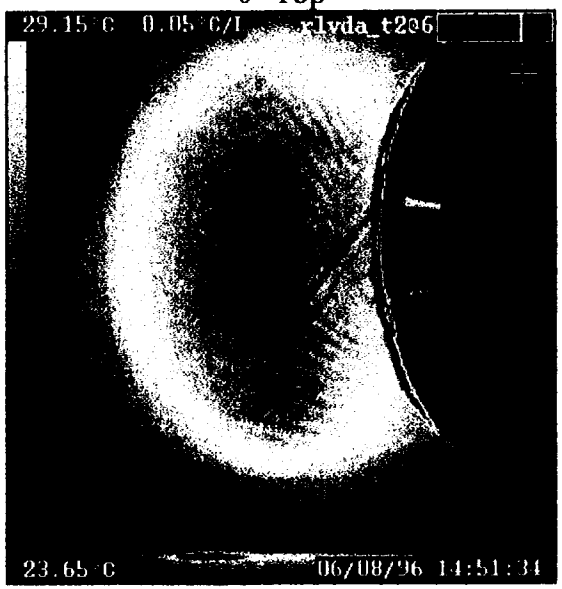

90° Top

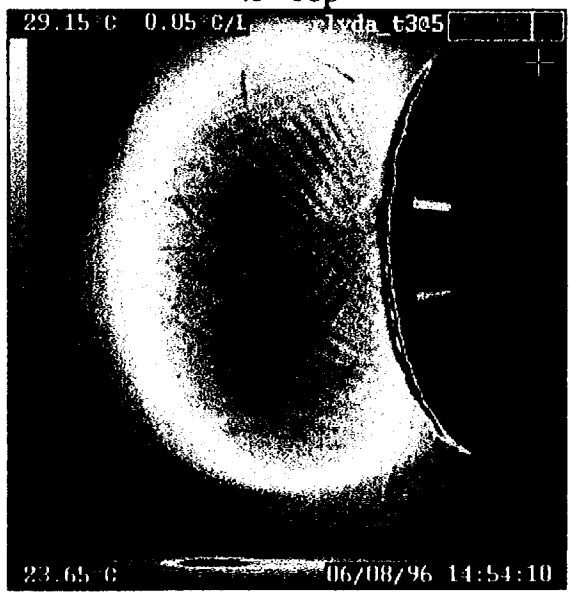

135° Top

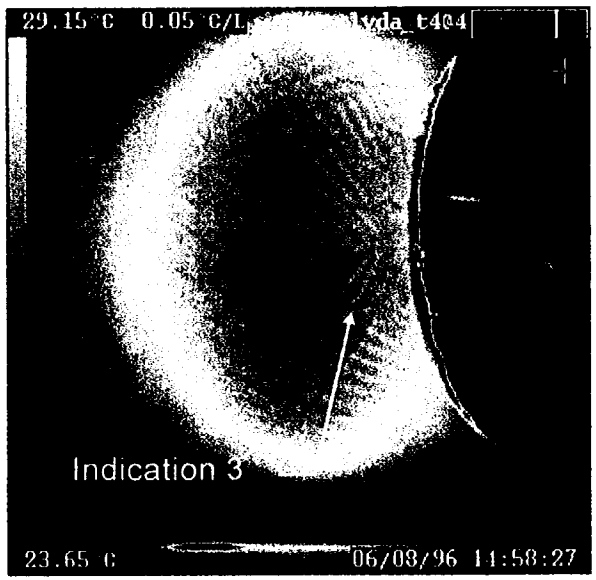

180° Top

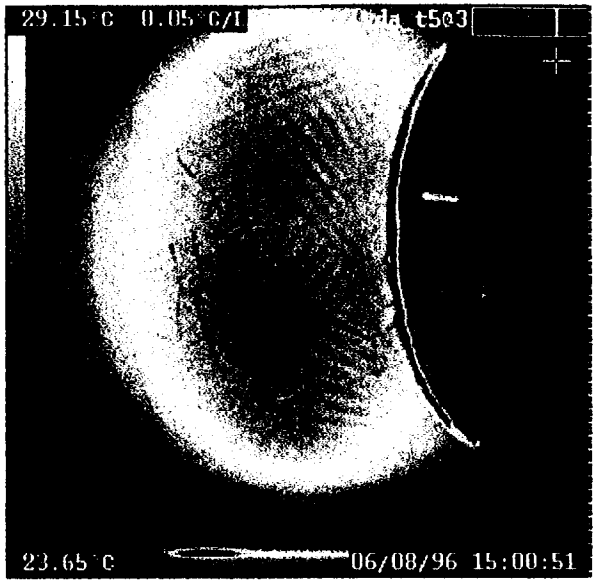

225° Top

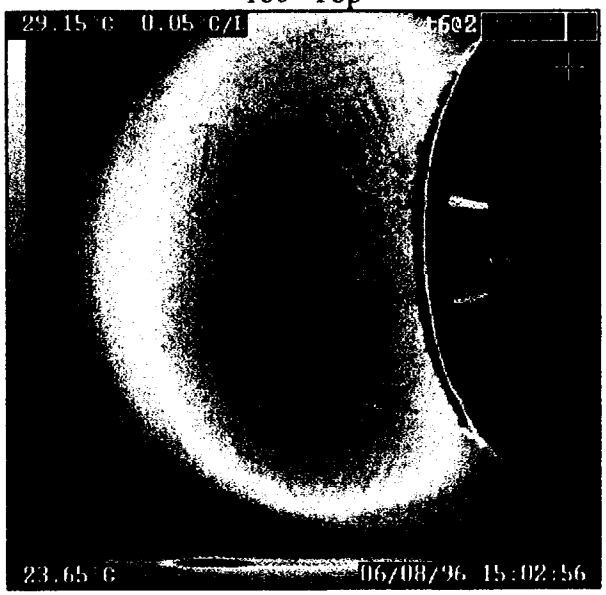

270° Top

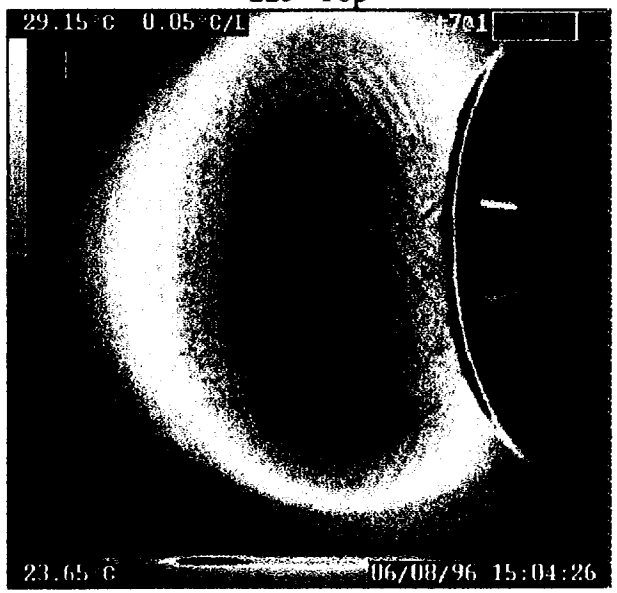

315° Top

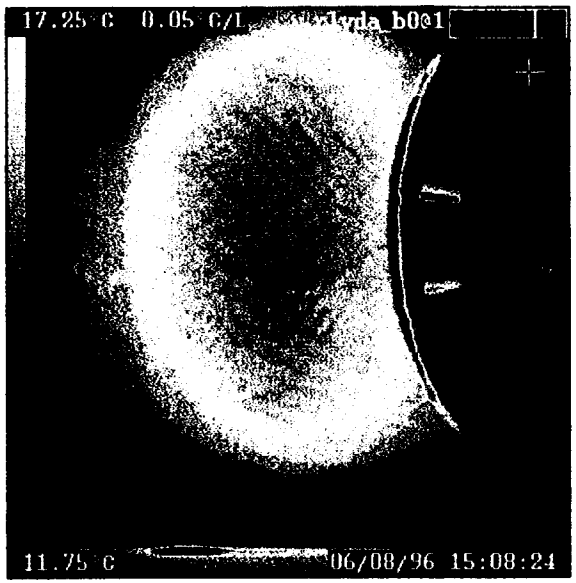

0° Bottom

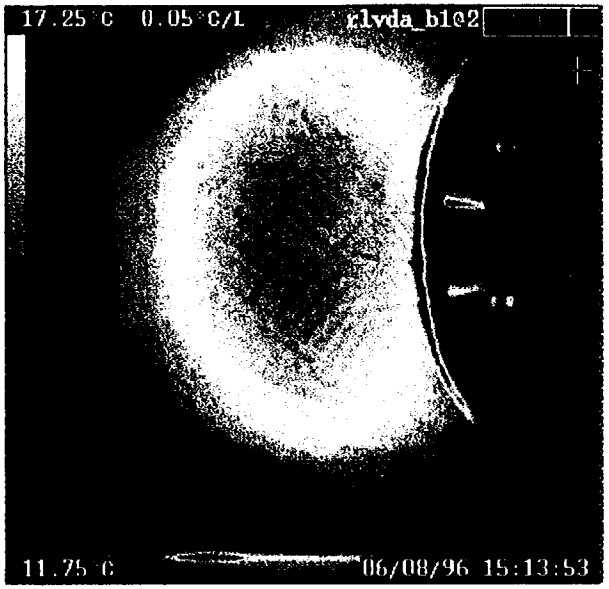

45° Bottom

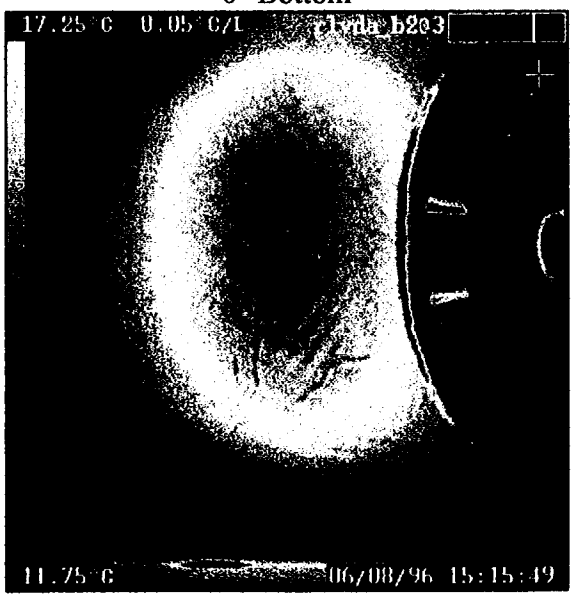

90° Bottom

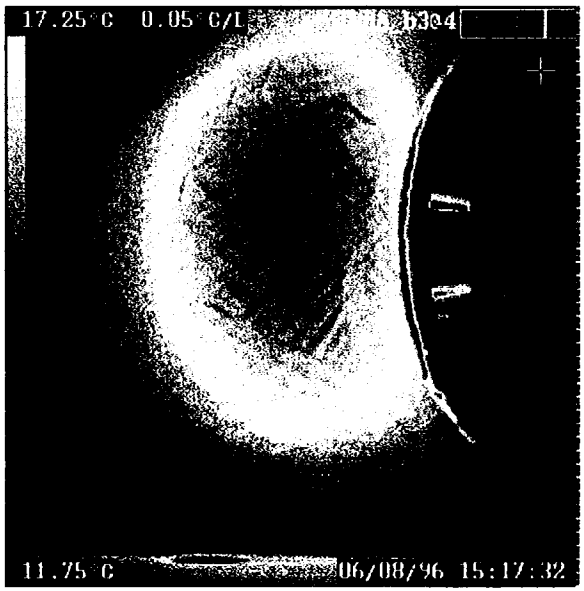

135° Bottom

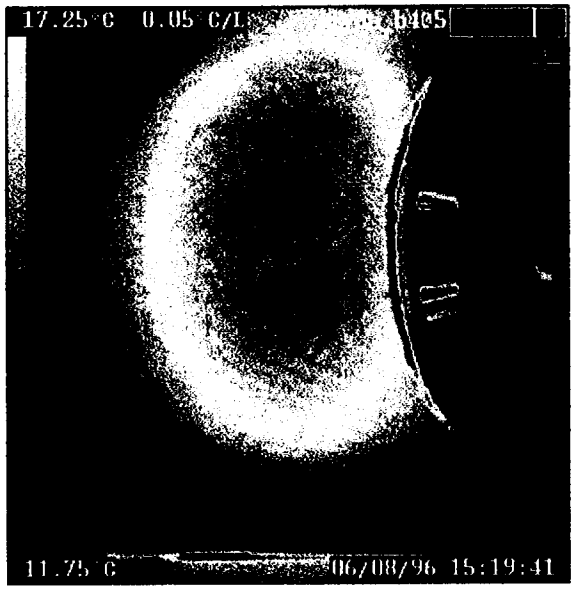

180° Bottom

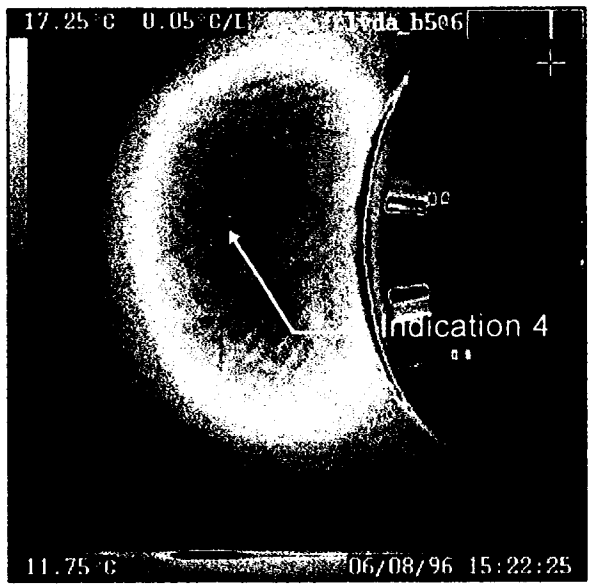

225° Bottom

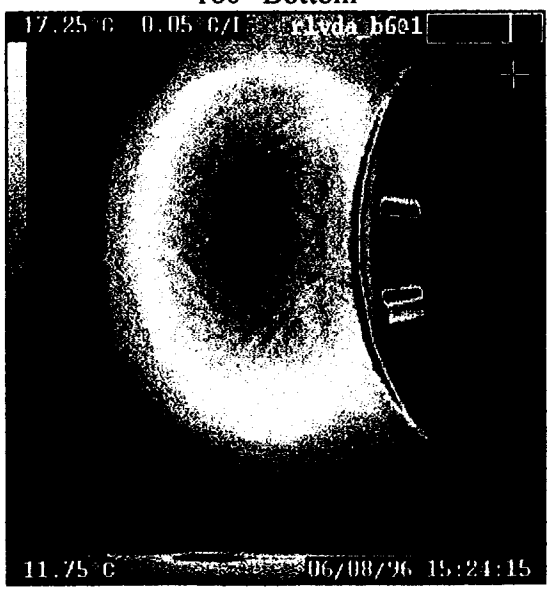

270° Bottom

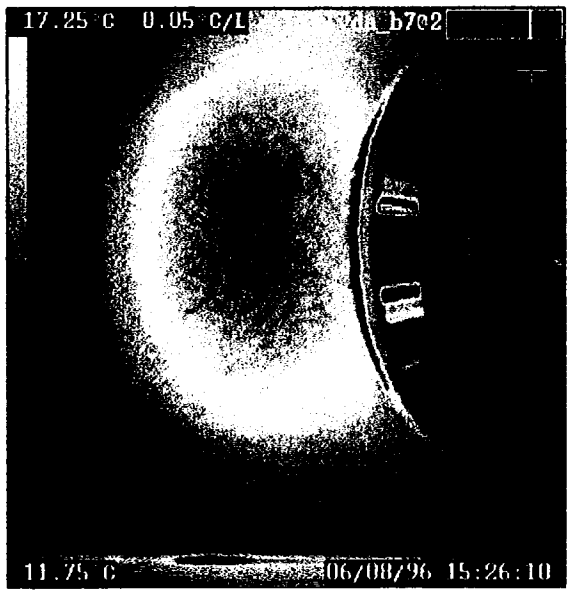

315° Bottom